Charles University in Prague

1st Faculty of Medicine

Study program: Biomedicine
Biochemistry and Pathobiochemistry

Academy of Sciences of the Czech Republic
Institute of Physiology, v.v.i.

M.Sc. Daša Medříková

Studium metabolického syndromu na myším modelu: úloha lipidů v potravě, tukové tkáně a AMP-aktivované proteinové kinázy

Study of metabolic syndrome in mice model: roles of dietary lipids, adipose tissue and AMP-activated protein kinase

Ph.D. Thesis

Supervisor: Jan Kopecký, MD, DSc.

Prague, 2011

Prohlášení:

Prohlašuji, že jsem závěrečnou práci zpracovala samostatně a že jsem uvedla všechny použité informační zdroje. Současně dávám svolení k tomu, aby tato závěrečná práce byla archivována v Ústavu vědeckých informací 1. lékařské fakulty Univerzity Karlovy v Praze a zde užívána ke studijním účelům. Za předpokladu, že každý, kdo tuto práci použije pro svou přednáškovou nebo publikační aktivitu, se zavazuje, že bude tento zdroj informací řádně citovat.

Souhlasím se zpřístupněním elektronické verze mé práce v Digitálním repozitáři Univerzity Karlovy v Praze (http://repozitar.cuni.cz). Práce je zpřístupněna pouze v rámci Univerzity Karlovy v Praze.

Souhlasím – Nesouhlasím *

V Praze dne Mgr. Daša Medříková

* **Nehodící se škrtněte**

Identifikační záznam:

Medříková, Daša. *Studium metabolického syndromu na myším modelu: úloha lipidů v potravě, tukové tkáně a AMP-aktivované proteinové kinázy. [Study of metabolic syndrome in mice model: roles of dietary lipids, adipose tissue nd a role of AMP-activated protein kinase]*. Praha, 2011. 68, 4. Dizertační práce (Ph.D.). Univerzita Karlova v Praze, 1. lékařská fakulta. Vedoucí práce Kopecký, Jan.

Acknowledgements

I would like to express my thanks to my supervisor Jan Kopecký for the scientific support during my PhD studies and to all the collaborators and co-authors of our publications.

This thesis is based on the following papers, referred to by their capital letters in the text as indicated here:

A. Rossmeisl M, Jelenik T, Jilkova Z, Slamova K, Kus V, Hensler M, **Medrikova D**, Povysil C, Flachs P, Mohamed-Ali V, Bryhn M, Berge K, Holmeide K, Kopecky J. DHA-derivatives in the prevention and reversal of obesity and glucose intolerance in mice. *Obesity*. 17:1023–1031, 2009 (IF = 2.798)

B. Kus V, Prazak T, Brauner P, Hensler M, Kuda O, Flachs P, Janovska P, **Medrikova D**, Rossmeisl M, Jilkova Z, Stefl B, Pastalkova E, Drahota Z, Houstek J, Kopecky J. Induction of muscle thermogenesis by high-fat diet in mice: association with obesity-resistance. *Am J Physiol Endocrinol Metab*. 295:E356-E367, 2008 (IF = 4.129)

C. Jelenik T, Rossmeisl M, Kuda O, Macek Jilkova Z, **Medrikova D**, Kus V, Hensler M, Janovska P, Miksik I, Baranowski M, Gorski , Jensen TE, Flachs P, Viollet B, Kopecky J. AMP-activated protein kinase α2 subunit is required for the preservation of hepatic insulin sensitivity by n-3 polyunsaturated fatty acids. *Diabetes.* 59:2737-2746, 2010 (IF = 8.261)

D. **Medrikova D,** Macek Jilkova Z, Bardova K, Janovska P, Rossmeisl M, Kopecky J. Sex differences during the course of diet-induced obesity in mice: adipose tissue expandability and glycemic control. Accepted in: *Int J Obes.* (IF = 4.343)

The above papers are included in full in this Ph.D. thesis. For the complete list of my published articles, see List of publications (Section 6).

LIST OF ABBREVIATIONS

AMP	adenosine monophosphate
AMPK	AMP–activated protein kinase
Aox1	acyl-CoA oxidase 1
ATP	adenosine triphosphate
BAT	brown adipose tissue
Cd68	Cd68 antigen
CLS	crown-like structures
CoA	coenzyme A
Cpt-1	carnitine palmitoyltransferase-1
DAG	diacylglycerols
DHA	docosahexaenoic acid (22:6 n–3)
EPA	eicosapentaenoic acid (20:3 n–5)
Fdps	farnesyl diphosphate synthase
gWAT	gonadal WAT
HF	high-fat
HMW	high molecular weight form of adiponectin
IL-6	interleukin-6
IP GTT	intraperitoneal glucose tolerance test
IR	insulin receptor
IRS	insulin receptor substrate
LC-PUFA	long chain polyunsaturated fatty acids
LF	low-fat
LMW	low molecular weight form of adiponectin
MCP-1	monocyte chemoattractant protein-1
MMW	medium molecular weight form of adiponectin
NEFA	non-esterified fatty acids
NF-κB	nuclear factor-κB
PDK-4	pyruvate dehydrogenase kinase 4
PPAR	peroxisome proliferator–activated receptor

PUFA	polyunsaturated fatty acids
RT-PCR	real-time polymerase chain reaction
SCD-1	stearoyl-CoA desaturase
SPOT14	thyroid hormone responsive SPOT14
SREBP	sterol regulatory element binding protein
ST	standard diet
scWAT	subcutaneous WAT
TAG	triacylglycerols
TNF-α	tumour necrosis factor-α
UCP1	uncoupling protein 1
WAT	white adipose tissue

CONTENT

1 INTRODUCTION

1.1 Induction of obesity

The incidence of obesity has reached epidemic dimension and it is still increasing worldwide. Overweight and obesity represent a considerable threat for modern society, as they are associated with a markedly increased risk of developing many severe health disturbances (1). Besides atherosclerosis, non-alcoholic fatty liver disease and certain type of cancer, one of the most devastating seems to be metabolic syndrome (2;3). Metabolic syndrome is a cluster of conditions including abdominal obesity, dyslipidaemia, high blood pressure or insulin resistance, which represent higher risk for cardiovascular disease and type 2 diabetes.

1.1.1 Energy homeostasis – energy intake and expenditure

In an organism, energy is stored in the form of glycogen in liver and skeletal muscle, and in the form of triacylglycerols (TAG) in adipose tissue. According to the first law of thermodynamics, energy cannot be created or disappear, it can be only transformed from one form to another. Mammalian species receive required energy for their vital processes as food. This form of chemical energy is converted by metabolic processes in the body to physical work or heat and enables survival of an organism. Unused energy is stored and can be reused in conditions of negative energy balance.

Food intake, energy expenditure and preservation of body energy stores are subjected to complex regulation with the brain as the main coordinator. Parts of brain responsible for food intake and body weight maintenance respond to afferent signals from circulation and regulate food intake according to the actual needs of an organism (4). Two main players in the control of food intake are adipose tissue-derived hormone leptin as well as hormone insulin produced by pancreatic β-cells. While leptin circulates in plasma at the levels corresponding to body fat stores, the receptors for both hormones are located in the parts of brain involved in the control of food intake, their stimulation causes reduction in energy intake (5;6).

Total energy expenditure can be divided into three main components: energy expenditure required for 1) basal metabolism, 2) physical work and 3) adaptive thermogenesis. Adaptive thermogenesis is defined as the regulated production of the heat in response to environmental temperature or diet (7). In response to low temperature, adaptive thermogenesis can be classified as shivering and non-shivering thermogenesis. Shivering thermogenesis is caused by the activation of muscle contractions, thus protecting an organism from cold by dissipation of energy in the form of heat. Non-shivering thermogenesis occurs after adaptation to cold and disappearance of shivering, when other tissues, such as brown adipose tissue (BAT) and skeletal muscle, undertake the heat production (8). Diet-induced thermogenesis belongs also to non-shivering thermogenesis, as feeding is known to increase energy expenditure (9).

Cold-induced non-shivering thermogenesis takes place mostly in BAT and is mediated by the mechanism of mitochondrial uncoupling. The principal molecule involved in this process is uncoupling protein 1 (UCP1), situated in the inner mitochondrial membrane of brown adipocytes. UCP1 enables re-entering of protons from mitochondrial intermembrane space back to mitochondrial matrix, bypassing the adenosine triphosphate (ATP)-synthase. Therefore, instead of using energy to ATP production, it is dissipated as a heat (10). For a long time, it was believed that the mechanism of mitochondrial uncoupling is present only in mammalian neonates and small mammals, while in adulthood it is insignificant. However, recent publications suggest that non-shivering thermogenesis mediated by BAT is relevant also in adults and it can importantly contribute to energy expenditure (11-13).

Part of adaptive thermogenesis can be attributed to skeletal muscle. Mechanism by which skeletal muscle contributes to adaptive thermogenesis is still unclear. For instance, leptin may stimulate lipid oxidation in the skeletal muscle, and increase energy expenditure, calcium cycling (14) or mitochondrial uncoupling (15).

Obesity develops when the balance between energy intake and expenditure is disturbed. This is usually caused by increased food intake and inability to induce adaptive thermogenesis associated with a decrease in physical activity. Development of obesity is further accompanied by an increased risk of metabolic disorders clustered into the so called metabolic syndrome.

1.2 Linking obesity to insulin resistance and type 2 diabetes

As mentioned above, obesity, resulting from positive energy balance, is a key factor in developing insulin resistance (one of the underlying features of metabolic syndrome), a state characterised by improper response of insulin target tissues to insulin action. In a normal, non-obese state, the main role of insulin is to stimulate glucose uptake by peripheral tissues, suppress hepatic glucose production as well as lipolysis in the adipose tissue in a postprandial state. Impaired insulin sensitivity is characterised by decreased efficiency of insulin to stimulate insulin-responsive signalling pathways, which eventually results in hyperglycaemia and/ or dyslipidaemia. Deficient insulin efficacy can be partially compensated by increased insulin secretion; however, chronically enhanced insulin secretion caused by overloaded metabolic pathways can lead to β-cells exhaustion and the onset of type 2 diabetes.

1.2.1 Role of adipose tissue

For a long period of time, adipose tissue was considered a passive storage place for excessive energy in a form of TAG, protecting an organism from lipotoxicity, additionally providing insulation and mechanical support for other organs. Whereas when food was scarce or energy expenditure increased, lipid reserves supplied fuel for energy generation in a form of glycerol and fatty acids that can be transported to muscle, liver and BAT and used in fatty acid oxidation (16). However, accordingly to recent studies, adipose tissue is now considered to be metabolically active and one of the largest endocrine organs that considerably influences metabolic homeostasis. It secretes numerous hormones and cytokines, which act in an endocrine and paracrine manner (17;18) and are involved in a regulation of metabolic homeostasis (see also section 1.3).

In mammalian species, white adipose tissue (WAT) develops in different locations throughout the body. Two principal fat depots are recognised: visceral/ intra-abdominal and subcutaneous adipose tissue. However, among these fat depots other subdivisions exist. Moreover, depot-specific differences in metabolic activity, adipocyte

size, innervation and vascularization are apparent (19), and various fat depots contribute to obesity-related disorders differently.

During the time of positive energy balance, adipose tissue has the capability to expand by increasing lipid accumulation in adipocytes. In obesity, adipocytes and subsequently the whole adipose tissue become larger. The process of enlargement is called adipocyte hypertrophy, and was originally considered the only means by which adipose tissue mass can expand. However, adipocyte hyperplasia, representing the formation of new adipocytes, also occurs in adipose tissue. Hyperplasia takes place predominantly in young age, nevertheless, it has been discovered recently, that approximately 10 % of adipocytes are renewed every year (20). This mechanism can significantly contribute to a progression of obesity.

Hypertrophied adipocytes are resistant to antilipolytic effect of insulin (21), resulting in an increased release of non-esterified fatty acids (NEFA). Moreover, elevated NEFA levels are associated with obesity, occurrence of metabolic syndrome, insulin resistance and type 2 diabetes (22).

1.2.2 Ectopic lipid accumulation

Adipocytes cannot expand beyond a “critical size” (23). After reaching it, the capacity of adipose tissue for storing excessive lipids is depleted, so the surplus fat is accumulated ectopically in organs such as liver, skeletal muscle and heart. This negatively affects the normal metabolic response of these tissues, as they are not adapted to store large amounts of fat (24). Thus, expandability of adipose tissue could be important for at least partial protection from ectopic lipid accumulation and subsequent insulin resistance (16).

Excessive lipid accumulation is detrimental to metabolically active organs such as liver and skeletal muscle. Increased influx of NEFA to the liver together with decreased fatty acid oxidation can result in hepatic steatosis, which is associated with insulin resistance (25). Whether hepatic steatosis is a cause of insulin resistance or its consequence, still remains to be determined (26). Moreover, byproducts of impaired TAG synthesis, namely diacylglycerol (DAG) accumulation, might contribute to the development of insulin resistance by activating protein kinase C-ε, which interferes with

insulin-stimulated phosphorylation of the substrate of insulin receptor 2 (IRS-2), thus impairing insulin signalling (27). Similarly, oversupply of fatty acids to skeletal muscle can lead to accumulation of various lipid metabolites, such as ceramides and DAG, with a detrimental effect on insulin sensitivity (28). Lipid overload in pancreatic β-cells leads to dysregulated insulin secretion (29;30), and apoptotic cell death (31), both of which may result in diabetic state.

1.2.3 AMP-activated protein kinase

Obesity-related insulin resistance and type 2 diabetes are characterised by defective energy metabolism. Adenosine monophosphate (AMP)-activated protein kinase (AMPK) controls whole body glucose and lipid homeostasis by regulating metabolism in liver, skeletal muscle, adipose tissue and pancreatic β-cells (Fig.1) – key tissues in the pathogenesis of type 2 diabetes. AMPK represents an energy sensor and master regulator of metabolism, placing it in the center of studies of obesity and metabolic syndrome (32).

AMPK is a heterotrimeric protein consisting of catalytic α subunit and regulatory β and γ subunits (33). The protein is activated by an decrease in the ATP/ AMP ratio, exercise, hypoxia, nutrient deprivation, adipose tissue-derived hormones such as leptin and adiponectin, or pharmacologically by antidiabetic drugs thiazolidinediones and metformin (34). AMP binding to γ subunit allosterically activates AMPK and facilitates a phosphorylation of a threonine residue (Thr-172) in α subunit by upstream tumour suppressor LKB1 (serine/threonine-protein kinase 11) kinase. However, AMPK activation can be triggered also in AMP-independent manner through Ca^{2+}/calmodulin-dependent protein kinase β in response to increased calcium ion concentration, such as during contraction of skeletal muscle (35). In general, AMPK activation triggers catabolic pathways that produce ATP and represses ATP consuming processes in order to restore cellular energy stores. Thus, it supports fatty acid oxidation and glucose uptake together with repression of gluconeogenesis and lipolysis. The ability of AMPK to induce lipid oxidation and thereby decrease muscle and liver TAG content is

considered an important feature of its insulin-sensitising effect and thus its activation could be beneficial for type 2 diabetes treatment.

Figure 1 Role of AMPK in the regulation of glucose and lipid homeostasis

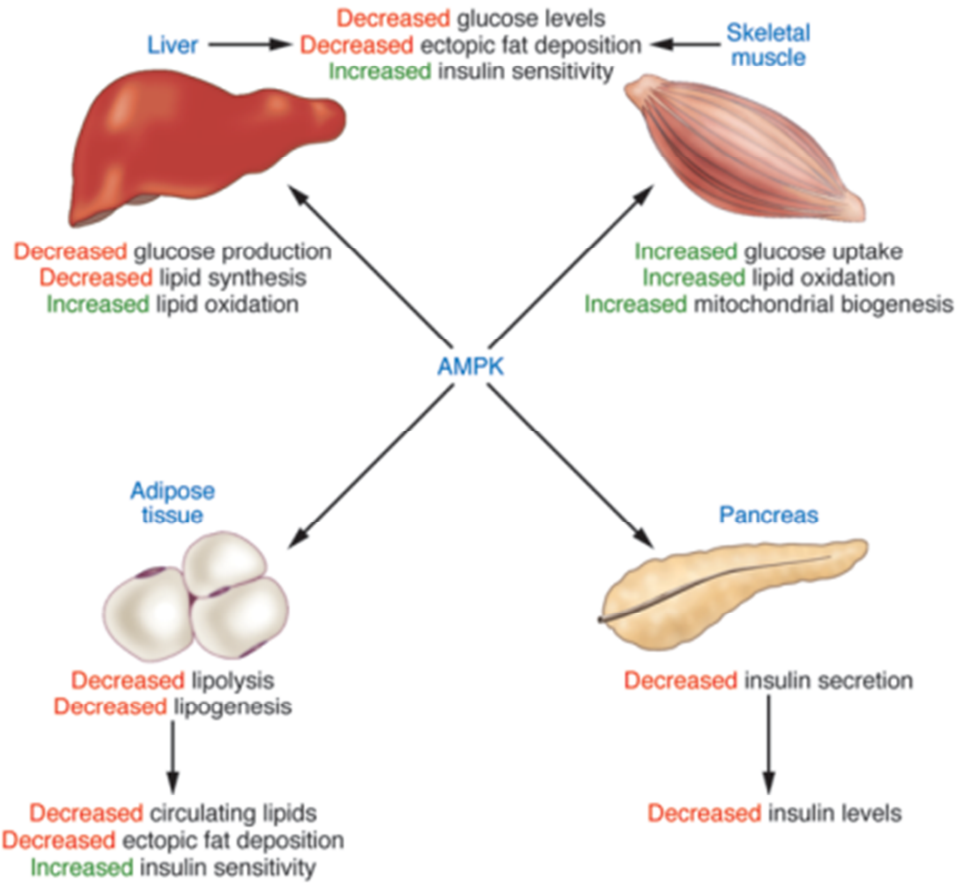

Activation of AMPK in liver, skeletal muscle and adipose tissue decreases glucose production and lipid synthesis, while increases glucose uptake and lipid oxidation at the same time. Thus, AMPK activation results in favourable metabolic environment for the prevention or treatment of type 2 diabetes. Activation of pancreatic AMPK is associated with decreased insulin secretion, probably a protective measure to prevent hypoglycaemia during fasting (adapted from (36)).

1.3 Secretory function of adipose tissue

Besides adipocytes, which represent the most abundant cell type, adipose tissue also contains pre-adipocytes, endothelial cells, fibroblasts and macrophages (37). As mentioned above, adipose tissue plays an important role in the regulation of many physiological and obesity-related pathological processes. By now, various products secreted by adipose tissue, termed adipocytokines, have been characterised (17;38). To their production contribute adipocytes as well as other cell types, such as macrophages. They act in an autocrine/ paracrine or endocrine level as important signalling mediators, and are fundamental to the pathogenesis of the metabolic syndrome (Fig. 2). Magnitude of their production depends highly on the body fat mass, subsequently on the degree of obesity and adipocyte size (39).

Figure 2 Adipocytokines involved in the pathogenesis of metabolic syndrome

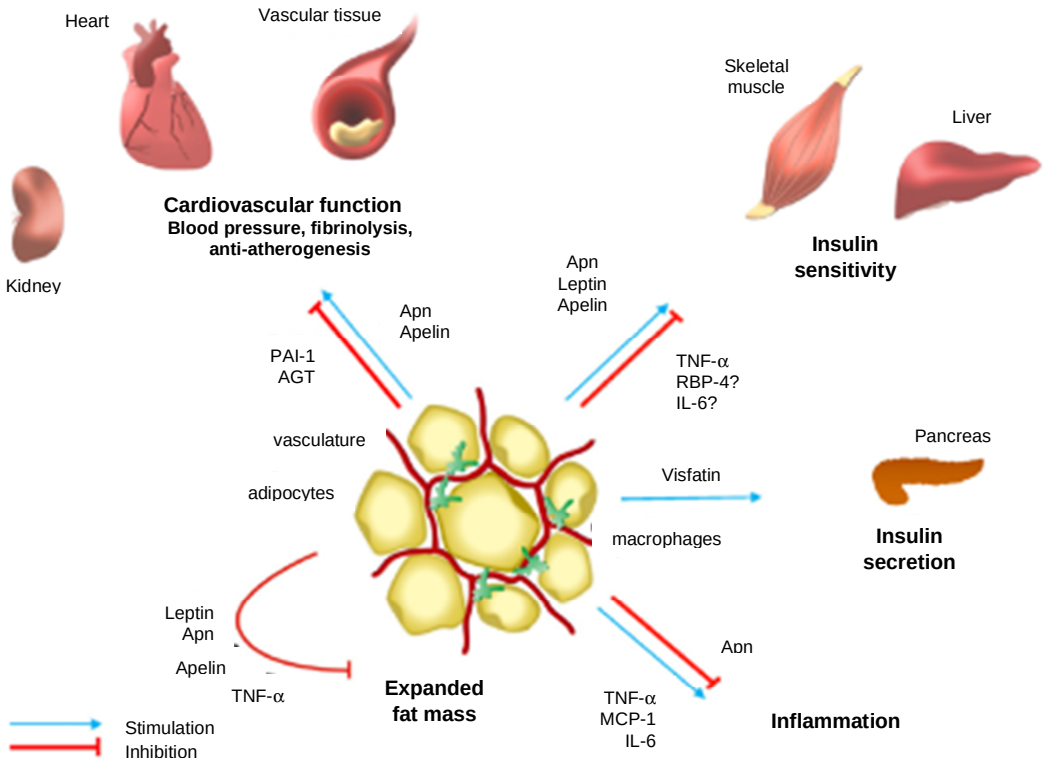

Adipocytokines modulate insulin sensitivity, cardiovascular function and inflammation. AGT, angiotensinogen; IL-6, interleukin-6; MCP-1, monocyte chemoattractant protein-1; PAI-1, plasminogen activator inhibitor type 1; RBP-4, retinol binding protein-4; TNF-α, tumour necrosis factor-α; adapted from (40)

1.3.1 Leptin

Leptin is an anorexigenic hormone secreted mainly from differentiated adipocytes (41). It regulates food intake and energy expenditure by acting at central nervous system (42), where it inhibits orexigenic neuropeptides and stimulates anorexigenic neurotransmitters (43-45) in hypothalamus. Leptin secretion and its circulating levels are positively correlated with total body fat mass (46). Thus, obesity is characterised by hyperleptinaemia. However, leptin transport across the blood-brain barrier and its postreceptor signalling are impaired in obesity (47;48), leading to desensitization of the leptin signalling, a phenomenon referred to as leptin resistance.

Besides acting at neural tissues, leptin has also direct pleiotrophic effects in peripheral tissues. It stimulates fatty acid oxidation by activating of the α2 subunit of AMPK (49). Once activated, AMPK phosphorylates the enzyme acetyl coenzyme A (CoA) carboxylase, resulting in its inhibition and decrease of malonyl-CoA levels, which subsequently activates carnitine palmitoyl-transferase 1 and mitochondrial fatty acid oxidation. By activating AMPK, leptin contributes to a decrease in tissue lipid content, for instance in muscle, liver and pancreatic cells, thus protecting these tissues from excessive fat accumulation, lipotoxicity, and tissue damage. Leptin is also involved in a modulation of lipogenic gene expression, by decreasing the expression of lipogenic transcription factor sterol regulatory element binding protein (SREBP)-1c (50). Furthermore, leptin stimulates glucose utilization (51) and activates in skeletal muscle thermogenesis in a phosphatidylinositol 3 kinase-dependent manner (52).

1.3.2 Adiponectin

Adiponectin is an abundant serum protein almost exclusively expressed in mature adipocytes (53;54). Its circulating levels are, in contrast to majority of adipocytokines, negatively correlated with body fat (46;55), and it is associated with insulin sensitivity in adult both mice and humans (56). Adiponectin is present in serum in the form of higher order oligomeric complexes. It exists in three distinct forms, i.e. low-molecular weight (LMW, trimer), medium-molecular weight (MMW, hexamer) and high-molecular

weight (HMW, 12-18-mer) adiponectin (57), with each of the form having different biological effectiveness (58). Multimerization of adiponectin molecules is enabled by the interaction between collagenous domains in the process of trimerization and further formation of disulfide bonds between trimers (57;59).

Adiponectin has potent insulin-sensitising effects. It enhances insulin-dependent suppression of hepatic glucose production (60) and thereby has a substantial lowering effect on glycaemia. Moreover, it increases glucose uptake and fatty acid oxidation in several tissues including liver and muscle via AMPK activation (61;62). Inactivation of adiponectin gene in mice results in reduced hepatic insulin sensitivity (63), while adiponectin overexpression is associated with protection from diet-induced insulin resistance (64). Increased adiponectin levels protect from hepatic lipid accumulation and contribute to the preservation of insulin sensitivity by promoting adipocyte differentiation (65). This mechanism augments the ability of adipose tissue to store excessive lipids and maintain its proper function (66). Furthermore, adiponectin has eventually anti-inflammatory properties mediated through the inhibition of tumour necrosis factor-α (TNF-α)-induced activation of pro-inflammatory nuclear factor-κB (NF-κB) signalling pathway (67).

1.3.3 Tumour necrosis factor-α

TNF-α is a pro-inflammatory cytokine, the expression of which in adipose tissue as well as its circulating levels are elevated in an obese state (38). Adipose tissue-derived TNF-α originates to a great extent from macrophages infiltrating fat tissue and not from adipocytes themselves, and increased levels of this cytokine in obese states are due to an elevated number of adipose tissue macrophages (68).

TNF-α represents a promising link between obesity, inflammation and impaired insulin signalling (38). TNF-α contributes to the development of insulin resistance by inhibiting the insulin-stimulated phosphorylation of insulin receptor (IR) and IRS-1 and thereby disrupting signalling from IR (69). Further, TNF-α is implicated in the pathogenesis of obesity by modulating the gene expression in adipocytes and liver (70),

including reduction in adiponectin mRNA (71) and activation of pro-inflammatory NF-κB signalling pathway (71) that has been shown to be involved in adipose tissue inflammation. As a proof of concept, TNF-α-deficient mice demonstrated better insulin sensitivity and glucose tolerance (72).

1.3.4 Interleukin-6

Interleukin-6 (IL-6) is an adipocytokine produced by several cell types within adipose tissue, including fibroblasts, monocytes and adipocytes. Its production is increased in obesity (73), while is implicated in the origin of hepatic insulin resistance mediated by increased expression of suppressor of cytokine signalling-3 that further impairs insulin signalling by inhibiting IRS phosphorylation (74;75). In contrast, IL-6 has divergent effects on skeletal muscle, where its concentration is increased in response to exercise, while skeletal muscle insulin sensitivity is enhanced (76). These data suggest tissue-specificity of IL-6 effect as well as differences in its chronic and acute action.

1.3.5 Monocyte chemoattractant protein-1

Monocyte chemoattractant protein-1 (MCP-1) is secreted by adipocytes and adipose tissue macrophages and its release is in proportion to progressive accumulation of fat and adipose tissue inflammation (77). It is a potent chemotactic factor responsible for recruiting monocytes/ macrophages into adipose tissue (78;79), which is the major cause of obesity-associated low-grade inflammatory state (80). Further, it possibly contributes to insulin resistance as well, since increased expression of MCP-1 in WAT preceded insulin resistance in obese mice (78). In agreement with this, MCP-1 was found to directly affect insulin signalling in liver and skeletal muscle. A decreased tyrosine phosphorylation of IR and IRS molecules in both tissues was demonstrated concomitantly with a decreased protein kinase B (known also as Akt kinase) phosphorylation (81), all of which being the principal sites in insulin signalling cascade. In addition, MCP-1 deficient mice fed high-fat (HF) diet exhibited lower infiltration of

fat by macrophages and attenuated insulin resistance and hepatic steatosis (79;82). In contrast, mice overexpressing MCP-1 showed reverse phenotype (79). These results strongly suggest that MCP-1 negatively affects insulin signalling.

1.3.6 Adipose tissue inflammation

Body weight gain is accompanied by a profound alteration of adipose tissue function. In a lean healthy state, adipose tissue is sensitive to lipogenic action of insulin, adipocytes display normal size and secretory function and the tissue is populated by M2 macrophages (alternatively activated), producing anti-inflammatory cytokines. However, with progressive overnutrition, obesity develops, which is characterised by adipocyte hypertrophy and/ or hyperplasia as well as by increased macrophage infiltration (Fig. 3). Increased fat storage results in adipocyte enlargement associated with a dysregulation of adipocytokine expression (39) and its shift toward dominance of pro-inflammatory adipocytokines, as well as higher propensity of enlarged adipocytes to necrotic cell death (83). Enhanced secretion of chemoattractants in obese state promotes migration of macrophages into adipose tissue (79;81) accompanied by the phenotypic switch of macrophages to a pro-inflammatory state (M1, classically activated macrophages) (84;85). Macrophages are preferentially recruited to the omental fat depot in comparison with subcutaneous fat (86), further confirming the importance of abdominal fat accumulation in the development of insulin resistance. Macrophages are predominantly situated around the dead or dying adipocytes, forming syncytia called crown-like structures (CLS), and scavenge residual lipids and cell debris (83). Higher release of pro-inflammatory cytokines into the circulation, like MCP-1, TNF-α and IL-6, may disrupt insulin signalling in other tissues (78;87;88). In agreement with this, obese and usually insulin resistant subjects are characterised by elevated circulating levels of inflammatory markers, such as IL-6 and TNF-α (89). Furthermore, large adipocytes are less insulin sensitive in comparison to smaller ones (90;91), and as adipocytes are not able to expand beyond a “critical size”, large adipocytes have limited storage capacity for excessive lipids. As mentioned above, this promotes ectopic lipid accumulation in

non-adipose tissues (92). To summarise, larger fat cells are associated with a chronic low-grade adipose tissue inflammation that represents a key factor linking obesity with insulin resistance (91;93;94).

Figure 3 The alterations in adipose tissue accompanying body weight gain

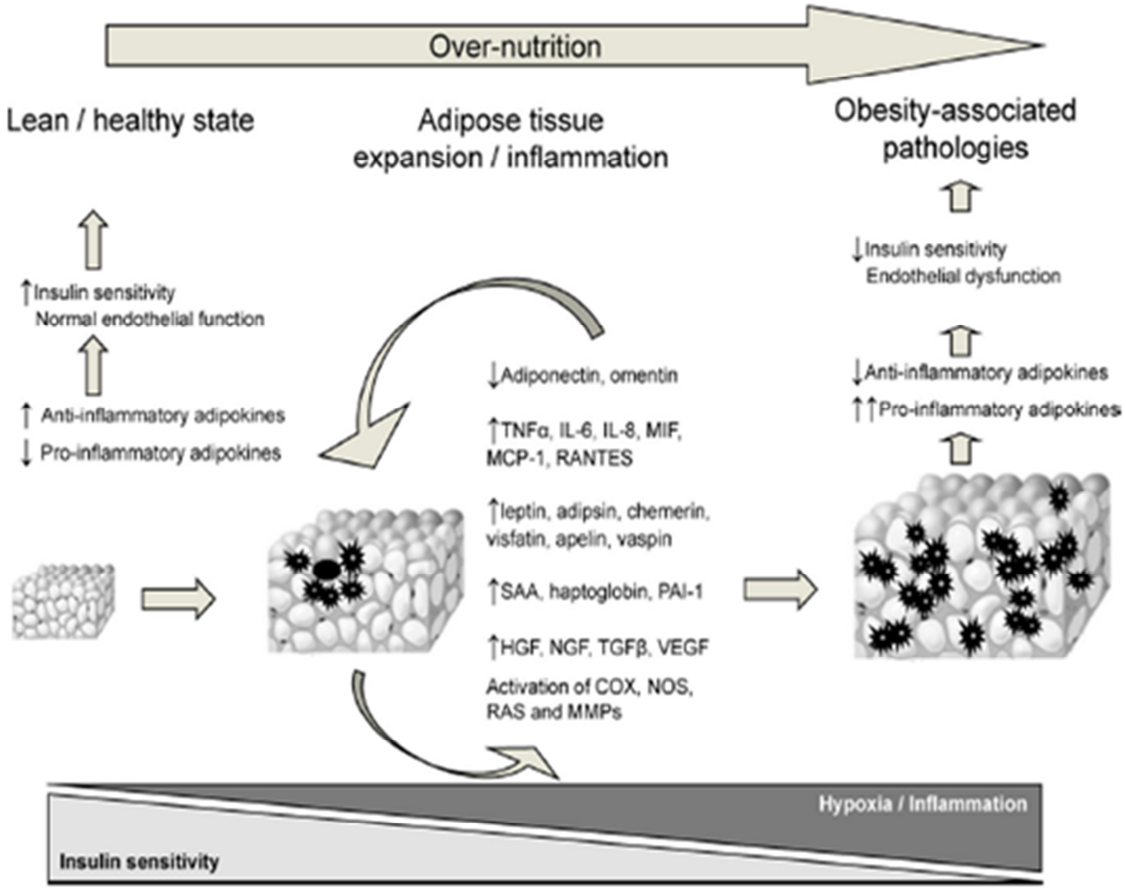

In the lean state, adipose tissue secretes anti-inflammatory adipocytokines and is insulin responsive. Increased energy intake is associated with adipocyte hypertrophy and death, resulting in chemotactic adipocytokine release, followed by macrophage infiltration into adipose tissue and aggravation of inflammatory state. These secretory changes are accompanied by insulin resistance of adipose tissue. IL, interleukin; COX, cyclooxygenase; HGF, hepatocyte growth factor; MCP-1, monocyte chemoattractant protein-1; MIF, macrophage migration inhibitory factor; MMP, matrix metalloproteinase; NGF, nerve growth factor; NOS, nitric oxide synthase; PAI-1, plasminogen activator inhibitor type 1; RANTES, regulated upon activation, normally T-cell expressed and secreted; RAS, rennin-angiotensin system; SAA, serum amyloid A cluster; TGFβ, transforming growth factor β; TNF-α, tumour necrosis factor-α; VEGF, vascular endothelial growth factor; (adapted from (95)).

1.4 Attenuation of obesity-associated pathogenesis by n-3 PUFA

1.4.1 Biological effects of n-3 LC-PUFA

Long chain polyunsaturated fatty acids (LC-PUFA) of n-3 and n-6 series are essential for many mammalian species including humans, as they cannot be synthesised *de novo*. Eicosapentaenoic acid (EPA) and docosahexaenoic acid (DHA) are the end-products of the n-3 fatty acid series formed from essential α-linolenic acid by several steps of elongation and desaturation. The rate of conversion is, especially for DHA, quite poor in humans, because the biosynthetic pathways of fatty acids belonging to both the n-3 and the n-6 series share the same Δ6-desaturase enzyme. Due to a high dietary intake of n-6 PUFA, the biosynthetic pathway is shifted towards the n-6 series. Thus, the dietary supplementation of n-3 LC-PUFA is highly recommended.

n-3 LC-PUFA are abundant in fish oils, especially of marine origin. They act as hypolipidemics, reduce the incidence of cardiac events and prevent progression of atherosclerosis (96). Since DHA is abundantly incorporated in the membrane phospholipids of brain and retina, it plays an important role in the development of these organs, learning abilities and visual acuity (97). Moreover, n-3 LC-PUFA have immunomodulatory effects, as they are capable of changing membrane lipid composition of immune cells resulting in altered immune response and possible amelioration of inflammatory response (98). In rodents, n-3 LC-PUFA have been shown to prevent obesity, impaired glucose tolerance, as well as adipose tissue inflammation (99;100).

1.4.2 Mechanism of action of n-3 LC-PUFA

Metabolic actions of n-3 LC-PUFA are largely mediated through the altered expression of genes involved in carbohydrate and lipid metabolism. n-3 LC-PUFA regulate gene expression in various tissues by acting as ligands to different transcription factors, i.e. peroxisome-proliferator activated receptors (PPARs), retinoid X receptors, liver X

receptors, hepatic nuclear factor-4 and SREBPs (101;102). Feeding n-3 LC-PUFA causes upregulation of genes responsible for fatty acid oxidation in skeletal muscle and liver, simultaneously with a downregulation of lipogenic genes in adipose tissue (103;104). This shift in metabolism results in preferential fat oxidation and reduction of fat storage.

Besides direct actions, n-3 LC-PUFA act through their active metabolites including resolvines, protectines, eicosanoids, and docosanoids. EPA and DHA give rise to lipid mediators with anti-inflammatory properties (105) through the action of lipoxygenase and cyclooxygenase enzymes (106). In addition, besides EPA and DHA conferring anti-inflammatory action, are also known for increasing adiponectin production, which can subsequently result in AMPK activation and facilitation of fatty acid oxidation (107).

1.5 Aspect of sex in control of insulin sensitivity

Human and animal studies proved that female subjects, although having higher total body fat mass, demonstrate milder phenotypes concerning obesity-related metabolic disorders and/ or showed later onset of metabolic impairment (108-111) in comparison to their male counterparts. Underlying mechanisms of this phenomenon remain largely unknown; however, they could be partially associated with differences in fat accumulation and adipose tissue inflammation.

It is well known, that males store the surplus of energy preferentially in the abdominal part of the body, while females accumulate excessive lipids more subcutaneously (112;113). Adipocytes in abdominal fat are more metabolically active and release more NEFA in states of obesity. As visceral fat is in a close proximity to portal vein, NEFA are transported to the liver and can cause its overload with lipids. This possibly contributes to hepatic insulin resistance and steatosis. Another important factor is a higher macrophage infiltration of omental fat, with a subsequent release of detrimental pro-inflammatory adipocytokines negatively affecting insulin sensitivity.

It has been shown that female mice fed a HF diet demonstrated lower adipose tissue inflammation compared to males (94). Furthermore, females present higher circulating adiponectin concentrations (59;114;115). As adiponectin exerts anti-inflammatory effects (116) and activates AMPK (61), higher adiponectin levels in females can contribute to lower infiltration of their adipose tissue by macrophages and/ or can promote macrophage polarization towards an anti-inflammatory phenotype (116) and decreased tendency to ectopic lipid accumulation.

However, since the protective effect is apparent only until the menopause, beneficial effects of oestrogens on metabolism cannot be ruled out. Some studies showed anti-inflammatory oestrogen action (117-119), but further research is needed to elucidate these mechanisms.

2 AIMS OF THE THESIS

The general aim of the thesis was to evaluate metabolic changes of an organism after challenge with HF-feeding with respect to development of specific components of the metabolic syndrome. Part of the work focused on the role of lipid composition in the diet, namely the beneficial effects of partial replacement of dietary lipids with n-3 LC-PUFA concentrate (specific aims 1 and 3). Furthermore, this thesis was aimed to contribute to the elucidation of the role of widely expressed enzyme AMPK in the protection from obesity and insulin resistance (specific aims 2 and 3). And finally, regarding significant differences in the incidence, prevalence and severity, by which males and females experience diseases associated with the metabolic syndrome, this thesis attempted to elucidate the disparity in the development of obesity in males and females by evaluating adipose tissue function at the onset of insulin resistance using a model of HF-feeding in mice.

The specific aims of this thesis were:

1. to characterise a role of lipid composition, namely with respect to n-3 LC-PUFA and their derivatives, in the induction of obesity and insulin resistance associated with the metabolic syndrome;

2. to examine the involvement of leptin-AMPK axis in lipid metabolism of skeletal muscle in response to HF-feeding, using a model of obesity-resistant (A/J) and obesity-prone (C57BL/6) strain of mice;

3. to investigate the role of AMPK in preservation of insulin sensitivity induced by n-3 LC-PUFA feeding using a model of AMPKα2 knock-out mouse model;

4. to investigate sex-dependent changes in adipocyte hypertrophy, low-grade inflammation and secretory function of adipose tissue with respect to the development of insulin resistance induced by HF-feeding in C57BL/6 mice.

3 RESULTS TO SELECTED PUBLICATIONS

3.1 Publication A: DHA-derivatives

Prevention and reversal of obesity and glucose intolerance in mice by DHA derivatives

The aim of this work was to determine the efficiency of four different chemical α-derivatives of DHA compared to pure, non-modified DHA in the prevention and reversal of obesity and associated metabolic disorders.

The *"Prevention study"* was performed on male mice of C57BL/6 strain. Three-month-old mice were randomly assigned either to high-fat diet (35 % wt/wt; cHF) or to cHF diet, where 1.5 % of total lipids was replaced with α-methyl DHA ethyl ester (Substance 1), α-ethyl DHA ethyl ester (Substance 2), α,α-di-methyl DHA ethyl ester (Substance 3) or α-thioethyl DHA ethyl ester (Substance 4). The experimental diets were administered for a period of four months. In the *"Reversal study"*, the effect of Substance 2 was evaluated in C57BL/6 mice with diet-induced obesity. After 4 months of cHF-feeding, mice were administered cHF diet supplemented with Substance 2 (1.5 % of total lipids) for 2 subsequent months. To evaluate the effect of a concentrate of DHA/EPA and a pure DHA, the separate experiment was performed in the same experimental setup as the *"Reversal study"*.

All DHA-derivatives, only with the exception of Substance 3, reduced body weight gain, while Substance 2 had the most pronounced effect in the *"Prevention study"*. It reduced weight of subcutaneous (scWAT) and gonadal (gWAT) fat by 73 % and 42 % respectively, and the effect on reduction of food intake was demonstrated as well. Since Substance 2 was proven as the most effective derivative in the suppression of obesity and its detrimental metabolic consequences, it was also tested in the *"Reversal study"* using obese mice with impaired glucose tolerance.

In both types of experiments, Substance 2 prevented or normalised adipocyte hypertrophy and macrophage infiltration to WAT and formation of CLS, representing

the degree of inflammatory state of adipose tissue (see publication). The immunohistochemical analysis was confirmed by real-time PCR (RT-PCR), showing that Substance 2 reduced the expression of macrophage markers CD68 antigen and MCP-1 in WAT by 91 % and 56 % respectively in *"Prevention study"* and by 32 % and 50 % respectively in *"Reversal study"* (see Table 1).

In liver, genes implicated in fatty acid oxidation were influenced by the treatment. Acyl-CoA oxidase-1 (*Aox-1*) and carnitine palmitoyltransferase-1α (*Cpt-1α*) were strongly upregulated by Substance 2, in agreement with a marked increase in mRNA expression of their regulatory transcription factor *Pparα*. Pure DHA and DHA in combination with EPA also increased transcription of *Cpt-1α,* but not *Aox-1*, however, the observed changes were much smaller than changes caused by the ingestion of Substance 2 (Table 1). The differences are striking, especially when we take into account a 10-fold lower concentration of Substance 2 in comparison with n-3 LC-PUFA (EPA/DHA) concentrate. Lipogenic genes, such as stearoyl-CoA desaturase (*Scd-1*), thyroid hormone responsive SPOT 14 (*Spot 14)*, farnesyl diphosphate synthase (*Fdps*), are known to be downregulated by n-3 LC-PUFA. In accordance, DHA and EPA/DHA decreased the expression of *Scd-1*and *Spot 14*, however, Substance 2 increased mRNA expression of *Scd-1*and *Fdps* (Table 1). Effect of Substance 2 on skeletal muscle was insignificant (Table 1).

To conclude, from the four tested DHA derivatives, Substance 2 appeared as most effective in obesity prevention as well as in the treatment of dyslipidaemia and insulin resistance associated with dietary obesity. It showed similar range of beneficial effects as naturally occurring n-3 LC-PUFA, but exerted much higher efficiency. Substance 2 also prevented macrophage accumulation in adipose tissue, which can have beneficial systemic effects on inflammatory state associated with obesity and consequently on insulin resistance. Furthermore, Substance 2 reduced ectopic lipid accumulation via enhanced lipid catabolism and possibly futile substrate cycling, as indicated by simultaneous activation of lipogenic genes (*Scd-1*, *Fdps*) and genes responsible for lipid oxidation (*Cpt-1α, Aox-1*) in the liver. Therefore, Substance 2 could be qualified as a novel drug for obesity treatment.

My main contribution to this work was the RNA isolation, control of quality of isolated RNA, reverse transcription and quantification of gene expression using RT-PCR.

Table 1 The effect of Substance-2 on mRNA levels of selected genes

	Prevention study			*Reversal study*				
	STD	cHF	Substance-2	STD	cHF	Substance-2	EPA/DHA	DHA
Adipose tissue								
Cd68	7 ± 1*	100 ± 24	9 ± 3*	17 ± 2*	100 ± 16	68 ± 16	NM	NM
Mcp-1	20 ± 3*	100 ± 15	44 ± 19*	33 ± 3*	100 ± 13	50 ± 14 *	NM	NM
Pgc-1α	109 ± 3*	100 ± 2	100 ± 2	99 ± 8	100 ± 3	101 ± 4	NM	NM
Glut-4	647 ± 61*	100 ± 24	193 ± 45	229 ± 72*	100 ± 16	68 ± 16	NM	NM
Liver								
Cpt-1α	52 ± 6*	100 ± 7	140 ± 13*	14 ± 2*	100 ± 24	563 ± 2 03*	196 ± 54*	145 ± 49
Aox-1	68 ± 10	100 ± 8	308 ± 23*	12 ± 5*	100 ± 27	1477 ± 500*	88 ± 35	114 ± 33
Pparα	73 ± 8*	100 ± 8	135 ± 10*	6 ± 2*	100 ± 19	296 ± 10 0*	113 ± 31	78 ± 15
Scd-1	243 ± 39*	100 ± 7	410 ± 34*	293 ± 71*	100 ± 15	100 4 ± 98*	44 ± 19	23 ± 11*
Spot 14	155 ± 49	100 ± 17	65 ± 17	132 ± 22	100 ± 14	149 ± 31	49 ± 18	43 ± 10*
Fdps	211 ± 24*	100 ± 13	260 ± 28*	174 ± 43	100 ± 13	452 ± 46*	84 ± 21	81 ± 23
Skeletal muscle								
Glut4	139 ± 6*	100 ± 15	109 ± 13	83 ± 9	100 ± 6	79 ± 5	N M	NM
Pdk-4	31 ± 6*	100 ± 13	96 ± 12	23 ± 10*	100 ± 14	89 ± 10	NM	NM
Scd-1	319 ± 151	100 ± 25	49 ± 6*	79 ± 12	100 ± 8	87 ± 5	NM	NM

The data represent the mean ± S.E. (*n* = 7-9 except for STD-fed mice in the „*Reversal study*"; *n* = 4). **P* < 0.05 vs. cHF (ANOVA).
Gene expression data were expressed as a percentage of the cHF-fed controls.
Aox-1, acyl-CoA oxidase-1; *Cd68*, CD68 antigen; *Cpt-1α,* carnitine palmitoyltransferase-1α; *Fdps*, farnesyl diphosphate synthase; *Glut-4*, glucose transporter-4; *Mcp-1*, monocyte chemoattractant protein-1; *Pdk-4*, pyruvate dehydrogenase kinase-4; *Pgc-1α,* peroxisome proliferator-activated receptor-γ coactivator-1α; *Pparα,* peroxisome proliferator-activated receptor-α; *Scd-1*, stearoyl-coenzyme A desaturase-1; *Spot 14*, thyroid hormone responsive SPOT 14; NM, not measured. (See Supplementary Table S4 of the respective publication).

3.2 Publication B: HF-feeding and muscle thermogenesis

Induction of muscle thermogenesis by high fat diet in mice: association with obesity-resistance

The main goal of this study was to elucidate, whether HF diet could stimulate muscle non-shivering thermogenesis and determine possible involvement of leptin-AMPK axis in this process.

The experiments were performed on male mice of obesity prone (C57BL/6) and obesity resistant (A/J) strain, born and maintained at nearly thermoneutral temperature of 30°C, to eliminate the possible confounding effect of shivering thermogenesis and adaptation to cold. At the age of four weeks, mice were randomly assigned to low fat (LF) or HF diet and maintained on these diets for two more weeks until sacrifice.

After 2 weeks on diets, no differences either in body weight, body weight gain or food consumption were observed. However, HF diet increased the weight of fat depots with a more pronounced effect in A/J mice, which was accompanied by a higher induction of plasma leptin levels in these mice (for the results, see publication). Different propensity to dietary-induced obesity was apparent only after longer exposure to HF diet and did not depend on stronger induction of energy expenditure of A/J mice in response to cold. A/J and C57BL/6 mice strains differed in their thermogenic capacity. After cold exposure (4°C), A/J LF mice became hypothermic, while the activation of shivering was similar as in C57BL/6 LF mice. HF diet reversed this phenotype and A/J HF mice were able to maintain their body temperature in cold. Measurement of norepinephrine-stimulated metabolic rate revealed stronger inducibility of UCP1-mediated thermogenesis by HF-diet in A/J compared to C57BL/6 mice (for data see publication). Protein content of UCP1 in interscapular BAT demonstrated induction by HF diet, while the increase was significantly higher in A/J when compared to C57BL/6 mice (Table 2). Furthermore, protein levels of UCP1 and its mRNA expression were measured in subcutaneous fat depot and skeletal muscles, respectively (Table 2); however, UCP1 levels were too low to be physiologically important for thermogenesis.

Table 2 Quantification of UCP1 and UCP2 expression in fat depots

Fat depot	C57BL/6		A/J	
	LF	HF	LF	HF
BAT				
UCP1-protein	9.6 ± 0.7	32.0 ± 4.1*	6.0 ± 0.8†	63.8 ± 10.5*†
UCP2-transcript	1.26 ± 0.30	0.81 ± 0.27	0.61 ± 0.17	0.69 ± 0.39
DL				
UCP1-protein	0.016 ± 0.005	0.043 ± 0.007*	0.043 ± 0.013†	0.065 ± 0.011
UCP2-transcript	0.62 ± 0.10	1.08 ± 0.36	0.95 ± 0.20	1.53 ± 0.16
EPI				
UCP2-transcript	1.23 ± 0.22	1.00 ± 0.10	2.17 ± 0.69	1.59 ± 0.34

Mice adapted to 30 ^{o}C and fed either LF of HF diet for 2 weeks after weaning were studied. UCP1 protein (mg/g membrane protein) was quantified using Western blots in 100,000 x g membranes isolated from adipose tissue homogenates. UCP2 transcript levels (AU) were measured using qRT-PCR in total RNA isolated from fat depots. BAT, interscapular brown fat; DL, dorsolumbar white fat; EPI, epididymal white fat. Data are means ± S.E. (n = 4-8). *Significant effect of diet; †significant effect of genotype. (See Table S2 in online Appendix of the respective publication).

To assess skeletal muscle metabolism and its possible involvement in non-shivering thermogenesis, gene expression in glycolytic *gastrocnemius* and oxidative *soleus* muscles were determined (Table 3). HF diet upregulated the expression of pyruvate dehydrogenase kinase 4 (*Pdk-4*) that is associated with suppression of glucose oxidation. Moreover, HF diet downregulated the expression of *Scd-1* in all studied subgroups with the most potent suppression in *soleus* muscle of A/J HF mice. This is in agreement with higher plasma leptin concentrations in this muscle, since *Scd-1* is suppressed by leptin. In addition, aminoimidazole carboxamid ribonucleotide-stimulated fatty acid oxidation was elevated in *soleus* of A/J HF mice, reflecting higher activation of AMPK (see publication).

These results indicated increased fatty acid oxidation and enhanced thermogenesis in oxidative skeletal muscle in response to HF diet in A/J mice, with a likely involvement of leptin-AMPK axis. Together with increased UCP1-mediated thermogenesis in BAT, both mechanisms could lead to obesity resistance in A/J mice fed HF diet.

My main contribution to this work was RNA isolation, reverse transcription and quantification of gene expression using RT-PCR. Further, I performed quantification of UCP1 protein in BAT and WAT by western blot analysis.

Table 3 Gene expression in glycolytic and oxidative skeletal muscles

Muscle	C57BL/6		A/J	
	LF	HF	LF	HF
Gastrocnemius				
Acot1	0.94 ± 0.13	0.86 ± 0.06	1.00 ± 0.21	0.97 ± 0.04
Acot2	1.55 ± 0.31	3.28 ± 0.33*†	0.88 ± 0.18	1.73 ± 0.16
Acsl1	1.11 ± 0.22	1.36 ± 21	1.15 ± 0.28	1.33 ± 0.13
Cox6a	0.67 ± 0.06	0.68 ± 0.07	0.59 ± 0.15	0.49 ± 0.08
Cpt-1α	2.08 ± 0.27	2.59 ± 0.33	1.77 ±0.33	1.22 ± 0.21†
Cpt-1β	0.35 ± 0.04	0.50 ± 0.05	0.50 ± 0.03	0.63 ± 0.07
Nrf-1	1.82 ± 0.21	1.84 ± 0.34	1.92 ± 0.45	1.72 ± 0.23
Pdk-4	0.62 ± 0.09	1.11 ± 0.48*	1.11 ± 0.48†	0.93 ± 0.24
Pgc-1α	0.71 ± 0.01	1.04 ± 0.27	1.71 ± 0.69†	1.12 ± 0.80
Pparα	0.43 ± 0.15	0.33 ± 0.10	0.50 ± 0.24	0.46 ± 0.23
Scd-1	1.31 ±0.35	0.48 ± 0.05*	1.79 ± 0.47	0.82 ± 0.20*
Sod1	1.07 ± 0.13	1.16 ± 0.13	1.23 ± 0.28	0.81 ± 0.14
Ucp1	0.30 ± 0.01	0.44 ± 0.03	0.91 ± 0.04†	1.10 ± 0.06†
Ucp3	2.09 ± 0.44	3.55 ± 0.69	2.73 ± 0.52	1.97 ± 0.45
Soleus				
Acot1	1.31 ± 0.11	1.90 ± 0.22*	1.25 ± 0.14	1.84 ± 0.10*
Acot2	1.62 ± 0.36	4.32 ± 0.13*	1.96 ± 0.34	3.58 ± 0.60*
Acsl1	2.94 ± 0.28	4.14 ± 0.41*†	3.17 ± 0.30	2.83 ± 0.24
Aox1	1.42 ± 0.12	1.64 ± 0.12	1.77 ± 0.30	1.56 ± 0.13
Cox6a	0.72 ± 0.05	0.64 ± 0.03	0.58 ± 0.04†	0.56 ± 0.03
Cpt-1α	1.06 ± 0.11	1.29 ± 0.09	2.54 ± 0.12†	2.25 ± 0.12†
Cpt-1β	0.79 ± 0.04	0.79 ± 0.04	0.76 ± 0.05	0.86 ± 0.05
Nrf-1	0.63 ± 0.15	0.69 ± 0.07	0.61 ± 0.09	0.83 ± 0.36
Pdk-4	1.27 ± 0.10	2.26 ± 0.15*	2.40 ± 0.60†	2.33 ± 0.23
Pgc-1α	2.52 ± 0.64	2.14 ± 0.24	1.68 ± 0.59†	1.38 ± 0.24†
Pparα	1.32 ± 0.12	1.07 ± 0.12	0.77 ± 0.09†	0.83 ± 0.14
Scd-1	1.00 ± 0.12	0.44 ± 0.07*	2.22 ± 0.37†	0.56 ± 0.06*
Serca1	1.21 ± 0.11	0.98 ± 0.02*	1.09 ± 0.19	0.71 ± 0.06*†
Serca2‡	1.18 ± 0.07	1.13 ± 0.06	1.65 ± 0.11†	1.25 ± 0.12*
Sod1	0.85 ± 0.03	0.82 ± 0.04	0.88 ± 0.08	0.78 ± 0.03
Ucp1	0.36 ± 0.04	0.43 ± 0.02	0.37 ± 0.02	0.44 ± 0.01
Ucp3	1.57 ±0.23	2.34 ± 0.18*	1.68 ± 0.11	1.90 ± 0.33

Transcript levels (AU) were measured using qRT-PCR in total RNA isolated from skeletal muscles of mice adapted to 30 ^{o}C and fed either LF or HF diet. Data are means ± S.E. (n = 6-7). *Significant effect of diet; †significant effect of genotype; ‡both *Serca2a* and *Serca2b* mRNA were quantified; *Acot1*, cytosolic acyl-CoA thioesterase; *Acot2*, mitochondrial acyl-CoA thioesterase; *Acsl1*, long-chain acyl-CoA synthetase; *Aox1*, acyl-CoA oxidase 1; *Cox6a*, subunit VIa of mitochondrial cytochrome oxidase; *Cpt-1*, carnitine palmitoyltranferase-1; *Nrf-1*, nuclear respiratory factor 1; *Pdk-4*, pyruvate dehydrogenase kinase-4; *Pgc-1α,* peroxisome proliferator-activated receptor-γ coactivator-1α; *Pparα,* peroxisome proliferator-activated receptor-α; *Scd-1*, stearoyl-CoA desaturase-1; *Serca*, sarcoplasmic reticulum Ca^{2+} ATPase; *Sod1*, superoxide dismutase 1; *Ucp,* uncoupling protein. (See Table 3 in the respective publication).

3.3 Publication C: n-3 PUFA, AMPK and insulin sensitivity

AMP-activated protein kinase α2 subunit is required for the preservation of hepatic insulin sensitivity by n-3 polyunsaturated fatty acids

Our objective was to test the hypothesis, whether AMPK is implicated in the beneficial effects of n-3 PUFA in the prevention of obesity, dyslipidaemia and insulin resistance.

Four-month-old whole-body AMPKα2 knock-out (AMPKα2$^{-/-}$) mice on C57BL/6J background and their wild-type littermate controls were used in this study. Mice were fed either a low-fat chow diet (chow), high-fat diet (cHF), or cHF diet, in which 15 % of total lipids were replaced with n-3 LC-PUFA concentrate (cHF+F) for 9 weeks.

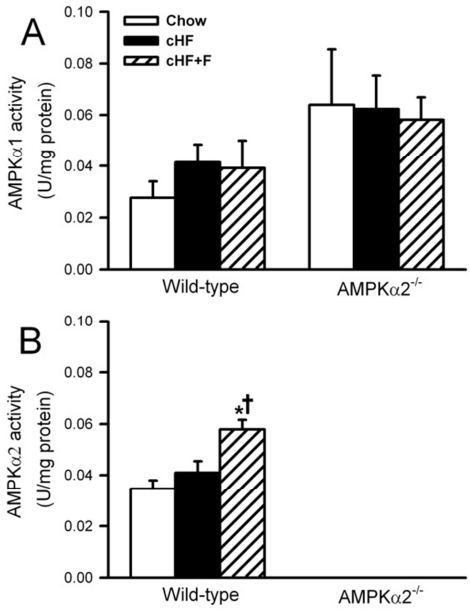

Figure 4 Liver AMPKα1 (A) and AMPKα2 (B) activity in wild type and AMPKα2$^{-/-}$ mice. The data are the means ± SE (n=5-8). In the AMPKα2$^{-/-}$ mice, AMPKα2 activity was below the detection limit. *P < 0.05 vs. genotype Chow; † P < 0.05 vs. genotype cHF. (See Figure 1 in the respective publication).

When specific activities of hepatic AMPKα1 and AMPKα2 subunits were evaluated, an increase in the activity of AMPKα2 subunit in response to n-3 LC-PUFA supplementation was observed. AMPKα1 activity did not show any significant compensatory changes in AMPKα2$^{-/-}$ mice, however, its activity tended to be increased (Fig. 4).

Administration of cHF diet resulted in higher body weight gain in wild-type and AMPKα2$^{-/-}$ mice when compared to chow-fed animals. However, the effect was less pronounced in AMPKα2$^{-/-}$. cHF+F diet induced smaller body weight gain regardless of the genotype. Similarly, cHF+F diet decreased plasma lipids independently of AMPKα2 subunit (for the data see publication). However, n-3 LC-PUFA-containing diet prevented high plasma insulin levels

associated with cHF diet feeding only in wild-type animals. Assessment of insulin sensitivity by hyperinsulinemic-euglycaemic clamp revealed protective effects of n-3 LC-PUFA from detrimental effects of cHF feeding only in wild-type mice, while no beneficial effects were observed in AMPK$\alpha 2^{-/-}$ mice. In line with these observations, plasma levels of insulin-sensitising hormone adiponectin, were increased (both total adiponectin as well as its biologically active HMW form) only in wild-type animals in response to n-3 LC-PUFA (Fig. 5).

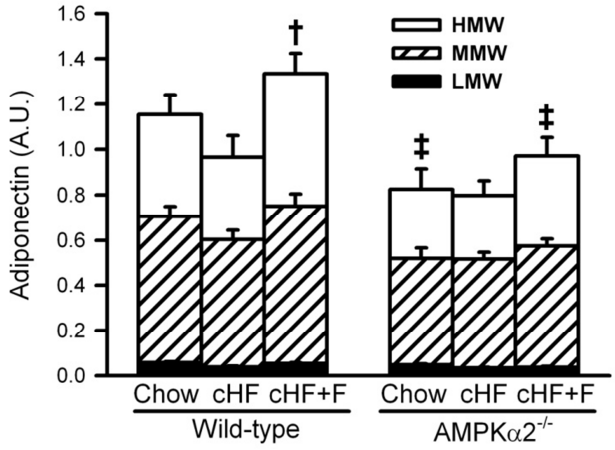

Figure 5 Adiponectin levels in plasma of wild-type and AMPK$\alpha 2^{-/-}$ mice fed either a Chow diet or corn oil-based high-fat diets without (cHF) or with 15% of the lipids in the form of n-3 LC-PUFA concentrate (cHF+F) for 9 weeks, and killed in *ad libitum* fed state. The total adiponectin levels and the distribution of adiponectin multimeric complexes were determined using Western blotting. The data are the means ± SE (n = 13-15). **P* < 0.05 vs. genotype Chow; †*P* < 0.05 vs. genotype cHF; ‡*P* < 0.05 vs. wild-type on respective diet. Significance evaluated for the total adiponectin levels. A.U., arbitrary units; LMW – low molecular weight; MMW – medium molecular weight; HMW – high molecular weight. (See Supplementary Figure 2 of the respective publication).

Liver TAG under the clamp conditions were decreased by n-3 LC-PUFA in AMPKα2-dependent manner. Moreover, experiments on isolated hepatocytes confirmed AMPK-dependent induction of fatty acid oxidation by n-3 LC-PUFA in the liver (see publication). The composition of hepatic lipids is very important for insulin sensitivity. While hepatic ceramides and phospholipids were not affected, the content of polyunsaturated DAG was modified by both diet and genotype. Dietary supplementation by n-3 LC-PUFA prevented accumulation of total DAG in wild-type mice compared to mice without functional AMPKα2 subunit (for details see publication).

To summarise, our results suggest that regulatory α2 subunit of AMPK is not necessary for anti-obesity and hypolipidemic effects of n-3 LC-PUFA, however, it is required for the preservation of insulin sensitivity, especially in the liver. Nevertheless, the activation of AMPKα2 by n-3 LC-PUFA is likely independent of their on direct interaction since it is most probably mediated by n-3 LC-PUFA-dependent increase in adiponectin plasma concentration and subsequent AMPK activation in target tissues.

My main contribution to this work was the measurement of enzymatic activity of AMPK and the assessment of adiponectin multimeric complexes in plasma of experimental animals.

3.4 Publication D: Sex-based differences of adipose tissue function

Sex differences during the course of diet-induced obesity in mice: adipose tissue expandability and glycaemic control

Our objective was to evaluate sex-based differences in adipose tissue plasticity with respect to adipose tissue inflammation and propensity to deterioration of insulin signalling between male and female mice.

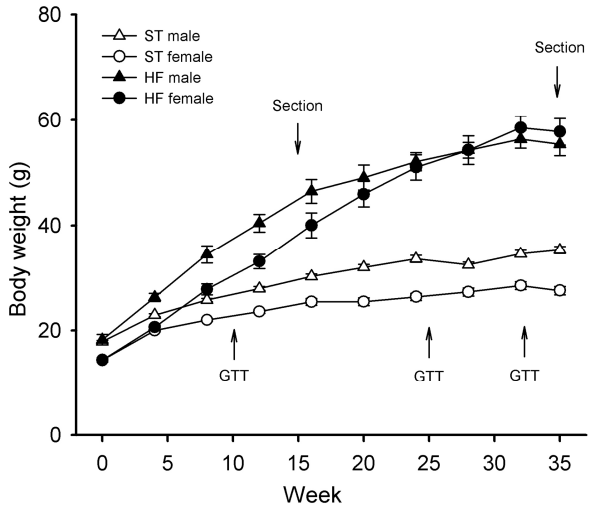

Figure 6 Growth curves. Mice of both sexes were weaned to either ST or HF diet at four weeks of age (week 0). Some mice (*n=10* from each sex) were killed at week 15, while the remaining mice were killed at week 35. Data are means ± SE (*n=20* between week 0-15; and *n=10* between week 16-35). Intraperitoneal glucose tolerance test (GTT) was performed at week 10, 25 and 33, respectively. (See Figure 1 of the respective publication).

This study was performed on male and female mice of C57BL/6N strain. Mice were randomly assigned to a control (3.4 % wt/wt of fat; ST) or high fat (35 % wt/wt of fat; HF) diet at the time of weaning (four weeks of age) and remained on their respective diets for 15 or 35 weeks. These time points were chosen to compare different states of body weight development after long-term HF diet administration (lower body weight in female compared to male mice at week 15; equalised body weight in female and male mice at week 35). Mice on HF diet became significantly heavier than their ST diet-fed controls and males weighed more than females until week 20. From the week 20 onwards, body weights of males and females equalised, which suggests higher propensity to fat accumulation in response to HF-feeding in female mice (Fig. 6).

In control mice, no significant differences either in weight of gonadal (gWAT) or subcutaneous (scWAT) adipose tissue were observed between the sexes, although males

tended to accumulate more fat. In mice fed HF-diet, the situation was opposite, i.e. females tended to have greater gWAT and scWAT depots than males at week 15. The differences were more pronounced at week 35, when females exhibited significantly larger scWAT and even ~3.8-fold larger gWAT compared to males (Table 4). Higher adiposity in females at week 35 were also reflected in higher plasma leptin levels in these animals (Table 5).

Table 4 Growth characteristics, adiposity, liver weight and TAG content

	ST		*HF*	
	Male	*Female*	*Male*	*Female*
BW (g)				
Week 0	17.8 ± 0.2	14.3 ± 0.3*	18.2 ± 1.0	14.3 ± 0.3*
Week 15	28.5 ± 0.4	24.1 ± 0.4*	43.6 ± 1.9$^{\#}$	36.4 ± 1.7$^{\#}$*
Week 35	35.3 ± 0.7	27.6 ± 0.8*	55.4 ± 2.2$^{\#}$	57.7 ± 2.6$^{\#}$
BWG (g)				
Week 15	11.6 ± 0.6	10.6 ± 0.5	27.2 ± 1.4$^{\#}$	23.1 ± 2.3$^{\#}$*
Week 35	17.5 ± 0.6	13.2 ± 0.6	37.2 ± 1.8$^{\#}$	43.4 ± 2.4$^{\#}$
FC (kJ/g/day)				
Week 4-14	2.39 ± 0.01	2.53 ± 0.04	1.88 ± 0.03	2.64 ± 0.10*
Week 17-30	1.99 ± 0.01	2.32 ± 0.03*	1.38 ± 0.09	1.42 ± 0.02
gWAT (mg)				
Week 15	484 ± 31	364 ± 26	1881 ± 158$^{\#}$	2147 ± 301$^{\#}$
Week 35	1032 ± 107	711 ± 97	1565 ± 95	5989 ± 470$^{\#}$*
scWAT (mg)				
Week 15	217 ± 14	195 ± 11	797 ± 95$^{\#}$	873 ± 117$^{\#}$
Week 35	312 ± 35	271 ± 24	1297 ± 113$^{\#}$	1590 ± 133$^{\#}$*
Liver (mg)				
Week 15	1247 ± 55	1144 ± 29	1606 ± 130$^{\#}$	1236 ± 56*
Week 35	1544 ± 51	1160 ± 56*	2541 ± 231$^{\#}$	1806 ± 111$^{\#}$*
Liver TAG (mg/g of tissue)				
Week 15	28 ± 1	32 ± 3	109 ± 20$^{\#}$	72 ± 6$^{\#}$*
Week 35	34 ± 3	38 ± 3	197 ± 27$^{\#}$	121 ± 8$^{\#}$*

Male and female mice weaned at four weeks of age (week 0) onto ST or HF diet were analysed after 15 weeks or 35 weeks (n=10) feeding of their respective diets. BW, body weight; BWG, body weight gain since week 0; FC, mean food consumption; gWAT, gonadal white adipose tissue; scWAT, subcutaneous white adipose tissue; TAG, triglycerides. Data are means ± SE. $P < 0.05$, *significant differences between sexes within diet, $^{\#}$significant differences between diets within sex (ANOVA). (See Table 1 of the respective publication).

HF-feeding induced accumulation of TAG in the livers of both sexes with a more pronounced effect in male mice that also resulted in higher liver weight (Table 4). Higher TAG accumulation in the liver together with smaller gWAT and scWAT suggested decreased capacity for adipose tissue enlargement and thereby higher ectopic lipid deposition in male mice as compared to their female counterparts. Since ectopic lipid

accumulation is known to be associated with insulin resistance, blood glucose levels in response to meal ingestion were elevated after a period of fasting at week 15.

Table 5 Plasma hormones

	ST		*HF*	
	Male	*Female*	*Male*	*Female*
Insulin (ng/ml)				
Week 15	0.88 ± 0.21	0.38 ± 0.04*	2.71 ± 0.54$^{\#}$	1.15 ± 0.23$^{\#}$*
Week 35	0.97 ± 0.16	0.21 ± 0.03*	4.68 ± 0.45$^{\#}$	2.30 ± 0.46$^{\#}$*
Leptin (ng/ml)				
Week 15	6.2 ± 0.7	8.8 ± 0.8	45.5 ± 7.6$^{\#}$	41.7 ± 8.0$^{\#}$
Week 35	17.7 ± 2.0	9.1 ± 1.7*	71.9 ± 4.7$^{\#}$	89.6 ± 2.8$^{\#}$*
Adiponectin (A.U.)				
Week 15				
HMW	0.45 ± 0.03	0.62 ± 0.05*	0.33 ± 0.02$^{\#}$	0.63 ± 0.03*
MMW	0.46 ± 0.02	0.65 ± 0.04*	0.44 ± 0.02	0.60 ± 0.03*
LMW	0.02 ± 0.00	0.02 ± 0.00	0.01 ± 0.00	0.02 ± 0.00*
Total	0.94 ± 0.05	1.29 ± 0.08*	0.78 ± 0.03$^{\#}$	1.25 ± 0.05*
Week 35				
HMW	0.46 ± 0.04	0.86 ± 0.10*	0.40 ± 0.06	0.63 ± 0.07$^{\#}$*
MMW	0.55 ± 0.03	0.80 ± 0.06*	0.50 ± 0.02	0.78 ± 0.07*
LMW	0.04 ± 0.01	0.03 ± 0.00	0.02 ± 0.00$^{\#}$	0.03 ± 0.00
Total	1.06 ± 0.06	1.69 ± 0.15*	0.92 ± 0.07	1.44 ± 0.13*

Male and female mice weaned at four weeks of age onto ST or HF diet were analysed after 15 weeks or 35 weeks (*n*=10) feeding of their respective diets. A.U., arbitrary units; HMW, high molecular weight; MMW, medium molecular weight; LMW, low molecular weight. Data are means ± SE. *significant differences between sexes within diet; $^{\#}$significant differences between diets within sexes (ANOVA). (See Table 2 of the respective publication).

Mice of both sexes fed ST diet together with female mice fed HF diet showed the ability to decrease plasma glucose levels in response to fasting. The opposite was observed in male mice fed HF diet, which demonstrated the inability to decrease blood glucose, indicating metabolic inflexibility in these animals (Fig. 7a). Furthermore, glucose homeostasis was evaluated by three subsequent intraperitoneal glucose tolerance tests (IP GTT) at weeks 10, 25 and 33. Fasting blood glucose levels already suggested better glucose tolerance in female mice fed ST diet in comparison with males at all three time points analysed. HF-feeding exacerbated glucose intolerance associated with aging in both sexes, however, male mice were affected earlier (already at week 10) in contrast to females, and exhibited much earlier deterioration of glucose tolerance (Fig. 7b,c). To further characterise glucose homeostasis, at week 33 plasma insulin levels were determined at the baseline and 30 minutes after glucose load during IP GTT, when the highest response of insulin is expected. Mice of both sexes on ST diet showed similar

insulin levels at both time points. Animals fed HF diet differed from ST-fed animals already at the baseline, when they exhibited significantly higher fasted insulin levels. Insulin increased further in response to glucose load with a more pronounced increase in male mice (Fig. 7d). Moreover, female mice exhibited substantially decreased insulin levels also in *ad libitum* fed state (Table 5) at week 15 and week 35. These results suggest that females need lower insulin levels to maintain the same glucose tolerance as males.

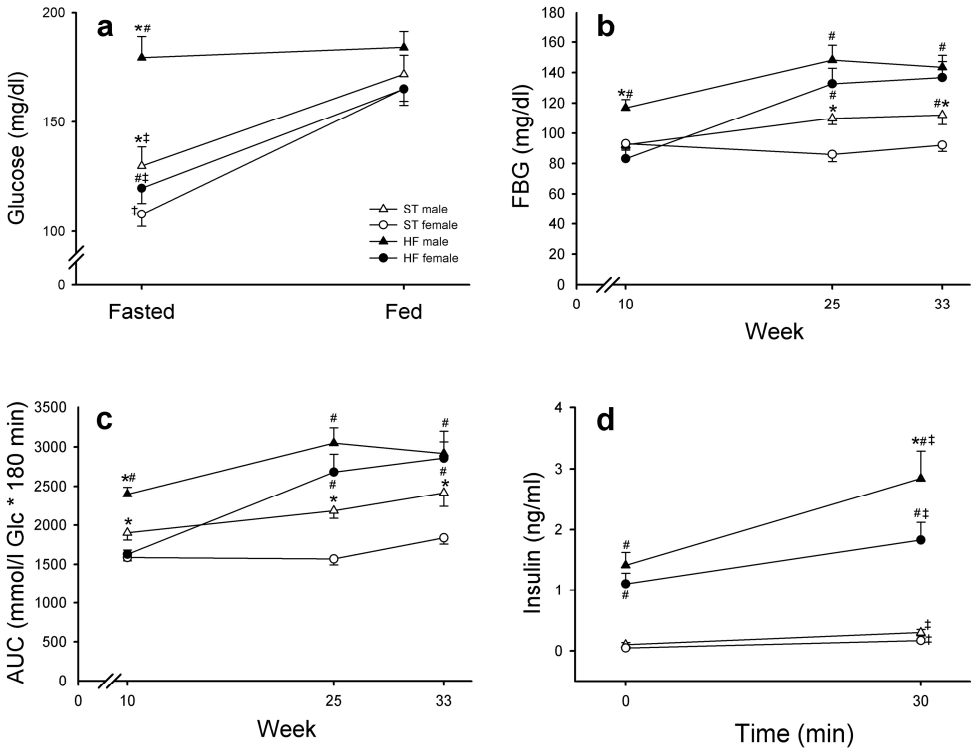

Figure 7 Glucose homeostasis. (a) Plasma glucose levels in fasted and fed mice at week 15 (see text for details). **(b-d)** Intraperitoneal glucose tolerance (GTT) test was performed at week 10, 25 and 33, respectively, after weaning to either ST or HF diet (see also Supp. Fig. 1). **(b)** Fasting blood glucose (FBG) at time 0 of the GTT performed at week 10, 25 and 33, respectively. **(c)** Area under the glycaemic curve (AUC) of the tests performed at week 10, 25 and 33, respectively. **(d)** Plasma insulin levels at time 0 and 30 min of the test performed at week 33. Data are means ± SE (*n=10*; at week 10, only part of mice was randomly selected for the testing). *significant difference between sexes within diet, #significant difference between diets within sexes (ANOVA), ‡significant difference before and after respective treatment (RM ANOVA). (See Figure 3 of the respective publication).

Moreover, this could delay the exhaustion of pancreatic β-cells and the onset of type 2 diabetes. Since adiponectin possess substantial insulin-sensitising effect mediated through activation of AMPK, better sensitivity to insulin action in females can be also

related to higher plasma adiponectin levels including the biologically active HMW form (Table 5).

The above results showed a lower ectopic fat storage and better metabolic profile of female mice in spite of higher degree of obesity. Therefore, further analysis of adipose tissue was performed, as insulin resistance is closely associated with adipose tissue inflammation and correlates with adipocyte size. Histological analysis of gWAT and scWAT combined with morphometry of adipocytes showed that adipocyte size in animals fed ST diet was similar in both sexes, and it did not differ between week 15 and 35, while almost no macrophages were detected in gWAT and scWAT (see publication). This leads us to a conclusion that adipose tissue of ST-fed lean animals is populated only with resident macrophages without any inflammatory activity. The opposite situation was observed in HF-fed animals. As expected, HF-feeding increased adipocyte size as well as macrophage infiltration, detected as a frequency of CLS, in gWAT and scWAT of both sexes. In agreement with a widely accepted concept that adipocyte size correlates with adipose tissue inflammation, males demonstrated adipocyte hypertrophy accompanied by a markedly increased number of CLS especially in gWAT both at week 15 and 35. Surprisingly, the dissociation of adipocyte size from macrophage infiltration was observed in female mice. At week 15, adipocyte size tended

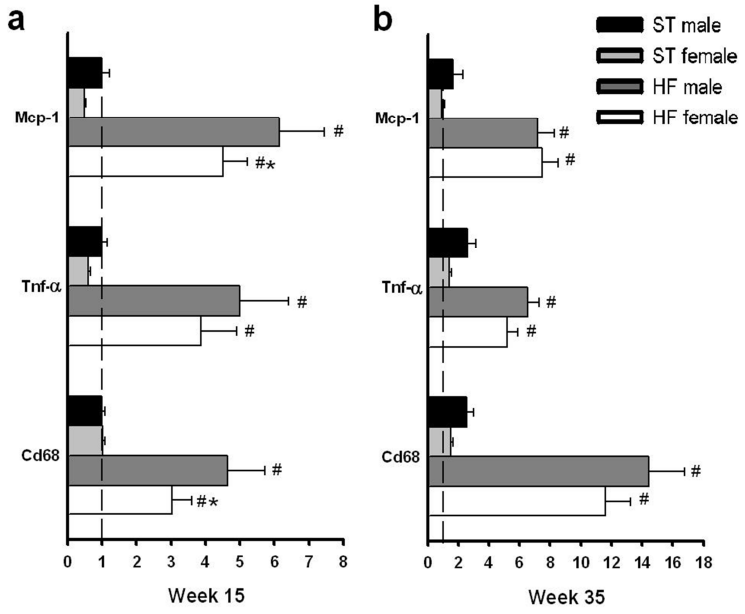

Figure 8 Quantification of gene expression in gWAT of male and female mice fed ST or HF diet at **(a)** week 15 and **(b)** week 35. Expression of selected genes was evaluated using qRT-PCR and standardised relative to ST diet fed male mice at week 15. Data are means ± SE (*n=7-10*). *significant difference between sexes within diet, #significant difference between diets within sexes (ANOVA). *Mcp-1*, monocyte chemoattractant protein-1; *Tnf-α* tumour necrosis factor α; *Cd68*, Cd68 antigen. (See Figure 5 of the respective publication).

to be larger in female gWAT and scWAT than in male and at week 35, the difference reached the statistical significance. However, adipose tissue macrophage infiltration remained considerably lower in females (see publication).

To further characterise the inflammatory status of adipose tissue of HF-fed mice, gene expression of several pro-inflammatory markers was assessed in gWAT, since this depot showed higher inflammatory response. As shown in Fig. 8a,b, HF-feeding markedly induced expression of *Mcp-1, Tnf-α* and *Cd68* in both sexes. At week 15, females fed HF diet showed lower expression of all three genes (although the decrease in did not reach statistical significance) as compared to males. Although at week 35 only a trend for decreased expression of *Tnf-α* and *Cd68* in female gWAT was observed, histological analysis clearly demonstrated lower degree of inflammation in adipose tissue depots of female mice, independent from the expression levels of pro-inflammatory markers.

To conclude, using a model of morbid dietary obesity in mice, females demonstrated higher adiposity as reflected by larger adipocytes and higher leptinaemia as compared to males. However, in spite of larger adipocytes, frequency of CLS was reduced in both gWAT and scWAT in female mice. Together with substantially lowered insulin levels, markedly increased adiponectin and less pronounced hepatosteatosis, these results indicate that better insulin sensitivity in female as compared to male mice challenged with HF-feeding might be due to their increased capacity for adipocyte enlargement and generally greater adipose tissue expandability.

My main contribution to this work was the management and coordination of all the experiments, biochemical analysis of plasma samples, assessment of adiponectin multimeric complexes by western blot technique, determination of glucose homeostasis (except of measuring insulin levels (ZMJ), and quantification of gene expression.

4 DISCUSSION

Diet-induced obesity represents a marked risk for developing metabolic syndrome, a cluster of diseases posing a substantial health threat for the human population. Understanding the principles and mechanisms connecting obesity with the propensity to develop metabolic syndrome is important for designing treatment strategies for the prevention of disturbed metabolic states. The results of publications described in this thesis contribute to our understanding of obesity development and are also relevant to approaches for the treatment of metabolic syndrome. Briefly, the first publication is related to the topic of dietary lipid composition, specifically with respect to dietary supplementation with EPA/ DHA concentrates and chemical DHA-derivatives, thereby modulating lipid accumulation, impaired glucose tolerance and WAT inflammation (Publication A). The second publication relates to the induction of muscle thermogenesis by HF-feeding in obesity-resistant A/J mice by means of increased leptinaemia and subsequent activation of AMPK (Publication B). Third paper deepens our knowledge about the mechanism, by which EPA/ DHA exert their beneficial effects on metabolism, and whether AMPK is involved in the process (Publication C). Finally, the last part of my work concerned the examination of different properties of adipose tissue associated with distinct predisposition for suffering from metabolic syndrome in male and female mice (Publication D).

Type of dietary lipids plays an important role in the development of obesity and associated diseases. The ingestion of saturated fat contributes to the onset of obesity and subsequently to the appearance of metabolic syndrome. To the contrary, PUFA, and particularly PUFA of n-3 series, are known to provide health benefits. Replacing a part of dietary lipids with EPA and especially with DHA confers the anti-inflammatory action in obese adipose tissue, improves metabolic profile, while in rodents it also prevents lipid accumulation (99;100). Inflammation of WAT represents a dysfunctional state of adipose tissue with a dysregulated secretory profile, which is characterised by a shift from releasing anti-inflammatory cytokines like adiponectin to the production of pro-inflammatory molecules. Adipocytokines such as TNF-α, MCP-1 or IL-6 are released from WAT, act at the local as well as systemic level and thereby worsen insulin

sensitivity in peripheral tissues (17). Additionally, obese adipose tissue, characterised by hypertrophied adipocytes, has limited capacity for TAG storage. Thus, it leads to ectopic fat accumulation in muscle and liver, further promoting insulin resistance. Given the fact that naturally occurring PUFA have beneficial effects in ameliorating obesity and associated metabolic disturbances (99), chemical derivatives of DHA have been developed with the view of improved action. In our study, four DHA derivatives were tested. Substance 2 (α-ethyl DHA ethyl ester) proved to be the most effective in prevention and reversal of obesity and impaired glucose tolerance (Publication A). It reduced macrophage WAT infiltration, thereby improving insulin resistance, as macrophages are the main source of pro-inflammatory cytokines counteracting insulin action (2). Substance 2 further reduced accumulation of TAG by simultaneous activation of lipogenesis (*Scd-1, Fdps*) and lipid catabolism (*Aox-1, Cp1-1α*), suggesting futile substrate cycling. Therefore, it could be qualified as a novel promising drug in the treatment of obesity and insulin resistance.

AMPK represents another notable drug target for diabetes and metabolic syndrome. The most widespread antidiabetic drugs, such as thiazolidinediones and metformin, act through the activation of AMPK (120;121). Furthermore, we showed for the first time, that AMPKα2 subunit is required for the effect of n-3 LC-PUFA to preserve hepatic insulin sensitivity (Publication C). The study was performed using transgenic mice with the whole-body inactivation of the catalytic α2 subunit of AMPK. First, we showed that AMPKα2 is activated in response to dietary n-3 LC-PUFA in wild-type but not in transgenic mice. However, concerning AMPK activation in response to n-3 LC-PUFA, contradictory results were obtained previously (122;123). This discrepancy could be caused by the differences in dietary intake of n-3 LC-PUFA or by the nutritional state of experimental animals. Moreover, no AMPK activation was observed in cultured hepatocytes treated directly with n-3 LC-PUFA (26). This suggests that AMPKα2 is activated by n-3 LC-PUFA indirectly, possibly by the stimulation of adiponectin release (124), since adiponectin is known to activate AMPK (61) and improve insulin sensitivity. Additionally, accumulation of DAG in the liver could mediate hepatic insulin resistance (125), and we showed that hepatic DAG levels are regulated in AMPKα2-dependent manner in response to dietary n-3 LC-PUFA.

Besides adiponectin, AMPK is also activated by other important adipocytokine, leptin. Leptin stimulates fatty acids oxidation and induces energy expenditure through AMPK, thereby protecting from ectopic fat accumulation. We demonstrated that leptin induced muscle non-shivering thermogenesis in an AMPK-dependent manner in response to HF-feeding in obesity resistant A/J, but not in obesity prone C57BL/6 mice (Publication B). HF-feeding exert stronger obesogenic effect in C57BL/6 mice compared to A/J. Low energy expenditure in A/J, which presumably predisposes these mice to obesity, is markedly enhanced by HF-feeding when compared with C57BL/6 mice. Increased energy expenditure is accompanied by higher body temperature and stronger induction of UCP1 in BAT. It has been shown before, that A/J mice are able to retain the sensitivity of adipose tissue to leptin (126) and β-adrenergic stimuli (127). Additionally, we demonstrated stronger AMPK phosphorylation/ activation and higher VO_2 in oxidative muscle in A/J mice, suggesting a preferential use of lipids for non-shivering thermogenesis. Increased lipid oxidation was also supported by higher *Scd-1* (128) and lower *Pdk-4* (129) expression. To conclude, our results suggest that UCP1 mediated thermogenesis in BAT together with non-shivering skeletal muscle thermogenesis contribute to the resistance to dietary obesity in A/J mice.

The above discussion outlines possibilities for the prevention and treatment of obesity and metabolic syndrome. Studies on animal models help to develop treatment strategies for numerous diseases including the metabolic syndrome. However, it is important to realise that significant differences resulting from biological diversity between the sexes exist regarding the manifestation of these diseases. Therefore, in the context of treating metabolic syndrome it is important to understand the inherent differences between the sexes regarding adipose tissue biology and the ability of an organism to cope with the HF diet challenge. We documented profound differences in a capability of adipose tissue to handle excess calories during the long-term administration of HF diet (Publication D). A murine model of morbid obesity with equalised BW of males and females was used, so that the differences in metabolic phenotypes cannot be attributed to a lower BW and smaller fat cells in female mice as described previously (94;110). Moreover, sex-dependent differences in adipocyte size and the frequency of CLS in WAT were demonstrated. In contrast to a generally accepted view that

hypertrophy of adipocytes correlates with macrophage infiltration of WAT (91;93), female mice exhibited a markedly reduced number of CLS in spite of their larger fat cells. This suggests a higher capacity of females' adipocytes to expand and thereby keep the adipose tissue inflammation at a relatively low level as compared to males that demonstrate considerable macrophage WAT infiltration. Increased expandability of WAT in females likely resulted in lower ectopic fat deposition and therefore lower lipotoxicity. Furthermore, our results confirm previously published data on sex-dependent differences in insulin sensitivity (90;130), as documented by females exhibiting later onset of impaired glucose tolerance associated with lower insulin levels to maintain the same glycaemia as compared to males. Another factor likely contributing to a better insulin sensitivity in female mice, while possess anti-inflammatory action (61), is adiponectin, showing consistently increased plasma levels in female as compared to male mice.

In summary, the results presented in this thesis help to understand primary mechanisms linking dietary obesity to metabolic syndrome and outline possible concepts for the prevention and treatment of these metabolic diseases with respect to sex-dependent differences in the way how the organism handle energy surplus.

5 CONCLUSIONS

Concerning the specific aims of this thesis, the following conclusions may be formulated:

1. Naturally occurring n-3 LC-PUFA exhibited beneficial effects in the prevention and treatment of obesity and metabolic syndrome. However, chemical DHA-derivatives manifested the same range of health benefits, but with a higher efficacy. Substance 2 (α-ethyl DHA ethyl ester) profoundly reduced adipocyte size and adipose tissue inflammation in obese mice, which was associated with improved insulin sensitivity.

2. Differences in plasma leptin levels between obesity resistant A/J and obesity prone C57BL/6 mice were identified. A/J mice exhibited a cold sensitive phenotype when fed LF diet. However, HF diet normalised cold tolerance by inducing both, UCP1 mediated thermogenesis and non-shivering thermogenesis in oxidative skeletal muscle. Muscle thermogenesis was accompanied by a preferential oxidation of lipids, suggesting the involvement of leptin-AMPK axis.

3. α2 subunit of AMPK was required for the preservation of hepatic insulin sensitivity mediated by n-3 LC-PUFA in mice fed HF diet. Dietary n-3 LC-PUFA modulated the type of accumulated hepatic DAG and completely prevented an increase of polyunsaturated DAG in AMPKα2-dependent manner.

4. Sex-dependent differences in adipose tissue in response to HF-feeding were described. Female mice demonstrated higher adiposity, however, in spite of larger adipocytes, the frequency of CLS was significantly lower than in males. Females accumulated less fat in non-adipose tissues, which together with lower inflammation of WAT and constantly increased adiponectin levels corresponded with their improved sensitivity. Thus, adipose tissue expandability and its capability to handle energy surplus rather than total body fat content contributed to a resistance of female mice to metabolic derangements associated with obesity.

6 LIST OF PUBLICATIONS

Published articles

- Flachs P, Sponarova J, Kopecky P, Horvath O, Sediva A, Nibbelink M, Casteilla L, **Medrikova D**, Neckar J, Kolar F, Kopecky J. Mitochondrial uncoupling protein 2 gene transcript levels are elevated in maturating erythroid cells. *FEBS Lett*. 581:1093-1097, 2007 (IF = 3.263)

- Kus V, Prazak T, Brauner P, Hensler M, Kuda O, Flachs P, Janovska P, **Medrikova D**, Rossmeisl M, Jilkova Z, Stefl B, Pastalkova E, Drahota Z, Houstek J, Kopecky J. Induction of muscle thermogenesis by high-fat diet in mice: association with obesity-resistance. *Am J Physiol Endocrinol Metab.* 295:E356-E367, 2008 (IF = 4.129)

- Rossmeisl M, Jelenik T, Jilkova Z, Slamova K, Kus V, Hensler M, **Medrikova D**, Povysil C, Flachs P, Mohamed-Ali V, Bryhn M, Berge K, Holmeide AK, Kopecky J. DHA-derivatives in the prevention and reversal of obesity and glucose intolerance in mice. *Obesity.* 17:1023–1031, 2009 (IF = 2.798)

- Jelenik T, Rossmeisl M, Kuda O, Macek Jilkova Z, **Medrikova D**, Kus V, Hensler M, Janovska P, Miksik I, Baranowski M, Gorski , Jensen TE, Flachs P, Viollet B, Kopecky J. AMP-activated protein kinaṣe α2 subunit is required for the preservation of hepatic insulin sensitivity by n-3 polyunsaturated fatty acids. *Diabetes.* 59:2737-2746, 2010 (IF = 8.261)

- Benes J, Kazdova L, Drahota Z, Houstek J, **Medrikova D**, Kopecky J, Kovarova N, Vrbacky M, Sedmera D, Strnad H, Kolar M, Petrak J, Benada O, Skaroupkova P, Cervenka L, Melenovsky V. The effect of metformin therapy on cardiac function and survival in volume-overload model of heart failure in rats. *Clin Sci. (Lond.) [Epub ahead of print], 2011* (IF = 3.982)

- **Medrikova D,** Macek Jilkova Z, Bardova K, Janovska P, Rossmeisl M, Kopecky J. Sex differences during the course of diet-induced obesity in mice: adipose tissue expandability and glycemic control. Accepted in: *Int J Obes.* (IF = 4.343)

7 REFERENCES

1. Kopelman,PG: Obesity as a medical problem. *Nature.* 404:635-643, 2000

2. Wellen,KE, Hotamisligil,GS: Inflammation, stress, and diabetes. *J Clin Invest.* 115:1111-1119, 2005

3. Calle,EE, Kaaks,R: Overweight, obesity and cancer: Epidemiological evidence and proposed mechanisms. *Nat Rev Cancer.* 4:579-591, 2004

4. Schwartz,MW, Woods,SC, Porte,D, Jr., Seeley,RJ, Baskin,DG: Central nervous system control of food intake. *Nature.* 404:661-671, 2000

5. Woods,SC, Seeley,RJ, Porte Jr.,D, Schwartz,MW: Signals that regulate food intake and energy homeostasis. *Science.* 280:1378-1383, 1998

6. Bruning,JC, Gautam,D, Burks,DJ, Gillette,J, Schubert,M, Orban,PC, Klein,R, Krone,W, Muller-Wieland,D, Kahn,CR: Role of brain insulin receptor in control of body weight and reproduction. *Science.* 289:2122-2125, 2000

7. Wijers,SL, Saris,WH, van Marken Lichtenbelt,WD: Recent advances in adaptive thermogenesis: potential implications for the treatment of obesity. *Obes Rev.* 10:218-226, 2009

8. Lowell,BB, Spiegelman,BM: Towards a molecular understanding of adaptive thermogenesis. *Nature.* 404:652-660, 2000

9. Rothwell,NJ, Stock,MJ, Stribling,D: Diet-induced thermogenesis. *Pharmacol Ther.* 17:251-268, 1982

10. Rothwell,NJ, Stock,MJ: A role for brown adipose tissue in diet-induced thermogenesis. *Nature.* 281:31-35, 1979

11. Zingaretti,MC, Crosta,F, Vitali,A, Guerrieri,M, Frontini,A, Cannon,B, Nedergaard,J, Cinti,S: The presence of UCP1 demonstrates that metabolically active adipose tissue in the neck of adult humans truly represents brown adipose tissue. *FASEB J.* 23:3113-3120, 2009

12. van Marken Lichtenbelt,WD, Vanhommerig,JW, Smulders,NM, Drossaerts,JM, Kemerink,GJ, Bouvy,ND, Schrauwen,P, Teule,GJ: Cold-activated brown adipose tissue in healthy men. *N Engl J Med.* 360:1500-1508, 2009

13. Cypess,AM, Lehman,S, Williams,G, Tal,I, Rodman,D, Goldfine,AB, Kuo,FC, Palmer,EL, Tseng,Y, Doria,A, Kolodny,GM, Kahn,CR: Identification and importance of brown adipose tissue in adult humans. *N Engl J Med.* 360:1509-1517, 2009

14. O'Brien,J, Block,BA: Effects of Ca2+ on oxidative phosphorylation in mitochondria from the thermogenic organ of marlin. *J Exp Biol.* 199:2679-2687, 1996

15. Wijers,SL, Schrauwen,P, Saris,WH, van Marken Lichtenbelt,WD: Human skeletal muscle mitochondrial uncoupling is associated with cold induced adaptive thermogenesis. *PLoS One.* 3:e1777, 2008

16. Sethi,JK, Vidal-Puig,AJ: Adipose tissue function and plasticity orchestrate nutritional adaptation. *J Lipid Res.* 48:1253-1262, 2007

17. Cao,H, Gerhold,K, Mayers,JR, Wiest,MM, Watkins,SM, Hotamisligil,GS: Identification of a lipokine, a lipid hormone linking adipose tissue to systemic metabolism. *Cell.* 134:933-944, 2008

18. Fonseca-Alaniz,MH, Takada,J, Alonso-Vale,MI, Lima,FB: Adipose tissue as an endocrine organ: from theory to practice. *J Pediatr (Rio J).* 83:S192-S203, 2007

19. Wajchenberg,BL: Subcutaneous and visceral adipose tissue: their relation to the metabolic syndrome. *Endocr Rev.* 21:697-738, 2000

20. Spalding,KL, Arner,E, Westermark,PO, Bernard,S, Buchholz,BA, Bergmann,O, Blomqvist,L, Hoffstedt,J, Naslund,E, Britton,T, Concha,H, Hassan,M, Ryden,M, Frisen,J, Arner,P: Dynamics of fat cell turnover in humans. *Nature.* 453:783-787, 2008

21. Campbell,PJ, Carlson,MG, Hill,JO, Nurjhan,N: Regulation of free fatty acid metabolism by insulin in humans: role of lipolysis and reesterification. *Am J Physiol.* 263:E1063-E1069, 1992

22. Boden,G: Role of fatty acids in the pathogenesis of insulin resistance and NIDDM. *Diabetes.* 46:3-10, 1997

23. Farnier,C, Krief,S, Blache,M, Diot-Dupuy,F, Mory,G, Ferre,P, Bazin,R: Adipocyte functions are modulated by cell size change: potential involvement of an integrin/ERK signalling pathway. *Int J Obes Relat Metab Disord.* 27:1178-1186, 2003

24. Yki-Jarvinen,H: Ectopic fat accumulation: an important cause of insulin resistance in humans. *J R Soc Med.* 95:39-45, 2002

25. Sakurai,M, Takamura,T, Ota,T, Ando,H, Akahori,H, Kaji,K, Sasaki,M, Nakanuma,Y, Miura,K, Kaneko,S: Liver steatosis, but not fibrosis, is associated with insulin resistance in nonalcoholic fatty liver disease. *J Gastroenterol.* 42:312-317, 2007

26. Dentin,R, Benhamed,F, Pegorier,JP, Foufelle,F, Viollet,B, Vaulont,S, Girard,J, Postic,C: Polyunsaturated fatty acids suppress glycolytic and lipogenic genes through the inhibition of ChREBP nuclear protein translocation. *J Clin Invest.* 115:2843-2854, 2005

27. Samuel,VT, Liu,ZX, Wang,A, Beddow,SA, Geisler,JG, Kahn,M, Zhang,XM, Monia,BP, Bhanot,S, Shulman,GI: Inhibition of protein kinase C epsilon prevents hepatic insulin resistance in nonalcoholic fatty liver disease. *J Clin Invest.* 117:739-745, 2007

28. Koves,TR, Ussher,JR, Noland,RC, Slentz,D, Mosedale,M, Ilkayeva,O, Bain,J, Stevens,R, Dyck,JR, Newgard,CB, Lopaschuk,GD, Muoio,DM: Mitochondrial overload and incomplete fatty acid oxidation contribute to skeletal muscle insulin resistance. *Cell Metab.* 7:45-56, 2008

29. Zhou,YP, Grill,V: Long-Term Exposure to Fatty-Acids and Ketones Inhibits B-Cell Functions in Human Pancreatic Islets of Langerhans. *J Clin Endocrinol Metab.* 80:1584-1590, 1995

30. Prentki,M, Vischer,S, Glennon,MC, Regazzi,R, Deeney,JT, Corkey,BE: Malonyl-CoA and long chain acyl-CoA esters as metabolic coupling factors in nutrient-induced insulin secretion. *J Biol Chem.* 267:5802-5810, 1992

31. Shimabukuro,M, Zhou,YT, Levi,M, Unger,RH: Fatty acid-induced beta cell apoptosis: A link between obesity and diabetes. *Proc Natl Acad Sci U S A.* 95:2498-2502, 1998

32. Hardie,DG, Carling,D, Carlson,M: The AMP-activated/SNF1 protein kinase subfamily: metabolic sensors of the eukaryotic cell? *Annu Rev Biochem.* 67:821-855, 1998

33. Woods,A, Cheung,PCF, Smith,FC, Davison,MD, Scott,J, Beri,RK, Carling,D: Characterization of AMP-activated protein kinase beta and gamma subunits - Assembly of the heterotrimeric complex in vitro. *J Biol Chem.* 271:10282-10290, 1996

34. Hardie,DG: AMPK: a key regulator of energy balance in the single cell and the whole organism. *Int J Obes (Lond).* 32 Suppl 4:S7-12, 2008

35. Hawley,SA, Pan,DA, Mustard,KJ, Ross,L, Bain,J, Edelman,AM, Frenguelli,BG, Hardie,DG: Calmodulin-dependent protein kinase kinase-beta is an alternative upstream kinase for AMP-activated protein kinase. *Cell Metab.* 2:9-19, 2005

36. Long,YC, Zierath,JR: AMP-activated protein kinase signaling in metabolic regulation. *J Clin Invest.* 116:1776-1783, 2006

37. Cinti S: The adipose organ. Milano, Italy, Editrice Kurtis, 1999,

38. Hotamisligil,GS, Shargill,NS, Spiegelman,BM: Adipose expression of tumor necrosis factor-alpha: direct role in obesity-linked insulin resistance. *Science.* 259:87-91, 1993

39. Skurk,T, Alberti-Huber,C, Herder,C, Hauner,H: Relationship between adipocyte size and adipokine expression and secretion. *J Clin Endocrinol Metab.* 92:1023-1033, 2007

40. Maury,E, Brichard,SM: Adipokine dysregulation, adipose tissue inflammation and metabolic syndrome. *Mol Cell Endocrinol.* 314:1-16, 2010

41. Zhang,Y, Proenca,R, Maffei,M, Barone,M, Leopold,L, Friedman,JM: Positional cloning of the mouse obese gene and its human homologue. *Nature.* 372:425-432, 1994

42. Morton,GJ, Cummings,DE, Baskin,DG, Barsh,GS, Schwartz,MW: Central nervous system control of food intake and body weight. *Nature.* 443:289-295, 2006

43. Seeley,RJ, Yagaloff,KA, Fisher,SL, Burn,P, Thiele,TE, van Dijk,G, Baskin,DG, Schwartz,MW: Melanocortin receptors in leptin effects. *Nature.* 390:349, 1997

44. Ebihara,K, Ogawa,Y, Katsuura,G, Numata,Y, Masuzaki,H, Satoh,N, Tamaki,M, Yoshioka,T, Hayase,M, Matsuoka,N, Aizawa-Abe,M, Yoshimasa,Y, Nakao,K: Involvement of agouti-related protein, an endogenous antagonist of hypothalamic melanocortin receptor, in leptin action. *Diabetes.* 48:2028-2033, 1999

45. Muhlhausler,BS, McMillen,IC, Rouzaud,G, Findlay,PA, Marrocco,EM, Rhind,SM, Adam,CL: Appetite regulatory neuropeptides are expressed in the sheep hypothalamus before birth. *J Neuroendocrinol.* 16:502-507, 2004

46. Staiger,H, Tschritter,O, Machann,J, Thamer,C, Fritsche,A, Maerker,E, Schick,F, Haring,HU, Stumvoll,M: Relationship of serum adiponectin and leptin concentrations with body fat distribution in humans. *Obes Res.* 11:368-372, 2003

47. Scarpace,PJ, Zhang,Y: Elevated leptin: consequence or cause of obesity? *Front Biosci.* 12:3531-3544, 2007

48. Banks,WA, Coon,AB, Robinson,SM, Moinuddin,A, Shultz,JM, Nakaoke,R, Morley,JE: Triglycerides induce leptin resistance at the blood-brain barrier. *Diabetes.* 53:1253-1260, 2004

49. Minokoshi,Y, Kim,YB, Peroni,OD, Fryer,LG, Muller,C, Carling,D, Kahn,BB: Leptin stimulates fatty-acid oxidation by activating AMP-activated protein kinase. *Nature.* 415:339-343, 2002

50. Kakuma,T, Lee,Y, Higa,M, Wang,ZW, Pan,WT, Shimomura,I, Unger,RH: Leptin, troglitazone, and the expression of sterol regulatory element binding proteins in liver and pancreatic islets. *Proc Natl Acad Sci U S A.* 97:8536-8541, 2000

51. Kamohara,S, Burcelin,R, Halaas,JL, Friedman,JM, Charron,MJ: Acute stimulation of glucose metabolism in mice by leptin treatment. *Nature.* 389:374-377, 1997

52. Dulloo,AG, Stock,MJ, Solinas,G, Boss,O, Montani,JP, Seydoux,J: Leptin directly stimulates thermogenesis in skeletal muscle. *FEBS Lett.* 515:109-113, 2002

53. Scherer,PE, Williams,S, Fogliano,M, Baldini,G, Lodish,HF: A novel serum protein similar to C1q, produced exclusively in adipocytes. *J Biol Chem.* 270:26746-26749, 1995

54. Halleux,CM, Takahashi,M, Delporte,ML, Detry,R, Funahashi,T, Matsuzawa,Y, Brichard,SM: Secretion of adiponectin and regulation of apM1 gene expression in human visceral adipose tissue. *Biochem Biophys Res Commun.* 288:1102-1107, 2001

55. Arita,Y, Kihara,S, Ouchi,N, Takahashi,M, Maeda,K, Miyagawa,J, Hotta,K, Shimomura,I, Nakamura,T, Miyaoka,K, Kuriyama,H, Nishida,M, Yamashita,S, Okubo,K, Matsubara,K, Muraguchi,M, Ohmoto,Y, Funahashi,T, Matsuzawa,Y: Paradoxical decrease of an adipose-specific protein, adiponectin, in obesity. *Biochem Biophys Res Commun.* 257:79-83, 1999

56. Hotta,K, Funahashi,T, Arita,Y, Takahashi,M, Matsuda,M, Okamoto,Y, Iwahashi,H, Kuriyama,H, Ouchi,N, Maeda,K, Nishida,M, Kihara,S, Sakai,N, Nakajima,T, Hasegawa,K, Muraguchi,M, Ohmoto,Y, Nakamura,T, Yamashita,S, Hanafusa,T, Matsuzawa,Y: Plasma concentrations of a novel, adipose-specific

protein, adiponectin, in type 2 diabetic patients. *Arterioscler Thromb Vasc Biol.* 20:1595-1599, 2000

57. Wang,Y, Lam,KSL, Chan,L, Chan,KW, Lam,JBB, Lam,MC, Hoo,RCL, Mak,WWN, Cooper,GJS, Xu,AM: Post-translational modifications of the four conserved lysine residues within the collagenous domain of adiponectin are required for the formation of its high molecular weight oligomeric complex. *J Biol Chem.* 281:16391-16400, 2006

58. Tsao,TS, Murrey,HE, Hug,C, Lee,DH, Lodish,HF: Oligomerization state-dependent activation of NF-kappa B signaling pathway by adipocyte complement-related protein of 30 kDa (Acrp30). *J Biol Chem.* 277:29359-29362, 2002

59. Waki,H, Yamauchi,T, Kamon,J, Ito,Y, Uchida,S, Kita,S, Hara,K, Hada,Y, Vasseur,F, Froguel,P, Kimura,S, Nagai,R, Kadowaki,T: Impaired multimerization of human adiponectin mutants associated with diabetes - Molecular structure and multimer formation of adiponectin. *J Biol Chem.* 278:40352-40363, 2003

60. Berg,AH, Combs,TP, Du,X, Brownlee,M, Scherer,PE: The adipocyte-secreted protein Acrp30 enhances hepatic insulin action. *Nat Med.* 7:947-953, 2001

61. Yamauchi,T, Kamon,J, Minokoshi,Y, Ito,Y, Waki,H, Uchida,S, Yamashita,S, Noda,M, Kita,S, Ueki,K, Eto,K, Akanuma,Y, Froguel,P, Foufelle,F, Ferre,P, Carling,D, Kimura,S, Nagai,R, Kahn,BB, Kadowaki,T: Adiponectin stimulates glucose utilization and fatty-acid oxidation by activating AMP-activated protein kinase. *Nat Med.* 8:1288-1295, 2002

62. Tomas,E, Tsao,TS, Saha,AK, Murrey,HE, Zhang,CC, Itani,SI, Lodish,HF, Ruderman,NB: Enhanced muscle fat oxidation and glucose transport by ACRP30 globular domain: Acetyl-CoA carboxylase inhibition and AMP-activated protein kinase activation. *Proc Natl Acad Sci U S A.* 99:16309-16313, 2002

63. Nawrocki,AR, Rajala,MW, Tomas,E, Pajvani,UB, Saha,AK, Trumbauer,ME, Pang,Z, Chen,AS, Ruderman,NB, Chen,H, Rossetti,L, Scherer,PE: Mice lacking adiponectin show decreased hepatic insulin sensitivity and reduced responsiveness to peroxisome proliferator-activated receptor gamma agonists. *J Biol Chem.* 281:2654-2660, 2006

64. Combs,TP, Pajvani,UB, Berg,AH, Lin,Y, Jelicks,LA, Laplante,M, Nawrocki,AR, Rajala,MW, Parlow,AF, Cheeseboro,L, Ding,YY, Russell,RG, Lindemann,D, Hartley,A, Baker,GR, Obici,S, Deshaies,Y, Ludgate,M, Rossetti,L, Scherer,PE: A transgenic mouse with a deletion in the collagenous domain of adiponectin displays elevated circulating adiponectin and improved insulin sensitivity. *Endocrinology.* 145:367-383, 2004

65. Fu,YC, Luo,NL, Klein,RL, Garvey,WT: Adiponectin promotes adipocyte differentiation, insulin sensitivity, and lipid accumulation. *J Lipid Res.* 46:1369-1379, 2005

66. Asterholm,IW, Scherer,PE: Enhanced metabolic flexibility associated with elevated adiponectin levels. *Am J Pathol.* 176:1364-1376, 2010

67. Ouchi,N, Kihara,S, Arita,Y, Okamoto,Y, Maeda,K, Kuriyama,H, Hotta,K, Nishida,M, Takahashi,M, Muraguchi,M, Ohmoto,Y, Nakamura,T, Yamashita,S, Funahashi,T, Matsuzawa,Y: Adiponectin, an adipocyte-derived plasma protein, inhibits endothelial NF-kappa B signaling through a cAMP-dependent pathway. *Circulation.* 102:1296-1301, 2000

68. Weisberg,SP, McCann,D, Desai,M, Rosenbaum,M, Leibel,RL, Ferrante,AW Jr.: Obesity is associated with macrophage accumulation in adipose tissue. *J Clin Invest.* 112:1796-1808, 2003

69. Hotamisligil,GS, Budavari,A, Murray,D, Spiegelman,BM: Reduced tyrosine kinase activity of the insulin receptor in obesity-diabetes. Central role of tumor necrosis factor-alpha. *J Clin Invest.* 94:1543-1549, 1994

70. Ruan,H, Miles,PD, Ladd,CM, Ross,K, Golub,TR, Olefsky,JM, Lodish,HF: Profiling gene transcription in vivo reveals adipose tissue as an immediate target of tumor necrosis factor-alpha: implications for insulin resistance. *Diabetes.* 51:3176-3188, 2002

71. Ruan,H, Hacohen,N, Golub,TR, Van Parijs,L, Lodish,HF: Tumor necrosis factor-alpha suppresses adipocyte-specific genes and activates expression of preadipocyte genes in 3T3-L1 adipocytes: nuclear factor-kappaB activation by TNF-alpha is obligatory. *Diabetes.* 51:1319-1336, 2002

72. Uysal,KT, Wiesbrock,SM, Marino,MW, Hotamisligil,GS: Protection from obesity-induced insulin resistance in mice lacking TNF-alpha function. *Nature.* 389:610-614, 1997

73. Mohamed-Ali,V, Goodrick,S, Rawesh,A, Katz,DR, Miles,JM, Yudkin,J, Klein,S, Coppack,SW: Subcutaneous adipose tissue releases interleukin-6, but not tumor necrosis factor-alpha, in vivo. *J CLin Endocrin Metab.* 82:4196-4200, 1997

74. Senn,JJ, Klover,PJ, Nowak,IA, Mooney,RA: Interleukin-6 induces cellular insulin resistance in hepatocytes. *Diabetes.* 51:3391-3399, 2002

75. Sabio,G, Das,M, Mora,A, Zhang,ZY, Jun,JY, Ko,HJ, Barrett,T, Kim,JK, Davis,RJ: A stress signaling pathway in adipose tissue regulates hepatic insulin resistance. *Science.* 322:1539-1543, 2008

76. Febbraio,MA, Pedersen,BK: Muscle-derived interleukin-6: mechanisms for activation and possible biological roles. *FASEB J.* 16:1335-1347, 2002

77. Sartipy,P, Loskutoff,DJ: Monocyte chemoattractant protein 1 in obesity and insulin resistance. *Proc Natl Acad Sci U S A.* 100:7265-7270, 2003

78. Xu,H, Barnes,GT, Yang,Q, Tan,G, Yang,D, Chou,CJ, Sole,J, Nichols,A, Ross,JS, Tartaglia,LA, Chen,H: Chronic inflammation in fat plays a crucial role in the development of obesity-related insulin resistance. *J Clin Invest.* 112:1821-1830, 2003

79. Kanda,H, Tateya,S, Tamori,Y, Kotani,K, Hiasa,K, Kitazawa,R, Kitazawa,S, Miyachi,H, Maeda,S, Egashira,K, Kasuga,M: MCP-1 contributes to macrophage infiltration into adipose tissue, insulin resistance, and hepatic steatosis in obesity. *J Clin Invest.* 116:1494-1505, 2006

80. Wellen,KE, Hotamisligil,GS: Obesity-induced inflammatory changes in adipose tissue. *J Clin Invest.* 112:1785-1788, 2003

81. Kamei,N, Tobe,K, Suzuki,R, Ohsugi,M, Watanabe,T, Kubota,N, Ohtsuka-Kowatari,N, Kumagai,K, Sakamoto,K, Kobayashi,M, Yamauchi,T, Ueki,K, Oishi,Y, Nishimura,S, Manabe,I, Hashimoto,H, Ohnishi,Y, Ogata,H, Tokuyama,K, Tsunoda,M, Ide,T, Murakami,K, Nagai,R, Kadowaki,T: Overexpression of monocyte chemoattractant protein-1 in adipose tissues causes macrophage recruitment and insulin resistance. *J Biol Chem.* 281:26602-26614, 2006

82. Weisberg,SP, Hunter,D, Huber,R, Lemieux,J, Slaymaker,S, Vaddi,K, Charo,I, Leibel,RL, Ferrante,AW Jr.: CCR2 modulates inflammatory and metabolic effects of high-fat feeding. *J Clin Invest.* 116:115-124, 2006

83. Cinti,S, Mitchell,G, Barbatelli,G, Murano,I, Ceresi,E, Faloia,E, Wang,S, Fortier,M, Greenberg,AS, Obin,MS: Adipocyte death defines macrophage localization and function in adipose tissue of obese mice and humans. *J Lipid Res.* 46:2347-2355, 2005

84. Lumeng,CN, Bodzin,JL, Saltiel,AR: Obesity induces a phenotypic switch in adipose tissue macrophage polarization. *J Clin Invest.* 117:175-184, 2007

85. Lumeng,CN, Delproposto,JB, Westcott,DJ, Saltiel,AR: Phenotypic switching of adipose tissue macrophages with obesity is generated by spatiotemporal differences in macrophage subtypes. *Diabetes.* 57:3239-3246, 2008

86. Cancello,R, Tordjman,J, Poitou,C, Guilhem,G, Bouillot,JL, Hugol,D, Coussieu,C, Basdevant,A, Bar,HA, Bedossa,P, Guerre-Millo,M, Clement,K: Increased infiltration of macrophages in omental adipose tissue is associated with marked hepatic lesions in morbid human obesity. *Diabetes.* 55:1554-1561, 2006

87. de Luca,C, Olefsky,JM: Inflammation and insulin resistance. *FEBS Lett.* 582:97-105, 2008

88. Hotamisligil,GS, Murray,DL, Choy,LN, Spiegelman,BM: Tumor necrosis factor alpha inhibits signaling from the insulin receptor. *Proc Natl Acad Sci U S A.* 91:4854-4858, 1994

89. Kern,PA, Ranganathan,S, Li,CL, Wood,L, Ranganathan,G: Adipose tissue tumor necrosis factor and interleukin-6 expression in human obesity and insulin resistance. *Am J Physiol Endocrinol Metab.* 280:E745-E751, 2001

90. Macotela,Y, Boucher,J, Tran,TT, Kahn,CR: Sex and depot differences in adipocyte insulin sensitivity and glucose metabolism. *Diabetes.* 58:803-812, 2009

91. Okuno,A, Tamemoto,H, Tobe,K, Ueki,K, Mori,Y, Iwamoto,K, Umesono,K, Akanuma,Y, Fujiwara,T, Horikoshi,H, Yazaki,Y, Kadowaki,T: Troglitazone increases the number of small adipocytes without the change of white adipose tissue mass in obese Zucker rats. *J Clin Invest.* 101:1354-1361, 1998

92. Danforth,E Jr: Failure of adipocyte differentiation causes type II diabetes mellitus? *Nat Genet.* 26:13, 2000

93. Kubota,N, Terauchi,Y, Miki,H, Tamemoto,H, Yamauchi,T, Komeda,K, Satoh,S, Nakano,R, Ishii,C, Sugiyama,T, Eto,K, Tsubamoto,Y, Okuno,A, Murakami,K, Sekihara,H, Hasegawa,G, Naito,M, Toyoshima,Y, Tanaka,S, Shiota,K, Kitamura,T, Fujita,T, Ezaki,O, Aizawa,S, Kadowaki,T: PPAR gamma mediates high-fat diet-induced adipocyte hypertrophy and insulin resistance. *Mol Cell.* 4:597-609, 1999

94. Grove,KL, Fried,SK, Greenberg,AS, Xiao,XQ, Clegg,DJ: A microarray analysis of sexual dimorphism of adipose tissues in high-fat-diet-induced obese mice. *Int J Obes (Lond).* 34:989-1000, 2010

95. Karastergiou,K, Mohamed-Ali,V: The autocrine and paracrine roles of adipokines. *Mol Cell Endocrinol.* 318:69-78, 2010

96. Ruxton,CH, Reed,SC, Simpson,MJ, Millington,KJ: The health benefits of omega-3 polyunsaturated fatty acids: a review of the evidence. *J Hum Nutr Diet.* 17:449-459, 2007

97. Salem,N, Litman,B, Kim,HY, Gawrisch,K: Mechanisms of action of docosahexaenoic acid in the nervous system. *Lipids.* 36:945-959, 2001

98. Calder,PC: Immunomodulation by omega-3 fatty acids. *Prostaglandins Leukot Essent Fatty Acids.* 77:327-335, 2007

99. Ruzickova,J, Rossmeisl,M, Prazak,T, Flachs,P, Sponarova,J, Vecka,M, Tvrzicka,E, Bryhn,M, Kopecky,J: Omega-3 PUFA of marine origin limit diet-induced obesity in mice by reducing cellularity of adipose tissue. *Lipids.* 39:1177-1185, 2004

100. Storlien,LH, Kraegen,EW, Chisholm,DJ, Ford,GL, Bruce,DG, Pascoe,WS: Fish oil prevents insulin resistance induced by high-fat feeding in rats. *Science.* 237:885-888, 1987

101. Mater,MK, Thelen,AP, Pan,DA, Jump,DB: Sterol response element-binding protein 1c (SREBP1c) is involved in the polyunsaturated fatty acid suppression of hepatic S14 gene transcription. *J Biol Chem.* 274:32725-32732, 1999

102. Jump,DB: Fatty acid regulation of gene transcription. *Crit Rev Clin Lab Sci.* 41:41-78, 2004

103. Sessler,AM, Kaur,N, Palta,JP, Ntambi,JM: Regulation of stearoyl-CoA desaturase 1 mRNA stability by polyunsaturated fatty acids in 3T3-L1 adipocytes. *J Biol Chem.* 271:29854-29858, 1996

104. Kim,JY, Nolte,LA, Hansen,PA, Han,DH, Kawanaka,K, Holloszy,JO: Insulin resistance of muscle glucose transport in male and female rats fed a high-sucrose diet. *Am J Physiol.* 276:R665-R672, 1999

105. Arita,M, Yoshida,M, Hong,S, Tjonahen,E, Glickman,JN, Petasis,NA, Blumberg,RS, Serhan,CN: Resolvin E1, an endogenous lipid mediator derived from omega-3 eicosapentaenoic acid, protects against 2,4,6-trinitrobenzene sulfonic acid-induced colitis. *Proc Natl Acad Sci U S A.* 102:7671-7676, 2005

106. Serhan,CN, Clish,CB, Brannon,J, Colgan,SP, Chiang,N, Gronert,K: Novel functional sets of lipid-derived mediators with antiinflammatory actions generated from omega-3 fatty acids via cyclooxygenase 2-nonsteroidal antiinflammatory drugs and transcellular processing. *J Exp Med.* 192:1197-1204, 2000

107. Todoric,J, Loffler,M, Huber,J, Bilban,M, Reimers,M, Kadl,A, Zeyda,M, Waldhausl,W, Stulnig,TM: Adipose tissue inflammation induced by high-fat diet

in obese diabetic mice is prevented by n-3 polyunsaturated fatty acids. *Diabetologia.* 49:2109-2119, 2006

108. Krotkiewski,M, Bjorntorp,P, Sjostrom,L, Smith,U: Impact of obesity on metabolism in men and women. Importance of regional adipose tissue distribution. *J Clin Invest.* 72:1150-1162, 1983

109. Frias,JP, Macaraeg,GB, Ofrecio,J, Yu,JG, Olefsky,JM, Kruszynska,YT: Decreased susceptibility to fatty acid-induced peripheral tissue insulin resistance in women. *Diabetes.* 50:1344-1350, 2001

110. Trevaskis,JL, Meyer,EA, Galgani,JE, Butler,AA: Counterintuitive effects of double-heterozygous null melanocortin-4 receptor and leptin genes on diet-induced obesity and insulin resistance in C57BL/6J mice. *Endocrinology.* 149:174-184, 2008

111. Hevener,A, Reichart,D, Janez,A, Olefsky,J: Female rats do not exhibit free fatty acid-induced insulin resistance. *Diabetes.* 51:1907-1912, 2002

112. Enzi,G, Gasparo,M, Biondetti,PR, Fiore,D, Semisa,M, Zurlo,F: Subcutaneous and visceral fat distribution according to sex, age, and overweight, evaluated by computed tomography. *Am J Clin Nutr.* 44:739-746, 1986

113. Clegg,DJ, Brown,LM, Woods,SC, Benoit,SC: Gonadal hormones determine sensitivity to central leptin and insulin. *Diabetes.* 55:978-987, 2006

114. Combs,TP, Berg,AH, Rajala,MW, Klebanov,S, Iyengar,P, Jimenez-Chillaron,JC, Patti,ME, Klein,SL, Weinstein,RS, Scherer,PE: Sexual differentiation, pregnancy, calorie restriction, and aging affect the adipocyte-specific secretory protein adiponectin. *Diabetes.* 52:268-276, 2003

115. Snijder,MB, Heine,RJ, Seidell,JC, Bouter,LM, Stehouwer,CD, Nijpels,G, Funahashi,T, Matsuzawa,Y, Shimomura,I, Dekker,JM: Associations of adiponectin levels with incident impaired glucose metabolism and type 2 diabetes in older men and women: the hoorn study. *Diabetes Care.* 29:2498-2503, 2006

116. Ohashi,K, Parker,JL, Ouchi,N, Higuchi,A, Vita,JA, Gokce,N, Pedersen,AA, Kalthoff,C, Tullin,S, Sams,A, Summer,R, Walsh,K: Adiponectin promotes macrophage polarization toward an anti-inflammatory phenotype. *J Biol Chem.* 285:6153-6160, 2010

117. Vegeto,E, Belcredito,S, Etteri,S, Ghisletti,S, Brusadelli,A, Meda,C, Krust,A, Dupont,S, Ciana,P, Chambon,P, Maggi,A: Estrogen receptor-alpha mediates the brain antiinflammatory activity of estradiol. *Proc Natl Acad Sci U S A.* 100:9614-9619, 2003

118. Vegeto,E, Belcredito,S, Ghisletti,S, Meda,C, Etteri,S, Maggi,A: The endogenous estrogen status regulates microglia reactivity in animal models of neuroinflammation. *Endocrinology.* 147:2263-2272, 2006

119. Ghisletti,S, Meda,C, Maggi,A, Vegeto,E: 17beta-estradiol inhibits inflammatory gene expression by controlling NF-kappaB intracellular localization. *Mol Cell Biol.* 25:2957-2968, 2005

120. Saha,AK, Avilucea,PR, Ye,JM, Assifi,MM, Kraegen,EW, Ruderman,NB: Pioglitazone treatment activates AMP-activated protein kinase in rat liver and adipose tissue in vivo. *Biochem Biophys Res Commun.* 314:580-585, 2004

121. Zhou,G, Myers,R, Li,Y, Chen,Y, Shen,X, Fenyk-Melody,J, Wu,M, Ventre,J, Doebber,T, Fujii,N, Musi,N, Hirshman,MF, Goodyear,LJ, Moller,DE: Role of AMP-activated protein kinase in mechanism of metformin action. *J Clin Invest.* 108:1167-1174, 2001

122. Suchankova,G, Tekle,M, Saha,AK, Ruderman,NB, Clarke,SD, Gettys,TW: Dietary polyunsaturated fatty acids enhance hepatic AMP-activated protein kinase activity in rats. *Biochem Biophys Res Commun.* 326:851-858, 2005

123. Dobrzyn,A, Dobrzyn,P, Miyazaki,M, Ntambi,JM: Polyunsaturated fatty acids do not activate AMP-activated protein kinase in mouse tissues. *Biochem Biophys Res Commun.* 332:892-896, 2005

124. Flachs,P, Mohamed-Ali,V, Horakova,O, Rossmeisl,M, Hosseinzadeh-Attar,MJ, Hensler,M, Ruzickova,J, Kopecky,J: Polyunsaturated fatty acids of marine origin induce adiponectin in mice fed high-fat diet. *Diabetologia.* 49:394-397, 2006

125. Wakelam,MJ: Diacylglycerol - when is it an intracellular messenger? *Biochim Biophys Acta.* 1436:117-126, 1998

126. Prpic,V, Watson,PM, Frampton,IC, Sabol,MA, Jezek,GE, Gettys,TW: Differential mechanisms and development of leptin resistance in A/J versus C57BL/6J mice during diet-induced obesity. *Endocrinology.* 144:1155-1163, 2003

127. Collins,S, Daniel,KW, Petro,AE, Surwit,RS: Strain-specific response to beta3-adrenergic receptor agonist treatment of diet-induced obesity in mice. *Endocrinology.* 138:405-413, 1997

128. Biddinger,SB, Miyazaki,M, Boucher,J, Ntambi,JM, Kahn,CR: Leptin suppresses stearoyl-CoA desaturase 1 by mechanisms independent of insulin and sterol regulatory element-binding protein-1c. *Diabetes.* 55:2032-2041, 2006

129. Sugden,MC, Holness,MJ: Recent advances in mechanisms regulating glucose oxidation at the level of the pyruvate dehydrogenase complex by PDKs. *Am J Physiol Endocrinol Metab.* 284:E855-E862, 2003

130. Guerre-Millo,M, Leturque,A, Girard,J, Lavau,M: Increased insulin sensitivity and responsiveness of glucose metabolism in adipocytes from female versus male rats. *J Clin Invest.* 76:109-116, 1985

8 SUPPLEMENT

1. Publication A
2. Publication B
3. Publication C
4. Publication D

Publication A

Rossmeisl M, Jelenik T, Jilkova Z, Slamova K, Kus V, Hensler M, **Medrikova D**, Povysil C, Flachs P, Mohamed-Ali V, Bryhn M, Berge K, Holmeide K, Kopecky J.

DHA-derivatives in the prevention and reversal of obesity and glucose intolerance in mice.

Obesity. 17: 1023–1031, 2009 (IF = 2.798)

Prevention and Reversal of Obesity and Glucose Intolerance in Mice by DHA Derivatives

Martin Rossmeisl[1], Tomas Jelenik[1], Zuzana Jilkova[1], Kristyna Slamova[1], Vladimir Kus[1], Michal Hensler[1], Dasa Medrikova[1], Ctibor Povysil[2], Pavel Flachs[1], Vidya Mohamed-Ali[3], Morten Bryhn[4], Kjetil Berge[4], Anne K. Holmeide[4] and Jan Kopecky[1]

The n-3 polyunsaturated fatty acids, especially eicosapentaenoic acid (EPA) and docosahexaenoic acid (DHA), exert hypolipidemic effects and prevent development of obesity and insulin resistance in animals fed high-fat diets. We sought to determine the efficacy of α-substituted DHA derivatives as lipid-lowering, antiobesity, and antidiabetic agents. C57BL/6 mice were given a corn oil–based high-fat (35% weight/weight) diet (cHF), or cHF with 1.5% of lipids replaced with α-methyl DHA ethyl ester (Substance 1), α-ethyl DHA ethyl ester (Substance 2), α,α-di-methyl DHA ethyl ester (Substance 3), or α-thioethyl DHA ethyl ester (Substance 4) for 4 months. Plasma markers of glucose and lipid metabolism, glucose tolerance, morphology, tissue lipid content, and gene regulation were characterized. The cHF induced obesity, hyperlipidemia, impairment of glucose homeostasis, and adipose tissue inflammation. Except for Substance 3, all other substances prevented weight gain and Substance 2 exerted the strongest effect (63% of cHF-controls). Glucose intolerance was significantly prevented (~67% of cHF) by both Substance 1 and Substance 2. Moreover, Substance 2 lowered fasting glycemia, plasma insulin, triacylglycerols, and nonesterified fatty acids (73, 9, 47, and 81% of cHF-controls, respectively). Substance 2 reduced accumulation of lipids in liver and skeletal muscle, as well as adipose tissue inflammation associated with obesity. Substance 2 also induced weight loss in dietary obese mice. In contrast to DHA administered either alone or as a component of the EPA/DHA concentrate (replacing 15% of dietary lipids), Substance 2 also reversed established glucose intolerance in obese mice. Thus, Substance 2 represents a novel compound with a promising potential in the treatment of obesity and associated metabolic disturbances.

Obesity (2009) **17,** 1023–1031. doi:10.1038/oby.2008.602

INTRODUCTION

Obesity, and especially abdominal obesity, is a risk factor for insulin resistance (IR), type 2 diabetes, and cardiovascular disease. "Dysfunctional" adipose tissue, which cannot properly handle the energy surplus resulting from a sedentary lifestyle combined with excessive calorie consumption, plays a central role in obesity-associated IR and type 2 diabetes (1). In general, IR develops as a consequence of exposure of insulin-responsive tissues to elevated dietary nutrients, resulting in the accumulation of lipid-derived metabolites and impairment of inter-organ communication networks that are mediated by peptide hormones and inflammatory molecules (2). Lifestyle modification therapies, such as reduced caloric intake and increased physical activity, for the obesity-associated IR and metabolic abnormalities have proved to be difficult for the general population. However, current pharmacological interventions often require the use of multiple agents and are also associated with adverse side effects, as documented in the case of the thiazolidinediones (3). Therefore, new treatment strategies are sought.

At the same time, the quality of dietary lipids is important. The n-3 long-chain polyunsaturated fatty acids (n-3 LC-PUFA), namely, eicosapentaenoic acid (EPA; 20:5n-3) and docosahexaenoic acid (DHA; 22:6n-3), which are abundant in marine fish oils, act as potent hypolipidemics in both rodents (4–6) and humans (7). The n-3 LC-PUFA also prevented development of obesity and IR in rodents fed high-fat diets (8). However, their beneficial effect on body weight and IR in overweight patients was only apparent when n-3 LC-PUFA were combined with

[1]Department of Adipose Tissue Biology and Center for Applied Genomics, Institute of Physiology, Academy of Sciences of the Czech Republic, Prague, Czech Republic; [2]Institute of Pathology, 1st Medical Faculty, Charles University, Prague, Czech Republic; [3]Adipokines and Metabolism Research Group, Centre for Clinical Pharmacology, Department of Medicine, University College London, London, UK; [4]Pronova BioPharma AS, Lysaker, Norway. Correspondence: Jan Kopecky (kopecky@biomed.cas.cz)

Received 6 June 2008; accepted 3 October 2008; published online 15 January 2009. doi:10.1038/oby.2008.602

a weight-loss regimen (9). In general, the insulin-sensitizing effects of n-3 LC-PUFA in subjects with impaired glucose tolerance (IGT) are minimal (10).

The hypolipidemic and antiobesity actions of n-3 LC-PUFA depend on a suppression of lipogenesis combined with increased fatty acid oxidation in the liver (4,11). However, enhanced mitochondrial biogenesis and β-oxidation in white adipose tissue (WAT) may also contribute (12). Moreover, n-3 LC-PUFA reduce WAT inflammation associated with obesity (13), while stimulating secretion of the insulin-sensitizing hormone adiponectin (6,14). The effects of n-3 LC-PUFA are largely mediated by peroxisome proliferator–activated receptors (PPARs), with PPAR-α and PPAR-δ (-β) representing the main targets for n-3 LC-PUFA (15,16); however, other factors, such as liver X receptor, hepatocyte nuclear factor-4α, and sterol-regulatory element binding protein, are also involved (for review see refs. 17,18). Decreased binding of both sterol-regulatory element binding protein–1c and nuclear factor-Y to promoters of lipogenic genes (19), as well as activation of AMP-activated protein kinase (20), may be of great importance for the liver effects. In addition to being ligands themselves, n-3 LC-PUFA might also act indirectly through their metabolites, eicosanoids, and other lipid molecules (21).

Concerning new pharmacotherapies for obesity-associated IR and type 2 diabetes, mixed agonists of various PPARs (22) or higher-affinity analogues of currently available agonists are being developed. Based on a relatively low efficiency of EPA/DHA in the treatment of IR in humans, the aim of this study was to explore several chemical DHA derivatives, substituted at the C(2)-position, as potential antiobesity and antidiabetic agents. In a mouse model of high-fat feeding, the efficiency of DHA derivatives in the prevention and reversal of obesity, IGT, dyslipidemia, WAT inflammation, and lipid accumulation in nonadipose tissues was analyzed.

METHODS AND PROCEDURES

Animals and experimental design

Male mice of either C57BL/6N genetic background (Charles River, Sulzfeld, Germany) or C57BL/6J background were maintained on a 12:12-h light–dark cycle at 22 °C (2–4 animals/cage). Mice were allowed an unrestricted access to water and a standard chow (STD; extruded Ssniff R/M-H diet; Ssniff Spezialdieten GmbH, Soest, Germany). At 3 months of age, mice were randomly assigned to a composite high-fat diet (cHF; lipids ~35% wt/wt, mostly corn oil), while some mice were maintained on STD diet. Energy content of STD and cHF diet was 13.0 and 22.8 kJ/g, respectively (see http://www.ssniff.com, and (5)). STD diet served as a control for the obesogenic effect of the HF diet. Two experimental approaches were used (see also **Figure 1**):

1. In the "prevention study," various DHA derivatives (Substance 1–4; see below) were admixed to the cHF diet (1.5% of dietary lipids replaced by a DHA derivative) and administered to the 3-month-old C57BL/6N mice for a period of 4 months. The DHA derivatives were tested in three separate experiments A, B, and C (Experiment A: Substance 1; Experiment B: Substance 2 and 3; Experiment C: Substance 4).
2. In the "reversal study," obesity and IGT were induced in C57BL/6J mice by feeding cHF diet for a period of 4 months prior to the subsequent 2-month-long administration of Substance 2 admixed to the cHF diet (1.5% of dietary lipids). To analyze potential contribution of a lower food intake in the beneficial effect of Substance 2 on glucose homeostasis (as observed in the "prevention study"), food intake in a subgroup of cHF-fed mice was reduced by 12% compared with mice fed cHF diet *ad libitum* during the final 2 months of the "reversal study." A separate experiment was also performed to evaluate the effect of EPAX1050 TG (Pronova BioPharma AS, Lysaker, Norway), a triglyceride concentrate of EPA (~15%) and DHA (~45%; EPA/DHA), as well as of pure DHA (~99%; ethyl ester; Pronova BioPharma AS) in *ad libitum*–fed mice; compared with all the experiments with DHA derivatives, a tenfold higher fraction of dietary lipids (i.e., 15% of lipids) was replaced by either EPA/DHA or DHA alone (see also our previous studies (5,6) and **Figure 1**).

The cHF-fed mice always served as controls. Body weight and food intake were monitored weekly, while a fresh ration was offered daily. Mice were killed by cervical dislocation under diethylether anesthesia between 9–11 AM, subcutaneous dorsolumbar and epididymal WAT, interscapular brown adipose tissue, liver, and skeletal muscle (*musculus quadriceps femoris*) were dissected and snap-freezed in liquid nitrogen. Truncal blood was collected into the EDTA-containing tubes and plasma was isolated by centrifugation at 5,000*g* for 10 min at 4 °C. Tissues and plasma were stored at −70 °C for future analyses. The experiments were conducted under the guidelines for the use and care of laboratory animals of the Institute of Physiology.

Chemical α-substituted DHA derivatives

DHA derivatives (for chemical structures, see **Supplementary Figure S1** online) were provided by Pronova BioPharma AS, including α-methyl DHA ethyl ester (Substance 1), α-ethyl DHA ethyl ester (Substance 2), α,α-di-methyl DHA ethyl ester (Substance 3), and α-thioethyl DHA ethyl ester (Substance 4).

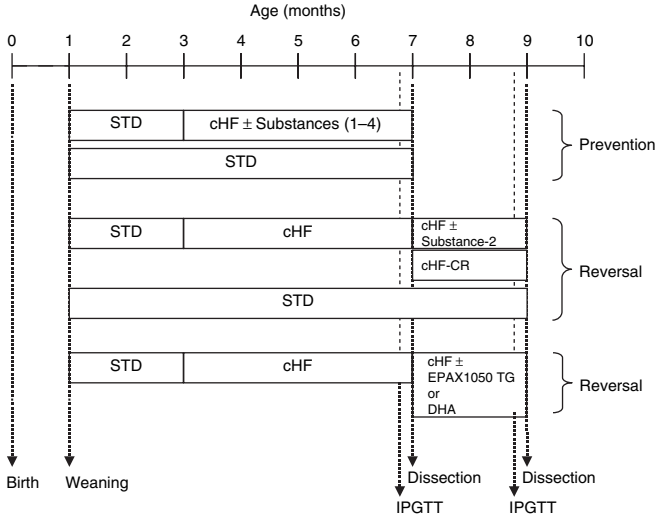

Figure 1 Timeline of experiments. In the "prevention study," 3-month-old mice were switched from a low-fat chow (STD) diet to either composite high-fat (cHF) diet, or cHF diets containing 1.5% of their lipids as DHA derivatives (Substance 1–4). In the "reversal study," 3-month-old mice were fed a cHF diet for a period of 4 months, followed by the treatment with Substance 2 for additional 2 months. A group of mice were also subjected to a 12% caloric restriction diet (cHF-CR; relative to food intake in the cHF group). In the "reversal study," an intraperitoneal glucose tolerance test (IPGTT) was performed 1 week before the end as well as 1 week before the initiation of dietary treatments. In a separate "reversal study" experiment, the effect of EPA/DHA concentrate (EPAX1050 TG) and DHA on *ad libitum*–fed mice was also studied using cHF diets containing 15% of their lipids as the tested compounds (using cHF-fed mice as controls).

Preparation of DHA derivatives

The NMR spectra were recorded in $CDCl_3$, with a Bruker Avance DPX 200 instrument. Mass spectra were recorded with a LC/MS Agilent 1100 series, with a G 1956 A mass spectrometer (electrospray, 3000 V). (University of Oslo, Norway). All reactions were performed under nitrogen or argon atmosphere.

Ethyl (all-Z)-2-methyl-4,7,10,13,16,19-docosahexaenoate (Substance 1)

In this phase, *n*-Butyllithium (1.6 mol/l in hexane, 228 ml, 370 mmol) was added dropwise to a stirred solution of diisopropylamine (60 ml, 420 mmol) in dry tetrahydrofuran (THF; 800 ml) at 0 °C under N_2. The resulting solution was stirred at 0 °C for 30 min, cooled to −78 °C and stirred an additional 30 min before dropwise addition of ethyl (all-Z)-4,7,10,13,16,19-docosahexaenoate (100 g, 280 mmol) in dry THF (500 ml) during 2 h. The resulting solution was stirred at −78 °C for 30 min before methyl iodide (28 ml, 450 mmol) was added. The solution was allowed to reach −20 °C during 1.5 h and then poured into water (1.5 l). The resulting mixture was extracted with heptane (2 × 800 ml). The combined organic extracts were washed with 1 mol/l HCl (1 l), dried (Na_2SO_4) and evaporated *in vacuo*. The residue was purified by flash chromatography (SiO_2, heptane/ethyl acetate 99:1). Yield: 50 g (48%) as a slightly yellow oil. ^{1}H-NMR (200 MHz, $CDCl_3$): δ 1.02 (t, J = 7.5 Hz, 3H), 1.20 (d, J = 6.8 Hz, 3H), 1.29 (t, J = 7.1 Hz, 3H), 2.0–2.6 (m, 5H), 2.8–3.0 (m, 10H), 4.17 (t, J = 7.1 Hz, 2H), 5.3–5.5 (m, 12H), MS (ESI): 393 $[M+Na^+]^+$.

Ethyl (all-Z)-2-ethyl-4,7,10,13,16,19-docosahexaenoat (Substance 2)

n-Butyllithium (1.6 mol/l in hexane, 440 ml, 670 mmol) was added dropwise to a stirred solution of diisopropylamine (111 ml, 780 mmol) in dry THF (750 ml) at 0 °C under N_2. The resulting solution was cooled to −78 °C and stirred an additional 45 min before dropwise addition of ethyl (all-Z)-4,7,10,13,16,19-docosahexaenoate (200 g, 560 mmol) in dry THF (1.6 l) during 4 h. The resulting solution was stirred at −78 °C for 30 min before ethyl iodode (65 ml, 810 mmol) was added. The solution was allowed to reach −40 °C before an additional amount of ethyl iodide (5 ml, 60 mmol) was added, and finally reach −15 °C (during 3 h from −78 °C) before the mixture was poured into water. The resulting mixture was extracted with hexane (2×). The combined organic extracts were washed with 1 mol/l HCl and water, dried (Na_2SO_4) and evaporated *in vacuo*. The residue was purified by flash chromatography (SiO_2, heptane/ethyl acetate 99:1–50:1). Yield: 42 g (20%) as a yellow oil. ^{1}H-NMR (200 MHz; $CDCl_3$): δ 0.8–1.0 (m, 6H), 1.2–1.4 (m, 4H), 1.5–1.7 (m, 2H), 2.12 (m, 2H), 2.3–2.5 (m, 2H), 2.8–3.0 (m, 10H), 4.18 (t, J = 7.1 Hz, 2H), 5.3–5.6 (m, 12H), MS (ESI): 407 $[M+Na^+]^+$.

Ethyl (all-Z)-2,2-dimethyl-4,7,10,13,16,19-docosahexaenoate (Substance 3)

n-Butyllithium (1.6 mol/l in hexane, 100 ml, 170 mmol) was added dropwise to a stirred solution of diisopropylamine (28 ml, 200 mmol) in dry THF (100 ml) at 0 °C under N_2. The resulting solution was stirred at 0 °C for 30 min, cooled to −78 °C before dropwise addition of (50 g, 140 mmol) in dry THF (200 ml). The resulting solution was stirred at −78 °C for 30 min before methyl iodide (17 ml, 280 mmol) was added. The solution was allowed to reach −10 °C and then poured into water. The resulting mixture was extracted with hexane (2×). The combined organic extracts were washed with 1 mol/l HCl, dried (Na_2SO_4) and evaporated *in vacuo*. This procedure was repeated, but the crude product was used instead of ethyl (all-Z)-4,7,10,13,16,19-docosahexaenoate. The residue was purified by flash chromatography (SiO_2, heptane/ethyl acetate 99:1–98:2). Yield: 32 g (59%) as a slightly yellow oil.^{1}H-NMR (200 MHz; $CDCl_3$): δ 1.01 (t, J = 7.5 Hz, 3H), 1.21 (s, 6H), 1.28 (t, J = 7.1 Hz, 3H), 2.08 (m, 2H), 2.34 (d, J = 6.8 Hz, 2H), 2.8–3.0 (m, 10H), 4.15 (q, J = 7.5 Hz, 2H), 5.3–5.6 (m, 12H) ^{13}C-NMR (50 MHz; $CDCl_3$): δ 14.7, 21.0, 25.3, 26.0, 26.1, 38.3, 42.8, 60.7, 125.8, 127.4, 128.3, 128.5, 128.6, 128.7, 129.0, 130.7, 132.4, 177.9, MS (ESI): 385 $[M+H^+]^+$.

Ethyl (all-Z)-2-thioethyl-4,7,10,13,16,19-docosahexaenoate (Substance 4)

Step 1: Synthesis of ethyl (all-Z)-2-iodo-4,7,10,13,16,19-docosahexaenoate. *n*-Butyllithium (1.6 mol/l in hexane, 158 ml, 253 mmol,) was added dropwise to a stirred solution of diisopropylamine (42 ml, 298 mmol) in dry THF (150 ml) at 0 °C under N_2. The resulting solution was cooled to −78 °C and stirred for 35 min before dropwise addition of ethyl (all-Z)-4,7,10,13,16,19-docosahexaenoate (75 g, 210 mmol) in dry THF (300 ml). The resulting solution was stirred at −78 °C for 30 min before iodine (91 g, 359 mmol) in THF (200 ml) was added dropwise. The solution was stirred at −78 °C for 20 min, then poured into water (200 ml). The resulting mixture was extracted with heptane (300 ml). The organic extract was washed with 1 mol/l HCl (150 ml) and water (200 ml), dried (Na_2SO_4) and evaporated *in vacuo*. The residue was purified by flash chromatography (SiO_2, heptane/ethyl acetate 100:1). Yield: 26 g (26%) as a yellow oil. ^{1}H-NMR (200 MHz, $CDCl_3$): δ 0.94 (t, J = 7.5 Hz, 3H), 1.24 (t, J = 7.1 Hz, 3H), 2.04 (quint, J = 7.1 Hz, 2H), 2.69–2.84 (m, 12 H), 4.17 (q, J = 7.1 Hz, 2H), 4.22 (t, J = 7.9 Hz, 1H), 5.24–5.49 (m, 12 H), ^{13}C NMR (50 MHz, $CDCl_3$): δ 13.7, 14.2, 25.5, 26.0 (2 signals), 25.8, 34.0, 61.7, 126.1, 127.0, 127.4, 127.8, 127.9, 128.0, 128.2, 128.5, 128.5, 131.6, 131.9, 170.9 (4 signals hidden), MS (ESI): 505 $[M+Na^+]^+$.

Step 2: Synthesis of ethyl (all-Z)-2-thioethyl-4,7,10,13,16,19-docosahexaenoate. Sodium ethyl thiolate (2.1 g, 25 mmol) was added to a solution of ethyl (all-Z)-2-iodo-4,7,10,13,16,19-docosahexaenoate (11.0 g, 23 mmol) in THF (100 ml) at 0 °C under N_2. The resulting mixture was stirred at 0 °C for 1 h. 1 mol/l HCl was added followed by heptane. The phases were separated and the organic phase was washed with water (2×), dried (Na_2SO_4) and evaporated *in vacuo*. The residue was purified by flash chromatography (SiO_2, heptane/ethyl acetate 30:1. Yield: 7.3 g (76 %) as a pale yellow oil. ^{1}H-NMR (200 MHz, $CDCl_3$): δ 1.1–1.3 (m, 9H), 2.05 (m, 2H), 2.3–2.7 (m, 4H), 2.7–2.9 (m, 10H), 3.25 (m, 1H), 4.17 (q, J = 7.1 Hz, 2H), 5.3–5.5 (m, 12H), MS (ESI): 439 $[M+Na^+]^+$.

Plasma metabolites, hormones, and enzymes

Blood glucose was measured using calibrated glucometers OneTouch Ultra (Life Scan, Milpitas, CA). Plasma triglycerides, cholesterol, aspartate aminotransferase, alanine aminotransferase, and creatine kinase were measured using a clinical analyzer and enzymatic kits from Roche Diagnostics (Mannheim, Germany). Nonesterified fatty acids (NEFA) were measured by a kit from Waco Chemicals (Neuss, Germany). Plasma insulin levels were determined by the Sensitive Rat Insulin RIA Kit (LINCO Research, St Charles, MO), and total immunoreactive adiponectin and leptin were measured by a 2-site ELISA (R&D Systems, Minneapolis, MN; (6)).

Glucose tolerance test

An intraperitoneal glucose tolerance test was performed after an overnight fasting (15–16 h). Blood glucose was assessed by tail bleeds at the baseline (fasting blood glucose; FBG) and after the injection of D-glucose (1 g/kg body weight). In the "reversal study," intraperitoneal glucose tolerance test was performed 1 week before the start (baseline) and 1 week before the end (final) of the 2-month-long treatment period. Results were expressed either as area under the curve (AUC) for glucose or as a change in blood glucose levels (ΔBlood glucose; final–baseline), derived from the glycemic curves of intraperitoneal glucose tolerance test measured before and after the treatment. In the latter case, the greater was the beneficial effect on glucose tolerance after the treatment, the greater was the negative deviation of a glycemic curve from the baseline.

RNA extraction and real-time quantitative PCR analysis

Total RNA was isolated from samples of WAT, liver, and skeletal muscle stored in RNA*later* Solution (Ambion, Austin, TX) by using TRIzol Reagent (Invitrogen, Carlsbad, CA). Muscle samples were grinded

under liquid nitrogen prior to homogenization. A quantity of 0.5 µg of total RNA was reverse transcribed to cDNA, and gene expression was analyzed by real-time PCR, using the LightCycler Instrument (Roche Diagnostics, Mannheim, Germany) as before (6). Oligonucleotide primers, described in **Supplementary Table S1** online, were designed using Lasergene software (DNAStar, Madison, WI). Gene expression data were expressed as a percentage of the cHF-fed controls.

Tissue triglycerides

Tissue fragments (~50 mg) were digested in 0.15 ml of 3 mol/l alcoholic KOH and the resulting homogenates were diluted tenfold with H_2O. After neutralization by 2.5 N $HClO_4$, deliberated glycerol was assayed in supernatants (4 µl) by Free Glycerol Reagent (Sigma-Aldrich, Prague, Czech Republic). Tissue triglyceride concentration was calculated relative to a glycerol standard (1 mg/ml; Sigma-Aldrich, Prague, Czech Republic) using a ratio of 1:10 for molecular weights of glycerol:triglyceride.

Light microscopy and immunohistochemical analysis

Samples of epididymal WAT and liver were fixed in 4% formaldehyde, embedded in paraffin and cut into 5 µm-sections. The liver sections were stained by hematoxylin-eosine, while the sections of epididymal fat were processed to detect a macrophage marker, MAC-2/galectin-3, by the use of specific antibodies (23). Digital images were captured using Olympus AX70 light microscope and a DP 70 camera (Olympus, Tokyo, Japan). Adipocyte morphometry was performed using a Lucia IMAGE version 4.81 (Laboratory Imaging, Prague, Czech Republic).

Statistical analysis

Data are presented as means ± s.e. Data were analyzed by a one-way ANOVA or two-way Repeated Measures ANOVA (only the analysis of glucose tolerance in the "reversal study") using SigmaStat statistical software. Logarithmic transformation was used to stabilize variance in cells when necessary. The Holm–Sidak test for multiple comparisons was used. Threshold of significance was defined at $P < 0.05$.

RESULTS

Reduction of body weight and adiposity by DHA derivatives

The effect of four different DHA derivatives (Substance 1–4) on body weight, food intake, and adiposity in the "prevention study" is summarized in **Table 1**. Compared to the cHF-fed mice, all DHA derivatives except Substance 3 reduced weight gain and Substance 2 exerted the strongest effects. Mice fed Substance 2 had a reduced food intake, and the feeding efficiency was decreased by ~70% in these animals. Substance 2 reduced the weight of subcutaneous and epididymal WAT by 73 and 42%, respectively, while the remaining DHA derivatives had less effect on adiposity. The dramatic effect of Substance 2 could be partly explained by a reduction of cellularity of WAT, as reflected by a 66% decrease in the DNA content of epididymal WAT. Furthermore, Substance 2 and 3 also decreased the weight of interscapular brown adipose tissue.

The effect of the most potent DHA derivative, Substance 2, was also examined in dietary obese mice in the "reversal study" (**Table 2**). Administration of Substance 2 for a period of 2 months resulted in a net weight loss in obese mice. This effect could be explained, at least in part, by a decreased weight of fat depots, which was accompanied by a reduction of cellularity (DNA data in **Table 2**). In line with the "prevention study," the average food intake in Substance 2-fed mice was decreased

Table 1 The effect of DHA derivatives on energy balance and tissue parameters in the "prevention study"

	STD	cHF	Substance 1	Substance 2	Substance 3	Substance 4
Whole-body parameters						
Body weight (g)	32.4 ± 0.7*	49.6 ± 0.6	44.0 ± 1.5*	30.1 ± 1.1*	46.3 ± 1.6	45.9 ± 1.1*
Weight gain (g)[a]	7.8 ± 0.4*	25.2 ± 0.5	20.2 ± 1.3*	6.4 ± 0.8*	22.4 ± 1.4	21.7 ± 0.9*
Food intake[b]	3.64 ± 0.04*	2.70 ± 0.02	2.64 ± 0.03	2.38 ± 0.05*	2.62 ± 0.02	100 ± 1
Feeding efficiency[c]	0.13 ± 0.02*	0.62 ± 0.08	0.48 ± 0.07	0.17 ± 0.03*	0.57 ± 0.06	0.55 ± 0.06
Tissue weight (mg)						
Subcutaneous WAT	345 ± 31*	1,361 ± 55	916 ± 57*	357 ± 39*	1,189 ± 71	1,417 ± 131
Epididymal WAT	980 ± 102*	1,551 ± 99	2,029 ± 176	877 ± 112*	2,427 ± 186*	2,449 ± 194*
BAT	130 ± 9*	263 ± 7	251 ± 24	91 ± 9*	194 ± 14*	260 ± 29
Liver	1,612 ± 30*	2,122 ± 71	2,055 ± 220	2,404 ± 95	2,405 ± 175	2,109 ± 161
Epididymal WAT DNA						
µg DNA/depot	300 ± 37*	1043 ± 86	ND	355 ± 56*	ND	ND
µg DNA/mg tissue	0.31 ± 0.02*	0.74 ± 0.08	ND	0.42 ± 0.05*	ND	ND
Triglycerides (mg/g tissue)						
Liver	36 ± 2*	122 ± 8	ND	74 ± 10*	ND	ND
Skeletal muscle	25 ± 3*	56 ± 6	ND	22 ± 2*	ND	ND

The data represent the mean ± s.e. (STD, $n = 13$; cHF, $n = 27$; Substance 1–4, $n = 8$); the data for cHF-fed mice were pooled from three experiments (see also METHODS AND PROCEDURES and **Supplementary Table S2** online).
BAT, brown adipose tissue; cHF, composite high-fat diet; ND, not determined; STD, low-fat chow diet; WAT, white adipose tissue.
[a]Calculated for a period of 16 weeks, from the start of feeding until the time point, when glucose tolerance test was performed one week before the killing of animals. [b]Measured weekly and expressed as grams of diet consumed by a mouse per day. [c]Calculated as body weight gained for each week divided by the amount of food consumed for that week (grams/grams). *$P < 0.05$ vs. cHF. 1.5% of dietary lipids was replaced by a DHA derivative.

Table 2 The effect of Substance 2 in the "*reversal study*"

	STD	cHF	Substance 2
Whole-body parameters			
Body weight (g)	34.8 ± 1.1*	52.8 ± 1.9	41.2 ± 1.5*
Weight gain (g)[a]	1.38 ± 0.30*	5.88 ± 1.19	−7.61 ± 1.11*
Food intake[b]	ND	3.19 ± 0.05	2.89 ± 0.07*
Tissue weight (mg)			
Subcutaneous WAT	622 ± 66*	1,872 ± 191	986 ± 122*
Epididymal WAT	1,146 ± 147*	2,021 ± 90	1,364 ± 134*
BAT	158 ± 5*	330 ± 32	158 ± 11*
Liver	1,596 ± 28*	2,556 ± 161	3,017 ± 60*
Epididymal WAT DNA			
µg DNA/depot	335 ± 11*	750 ± 72	515 ± 47*
µg DNA/mg tissue	0.31 ± 0.04	0.37 ± 0.03	0.40 ± 0.04
Tissue triglycerides (mg/g tissue)			
Liver	66 ± 14*	268 ± 22	83 ± 7*
Skeletal muscle	49 ± 6*	190 ± 31	77 ± 10*
Blood/plasma			
Triglycerides (mmol/l)	1.56 ± 0.09	1.60 ± 0.09	0.72 ± 0.06*
NEFA (mmol/l)	0.89 ± 0.08	0.97 ± 0.05	0.73 ± 0.04*
Cholesterol (mmol/l)	1.76 ± 0.14*	5.24 ± 0.27	3.90 ± 0.13*
FBG (mg/dl)	86 ± 5*	118 ± 4	99 ± 4*
Insulin (ng/ml)	1.12 ± 0.54*	4.34 ± 0.33	1.40 ± 0.33*

The data are means ± s.e. (STD, $n = 4$; cHF, $n = 9$; Substance 2, $n = 9$).
BAT, brown adipose tissue; cHF, composite high-fat diet; FBG, fasting blood glucose; ND, not determined; NEFA, nonesterified fatty acids; STD, low-fat chow diet; WAT, white adipose tissue. [a]Calculated for a period of 7 weeks, from the start of feeding until the time point, when glucose tolerance test was performed one week before the killing of animals. [b]Measured weekly and expressed as grams of diet consumed by a mouse per day. *$P < 0.05$ vs. cHF. 1.5% of dietary lipids was replaced by Substance 2.

by 9%. A separate experiment revealed that the reduction in body weight gain induced by either DHA alone or EPA/DHA concentrate (admixed at a tenfold higher dose to cHF diet as compared to Substance 2; that is, replacing 15% vs. 1.5% of dietary lipids) was relatively mild, while no effect on food intake was observed (**Supplementary Table S2** online).

Prevention of adipocyte hypertrophy and macrophage infiltration of WAT by Substance 2

In the "prevention study," histological analysis of epididymal WAT (**Figure 2a,b,c**) revealed adipocyte hypertrophy in the cHF-fed mice, resulting in a approximately twofold increase in the mean cell size. This effect was completely prevented by Substance 2 (**Figure 2d**). Moreover, Substance 2 also completely prevented obesity-associated macrophage infiltration of WAT, as revealed by immunohistochemical detection of Mac-2 (**Figure 2**; white arrows). Macrophages aggregate in crown-like structures surrounding individual adipocytes (23). While the density of crown-like structures was ~77-fold higher in cHF-fed compared with STD-fed mice, Substance 2 completely prevented this effect (**Figure 2e**). Moreover, in

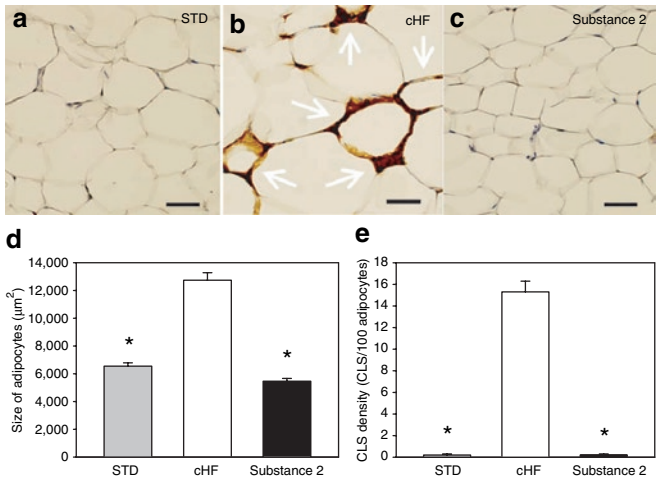

Figure 2 The effect of Substance 2 on adipose tissue morphology and macrophage infiltration in the "prevention study." The amount of MAC-2 immunoreactive macrophages (brownish color) was analyzed in epididymal fat. Sections were counterstained with hematoxylin-eosin. (**a**) Mice fed a low-fat chow (STD) diet. (**b**) Composite high-fat (cHF) diet. (**c**) Substance 2. Arrows indicate crown-like structures (CLS) surrounding individual adipocytes, where the majority of macrophages are lozalized. Bar = 50 µm. (**d**) Size of adipocytes. (**e**) CLS density. The morphometry data are based on >1,000 cells taken randomly from 5 different areas per animal ($n = 3$). *$P < 0.05$ vs. cHF diet (ANOVA).

epididymal WAT Substance 2 reduced mRNA levels of *CD68* and monocyte chemoattractant protein-1 (*MCP-1*), two factors that are closely linked to macrophage function, by 91 and 56%, respectively (**Supplementary Table S4** online). In the "reversal study," Substance 2 reduced the accumulation of macrophages in epididymal WAT by 65% (not shown) and expression of *CD68* and *MCP-1* by 32 and 50%, respectively (**Supplementary Table S4** online). Thus, Substance 2 completely prevents and even partially reverses adipocyte hypertrophy and macrophage infiltration of WAT, induced by the obesogenic cHF diet.

Given the strong effect of Substance 2 on adiposity and obesity-associated inflammation of WAT, two major adipokines, leptin and adiponectin, were evaluated after 2 months of treatment in the "prevention study." Compared with cHF-fed mice, plasma leptin levels were strongly reduced by Substance 2 (4.4 ± 0.3 vs. 86.0 ± 6.2 ng/ml; $P < 0.00001$) and reached the levels observed in the STD-fed mice (6.9 ± 0.9 ng/ml). Plasma adiponectin levels were also slightly reduced (Substance 2, 7.1 ± 0.6 vs. cHF, 9.3 ± 0.5; $P < 0.05$) and were similar to those observed in STD-fed mice (6.9 ± 0.4 ng/ml).

The effects on liver and muscle

In both "prevention" (**Table 1**) and "reversal" (**Table 2**) study, cHF diet significantly increased liver weight. Compared to cHF-fed mice, Substance 2 increased the liver weight in the "reversal study." Importantly, in both studies, Substance 2 reduced the accumulation of triglycerides in liver and skeletal muscle, normally induced after cHF feeding. The induction of liver steatosis by cHF diet and a decrease of triglyceride accumulation by Substance 2 in the "reversal

study" were also confirmed by light microscopy (**Figure 3**). Importantly, livers from mice treated with Substance 2 contained small parenchymal cells of normal morphology, a picture compatible with active regeneration and extensive remodelling of the tissue.

While aspartate aminotransferase levels in plasma of Substance-2-treated mice were unchanged (not shown), alanine aminotransferase levels were increased (Substance 2, 11.33 ± 2.61 vs. cHF, 1.04 ± 0.11 μkat/l; $P < 0.01$) in the "prevention study." Plasma levels of creatine kinase, a marker of muscle cell integrity, were unchanged (not shown). In the "reversal study," Substance 2 increased both aspartate aminotransferase (Substance 2, 12.07 ± 2.30 vs. cHF, 4.98 ± 0.55 μkat/l; $P < 0.05$) and alanine aminotransferase (Substance 2, 11.19 ± 2.45 vs. cHF, 0.97 ± 0.17 μkat/l; $P < 0.05$). The elevated plasma levels of hepatic markers in Substance-2-treated mice, especially in the "reversal study," can be explained by intense regeneration of liver parenchyma accompanying removal of lipid-engorged hepatocytes.

The expression of genes involved in fatty acid oxidation in the liver, such as acyl-CoA oxidase-1 (*Aox-1*) and carnitine palmitoyltransferase-1α (*Cpt-1α*), was higher in animals fed cHF compared with STD diet. This was evident in both the "prevention" and the "reversal" study. These genes were even more upregulated by Substance 2. There was a stronger induction of the peroxisomal (*Aox-1*) than the mitochondrial (*Cpt-1α*) pathway. In both cases, the induction was stronger in the "reversal" than in the "prevention" study (**Supplementary Table S4** online and **Figure 3f**). In a separate "reversal study" experiment, EPA/DHA concentrate and to a lesser extent also DHA alone upregulated *Cpt-1α* (but not *Aox-1*) mRNA levels. However, these changes were relatively small compared to the effects of Substance 2 admixed at a tenfold lower dose to cHF diet. Strong induction of *Aox-1* and *Cpt-1α* expression by Substance 2 correlated well with a marked increase in the expression of their regulatory transcription factor PPAR-α (**Supplementary Table S4** online).

n-3 LC-PUFA are known to decrease expression of lipogenic genes like stearoyl-coenzyme A desaturase-1 (*Scd-1*), as well as other genes (*Spot 14* and farnesyl diphosphate synthase (*Fdps*); (19)). Expression of *Scd-1, Spot 14*, and *Fdps* was downregulated by cHF when compared with STD diet. In the "reversal study," expression of *Scd-1* and *Spot 14* was decreased by both EPA/DHA and by DHA alone. In contrast, expression of *Scd-1* and *Fdps* was markedly induced by Substance 2, namely in the "reversal study" (**Supplementary Table S4** online).

In the skeletal muscle, Substance 2 exerted negligible effects on gene expression except for a downregulation of *Scd-1* (**Supplementary Table S4** online).

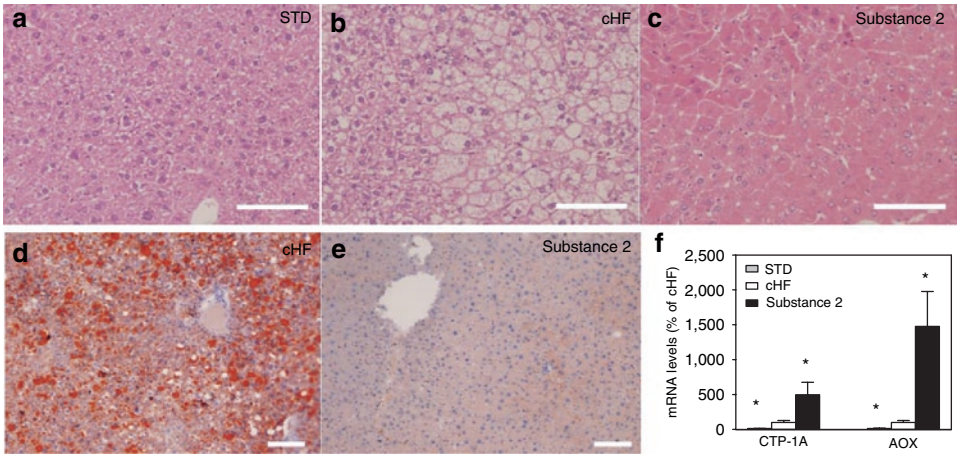

Figure 3 The effect of Substance 2 on liver histology and gene expression in the "reversal study." Liver morphology assessed by hematoxyline-eosin staining of liver sections from mice fed (**a**) low-fat chow (STD) diet, (**b**) composite high-fat (cHF) diet, and (**c**) Substance 2. Visualization of neutral lipids (in red) by Sudan III staining in the liver of mice fed (**d**) cHF diet and (**e**) Substance 2. Nuclei (in blue) were counterstained by hematoxyline. Bar = 50 μm. (**f**) The expression of genes involved in fatty acid oxidation in the liver. Values represent means ± s.e. (n = 4–8). AOX, acyl-CoA oxidase; CPT-1α, carnitine palmitoyltransferase-1α. *$P < 0.05$ vs. cHF diet (ANOVA).

Table 3 The effect of DHA derivatives on plasma markers of lipid metabolism in the *"prevention study"*

	STD	cHF	Substance 1	Substance 2	Substance 3	Substance 4
Triglycerides	89 ± 6	100 ± 6	99 ± 5	47 ± 7*	79 ± 4*	101 ± 7
NEFA	122 ± 11	100 ± 9	134 ± 7*	81 ± 5*	110 ± 8	100 ± 7
Cholesterol	53 ± 1*	100 ± 4	97 ± 4	80 ± 2*	85 ± 2*	83 ± 13

The data are expressed as percentages of the control cHF diet (~ 100%). 1.5% of dietary lipids was replaced by a DHA derivative. Means ± s.e. (STD, n = 13; cHF, n = 7–13; Substance 1–4, n = 8); the data for cHF-fed mice were pooled from three experiments (see METHODS AND PROCEDURES and **Supplementary Table S2** online).
STD, low-fat chow diet; cHF, composite high-fat diet; NEFA, nonesterified fatty acids.
*$P < 0.05$ vs. cHF.

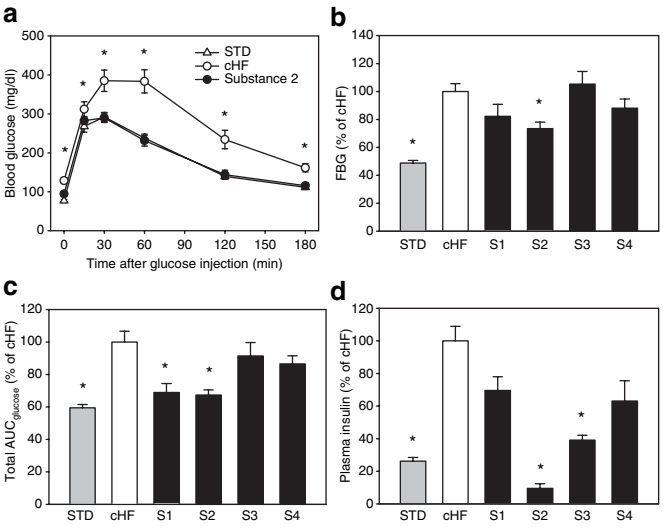

Figure 4 The effect of DHA derivatives on glucose homeostasis in the "prevention study." Mice were fed either a low-fat chow (STD), composite high-fat (cHF) diet, or cHF diet in which 1.5% of lipids was replaced by various DHA derivatives (S1, Substance 1; S2, Substance 2; S3, Substance 3; S4, Substance 4). (**a**) Intraperitoneal glucose tolerance test (IPGTT; glycemic curves for mice fed the STD, cHF, and Substance 2 diets are shown). *$P < 0.05$ vs. other groups (ANOVA). (**b**) Fasting blood glucose (FBG) corresponding to baseline blood glucose levels from IPGTT. (**c**) Total area under the curve for glucose ($AUC_{glucose}$) derived from IPGTT data. (**d**) Plasma insulin in *ad libitum*–fed mice at the time of killing, that is, 1 week after IPGTT. Data are expressed as percentages of the control cHF diet and represent means ± s.e. (STD, $n = 11$; cHF, $n = 7$–13; Substances, $n = 8$). *$P < 0.05$ vs. cHF diet (ANOVA).

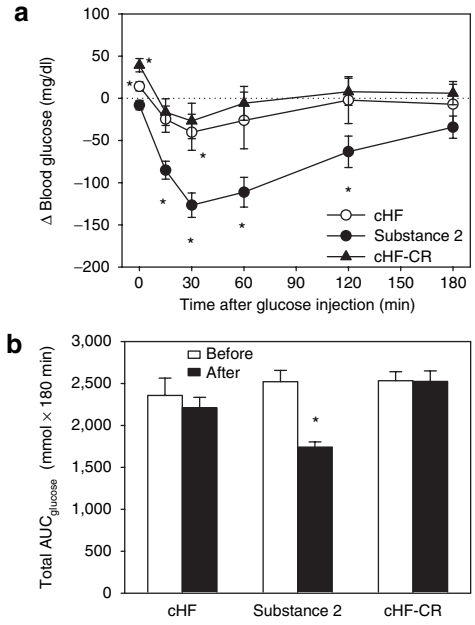

Figure 5 Reversal of impaired glucose tolerance in dietary obese mice by Substance 2 in the "reversal study." Glucose tolerance was assessed by intraperitoneal glucose tolerance test (IPGTT) performed 1 week before the start and 1 week before the end of 2-month-long treatment in mice fed *ad libitum* either a composite high-fat (cHF) diet or cHF diet, containig DHA derivative (Substance 2). Calorie-restricted cHF-fed mice (cHF-CR; 12% restriction) were also analyzed. (**a**) Glycemic curves, representing a change in blood glucose levels during IPGTT measured before and after the treatment. (**b**) Total area under the curve for glucose ($AUC_{glucose}$) derived from IPGTT data obtained before and after the treatment. Values represent means ± s.e. (cHF, $n = 20$; Substance 2, $n = 21$; cHF-CR, $n = 12$). *$P < 0.05$ before vs. after the treatment (two-way repeated measures ANOVA).

Beneficial effects of DHA derivatives on systemic markers of lipid metabolism

In the "prevention study" study, Substance 2 reduced plasma levels of total triglycerides, NEFA, and total cholesterol by 53, 19, and 20%, respectively (**Table 3**). The other substances exerted less pronounced lipid-lowering effects, while Substance 1 even increased plasma NEFA by 34%. In the "reversal study," Substance 2 lowered plasma triglycerides, NEFA, and cholesterol levels by 55, 24, and 25%, respectively (**Table 2**). A separate experiment revealed that DHA alone admixed at a tenfold higher dose to cHF diet compared to Substance 2 had no effect on plasma triglycerides, while EPA/DHA concentrate reduced plasma triglycerides by 40% (**Supplementary Table S2** online), that is, similarly to Substance 2 admixed at a tenfold lower dose (see above).

Beneficial effects of DHA derivatives on glucose homeostasis

In the "prevention study," FBG and glucose tolerance were markedly impaired by cHF feeding, while Substance 2 improved FBG and both Substance 1 and Substance 2 improved glucose tolerance (**Figure 4**). cHF-fed mice also demonstrated hyperinsulinemia, while Substance 2 and Substance 3 exerted protective effects (**Figure 4d**).

Substance 2 also lowered FBG and plasma insulin in dietary obese mice in the "reversal study" (**Table 2**). Importantly, glucose tolerance was also improved by Substance 2 (**Figure 5**). In contrast, neither EPA/DHA nor DHA alone (both admixed at a tenfold higher dose to cHF diet as compared to Substance 2) exerted significant effects on FBG and glucose tolerance (total AUC glucose) in dietary obese mice in the "reversal study," although there was a trend for EPA/DHA to improve glucose tolerance (**Supplementary Table S2** online).

Because Substance 2 reduced food intake by 12% during the "prevention" study, the effect of a 12% calorie restriction on glucose tolerance was analyzed in the "reversal study." Except for increasing FBG, calorie restriction did not have any significant effect on glycemia during intraperitoneal glucose tolerance test (**Figure 5a**) or on total AUC (**Figure 5b**) in obese cHF diet-fed mice. In contrast, calorie restriction decreased body weight by 1.25 ± 0.62 g as compared to a weight loss of 6.89 ± 1.23 g induced by Substance 2 ($P < 0.001$).

DISCUSSION

We report for the first time the metabolic effects of DHA derivatives substituted at the C(2)-position of the molecule. We show that replacement of 1.5% of dietary lipids by various DHA derivatives affected the development of diet-induced obesity and associated metabolic traits in C57BL/6 mice fed a high-fat diet. Substance 2 (α-ethyl DHA ethyl ester) completely prevented and even partially reversed the development

of obesity, fat accumulation, IGT, dyslipidemia, and WAT inflammation. Therefore, besides the general characterization of various DHA derivatives, our study was largely focused on a detailed description of the action of Substance 2.

In agreement with its effect on body weight and adiposity, Substance 2 profoundly affected WAT properties. Similar to the effect of EPA/DHA (5,13), Substance 2 reduced (i) tissue cellularity, (ii) the size of adipocytes, and (iii) macrophage infiltration of WAT. Small adipocytes are more insulin sensitive and less lipolytic, while releasing less inflammatory cytokines, including MCP-1 (24). The reduction of macrophage infiltration should have beneficial systemic effects, as macrophages represent an additional source of proinflammatory cytokines, which induce IR and contribute to a state of chronic low-level inflammation in obesity (25). Similar to the effects of n-3 LC-PUFA (5), Substance 2 also partially prevented downregulation of *Glut4* in WAT, otherwise induced by high-fat diet. WAT is also a source of antiinflammatory and insulin-sensitizing adipokines, leptin and adiponectin. Circulating leptin levels reflect adiposity and obesity is associated with leptin resistance (26,27). Substance 2 markedly decreased plasma leptin levels, reflecting the reduction of adiposity. However, downregulation of *Scd-1* in skeletal muscle of Substance-2-treated mice could also imply improved muscle leptin sensitivity and elevated fatty acid oxidation (28). In contrast to the induction of adiponectin by EPA/DHA (6), Substance 2 decreased plasma adiponectin by ~25% despite dramatically improving glucose tolerance. However, similar plasma adiponectin levels in Substance-2-treated mice and mice fed a low-fat STD diet suggest that plasma adiponectin might not be the best predictor of the metabolic state in this mouse model.

A relatively strong suppression of insulin levels by Substance 2 could hardly represent an indirect effect secondary to improvements in insulin sensitivity. It has been shown that n-3 LC-PUFA reversed glucose-stimulated insulin hypersecretion, normally induced by obesogenic diet, in rat islets (29,30). Therefore, in addition to its effects in other tissues, Substance 2 might act directly on pancreatic β-cells via reduction of insulin secretion. However, further studies are required to clarify this issue.

As published by others (31), DHA derivatives with a hydrophilic substituent at the C(4)-position could lower glucose levels in animal models of diabetes. However, they did not lower blood triglycerides. In contrast, Substance 2 not only prevented and even partially reversed IGT, but it also lowered plasma triglycerides, NEFA, and cholesterol levels. Substance 2 strongly reduced the accumulation of triglycerides in both liver as well as skeletal muscle, resembling the effects of n-3 LC-PUFA (30). The reduced lipid accumulation in the liver and muscle might be a major mechanism, by which Substance 2 counteracted development of IGT.

Substance 2, and to a lesser extent also EPA/DHA concentrate and DHA alone, upregulated *Ppar-α* and its target genes *Aox-1* and *Cpt-1α* in the liver, documenting induction of lipid catabolism and suggesting that Substance 2 acted as a potent PPAR-α agonist (18). In agreement with the known induction of lipogenic genes by pharmacological stimulation of PPAR-α in mouse liver (32), lipogenic *Scd-1* and *Fdps* were strongly induced by Substance 2. Importantly, hepatic *Scd-1* gene expression has been shown to be upregulated by PPARs directly, through a mechanism distinct from the regulation of this gene by polyunsaturated fatty acids (33). A set of sterol-regulatory element binding protein–1c target genes (*Scd-1, Spot 14, and Fdps*) was downregulated by EPA/DHA concentrate or DHA alone as expected (19).

The induction of *Scd-1* and other lipogenic genes by Substance 2 seems to be liver specific because it did not occur in skeletal muscle, where Substance 2 even downregulated *Scd-1* expression. The simultaneous stimulation of *in situ* lipogenesis and lipid oxidation by Substance 2 in the liver suggests induction of futile substrate cycling, which may be responsible for the reduced accumulation of triglycerides in the tissue and possibly also for decreased feeding efficiency of Substance-2-treated mice.

Besides increasing the expression of fatty acid oxidation genes, Substance 2 also lowered FBG in both "prevention" and "reversal" study, suggesting a reduction in hepatic glucose production and gluconeogenesis. This finding is in disagreement with previously published reports, linking increased oxidation of fatty acids to the activation of gluconeogenesis in the liver (34,35). However, the coordinated regulation of these metabolic pathways by physiological stimuli such as fasting (35) might be dramatically different from the situation, when hepatic fatty acid oxidation is stimulated by pharmacological activation of PPAR-α. In fact, improved liver insulin sensitivity in response to PPAR-α agonist treatment, as evidenced by lower endogenous glucose production, has been already observed before (36).

The efficacy of Substance 2 is striking because the dose used in our experiments (1.5% of dietary lipids replaced by the DHA derivative) was approximately six- to tenfold lower compared either with the dose of EPA/DHA concentrate (or DHA alone) also used in this study or with other animal studies in which significant effects of EPA and DHA on body weight, adiposity, and plasma lipids (5,6), or IR (8) were observed. Substance 2 reduced body weight gain in association with a reduced feeding efficiency; however, food intake was also slightly reduced. Calorie restriction itself exerts beneficial effects on lipid and glucose metabolism (6,37). However, the "reversal study," which also included the calorie-restricted cHF diet-fed mice, indicated that Substance 2 reversed glucose intolerance independently of the reduction in food intake. Nevertheless, the contribution of body weight change to improved glucose tolerance in Substance-2-treated mice could not be directly estimated. In contrast to Substance 2 and in agreement with human studies (10), EPA/DHA or DHA alone could not reverse established glucose intolerance.

In summary, among the four DHA derivatives tested, Substance 2 (α-ethyl DHA ethyl ester) appeared to exhibit a similar range of beneficial effects on obesity and associated metabolic traits as naturally occurring n-3 LC-PUFA, but with a higher efficacy. Therefore, this compound could qualify as a novel drug for the treatment of obesity, dyslipidemia, and insulin resistance.

SUPPLEMENTARY MATERIAL

Supplementary material is linked to the online version of the paper at http://www.nature.com/oby

ACKNOWLEDGMENTS

This study was supported by the grants from the Czech Science Foundation (303/08/0664 and 303/07/0708), Pronova BioPharma AS (Lysaker, Norway), and MITOFOOD (COST Action FA0602). We acknowledge Synthetica AS (Forskningsparken, Oslo) for the synthesis of the DHA derivatives. We also thank Saverio Cinti (University of Ancona, Italy) for advice concerning histological analysis.

DISCLOSURE

Dr Bryhn, Dr Berge, and Dr Holmeide were employees of Pronova BioPharma AS at the time of this study.

REFERENCES

1. Despres JP, Lemieux I. Abdominal obesity and metabolic syndrome. *Nature* 2006;444:881–887.
2. Muoio DM, Newgard CB. Mechanisms of disease: molecular and metabolic mechanisms of insulin resistance and beta-cell failure in type 2 diabetes. *Nat Rev Mol Cell Biol* 2008;9:193–205.
3. Nissen SE, Wolski K. Effect of rosiglitazone on the risk of myocardial infarction and death from cardiovascular causes. *N Engl J Med* 2007;356:2457–2471.
4. Rustan AC, Christiansen EN, Drevon CA. Serum lipids, hepatic glycerolipid metabolism and peroxisomal fatty acid oxidation in rats fed omega-3 and omega-6 fatty acids. *Biochem J* 1992;283:333–339.
5. Ruzickova J, Rossmeisl M, Prazak T *et al*. Omega-3 PUFA of marine origin limit diet-induced obesity in mice by reducing cellularity of adipose tissue. *Lipids* 2004;39:1177–1185.
6. Flachs P, Mohamed-Ali V, Horakova O *et al*. Polyunsaturated fatty acids of marine origin induce adiponectin in mice fed high-fat diet. *Diabetologia* 2006;49:394–397.
7. Woodman RJ, Mori TA, Burke V *et al*. Effects of purified eicosapentaenoic and docosahexaenoic acids on glycemic control, blood pressure, and serum lipids in type 2 diabetic patients with treated hypertension. *Am J Clin Nutr* 2002;76:1007–1015.
8. Storlien LH, Kraegen EW, Chisholm DJ *et al*. Fish oil prevents insulin resistance induced by high-fat feeding in rats. *Science* 1987;237:885–888.
9. Mori TA, Bao DQ, Burke V *et al*. Dietary fish as a major component of a weight-loss diet: effect on serum lipids, glucose, and insulin metabolism in overweight hypertensive subjects. *Am J Clin Nutr* 1999;70:817–825.
10. Fasching P, Ratheiser K, Waldhausl W *et al*. Metabolic effects of fish-oil supplementation in patients with impaired glucose tolerance. *Diabetes* 1991;40:583–589.
11. Berge RK, Madsen L, Vaagenes H, Tronstad KJ, Gottlicher M, Rustan AC. In contrast with docosahexaenoic acid, eicosapentaenoic acid and hypolipidaemic derivatives decrease hepatic synthesis and secretion of triacylglycerol by decreased diacylglycerol acyltransferase activity and stimulation of fatty acid oxidation. *Biochem J* 1999;343:191–197.
12. Flachs P, Horakova O, Brauner P *et al*. Polyunsaturated fatty acids of marine origin upregulate mitochondrial biogenesis and induce beta-oxidation in white fat. *Diabetologia* 2005;48:2365–2375.
13. Todoric J, Loffler M, Huber J *et al*. Adipose tissue inflammation induced by high-fat diet in obese diabetic mice is prevented by n-3 polyunsaturated fatty acids. *Diabetologia* 2006;49:2109–2119.
14. Neschen S, Morino K, Rossbacher JC *et al*. Fish oil regulates adiponectin secretion by a peroxisome proliferator-activated receptor-γ-dependent mechanism in mice. *Diabetes* 2006;55:924–928.
15. Forman BM, Chen J, Evans RM. Hypolipidemic drugs, polyunsaturated fatty acids, and eicosanoids are ligands for peroxisome proliferator-activated receptors α and δ. *Proc Natl Acad Sci USA* 1997;94:4312–4317.
16. Neschen S, Morino K, Dong J *et al*. N-3 fatty acids preserve insulin sensitivity *in vivo* in a PPARα-dependent manner. *Diabetes* 2007;56:1034–1041.
17. Sampath H, Ntambi JM. Polyunsaturated fatty acid regulation of genes of lipid metabolism. *Annu Rev Nutr* 2005;25:317–340.
18. Sanderson LM, de Groot PJ, Hooiveld GJ *et al*. Effect of synthetic dietary triglycerides: a novel research paradigm for nutrigenomics. *PLoS ONE* 2008;3:e1681.
19. Teran-Garcia M, Adamson AW, Yu G *et al*. Polyunsaturated fatty acid suppression of fatty acid synthase (FASN): evidence for dietary modulation of NF-Y binding to the Fasn promoter by SREBP-1c. *Biochem J* 2007;402:591–600.
20. Suchankova G, Tekle M, Saha AK *et al*. Dietary polyunsaturated fatty acids enhance hepatic AMP-activated protein kinase activity in rats. *Biochem Biophys Res Commun* 2005;326:851–858.
21. Serhan CN. Novel omega—3-derived local mediators in anti-inflammation and resolution. *Pharmacol Ther* 2005;105:7–21.
22. Fievet C, Fruchart JC, Staels B. PPARα and PPARγ dual agonists for the treatment of type 2 diabetes and the metabolic syndrome. *Curr Opin Pharmacol* 2006;6:606–614.
23. Cinti S, Mitchell G, Barbatelli G *et al*. Adipocyte death defines macrophage localization and function in adipose tissue of obese mice and humans. *J Lipid Res* 2005;46:2347–2355.
24. Yang X, Smith U. Adipose tissue distribution and risk of metabolic disease: does thiazolidinedione-induced adipose tissue redistribution provide a clue to the answer? *Diabetologia* 2007;50:1127–1139.
25. Wellen KE, Hotamisligil GS. Inflammation, stress, and diabetes. *J Clin Invest* 2005;115:1111–1119.
26. Frederich RC, Hamann A, Anderson S *et al*. Leptin levels reflect body lipid content in mice: evidence for diet-induced resistance to leptin action. *Nat Med* 1995;1:1311–1314.
27. Caro JF, Kolaczynski JW, Nyce MR *et al*. Decreased cerebrospinal-fluid/serum leptin ratio in obesity: a possible mechanism for leptin resistance. *Lancet* 1996;348:159–161.
28. Dobrzyn A, Dobrzyn P. Stearoyl-CoA desaturase—a new player in skeletal muscle metabolism regulation. *J Physiol Pharmacol* 2006;57:31–42.
29. Holness MJ, Greenwood GK, Smith ND, Sugden MC. Diabetogenic impact of long-chain omega-3 fatty acids on pancreatic β-cell function and the regulation of endogenous glucose production. *Endocrinology* 2003;144:3958–3968.
30. Lombardo YB, Chicco AG. Effects of dietary polyunsaturated n-3 fatty acids on dyslipidemia and insulin resistance in rodents and humans. A review. *J Nutr Biochem* 2006;17:1–13.
31. Yamamoto K, Itoh T, Abe D *et al*. Identification of putative metabolites of docosahexaenoic acid as potent PPARγ agonists and antidiabetic agents. *Bioorg Med Chem Lett* 2005;15:517–522.
32. Knight BL, Hebbachi A, Hauton D *et al*. A role for PPARα in the control of SREBP activity and lipid synthesis in the liver. *Biochem J* 2005;389:413–421.
33. Miller CW, Ntambi JM. Peroxisome proliferators induce mouse liver stearoyl-CoA desaturase 1 gene expression. *Proc Natl Acad Sci USA* 1996;93:9443–9448.
34. Williamson JR, Kreisberg RA, Felts PW. Mechanism for the stimulation of gluconeogenesis by fatty acids in perfused rat liver. *Proc Natl Acad Sci USA* 1966;56:247–254.
35. Koo SH, Satoh H, Herzig S *et al*. PGC-1 promotes insulin resistance in liver through PPAR-α-dependent induction of TRB-3. *Nat Med* 2004;10:530–534.
36. Haluzik MM, Lacinova Z, Dolinkova M *et al*. Improvement of insulin sensitivity after peroxisome proliferator-activated receptor-α agonist treatment is accompanied by paradoxical increase of circulating resistin levels. *Endocrinology* 2006;147:4517–4524.
37. Guarente L. Sirtuins as potential targets for metabolic syndrome. *Nature* 2006;444:868–874.

Publication B

Kus V, Prazak T, Brauner P, Hensler M, Kuda O, Flachs P, Janovska P, **Medrikova D**, Rossmeisl M, Jilkova Z, Stefl B, Pastalkova E, Drahota Z, Houstek J, Kopecky J.

Induction of muscle thermogenesis by high-fat diet in mice: association with obesity-resistance.

Am J Physiol Endocrinol Metab. 295: E356-E367, 2008 (IF = 4,129)

Am J Physiol Endocrinol Metab 295: E356–E367, 2008.
First published May 20, 2008; doi:10.1152/ajpendo.90256.2008.

Induction of muscle thermogenesis by high-fat diet in mice: association with obesity-resistance

Vladimir Kus,[1] Tomas Prazak,[1] Petr Brauner,[1] Michal Hensler,[1] Ondrej Kuda,[1] Pavel Flachs,[1] Petra Janovska,[1] Dasa Medrikova,[1] Martin Rossmeisl,[1] Zuzana Jilkova,[1] Bohumir Stefl,[4†] Eva Pastalkova,[3] Zdenek Drahota,[2] Josef Houstek,[2] and Jan Kopecky[1]

Departments of [1]Adipose Tissue Biology, [2]Bioenergetics, and [3]Neurophysiology of Memory and Computational Neuroscience, Institute of Physiology, Academy of Sciences of the Czech Republic; and [4]Department of Physiology and Developmental Biology, Faculty of Science, Charles University, Prague, Czech Republic

Submitted 27 February 2008; accepted in final form 20 May 2008

Kus V, Prazak T, Brauner P, Hensler M, Kuda O, Flachs P, Janovska P, Medrikova D, Rossmeisl M, Jilkova Z, Stefl B,† Pastalkova E, Drahota Z, Houstek J, Kopecky J. Induction of muscle thermogenesis by high-fat diet in mice: association with obesity-resistance. *Am J Physiol Endocrinol Metab* 295: E356–E367, 2008. First published May 20, 2008; doi:10.1152/ajpendo.90256.2008.—The obesogenic effect of a high-fat (HF) diet is counterbalanced by stimulation of energy expenditure and lipid oxidation in response to a meal. The aim of this study was to reveal whether muscle nonshivering thermogenesis could be stimulated by a HF diet, especially in obesity-resistant A/J compared with obesity-prone C57BL/6J (B/6J) mice. Experiments were performed on male mice born and maintained at 30°C. Four-week-old mice were randomly weaned onto a low-fat (LF) or HF diet for 2 wk. In the A/J LF mice, cold exposure (4°C) resulted in hypothermia, whereas the A/J HF, B/6J LF, and B/6J HF mice were cold tolerant. Cold sensitivity of the A/J LF mice was associated with a relatively low whole body energy expenditure under resting conditions, which was normalized by the HF diet. In both strains, the HF diet induced uncoupling protein-1-mediated thermogenesis, with a stronger induction in A/J mice. Only in A/J mice: *1*) the HF diet augmented activation of whole body lipid oxidation by cold; and *2*) at 30°C, oxygen consumption, total content, and phosphorylation of AMP-activated protein kinase (AMPK), and AICAR-stimulated palmitate oxidation in soleus muscle was increased by the HF diet in parallel with significantly increased leptinemia. Gene expression data in soleus muscle of the A/J HF mice indicated a shift from carbohydrate to fatty acid oxidation. Our results suggest a role for muscle nonshivering thermogenesis and lipid oxidation in the obesity-resistant phenotype of A/J mice and indicate that a HF diet could induce thermogenesis in oxidative muscle, possibly via the leptin-AMPK axis.

nonshivering thermogenesis; leptin; adenosine monophosphate-activated protein kinase

MANY HEALTH PROBLEMS IN AFFLUENT SOCIETIES are linked to the increased incidence of obesity. Especially meals with high content of fat are obesogenic, due to a low energetic cost of nutrient storage and a low potency of fat intake to promote fat oxidation (20). Induction of lipid catabolism is crucial for adaptive thermogenesis, which is regulated by the sympathetic nervous system, thyroid hormones, insulin (reviewed in Refs. 19 and 26), and leptin (see below) and is possibly involved in the regulation of body weight in humans (12, 26, 49). However, the mechanisms and organs contributing to adaptive thermogenesis need to be better characterized.

In small mammalian species, hibernators, and mammalian neonates, adaptive thermogenesis largely depends on uncoupling protein-1 (UCP1), which is located in brown adipose tissue. Thermogenesis in brown fat could be activated in response to both cold exposure and a meal (6), and its capacity is increased by adaptation to cold or intake of high-fat (HF) diets. Diet can even act as a preacclimation to cold (6, 36), and brown fat thermogenesis serves to maintain both body temperature and energy balance. However, the capacity does not exceed 60% of total adaptive nonshivering thermogenesis (reviewed in Ref. 19), suggesting a role for other organs in this process (16, 24, 50). Whether skeletal muscle can mediate adaptive nonshivering thermogenesis in mammals is a matter of a long-lasting controversy. Skeletal muscle is an important site of whole body energy expenditure, which can account for 20–30% of the total oxygen uptake in the resting state (6, 19, 25). Differences in resting muscle metabolism explain part of the variance in resting metabolic rate among adult humans and may play a role in the pathogenesis of obesity (55).

A unique role in the complex control of energy homeostasis and thermogenesis is played by adipocyte hormone leptin, which acts both centrally in the hypothalamus and also directly in the peripheral tissues (reviewed in Ref. 35). The administration of leptin reverts reduced metabolic rate, depression of body temperature, and excessive adiposity in genetically obese *ob/ob* mice lacking functional leptin (31). Even in normal mice, leptin induces the capacity for UCP1-mediated thermogenesis (38), and it also stimulates lipid oxidation and uptake of glucose in skeletal muscle by activating AMP-activated protein kinase [AMPK (29)]. The direct thermogenic effect of leptin was also demonstrated in murine skeletal muscle, where exogenous leptin stimulated oxygen consumption (41). Leptin's effects occurred primarily in the oxidative but not glycolytic type of muscle (29, 41).

We hypothesized that muscle nonshivering thermogenesis could be complementary to that mediated by UCP1 in brown fat and could be activated under the conditions of a strong thermogenic response to a HF diet, possibly in association with obesity resistance. Therefore, mice of two different inbred strains were studied: *1*) obesity-prone C57BL/6J (B/6J) mice and *2*) A/J mice, which are relatively resistant to the obeso-

† Deceased. 1 10, 2008.

Address for reprint requests and other correspondence: J. Kopecky, Dept. of Adipose Tissue Biology, Inst. of Physiology, Academy of Sciences of the Czech Republic, Videnska 1083, 142 20 Prague, Czech Republic (e-mail: kopecky@biomed.cas.cz).

The costs of publication of this article were defrayed in part by the payment of page charges. The article must therefore be hereby marked "*advertisement*" in accordance with 18 U.S.C. Section 1734 solely to indicate this fact.

genic environment (45, 46, 53). The different propensities to obesity have previously been shown to be associated with a stronger activation of thermogenesis mediated by UCP1 and UCP2 in brown (17, 48, 52) and white (8, 13, 48, 52) adipose tissue of A/J mice. Mice of the A/J strain also showed a much stronger induction of leptin by the HF diet especially during the early postweaning period (47, 52). In our experiments, to eliminate the confounding effect of cold-induced thermogenesis, all mice were born and maintained at 30°C, i.e., close to their thermoneutral temperature (1), weaned onto a low-fat (LF) or HF diet, and studied 2 wk after weaning. In contrast to B/6J mice, A/J mice could not maintain their body temperature in cold when fed the LF diet, reflecting their relatively low metabolic rate at 30°C. Our results suggest that HF diet induced nonshivering thermogenesis in oxidative skeletal muscle of A/J mice.

METHODS

Animals and study design. All procedures were in accordance with the guidelines for the use and care of laboratory animals of the Institute of Physiology, the directive of the European Communities Council (86/609/EEC), and the *Principles of Laboratory Animal Care* (NIH publication no. 85-23, revised 1985). B/6J and A/J mice were obtained from the Jackson Laboratory (Bar Harbor, ME) and bred at the Institute of Physiology for several generations. Animals were housed in a controlled environment (22°C; 12:12-h light-dark cycle; light from 6:00 AM) with free access to water and chow, a LF diet (ST-1 diet; Velaz, Prague, Czech Republic). The LF diet contained 25, 9, and 66% calories as protein, fat, and carbohydrate, respectively. To obtain animals for this study, pregnant mice were transferred to 30°C 1 wk before delivery, and newborn mice were maintained at this temperature until the end of the experiment. When indicated, some animals born and reared at 22°C were also analyzed. Only male pups were used. Mice were weaned at 4 wk of age, caged singly in Eurostandard type II mouse plastic cages (~6,000 ml; Techniplast, Milan, Italy), and assigned randomly to either the LF or HF diet. The HF diet, proven to be obesogenic in B/6J mice (22), contained 15, 59, and 26% calories as protein, fat, and carbohydrate, respectively. Fatty acid composition of both diets (LF vs. HF, in mol%) was characterized (29.7 vs. 19.6 for saturated fatty acid, 28.3 vs. 55.2 for monounsaturated fatty acid, and 42.1 vs. 25.2 for polyunsaturated fatty acid), and energy densities of LF and HF diets were 3.4 and 5.3 kcal/g, respectively (37). To eliminate the confounding effect of the large differences in adiposity, all analyses described below were performed 2 wk after weaning, except for *1*) 24-h food consumption measurements, which were performed at 2, 4, 9, and 13 days after weaning (Table 1); and *2*) a separate experiment at 30°C, in which the effect of the diet on body weight was followed until 4 mo after weaning (Fig. 1). For the collection of plasma and tissues, ad libitum-fed mice were killed by cervical dislocation between 9:00 and 10:00 AM. EDTA-plasma was prepared from truncal blood and stored at −70°C. Subcutaneous (dorsolumbar) and epididymal white adipose tissue, interscapular brown fat, and gastrocnemius and soleus muscles were dissected and stored in liquid nitrogen for analysis of gene expression. For measurements of oxygen consumption and fatty acid oxidation, freshly dissected muscles were used. For Western blot analysis, soleus muscle was dissected under pentobarbital sodium anesthesia and jet-frozen in liquid nitrogen (see below).

Body temperature and shivering during cold exposure. Two weeks after weaning, singly caged mice fed either the LF or HF diet were transferred to 4°C. Core body temperature was measured just before cold exposure (*time 0*) and at 1, 2, 3, 24, 48, and 72 h in the cold, using a temperature probe (Thermocouple Thermometer; Cole Parmer, Vernon Hills, IL) inserted into the colon. During the cold exposure, animals had free access to food and water.

Table 1. *Growth characteristics and plasma parameters*

	B/6J		A/J	
	LF	HF	LF	HF
BW, g	18.6±0.3	18.4±0.5	17.0±0.7	18.4±0.7
BWG, g	5.63±0.39	4.91±0.20	4.71±0.50	5.31±0.28
FC, kcal/day	7.74±0.8	7.78±0.4	8.06±0.7	8.11±0.4
Weight of fat depots, mg				
BAT	90±3	57±3*	69±3†	61±3*
DL	152±4	180±10*	167±9	252±14*†
EPI	160±8	239±21*	163±14	292±26*
Plasma levels				
TG, mg/dl	148±12	133±19	139±11	130±7
NEFA, μM	264±2	346±18*	274±10	273±18
Leptin, ng/ml	4.48±0.38	5.21±0.54	3.35±0.34†	9.42±1.15*†
T_4, nmol/l	37±2	46±2*	45±1†	45±3
T_3, nmol/l	1.5±0.2	1.9±0.2*	1.9±0.2†	1.9±0.2

Six-week-old mice reared at 30ºC and weaned at 4 wk after birth onto low-fat (LF) or high-fat (HF) diets were analyzed. Mean body weight at time of weaning was similar in all subgroups of mice (12.3–13.5 g). BW, body weight at 6 wk of age; BWG, body weight gain during 2 wk period after weaning; FC, mean food consumption measured at *days 2, 4, 9,* and *13* after weaning; BAT, interscapular brown fat; DL, dorsolumbar white fat; EPI, epididymal white fat; TG, triglyceride; NEFA, nonesterified fatty acid; T_4, thyroxine; T_3, triiodothyronine. Data are means ± SE (n = 11–14). *Significant effect of diet; †significant effect of genotype.

Shivering was monitored in a separate group of mice by means of electromyography (EMG). Before the experiment, mice were transferred to 20°C and anesthetized using diethyl ether, and 0.5-cm Ni-Cr wire (150 μm diameter) electrodes were inserted under the skin. Two recording electrodes were placed above the left and right shoulders of the forelimbs, and a reference electrode was implanted above the rear back. Immediately after recovery from anesthesia, mice were caged singly without bedding, water, or food. Action potentials were amplified (5,000 times), filtered (300–6,000 Hz), and digitized (32-bit resolution, 32 kHz), and data were stored for analysis performed using custom-made software (AcX; Andre A. Fenton, Institute of Physiology, Prague, Czech Republic). After a 20-min period of initial recording at 20°C, the cages were transferred to 4°C, and recording was performed for 50 min. After the experiment, mice were killed by cervical dislocation. During offline analysis of the data, moving artifacts were eliminated on the basis of their high amplitude and time intervals. Voltage values were integrated over 10-min periods.

Indirect calorimetry. Energy expenditure was evaluated using the indirect calorimetry system INCA (Somedic, Horby, Sweden) as described before (1). To minimize stress in the animals, measurements were performed in the standard cages, in which animals had been maintained since weaning (see above), and they were transferred into sealed chambers equipped with thermostatically controlled heat exchangers. Calibration of oxygen sensors was performed before each measurement. Measurements proceeded under a constant airflow rate (1,000 ml/min). Oxygen consumption ($\dot{V}O_2$) and carbon dioxide production ($\dot{V}CO_2$) were recorded every 2 min. The system allowed for four individually housed mice to be monitored simultaneously. During the measurements, lasting for 46 h and starting at 3:00 PM (12:12-h light-dark cycle; light from 6:00 AM), animals had ad libitum access to food (i.e., LF or HF diet, see above). During the initial 23 h, the temperature was set to 30°C followed by a drop to 15°C during a 30-min interval at the beginning of the second 23-h period and kept at 15°C until the end of the measurement. The level of substrate partitioning was estimated by calculating respiratory exchange ratio (RER; i.e., $\dot{V}CO_2/\dot{V}O_2$ ratio). To compare subtle differences between subgroups, the percent relative cumulative frequency (PRCF) curves were also drawn (see Fig. 5), based on RER values pooled from all animals within a given subgroup (24, 34).

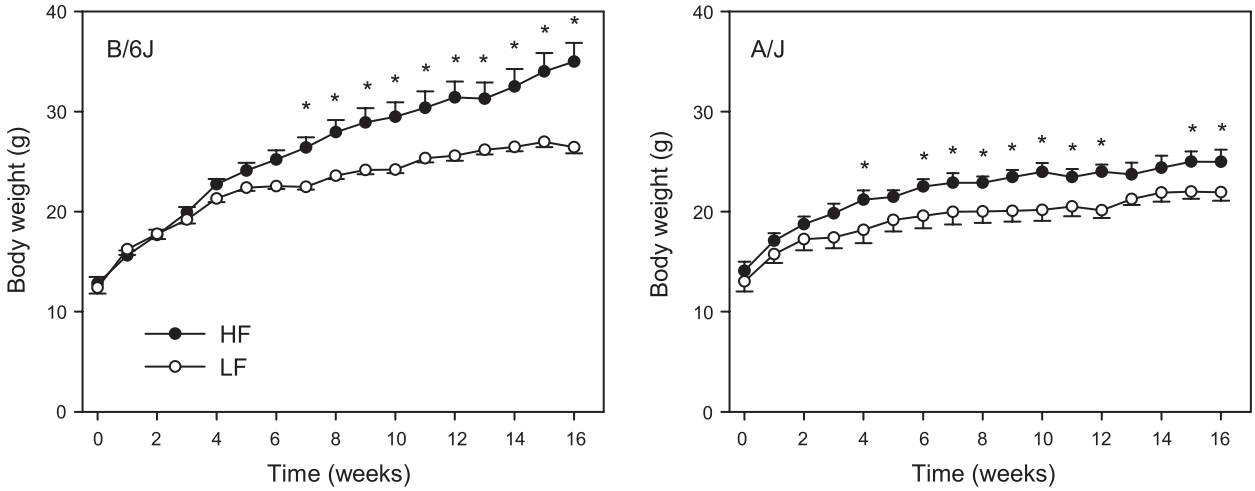

Fig. 1. Body weights in B/6J and A/J mice during prolonged feeding by low-fat (LF) and high-fat (HF) diets. Mice were born and maintained at 30°C. At 4 wk of age (*week 0*), animals were caged singly and weaned either on LF or HF diet. Data are means ± SE (n =7–8). *Significant effect of diet; there was also a significant interaction between diet and genotype (repeated-measures ANOVA).

Norepinephrine-stimulated metabolic rate (NEMR) was measured in anesthetized mice as described before (42) and calculated as a difference between $\dot{V}O_2$ measured 15–20 min before and after intraperitoneal injection of L-norepinephrine D-bitartrate (Sigma-Aldrich; in 5% D-glucose at a dose of 0.6 mg/kg body wt).

Lipids, metabolites, and hormones in plasma. Triglycerides (TG) were estimated using diagnostic kit no. 320-A (Sigma-Aldrich). The concentration of nonesterified fatty acids (NEFA) was evaluated enzymatically using a NEFA C kit (Wako Chemicals, Richmond, VA). Leptin content was assessed by a Mouse Leptin RIA Kit (Linco Research, St. Charles, MO). Serum triiodothyronine (T_3) and thyroxine (T_4) levels were determined with total T_4 and total T_3 RIA kits (Immunotech, Beckman Coulter, Czech Republic).

Measurements of $\dot{V}O_2$ in skeletal muscles. Dissected soleus or gastrocnemius muscle (10 mg wet wt) was placed in a respiratory chamber of Oroboros Oxygraph [Paar, Graz, Austria (15)] filled with 2 ml of freshly oxygenated (95% O_2, 5% CO_2) Krebs-Ringer bicarbonate buffer (pH 7.4), containing 10 mM glucose and warmed to 37°C. $\dot{V}O_2$ was measured continuously and recorded at 1-s intervals between 10 and 35 min after the start of incubation by use of a computer data acquisition system (Datlab; Oroboros, Innsbruck, Austria). Mean values of $\dot{V}O_2$ were calculated for 5-min intervals. Results were normalized to wet weight of the tissue and also to protein content estimated in the tissue homogenate by using the bicinchoninic acid procedure and BSA as a standard (40), prepared after the respirometry.

Measurements of fatty acid oxidation in muscles. Soleus and gastrocnemius muscle was incubated as described above, except that the final volume was 3 ml, and the Krebs-Ringer bicarbonate buffer contained 5 mM glucose and fatty acid-free bovine serum albumin (5 mg/ml, ICN Biomedicals, High Wycombe, UK) complexed (1:3) with palmitic acid (Sigma-Aldrich) and [U-^{14}C]palmitate (0.1 μCi/ml; LACOMED, Czech Republic); see online APPENDIX for details. Muscles from left and right limb were incubated in the absence or presence of AMPK activator 5-aminoimidazole-4-carboxamide-1-β-D-ribofuranoside (AICAR; Sigma-Aldrich) added at a 2 mM final concentration. After 1 h of shaking at 37°C in a closed glass vial (15 ml total volume), the reaction was terminated by injecting 0.3 ml of 5 M H_2SO_4 into the vial, and liberated CO_2 was trapped in 0.3 ml of hyamine hydroxide (PerkinElmer, Waltham, MA) contained in an Eppendorf tube inserted into the incubation vial. After 60 min of CO_2 trapping, $^{14}CO_2$ in hyamine hydroxide was quantified by liquid scintillation counting, and oxidation rate was normalized to tissue protein as above.

Gene expression analysis. Total RNA was isolated (Tri Reagent; MRC, Cincinnati, OH), and levels of different transcripts were evaluated using real-time quantitative PCR (qRT-PCR), a DyNamo Capillary SYBR Green qPCR kit (Finnzymes, Espoo, Finland), and a LightCycler 2.0 instrument (Roche Diagnostics, Mannheim, Germany) as before (11). Lasergene software (DNA Star, Madison, WI) was used to design oligonucleotide primers (see online APPENDIX, Supplemental Table S1). To correct for intersample variations, the level of each transcript was normalized to elongation factor-1α (EF-1α), used as an internal standard, and expressed in arbitrary units (AU). Similar results were obtained using cyclophilin-β as an internal standard (not shown).

Evaluation of UCP1 and protein content. UCP1 was quantified by Western blots (39) in crude cell membranes (100,000 *g*) prepared from homogenates of adipose tissue, using purified UCP1 as a standard (23). Total protein concentration was assessed as above (40).

Quantification of AMPK and acetyl-CoA carboxylase (ACC) in soleus muscle. Muscle lysates were prepared as before (27). Total amount of the α1 and α2 catalytic subunits of AMPK (AMPKα1, AMPKα2) and the phosphorylated form of AMPK (p-AMPK) were determined by Western blotting using a mixture of primary antibodies: *1*) sheep antibodies against AMPKα1 and -α2 [1:3,500; kind gift from D. Grahame Hardie, University of Dundee, UK (53)], and *2*) phosphospecific rabbit antibodies against the Thr^{172} of the α-subunits of AMPK (1:1,000; no. 2535, lot no. 6; Cell Signaling Technology, Danvers, MA). As secondary antibodies, a mixture of infrared dye-labeled antibodies was used: *1*) donkey anti-sheep IgG conjugated to infrared dye 680 (1:5,000, no. A-21102, Lot no. 93C2-1; Alexa fluor 680 donkey anti-sheep IgG; Molecullar Probes, Leiden, The Netherlands), and 2) donkey anti-rabbit IgG conjugated to infrared dye 800 (1:5,000, no. 611-732-127, Lot no. 13176; infrared dye 800 anti-rabbit IgG donkey; Rockland, Gilbertsville, PA). Both total and p-AMPK were quantified on the same blot using the Odyssey IR Imaging Systems (Li-Cor Biosciences, Lincoln, NE). Total content of ACC and its phosphorylated form were quantified using Western blotting and specific antibodies as before (3). Prestained protein M_r standards (PageRuler Prestained Protein Ladder; Fermentas, Burlington, ON, Canada) were used to locate positions of AMPK or ACC on the blots. Signals on different blots were compared using a standard prepared from the liver of adult LF diet-fed B/6J mice and expressed in arbitrary units. The value for each mouse represents the mean of values obtained from the left and right soleus muscles.

Statistics. The data were analyzed by a two-way ANOVA, using SigmaStat statistical software. Logarithmic transformation was used

to stabilize variance in cells when necessary. Repeated ANOVA measurements were performed to analyze $\dot{V}O_2$ in muscles. To the analyze statistical significance of differences in PRCF of RER values in the indirect calorimetry (see *Indirect calorimetry*), data from each mouse were treated separately. The PRCF curves were fitted with sigmoidal dose-response (variable slope) function using GraphPad Prism v. 4.03 for Windows (GraphPad Software, San Diego, CA). Both log EC_{50} and Hill slope values were compared in a two-way ANOVA (diet × temperature). Tukey's test for all pairwise multiple comparisons was used. All values are presented as means ± SE. Comparisons were judged to be significant at $P \leq 0.05$.

RESULTS

Gross phenotypes and plasma parameters. B/6J and A/J mice were born and maintained at 30°C, weaned onto LF or HF diet at 4 wk of age, and killed 2 wk later. At weaning, as well as at the time of euthanasia, mice of both strains had similar body weights independent of the type of diet. Accordingly, body weight gains during the 2-wk postweaning period were similar in all animal subgroups (Table 1). Caloric intake was also similar in all the subgroups. Feeding mice of both strains the HF diet resulted in a decrease of interscapular brown fat (with a significant effect only in B/6J mice). In accord with a previous study (52) performed at 20°C and using a HF diet of a similar composition as in our experiments, the weight of white fat depots was increased by HF diet at 2 wk after weaning, with a stronger effect seen in A/J mice (Table 1). However, when the animals were fed the HF diet for up to 4 mo while still maintained at 30°C, B/6J mice gained more weight than A/J mice, and only in the former mice a strong obesogenic effect of the HF diet on body weight was observed (Fig. 1). Thus, in adult mice, the different propensity to dietary obesity, as detected in previous studies in B/6J and A/J mice maintained at 20–22°C (45, 46, 53), became clearly apparent even close to thermoneutrality, indicating that obesity resistance of A/J mice did not depend on the induction of energy expenditure by cold. On the other hand, the induction of adiposity by HF diet in both strains after weaning may reflect relatively low protein intake for actively growing mice.

At 2 wk after weaning, plasma levels of TG and NEFA were not affected by the diet in either genotype, except for a small induction of NEFA by the HF diet in B/6J mice (Table 1). As expected (47, 52), the HF diet strongly increased (~2.8-fold) leptin levels in A/J mice, whereas no significant induction of leptin could be detected in B/6J mice (Table 1). In contrast, plasma levels of both T_4 and T_3 were not affected by the HF diet in A/J mice, but they were increased in B/6J mice, indicating the stimulatory effect of the HF diet on thyroid function in B/6J but not in A/J mice (Table 1).

Body temperature and shivering during cold exposure. Assuming that the difference between B/6J and A/J mice in their propensity to HF diet-induced obesity reflected different thermogenic capacity of these two strains, sensitivity of the animals to acute cold exposure might be affected by the diet. To verify this hypothesis, the mice adapted to 30°C were exposed to an ambient temperature of 4°C, and their deep body temperature was measured (Fig. 2). Before the cold exposure (*time 0*), body temperature was similar in all the subgroups, whereas the temperature tended to be increased by HF diet specifically in A/J mice (legend to Fig. 2). During the first hour in the cold, body temperature decreased in all the subgroups, while the most pronounced decrease (~2.5°C) was observed in the A/J LF mice. However, LF diet-fed mice of both strains showed similar activation of shivering in the cold (Fig. 3). During the next 2 h, body temperature remained stable in all subgroups except for the A/J LF mice, which became hypothermic, and this prompted us to terminate the experiment in this subgroup (Fig. 2). In contrast, all the other mice were able to maintain their body temperature relatively stable up to 3 days in the cold (not shown). The strain-specific response to cold was not apparent in mice born and reared at 22°C, since under these conditions even A/J LF mice were able to maintain their body temperature above 36°C during a 3-day period in the cold (not shown). Thus, the adaptation of the A/J LF mice to the temperature close to thermoneutrality was essential for unmasking the relatively low thermogenic potential of these mice

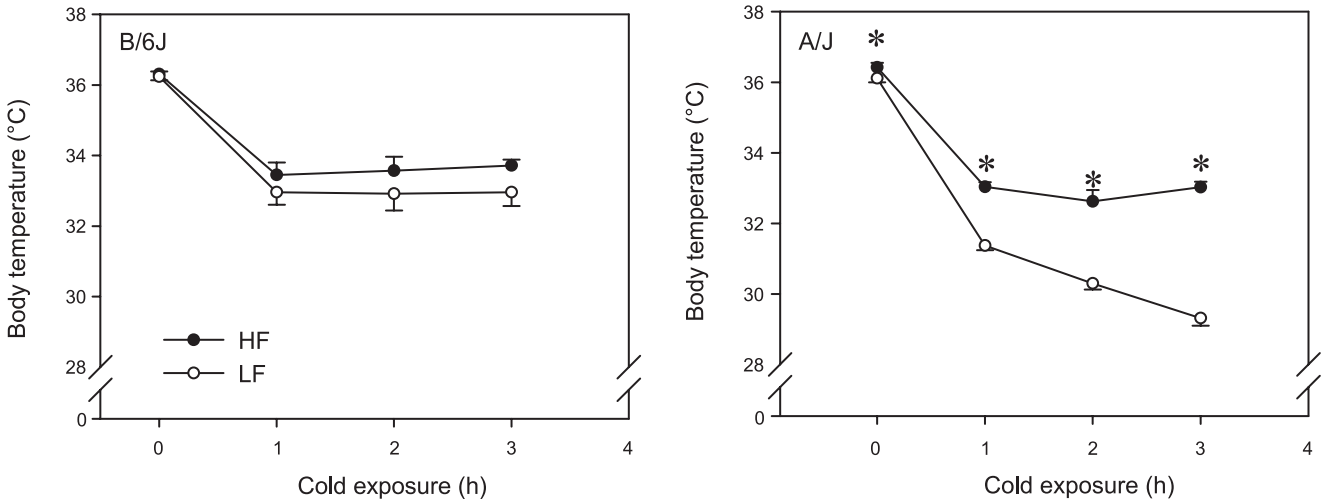

Fig. 2. Deep-body temperature in mice during cold exposure. Singly caged mice maintained at 30°C and fed either LF or HF diet for 2 wk after weaning were used. Animals in their cages containing food, water, and bedding were transferred from 30 to 4°C, and their colonic temperature was measured just before (36.24 ± 0.11, 36.31 ± 0.07, 36.05 ± 0.11, and 36.43 ± 0.13°C in B/6J LF, B/6J LH, A/J LF, and A/J HF, respectively) and during cold exposure. In A/J LF mice, cold exposure was finished after 3 h due to the development of severe hypothermia, whereas all the other mice could maintain their body temperature relatively constant for 3 days in the cold (not shown). Data are means ± SE (n = 7–8). *Significant effect of diet.

when exposed to cold and for demonstration of the induction of the thermogenic capacity of the A/J mice by HF diet.

Whole body energy expenditure in awake animals. To characterize whole body energy expenditure and its changes in response to diet in mice of both genotypes, indirect calorimetry was used to analyze $\dot{V}O_2$ and RER in ad libitum-fed mice reared at 30°C. Continuous monitoring in individually caged mice was performed for 23 h at 30°C, followed by a period of 23 h at 15°C (Fig. 4). When measured at 30°C and during the light phase of the day, energy expenditure in the A/J mice was affected by the type of diet, with a significant 38% increase in response to HF diet (Table 2). In fact, this increase was related to a relatively low $\dot{V}O_2$ during the light phase in the A/J LF mice compared with all other subgroups, and the $\dot{V}O_2$ values in A/J HF mice were similar to that in B/6J mice (Table 2). No effect of diet on energy expenditure was detected in the B/6J mice. During the dark phase, $\dot{V}O_2$ was not affected by diet in either strain of mice (Table 2). Upon a decrease of ambient temperature from 30 to 15°C, mean $\dot{V}O_2$ values increased approximately twofold in all the subgroups and the differences in $\dot{V}O_2$ between the genotypes and diets disappeared (Table 2).

The HF diet lowered RER in all animal subgroups, especially during the dark phase (Table 2), suggesting a shift toward lipid oxidation. This shift was also illustrated by the PRCF curves of RER values pooled from all the measurements performed within the same ambient temperature (Fig. 5). Since all the PRCF curves represented normally distributed data (not shown), the mean RER values corresponded to the 50th percentile values of the PRCF curves (34). In A/J but not in B/6J mice, RER values were also decreased in response to the lower ambient temperature. This shift was more significant in mice fed the HF compared with the LF diet (Table 2), resulting also in the steepest PRCF curve in the A/J HF mice when measured at 15°C (Fig. 5). The slope of the PRCF curve is a marker of metabolic flexibility, with a bigger slope suggesting a lower metabolic flexibility between oxidation of lipids and carbohydrates (34). Therefore, the results highlighted modulation of the resting energy expenditure in A/J mice by the dietary treatments and high reliance of A/J mice on fatty acid oxidation during cold exposure.

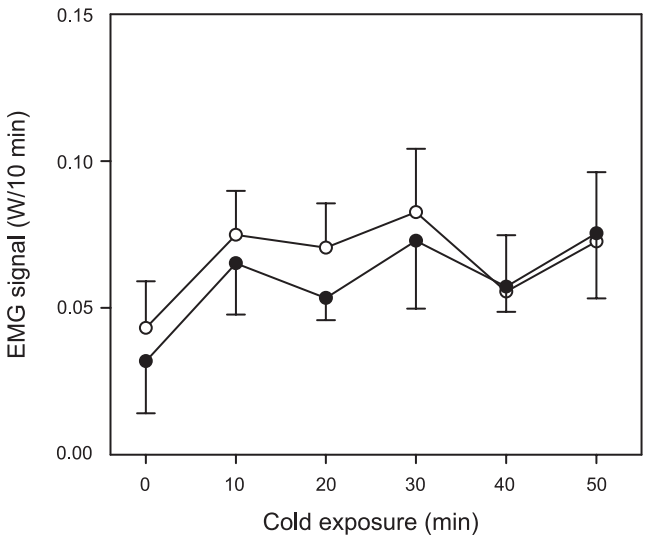

Fig. 3. Shivering during cold exposure. Singly caged B/6J (open symbols) and A/J (filled symbols) mice maintained at 30°C and fed LF diet for 2 wk after weaning were used. After implantation of recording and reference electrodes during anesthesia at 20°C, animals in their cages without food, water, and bedding were transferred to 4°C, and EMG recording was performed before (*time 0*) and during 50 min of cold exposure. Voltage values were integrated over 10-min periods before the indicated time points. Data are means ± SE (n = 7–8). In mice of both strains, shivering tended to be increased during the first 10 min, but the effect was not statistically significant.

UCP1-mediated nonshivering thermogenesis. Capacity for UCP1-mediated thermogenesis was assessed as an increment in metabolic rate after the injection of norepinephrine to anesthetized animals (NEMR; Refs. 16, 19, 42). NEMR was similar in LF diet-fed mice of both genotypes, it was stimulated by HF diet, and the stimulation was higher in A/J than in B/6J mice (Fig. 6). UCP1 protein content in interscapular brown fat was also increased by HF diet, and this increase was significantly higher in A/J mice (~10-fold) compared with B/6J mice (~3-fold), resulting in approximately twofold higher UCP1 levels in brown fat in A/J than in B/6J mice. Expression of UCP1 was also detected in subcutaneous white fat (see online APPENDIX, Table S2) and skeletal muscles (Table 3; see also Ref. 2) of mice of both genotypes, but the levels of UCP1 in these tissues were by at least two orders of magnitude lower than in the interscapular fat, indicating a negligible quantitative importance for thermogenesis. In some of the previous studies, UCP2 transcript levels in white fat have also been correlated with obesity resistance in A/J mice (13, 48, 52). However, in our experiments, UCP2 expression was similar in all fat depots studied, including interscapular brown and subcutaneous and epididymal white fat, and no effect of either genotype or diet on UCP2 expression was observed (see online APPENDIX, Table S2).

Thus, in both genotypes, the stimulation of NEMR by HF diet could be explained by the induction of UCP1 protein in the interscapular brown fat. A relatively strong induction in A/J mice was associated with the development of cold tolerance of these mice. On the other hand, the cold sensitivity of the A/J LF mice could be attributed to their relatively low whole body energy expenditure during the light phase of the day and could not be explained by an insufficient capacity of either UCP1-mediated energy expenditure or shivering thermogenesis, since no differences in this respect were detected between A/J and B/6J mice fed the LF diet.

Gene expression in muscles. A marked increase of $\dot{V}O_2$ in response to the HF diet in A/J mice during the light phase of the day, when the locomotor activity of animals is minimal (9), suggested involvement of an adaptive mechanism of energy expenditure, compatible with a sustained induction of nonshivering thermogenesis in muscle via the leptin-AMPK axis (see introductory remarks). Therefore, to characterize muscle metabolism, expression of several genes was assessed in gastrocnemius (a predominantly fast, glycolytic fiber type) and soleus (a predominantly slow, oxidative fiber type) muscle (Table 3). Strong effects of both diet and genotype were detected in the case of stearoyl-CoA desaturase-1 (SCD-1), a gene that is specifically repressed by leptin, which also stimulates fatty acid oxidation (4, 7). In both strains and in both types of muscles, the expression of SCD-1 was downregulated by the HF diet. The strongest suppression, approximately fourfold, was observed in the soleus muscle of A/J mice. These results were in agreement with the assumption that leptin was in-

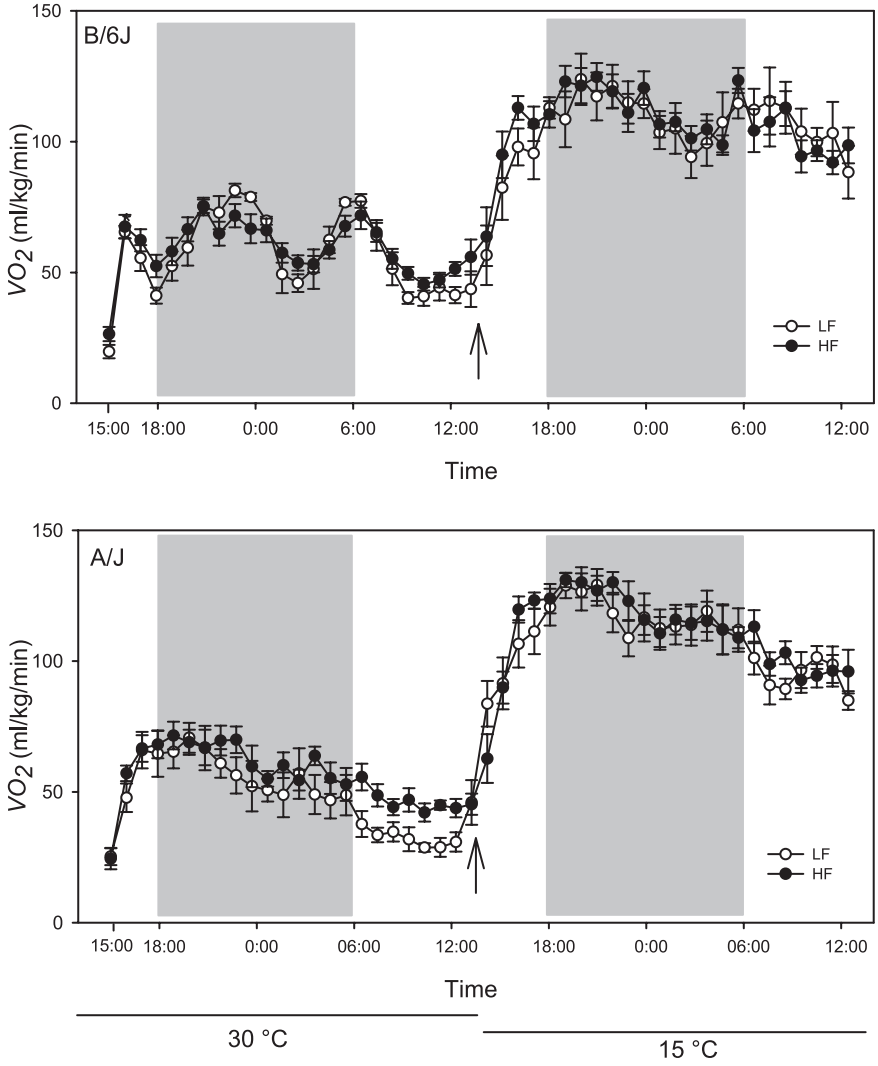

Fig. 4. Time course of $\dot{V}O_2$ measurements in mice maintained at 30°C and fed either LF or HF diet for 2 wk after weaning. Indirect calorimetry was performed on singly caged mice with free access to water and diet initially at 30°C for a period of 23 h followed by 23 h at 15°C. $\dot{V}O_2$ data were sampled at 60 s for every 2 min; however, only mean values of single recordings at 1-h intervals are shown. Arrows indicate beginning of a 30-min period during which the temperature was dropped. Gray areas represent the dark phases of diurnal cycle. A biphasic circadian rhythm of $\dot{V}O_2$ was observed in B/6J mice, with 2 maxima: 1 in the middle of the day and the other at the end of the dark phase. This pattern was only marginally affected by diet. In contrast, in A/J mice, a monophasic rhythm of $\dot{V}O_2$ was recorded, with maximum around the beginning of the dark phase of the day and lower $\dot{V}O_2$ values recorded during the light phase. Data are means ± SE (n = 6–8). For statistical analysis of these data, see Table 2.

volved in the induction of nonshivering thermogenesis in soleus muscle of A/J mice by HF diet.

There was no effect of genotype or diet on genes engaged in the control of mitochondrial biogenesis and oxidative capacity, as assessed by quantification of the transcripts for nuclear respiratory factor-1 and subunit VIa of mitochondrial cytochrome oxidase (21), respectively. The expression of PPARγ coactivator-1α (PGC-1α), which links nuclear receptors to the transcriptional program of mitochondrial biogenesis and oxidative metabolism (33), could not explain the stimulatory

Table 2. *Indirect calorimetry*

	30°C				15°C			
	B/6J		A/J		B/6J		A/J	
	LF	HF	LF	HF	LF	HF	LF	HF
$\dot{V}O_2$, ml·kg^{-1}·min^{-1}								
23 h	54.6±3.4	56.9±2.6	46.9±4.3	56.3±2.8	101.9±5.6	106.7±2.5	105.5±5.9	113.9±3.8
Light	51.2±1.8	56.3±2.8	35.6±2.6†	49.2±1.9*	103.3±2.9	103.5±3.1	92.0±3.8	104.9±2.6
Dark	63.7±2.1	64.7±2.4	59.2±4.2	63.7±3.8	109.7±2.2	113.6±2.4	119.1±3.6	117.6±3.4
RER								
23 h	0.91±0.02	0.81±0.02*	0.91±0.01	0.83±0.01*	0.89±0.01	0.81±0.01*	0.89±0.01	0.80±0.01*‡
Light	0.86±0.03	0.83±0.01	0.87±0.01	0.83±0.01	0.88±0.01	0.81±0.01*	0.85±0.02	0.79±0.01*‡
Dark	0.90±0.02	0.82±0.01*	0.94±0.01	0.84±0.01*	0.90±0.01	0.81±0.01*	0.92±0.01	0.81±0.01*

Singly caged mice were born and maintained at 30°C and fed LF or HF diet from weaning. Measurements proceeded at 30°C for 23 h, followed by exposure to 15°C for 23 h. $\dot{V}O_2$, O_2 consumption; RER, respiratory exchange ratio. See also Figs. 4 and 5. Data are means ± SE (n = 6–8, with ~700 data points per mouse per 23 h). *Significant effect of diet; †significant effect of genotype; ‡significant effect of temperature. All $\dot{V}O_2$ data were significantly affected by ambient temperature.

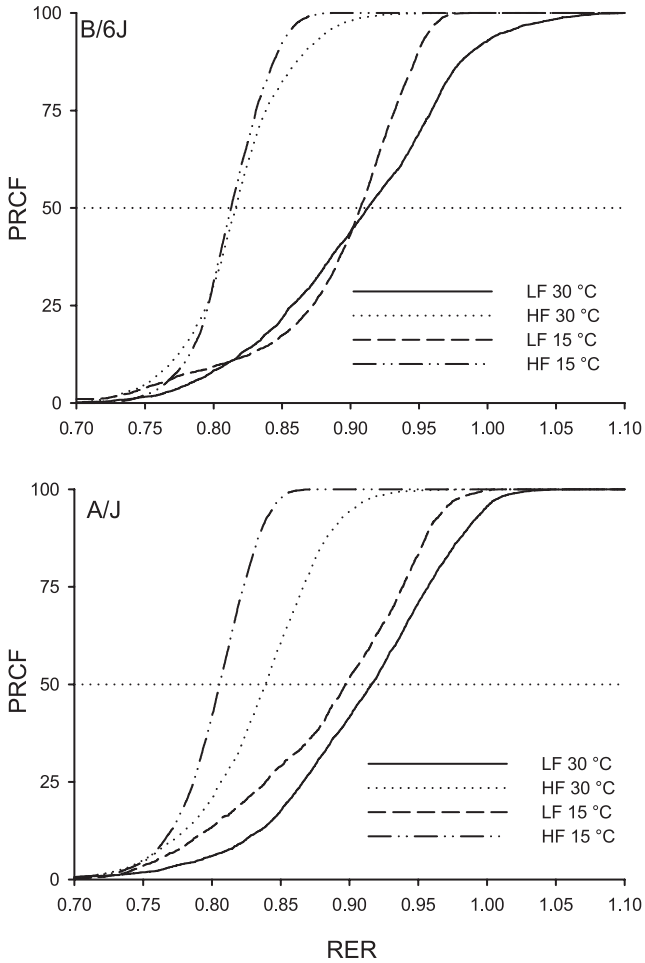

Fig. 5. Plots of percent relative cumulative frequency (PRCF) of respiratory exchange ratio (RER) values obtained by indirect calorimetry. RER data from the experiment (described in Table 2 and Fig. 4) were used to construct PRCF curves, each of which represents the data pooled from all mice (n = 6–8) within a given subgroup (~4,200–5,600 RER measurements per curve). For statistical analysis, see METHODS. Values of log EC_{50} (50th %ile values; see also corresponding RER data in Table 2) are significantly different between HF- and LF-fed mice within each genotype and irrespective of experimental temperature ($P < 0.001$). Only in A/J HF mice, values of log EC_{50} at 15 and 30°C are also significantly different ($P = 0.004$). At 15°C, the Hill-slope values are significantly different between HF- and LF-fed mice within each genotype, whereas at 30°C a significant difference between HF- and LF-fed mice was found only in B/6J mice.

effect of HF diet on energy expenditure in skeletal muscle of A/J mice either (Table 3). These results were in agreement with the lack of any effect of HF diet on the activity of cytochrome oxidase in soleus muscle of A/J mice (not shown).

The HF diet induced expression of mitochondrial acyl-CoA thioesterase, with the most pronounced effect in the soleus muscle of B/6J mice, and only in B/6J mice did it also upregulate UCP3 (Table 3). This was in agreement with the known stimulatory effect of thyroid hormones (30) on the expression of UCP3 and mitochondrial acyl-CoA thioesterase genes and with the B/6J strain-specific stimulation of thyroid status by HF diet (see above). The induction of UCP3 in both muscles of B/6J mice was associated with upregulation of long-chain acyl-CoA synthetase (required for activation and transport of fatty acid into mitochondria), whereas expression of cytosolic acyl-CoA thioesterase was unchanged (Table 3). These results suggest thyroid hormone-dependent induction of a mechanism of lipid handling by HF diet, which may preserve the CoASH pool in mitochondria, specifically in B/6J mice, independently of thermogenesis (18).

The expression of superoxide dismutase-1, a marker of reactive oxygen species formation, was similar in all the subgroups. Except for muscle type-specific differences in gene expression, relatively small variations in mRNA levels of PPARα, UCP1 (see above and Ref. 2), acyl-CoA oxidase-1, and the "muscle" isoform of carnitine palmitoyltransferase I (CPT IB) were observed in response to the diet. In contrast, strain-specific differences in the expression of CPT IA ("liver" isoform) were observed both in soleus and in gastrocnemius muscles. In this case, the expression was affected more by the genotype than by the diet, with the most pronounced effect in the soleus muscle, resulting in an approximately twofold higher CPT IA expression in A/J than in B/6J mice. An opposite effect of the genotype on the expression of CPT IA was observed in the gastrocnemius muscle of HF diet-fed mice (Table 3). Furthermore, high levels of mRNA for isoenzyme 4 of pyruvate dehydrogenase kinase (PDK-4) were found in soleus muscles of A/J mice, indicative of sustained lipid delivery and oxidation (Table 3; Ref. 44). Expression of PDK-4 mRNA in A/J mice was not affected in response to the HF diet; however, its expression was stimulated in both the soleus and the gastrocnemius muscles of B/6J mice. All together, the results above suggested a strain-specific loss of regulation of glucose/fatty acid partitioning in the soleus muscle of A/J mice, favoring oxidation of fatty acids.

Oxidative metabolism in muscles and AMPK. To analyze a possible induction of oxidative metabolism by HF diet in skeletal muscles of A/J mice, ex vivo measurements were performed. First, the rate of endogenous $\dot{V}O_2$ in the gastrocnemius and soleus muscles was assessed during a 35-min period (Fig. 7 and Table 4). Feeding mice the HF diet tended to increase the respiratory rate in gastrocnemius muscle of both B/6J and A/J mice, but this effect was not statistically significant. On the contrary, in the soleus muscle of A/J mice, HF

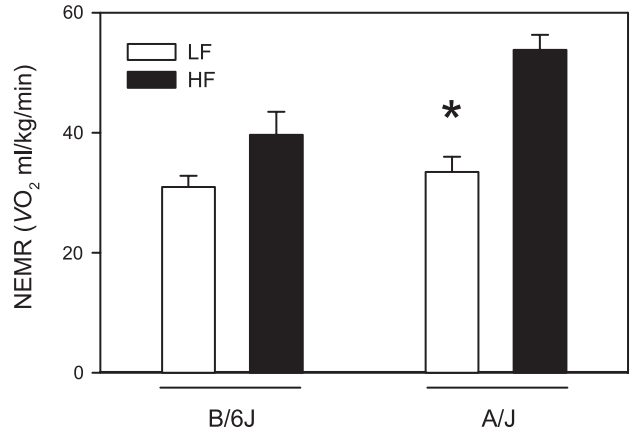

Fig. 6. Norepinephrine (NE)-induced thermogenesis. Mice maintained at 30°C and fed either LF or HF diet for 2 wk after weaning were anesthetized by pentobarbital sodium, and NE metabolic rate (NEMR) was measured as difference between $\dot{V}O_2$ before and after ip injection of NE. Before injection, $\dot{V}O_2$ values were similar in all subgroups of anesthetized mice (28.1 ± 3.1, 29.5 ± 3.0, 26.2 ± 2.7, and 25.6 ± 2.1 ml·kg^{-1}·min^{-1} in B/6J LF, B/6J HF, A/J LF, and A/J HF mice, respectively). Data are means ± SE (n = 6–9). *Significant effect of diet.

Table 3. *Gene expression in glycolytic and oxidative skeletal muscles*

	B/6J		A/J	
Muscle	LF	HF	LF	HF
Gastrocnemius				
ACOT1	0.94±0.13	0.86±0.06	1.00±0.21	0.97±0.04
ACOT2	1.55±0.31	3.28±0.33*†	0.88±0.18	1.73±0.16
ACSL1	1.11±0.22	1.36±21	1.15±0.28	1.33±0.13
COX6a	0.67±0.06	0.68±0.07	0.59±0.15	0.49±0.08
CPT IA	2.08±0.27	2.59±0.33	1.77±0.33	1.22±0.21†
CPT IB	0.35±0.04	0.50±0.05	0.50±0.03	0.63±0.07
NRF-1	1.82±0.21	1.84±0.34	1.92±0.45	1.72±0.23
PDK-4	0.62±0.09	1.11±0.48*	1.11±0.48†	0.93±0.24
PGC-1α	0.71±0.01	1.04±0.27	1.71±0.69†	1.12±0.80
PPARα	0.43±0.15	0.33±0.10	0.50±0.24	0.46±0.23
SCD-1	1.31±0.35	0.48±0.05*	1.79±0.47	0.82±0.20*
SOD1	1.07±0.13	1.16±0.13	1.23±0.28	0.81±0.14
UCP1	0.30±0.01	0.44±0.03	0.91±0.04†	1.10±0.06†
UCP3	2.09±0.44	3.55±0.69	2.73±0.52	1.97±0.45
Soleus				
ACOT1	1.31±0.11	1.90±0.22*	1.25±0.14	1.84±0.10*
ACOT2	1.62±0.36	4.32±0.13*	1.96±0.34	3.58±0.60*
ACSL1	2.94±0.28	4.14±0.41*†	3.17±0.30	2.83±0.24
AOX1	1.42±0.12	1.64±0.12	1.77±0.30	1.56±0.13
COX6a	0.72±0.05	0.64±0.03	0.58±0.04†	0.56±0.03
CPT IA	1.06±0.11	1.29±0.09	2.54±0.12†	2.25±0.12†
CPT IB	0.79±0.04	0.79±0.04	0.76±0.05	0.86±0.05
NRF-1	0.63±0.15	0.69±0.07	0.61±0.09	0.83±0.36
PDK-4	1.27±0.10	2.26±0.15*	2.40±0.60†	2.33±0.23
PGC-1α	2.52±0.64	2.14±0.24	1.68±0.59†	1.38±0.24†
PPARα	1.32±0.12	1.07±0.12	0.77±0.09†	0.83±0.14
SCD-1	1.00±0.12	0.44±0.07*	2.22±0.37†	0.56±0.06*
SERCA1	1.21±0.11	0.98±0.02*	1.09±0.19	0.71±0.06*†
SERCA2‡	1.18±0.07	1.13±0.06	1.65±0.11†	1.25±0.12*
SOD1	0.85±0.03	0.82±0.04	0.88±0.08	0.78±0.03
UCP1§	0.36±0.04	0.43±0.02	0.37±0.02	0.44±0.01
UCP3	1.57±0.23	2.34±0.18*	1.68±0.11	1.90±0.33

Transcript levels (AU) were measured using qRT-PCR in total RNA isolated from skeletal muscles of mice adapted to 30°C and fed LF or HF diet. Within a particular transcript, all groups can be compared. Data are means ± SE (n = 6–7). *Significant effect of diet; †significant effect of genotype; ‡both SERCA2a and SERCA2b mRNA were quantified; §both UCP1 transcript (qRT-PCR) and protein (measured by Western blots, not shown; see also METHODS) were detected at levels that were at least ~200-fold lower vs. that in BAT of mice reared at 20°C. ACOT1, cytosolic acyl-CoA thioesterase; ACOT2, mitochondrial ACOT; ACSL1, long-chain acyl-CoA synthetase; AOX1, acyl-CoA oxidase-1; COX6a, subunit VIa of mitochondrial cytochrome oxidase; CPT I, carnitine palmitoyltransferase I; PGC-1, PPARγ coactivator 1; NRF-1, SERCA, sarcoplasmic reticulum Ca^{2+} ATPase; nuclear respiratory factor 1; PDK-4, pyruvate dehydrogenase kinase-4; SOD1, superoxide dismutase-1.

diet increased the respiration ~1.8-fold, while no effect was observed in B/6J mice.

Second, oxidation of exogenous palmitate in the muscles was measured (Table 5). In either genotype, no significant effect of HF diet on palmitate oxidation was observed. However, when palmitate oxidation was evaluated in the presence of AICAR, an AMPK activator, an ~70% increase in the rate of oxidation was observed in the soleus muscle of the A/J HF mice. No stimulatory effect of AICAR was observed in the soleus muscle of either the A/J LF mice or the B/6J mice fed both types of diets. In the gastrocnemius muscle, no stimulation by AICAR or diet was detected in mice of either genotype (not shown).

To further investigate a possible involvement of AMPK in the strain-specific effect of HF diet, AMPK content and phosphorylation (p-AMPK) were measured in the soleus muscle (Fig. 8). In B/6J mice, the HF diet had no effect on either total AMPK or p-AMPK muscle content. In contrast, in A/J mice the HF diet caused an ~1.7- and ~1.4-fold increase in the content of AMPK and pAMPK, respectively; however, only the effect on total AMPK content reached statistical significance (two-way ANOVA). The stimulatory effect of HF diet on AMPK in soleus muscle of A/J mice was further confirmed by assessing the level of phosphorylation of ACC, a downstream target of AMPK, which showed an ~1.4-fold increase in response to HF diet, whereas no effect on ACC phosphorylation was found in B/6J mice (not shown). These results indicated a genotypic difference in the effect of HF diet on energy expenditure in soleus muscle, where the inducibility of respiration by HF diet in the A/J mice was associated with a relatively high potency of the AMPK regulatory pathway.

DISCUSSION

The principal finding of this study is the stimulation of muscle thermogenesis and lipid oxidation by HF diet in obesity-resistant A/J mice. Our results indicate that an HF diet could induce nonshivering thermogenesis in oxidative muscle, possibly by the leptin-AMPK axis.

We have demonstrated, for the first time, a profound difference between A/J and B/6J mice in their ability to resist acute cold exposure, providing that the animals were first adapted to the temperature close to thermoneutrality and maintained on an LF diet. Nevertheless, a relatively low whole body energy expenditure of the A/J LF mice, which would predispose these animals to obesity, was enhanced in response to the HF diet. This induction was apparently stronger than in B/6J mice, which exhibited higher energy expenditure than A/J mice when fed the LF diet but are prone to HF diet-induced obesity. That the HF diet induced a larger increase in whole body energy expenditure in A/J than in B/6J mice was also in agreement with the tendency of HF diet to increase body temperature in the former mice in this and in the previous study (47).

Without preacclimation to ambient temperatures around 20–22°C, as used in previous studies (8, 17, 48, 52), the capacity of nonshivering thermogenesis in brown adipose tissue was relatively low, but it was similar in both strains of mice, unless it was stimulated by HF diet. Since the ability to activate shivering was also similar in both B/6J and A/J mice fed the LF diet (Fig. 3), the cold sensitivity of the A/J LF mice could be explained, at least in part, by their relatively low $\dot{V}O_2$ as measured at 30°C during the light phase of the day. Although locomotor activity was not assessed in this study, it could have contributed to the differences in $\dot{V}O_2$ as well in cold sensitivity (5, 9, 14).

The stronger obesogenic effect of HF diet in B/6J compared with A/J mice has been previously explained by strain-specific differences in the adrenergic control of thermogenesis (8) and sensitivity to leptin (32), with only A/J mice retaining sensitivity of adipose tissue to both stimuli after several weeks of feeding on a HF diet. The present study confirmed the previous results (8, 17, 48, 52), indicating that the differential response to HF diet could be attributed to the relatively high induction of UCP1 in the interscapular brown fat of A/J mice. In addition, our study demonstrated a HF diet-induced increase of $\dot{V}O_2$ in soleus muscle, which was specific for A/J mice, and

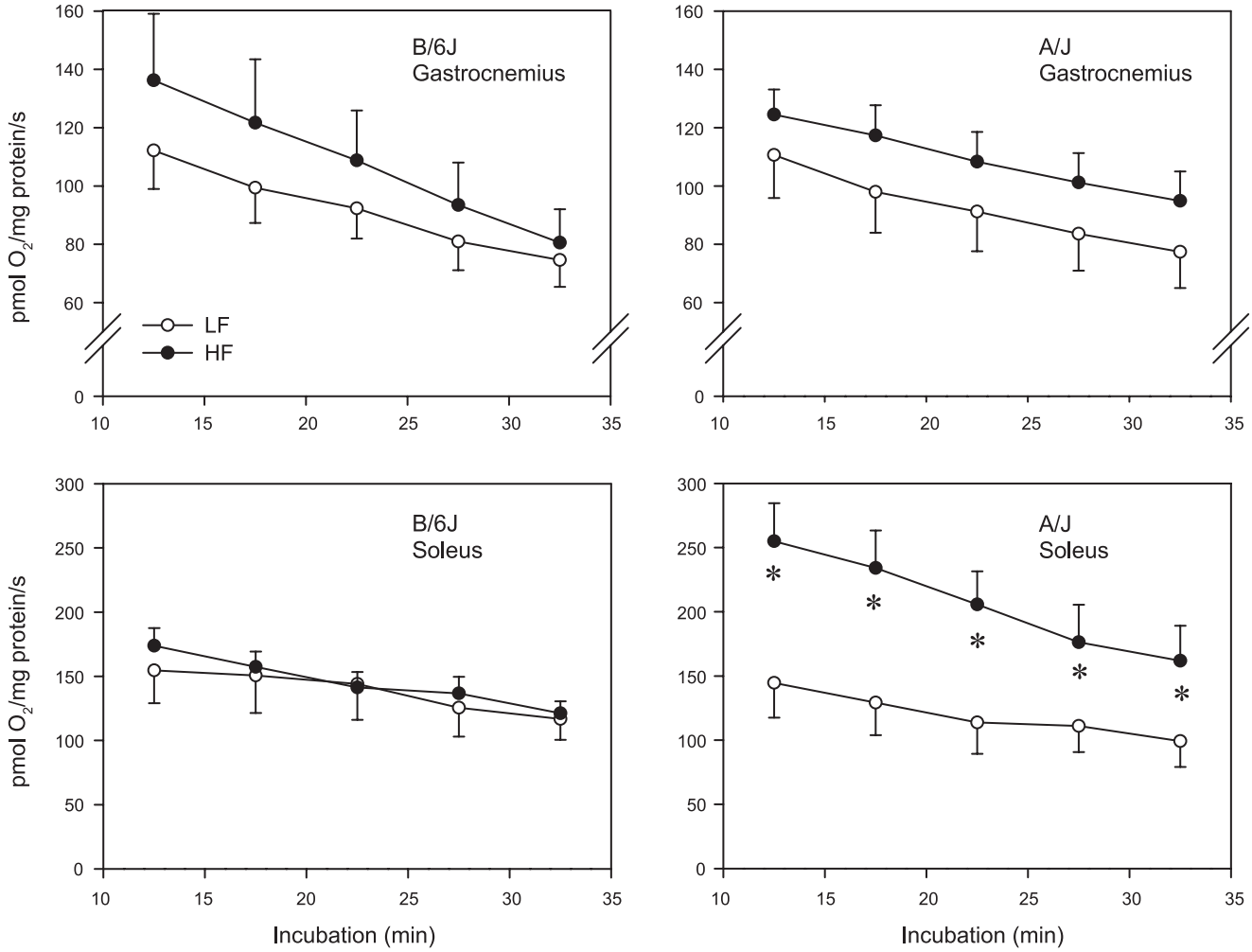

Fig. 7. Ex vivo muscle $\dot{V}O_2$ during 35-min incubation period at 37°C. Muscle samples were obtained from mice adapted to 30°C and fed either LF or HF diet. Fragments of gastrocnemius or whole soleus muscles were incubated in freshly oxygenated (95% O_2-5% CO_2) Krebs-Ringer bicarbonate buffer (pH 7.4) containing 10 mM glucose, and $\dot{V}O_2$ was measured using polarography (see also Table 4). Data are means ± SE for a 5-min interval, beginning 10 min after insertion of tissue fragments into measuring chambers. Results were normalized to tissue protein (n = 7–9). *Significant effect of diet (repeated-measures ANOVA: diet vs. time).

suggested activation of nonshivering thermogenesis in this muscle. The association with increased leptin levels, and the selective involvement of the oxidative muscle, strongly suggested the involvement of the leptin-AMPK axis (29, 41). AMPK plays a major role in the regulation of fatty acid oxidation in skeletal muscle while inhibiting ACC by phosphorylation, reducing malonyl-CoA levels, and, thus, enhancing activity of CPT I and β-oxidation of fatty acids (7, 29). Direct stimulation of muscle thermogenesis ex vivo required both AMPK and phosphatidylinositol 3-kinase and could be prevented by pharmacological inhibition of AMPK, and activation of the AMPK axis was required for leptin-induced substrate cycling between de novo lipogenesis and lipid oxidation (41).

Table 4. *$\dot{V}O_2$ in skeletal muscles*

	B/6J		A/J	
Muscle	LF	HF	LF	HF
Gastrocnemius	112±13	136±23	111±15	125±9.0
Soleus	155±26	174±14	145±27	255±30*†

$\dot{V}O_2$ was measured in muscles dissected from mice adapted to 30ºC and fed LF of HF diet, as described also in Fig. 4. Data are means ± SE for the 5-min interval, beginning 10 min after insertion of tissue fragments into measuring chambers. Results were normalized to tissue protein and expressed as pmol $O_2 \cdot$mg protein^{-1}s^{-1} (n = 7–9). *Significant effect of diet; †significant effect of genotypes. Similar results were observed when data were normalized to tissue wet weight (not shown).

Table 5. *Palmitate oxidation in soleus muscle*

	Palmitate Oxidation, dpm·mg protein^{-1}·s^{-1}			
	B/6J		A/J	
	LF	HF	LF	HF
–AICAR	10.6±1.3	11.1±1.6	10.9±1.8	11.4±1.5
+AICAR	13.0±2.2	12.1±1.2	14.6±1.3	19.2±1.2*†

Palmitate oxidation was assessed in soleus muscle dissected from mice adapted to 30ºC and fed LF or HF diet. Measurements were performed at 37°C using [U-^{14}C]palmitate in the absence or presence of 2 mM 5-aminoimidazole-4-carboxamide-1-β-D-ribonucleoside (AICAR). Data are means ± S.E (n = 8). *Significant effect of diet; †significant effect of genotype.

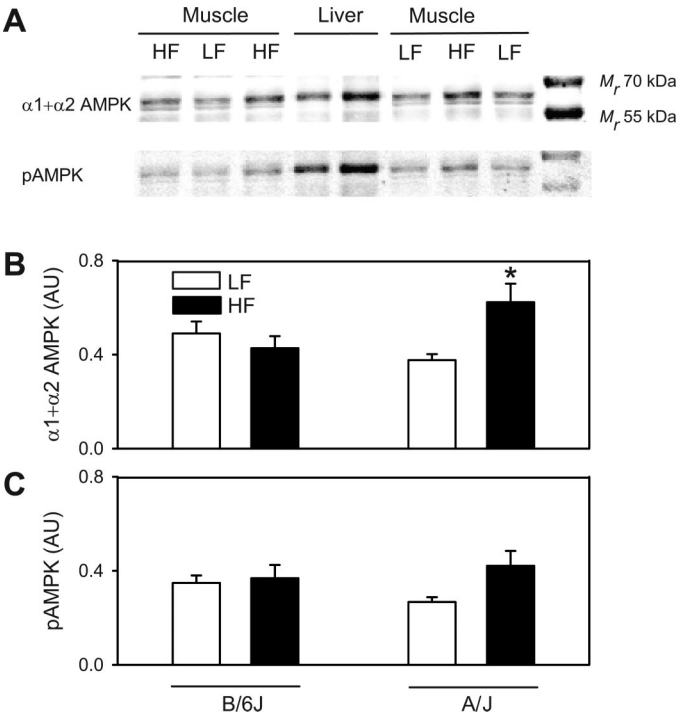

Fig. 8. Content and phosphorylation of AMPK in soleus muscle of B/6J and A/J mice. Mice maintained at 30°C and fed either LF (open bars) or HF (filled bars) diet for 2 wk after weaning were used. Total amount of AMPK (AMPKα1 + -α2) was assessed in tissue extracts with a mixture of primary antibodies against AMPKα1 and -α2 , whereas phosphorylated (p-)AMPK was detected using primary antibodies specific for phosphorylated Thr^{172}. Both forms of AMPK were visualized and quantified on the same blot using two different secondary infrared dye-labeled antibodies and the Odyssey IR Imager. *A*: picture of representative blot with muscle samples (15 μg protein/lane) from A/J mice, liver standards isolated from adult LF diet-fed B/6J mice (10 and 15 μg protein/lane), and prestained M_r standards. *B*: quantification of total amount of AMPK. *C*: quantification of p-AMPK. Data are means ± SE (B/6J, $n = 7–8$; A/J, $n = 10–11$). *Significant effect of diet.

The acute stimulation of AMPK by leptin reflects an increased phosphorylation of Thr^{172} in the enzyme α-subunit (29). On the other hand, chronic hyperleptinemia in rats resulted in an increased content of both total AMPK and p-AMPK and increased phosphorylation of ACC (43) similarly to the results of our experiments. Our results have documented the HF diet-induced increase of AICAR-dependent fatty acid oxidation in soleus muscle of A/J but not B/6J mice. These results suggest a much higher inducibility of lipid oxidation by AMPK in the soleus muscle of A/J than in B/6J mice. However, without AICAR, no effect on fatty acid oxidation was noticed. Perhaps, oxidation of the exogenously added fatty acids could be limited by the transport of fatty acids from the medium, unless the AMPK and CPT I activities are maximally stimulated by AICAR. In resting soleus muscle, exogenous fatty acid provide only a very small fraction (~2%) of total lipid metabolized while catabolism of intramuscular lipid represents the bulk [~98% (10)]. Oxidation of intramuscular lipid should be better reflected by the ex vivo measurements of endogenous respiration in the muscle. However, the quantitative interpretation of these measurements, even in a relatively small whole soleus muscle, is limited due, for example, to a diffusion barrier for oxygen or a release of electrolytes (particulary potassium), which can alter the respiration. Nevertheless, the combined results of both approaches strongly suggest induction of energy expenditure by HF diet in the soleus muscle of A/J mice involving AMPK-stimulated fatty acid oxidation.

The strongest suppression of SCD-1 expression, accompanied by the highest levels of PDK-4 transcript in soleus muscle of the A/J HF mice, further supports the preferential use of lipids for adaptive thermogenesis in the muscle. Downregulation of SCD-1 results in increased β-oxidation of fatty acids, enhanced thermogenesis, and resistance to obesity (reviewed in Refs. 4, 7, 25), whereas activation of PDK-4 leads to suppression of glucose oxidation (44). Of note, upregulation of PDK-4 was also detected in soleus muscle of cold-acclimated UCP1 knockout mice (50). A relatively high expression of CPT IA, the liver isoform of the enzyme, in the soleus muscle of the A/J HF mice is also in favor of intense β-oxidation of fatty acids, since it is primarily the muscle isoform that is more sensitive to inhibition by malonyl-CoA (28).

That lipid oxidation was important for the cold defense abilities of the A/J HF mice was further documented by indirect calorimetry. Lowering of ambient temperature during the measurements augmented the activation of lipid oxidation by HF diet in A/J but not in B/6J mice (see the PRCF data in Fig. 5, and RER data in Table 2). This strain-specific enhancement of the whole-body lipid oxidation in cold probably reflected the increased capacity for both UCP1-mediated and muscle thermogenesis by HF diet. On the other hand, the HF diet-induced elevation of $\dot{V}O_2$ during the light phase in A/J mice maintained at 30°C probably resulted from the sustained increase in muscle nonshivering thermogenesis, induced by leptin and independent of acute stimulation of sympathetic activity due to cold or meal (see also Ref. 6).

The role and mechanism of leptin-mediated adaptive thermogenesis have recently been investigated by Ukropec et al. (51) using *ob/ob* mice with a targeted inactivation of UCP1 gene ($Ucp1^{-/-}.Lep^{-/-}$ mice). These mice could not adapt to temperatures below 12°C unless they were administered either leptin or T_3 (51). Thermogenesis was possibly activated due to the induction of Ca^{2+} cycling associated with an increased expression of sarcoplasmic reticulum Ca^{2+} ATPase-2 (SERCA2) in oxidative muscle (51). On the contrary, the stimulation of thermogenesis in the oxidative muscle of the A/J HF mice was not associated either with upregulation of SERCA2 (in fact, in both the experiments on $Ucp1^{-/-}.Lep^{-/-}$ mice and in our study, both SERCA2a and SERCA2b mRNA were quantified together) or with changes of the thyroid hormone status (Tables 1 and 3). The qualitative difference in the thermogenic response between $Ucp1^{-/-}.Lep^{-/-}$ and A/J mice may thus reflect a much higher induction of thermogenic mechanisms required to substitute for defective UCP1-mediated thermogenesis in the transgenic mice. Additional thermogenic mechanisms may function in this transgenic model that do not operate in A/J mice. However, in both $Ucp1^{-/-}.Lep^{-/-}$ and A/J mice, oxidative but not glycolytic muscle was involved in the adaptive thermogenesis, supporting further the importance of lipid catabolism and mitochondria for muscle thermogenesis.

Our results do not answer the question whether the induction of muscle thermogenesis by leptin could result from a direct interaction of leptin with muscle or whether it is mediated centrally via the activation of the adrenergic system (29). With respect to a possible extrapolation to human subjects, where

the control and significance of adaptive nonshivering thermogenesis is less defined than in rodent species, an increase of sympathetic activity is known to be critical for resistance to obesity (see other references in Ref. 9).

In summary, our results demonstrate that both the UCP1-mediated thermogenesis in brown fat and muscle thermogenesis are associated with resistance to dietary obesity in mice. Only in the model of obesity-resistant A/J, but not in obesity-prone B/6J mice, stimulation of thermogenesis in oxidative skeletal muscle in response to an HF diet was observed. Our results further suggest the involvement of the leptin-AMPK axis, with a preferential use of lipids as metabolic substrates, in the induction of nonshivering thermogenesis in oxidative muscle by HF diet. Thus, at least in mice, the adaptive stimulation of lipid oxidation and muscle thermogenesis in response to increased fat content in the diet might contribute to cold resistance and obesity resistance.

ACKNOWLEDGMENTS

We thank Grahame D. Hardie (University of Dundee, Dundee, UK) for the generous gift of the sheep antibodies against AMPKα1 and -α2 and Leslie P. Kozak (Pennington Biomedical Research Center, Baton Rouge, LA) and Jan Bures (Institute of Physiology, Academy of Sciences of the Czech Republic, Prague) for critical reading of the manuscript.

GRANTS

This work was supported by Research Project AV0Z50110509 and by grants from the Ministry of Education, Youth and Sports of the Czech Republic (1M6837805002), the Czech Science Foundation (305/08/H037,303/07/0781, and the European Commission (Projects EARNEST: FOOD-CT-2005-007036 and EXGENESIS: LSHM-CT-2004-005272).

REFERENCES

1. **Alberts P, Johansson BG, McArthur RA.** Measurement and characterization of energy expenditure as a tool in the development of drugs for metabolic diseases, such as obesity and diabetes. In: *Current Protocols in Pharmacology*, edited by Enna SJ, Williams M, Ferkany JW, Kenakin T, Porsolt RD, Sullivan JP. Wiley and Sons, 2005, p. 1–15.
2. **Almind K, Manieri M, Sivitz WI, Cinti S, Kahn CR.** Ectopic brown adipose tissue in muscle provides a mechanism for differences in risk of metabolic syndrome in mice. *Proc Natl Acad Sci USA* 104: 2366–2371, 2007.
3. **Andersson U, Filipsson K, Abbott CR, Woods A, Smith K, Bloom SR, Carling D, Small CJ.** AMP-activated protein kinase plays a role in the control of food intake. *J Biol Chem* 279: 12005–12008, 2004.
4. **Biddinger SB, Miyazaki M, Boucher J, Ntambi JM, Kahn CR.** Leptin suppresses stearoyl-CoA desaturase 1 by mechanisms independent of insulin and sterol regulatory element-binding protein-1c. *Diabetes* 55: 2032–2041, 2006.
5. **Brownlow BS, Petro A, Feinglos MN, Surwit RS.** The role of motor activity in diet-induced obesity in C57BL/6J mice. *Physiol Behav* 60: 37–41, 1996.
6. **Cannon B, Nedergaard J.** Brown adipose tissue: function and physiological significance. *Physiol Rev* 84: 277–359, 2004.
7. **Cohen P, Friedman JM.** Leptin and the control of metabolism: role for stearoyl-CoA desaturase-1 (SCD-1). *J Nutr* 134: 2455S–2463S, 2004.
8. **Collins S, Daniel KW, Petro AE, Surwit RS.** Strain-specific response to beta3-adrenergic receptor agonist treatment of diet-induced obesity in mice. *Endocrinology* 138: 405–413, 1997.
9. **DeRuisseau LR, Parsons AD, Overton JM.** Adaptive thermogenesis is intact in B6 and A/J mice studied at thermoneutrality. *Metabolism* 53: 1417–1423, 2004.
10. **Dyck DJ, Bonen A.** Muscle contraction increases palmitate esterification and oxidation and triacylglycerol oxidation. *Am J Physiol Endocrinol Metab* 275: E888–E896, 1998.
11. **Flachs P, Horakova O, Brauner P, Rossmeisl M, Pecina P, Franssen-van Hal NL, Ruzickova J, Sponarova J, Drahota Z, Vlcek C, Keijer J, Houstek J, Kopecky J.** Polyunsaturated fatty acids of marine origin upregulate mitochondrial biogenesis and induce beta-oxidation in white fat. *Diabetologia* 48: 2365–2375, 2005.
12. **Flatt JP.** Exaggerated claim about adaptive thermogenesis. *Int J Obes (Lond)* 31: 1626–1628, 2007.
13. **Fleury C, Neverova M, Collins S, Raimbault S, Champigny O, Levi-Meyrueis C, Bouillaud F, Seldin MF, Surwit RS, Ricquier D, Warden CH.** Uncoupling protein-2: a novel gene linked to obesity and hyperinsulinemia. *Nat Genet* 15: 269–272, 1997.
14. **Gelegen C, Collier DA, Campbell IC, Oppelaar H, Kas MJ.** Behavioral, physiological, and molecular differences in response to dietary restriction in three inbred mouse strains. *Am J Physiol Endocrinol Metab* 291: E574–E581, 2006.
15. **Gnaiger E, Steinlechner-Maran R, Mendez G, Eberl T, Margreiter R.** Control of mitochondrial and cellular respiration by oxygen. *J Bioenerg Biomembr* 27: 583–596, 1995.
16. **Granneman JG, Burnazi M, Zhu Z, Schwamb LA.** White adipose tissue contributes to UCP1-independent thermogenesis. *Am J Physiol Endocrinol Metab* 285: E1230–E1236, 2003.
17. **Guerra C, Koza RA, Yamashita H, King KW, Kozak LP.** Emergence of brown adipocytes in white fat in mice is under genetic control. *Effects on body weight and adiposity J Clin Invest* 102: 412–420, 1998.
18. **Himms-Hagen J, Harper ME.** Physiological role of UCP3 may be export of fatty acids from mitochondria when fatty acid oxidation predominates: an hypothesis. *Exp Biol Med (Maywood)* 226: 78–84, 2001.
19. **Jansky I.** Humoral thermogenesis and its role in maintaining energy balance. *Physiol Rev* 75: 237–259, 1995.
20. **Jéquier E.** Regulation of thermogenesis and nutrient metabolism in the human: relevance for obesity. In: *Obesity*, edited by Björntorp P, Brodoff BN. Philadelphia, PA: Lippincott, 1992, p. 130–135.
21. **Kadenbach B, Huttemann M, Arnold S, Lee I, Bender E.** Mitochondrial energy metabolism is regulated via nuclear-coded subunits of cytochrome c oxidase. *Free Radic Biol Med* 29: 211–221, 2000.
22. **Kopecky J, Hodny Z, Rossmeisl M, Syrovy I, Kozak LP.** Reduction of dietary obesity in the *aP2-Ucp* transgenic mice: physiology and adipose tissue distribution. *Am J Physiol Endocrinol Metab* 270: E768–E775, 1996.
23. **Kopecky J, Rossmeisl M, Hodny Z, Syrovy I, Horakova M, Kolarova P.** Reduction of dietary obesity in the *aP2-Ucp* transgenic mice: mechanism and adipose tissue morphology. *Am J Physiol Endocrinol Metab* 270: E776–E786, 1996.
24. **Liu X, Rossmeisl M, McClaine J, Kozak LP.** Paradoxical resistance to diet-induced obesity in UCP1-deficient mice. *J Clin Invest* 111: 399–407, 2003.
25. **Mainieri D, Summermatter S, Seydoux J, Montani JP, Rusconi S, Russell AP, Boss O, Buchala AJ, Dulloo AG.** A role for skeletal muscle stearoyl-CoA desaturase 1 in control of thermogenesis. *FASEB J* 20: 1751–1753, 2006.
26. **Major GC, Doucet E, Trayhurn P, Astrup A, Tremblay A.** Clinical significance of adaptive thermogenesis. *Int J Obes (Lond)* 31: 204–212, 2007.
27. **Matejkova O, Mustard KJ, Sponarova J, Flachs P, Rossmeisl M, Miksik I, Thomason-Hughes M, Hardie DG, Kopecky J.** Possible involvement of AMP-activated protein kinase in obesity resistance induced by respiratory uncoupling in white fat. *FEBS Lett* 569: 245–248, 2004.
28. **McGarry JD, Mills SE, Long CS, Foster DW.** Observations on the affinity for carnitine, and malonyl-CoA sensitivity, of carnitine palmitoyltransferase I in animal and human tissues. Demonstration of the presence of malonyl-CoA in non-hepatic tissues of the rat. Biochem J 214: 21–28, 1983.
29. **Minokoshi Y, Kim YB, Peroni OD, Fryer LG, Muller C, Carling D, Kahn BB.** Leptin stimulates fatty-acid oxidation by activating AMP-activated protein kinase. *Nature* 415: 339–343, 2002.
30. **Moreno M, Lombardi A, de Lange P, Silvestri E, Ragni M, Lanni A, Goglia F.** Fasting, lipid metabolism, and triiodothyronine in rat gastrocnemius muscle: interrelated roles of uncoupling protein 3, mitochondrial thioesterase, and coenzyme Q. *FASEB J* 17: 1112–1114, 2003.
31. **Pelleymounter MA, Cullen MJ, Baker MB, Hecht R, Winters D, Boone T, Collins F.** Effects of the obese gene product on body weight regulation in ob/ob mice. *Science* 269: 540–543, 1995.
32. **Prpic V, Watson PM, Frampton IC, Sabol MA, Jezek GE, Gettys TW.** Differential mechanisms and development of leptin resistance in A/J versus C57BL/6J mice during diet-induced obesity. *Endocrinology* 144: 1155–1163, 2003.

33. **Puigserver P, Spiegelman BM.** Peroxisome proliferator-activated receptor-gamma coactivator 1 alpha (PGC-1 alpha): transcriptional coactivator and metabolic regulator. *Endocr Rev* 24: 78–90, 2003.
34. **Riachi M, Himms-Hagen J, Harper ME.** Percent relative cumulative frequency analysis in indirect calorimetry: application to studies of transgenic mice. *Can J Physiol Pharmacol* 82: 1075–1083, 2004.
35. **Rosen ED, Spiegelman BM.** Adipocytes as regulators of energy balance and glucose homeostasis. *Nature* 444: 847–853, 2006.
36. **Rothwell NJ, Stock MJ.** Similarities between cold- and diet- induced thermogenesis in the rat. *Can J Physiol Pharmacol* 58: 842–848, 1980.
37. **Ruzickova J, Rossmeisl M, Prazak T, Flachs P, Sponarova J, Vecka M, Tvrzicka E, Bryhn M, Kopecky J.** Omega-3 PUFA of marine origin limit diet-induced obesity in mice by reducing cellularity of adipose tissue. *Lipids* 39: 1177–1185, 2004.
38. **Scarpace PJ, Matheny M.** Leptin induction of UCP1 gene expression is dependent on sympathetic innervation. *Am J Physiol Endocrinol Metab* 275: E259–E264, 1998.
39. **Skarka L, Bardova K, Brauner P, Flachs P, Jarkovska D, Kopecky J, Ostadal B.** Expression of mitochondrial uncoupling protein 3 and adenine nucleotide translocase 1 genes in developing rat heart: putative involvement in control of mitochondrial membrane potential. *J Mol Cell Cardiol* 35: 321–330, 2003.
40. **Smith PK, Krohn RI, Hermanson GT, Mallia AK, Gartner FH, Provenzano MD, Fujimoto EK, Goekke NM, Olson BJ, Klenk BC.** Measurement of protein using bicinchoninic acid. *Anal Biochem* 150: 76–85, 1985.
41. **Solinas G, Summermatter S, Mainieri D, Gubler M, Pirola L, Wymann MP, Rusconi S, Montani JP, Seydoux J, Dulloo AG.** The direct effect of leptin on skeletal muscle thermogenesis is mediated by substrate cycling between de novo lipogenesis and lipid oxidation. *FEBS Lett* 577: 539–544, 2004.
42. **Stefl B, Janovska A, Hodny Z, Rossmeisl M, Horakova M, Syrovy I, Bemova J, Bendlova B, Kopecky J.** Brown fat is essential for cold-induced thermogenesis but not for obesity resistance in aP2-Ucp mice. *Am J Physiol Endocrinol Metab* 274: E527–E533, 1998.
43. **Steinberg GR, Rush JW, Dyck DJ.** AMPK expression and phosphorylation are increased in rodent muscle after chronic leptin treatment. *Am J Physiol Endocrinol Metab* 284: E648–E654, 2003.
44. **Sugden MC, Holness MJ.** Recent advances in mechanisms regulating glucose oxidation at the level of the pyruvate dehydrogenase complex by PDKs. *Am J Physiol Endocrinol Metab* 284: E855–E862, 2003.
45. **Surwit RS, Feinglos MN, Rodin J, Sutherland A, Petro AE, Opara EC, Kuhn CM, Rebuffe-Scrive M.** Differential effects of fat and sucrose on the development of obesity and diabetes in C57BL/6J and A/J mice. *Metabolism* 44: 645–651, 1995.
46. **Surwit RS, Kuhn CM, Cochrane C, McCubbin JA, Feinglos MN.** Diet-induced type II diabetes in C57BL/6J mice. *Diabetes* 37: 1163–1167, 1988.
47. **Surwit RS, Petro AE, Parekh P, Collins S.** Low plasma leptin in response to dietary fat in diabetes- and obesity-prone mice. *Diabetes* 46: 1516–1520, 1997.
48. **Surwit RS, Wang S, Petro AE, Sanchis D, Raimbault S, Ricquier D, Collins S.** Diet-induced changes in uncoupling proteins in obesity-prone and obesity-resistant strains of mice. *Proc Natl Acad Sci USA* 95: 4061–4065, 1998.
49. **Tremblay A, Pelletier C, Doucet E, Imbeault P.** Thermogenesis and weight loss in obese individuals: a primary association with organochlorine pollution. *Int J Obes Relat Metab Disord* 28: 936–939, 2004.
50. **Ukropec J, Anunciado RP, Ravussin Y, Hulver MW, Kozak LP.** UCP1-independent thermogenesis in white adipose tissue of cold-acclimated Ucp1−/− mice. *J Biol Chem* 281: 31894–31908, 2006.
51. **Ukropec J, Anunciado RV, Ravussin Y, Kozak LP.** Leptin is required for uncoupling protein-1-independent thermogenesis during cold stress. *Endocrinology* 147: 2468–2480, 2006.
52. **Watson PM, Commins SP, Beiler RJ, Hatcher HC, Gettys TW.** Differential regulation of leptin expression and function in A/J vs. C57BL/6J mice during diet-induced obesity. *Am J Physiol Endocrinol Metab* 279: E356–E365, 2000.
53. **West DB, Boozer CN, Moody DL, Atkinson RL.** Dietary obesity in nine inbred mouse strains. *Am J Physiol Regul Integr Comp Physiol* 262: R1025–R1032, 1992.
54. **Woods A, Salt I, Scott J, Hardie DG, Carling D.** The alpha1 and alpha2 isoforms of the AMP-activated protein kinase have similar activities in rat liver but exhibit differences in substrate specificity in vitro. *FEBS Lett* 397: 347–351, 1996.
55. **Zurlo F, Larson K, Bogardus C, Ravussin E.** Skeletal muscle metabolism is a major determinant of resting energy expenditure. *J Clin Invest* 86: 1423–1427, 1990.

Publication C

Jelenik T, Rossmeisl M, Kuda O, Macek Jilkova Z, **Medrikova D**, Kus V, Hensler M, Janovska P, Miksik I, Baranowski M, Gorski J, Hebrard S, Jensen TE, Flachs P, Hawley S, Viollet B, Kopecky J.

AMP-activated protein kinase a2 subunit is required for the preservation of hepatic insulin sensitivity by n-3 polyunsaturated fatty acids.

Diabetes. 59: 2737-2746, 2010 (IF = 8.261)

AMP-activated Protein Kinase α2 Subunit Is Required for the Preservation of Hepatic Insulin Sensitivity by n-3 Polyunsaturated Fatty Acids

Tomas Jelenik,[1] Martin Rossmeisl,[1] Ondrej Kuda,[1] Zuzana Macek Jilkova,[1] Dasa Medrikova,[1] Vladimir Kus,[1] Michal Hensler,[1] Petra Janovska,[1] Ivan Miksik,[2] Marcin Baranowski,[3] Jan Gorski,[3] Sophie Hébrard,[4,5] Thomas E. Jensen,[6] Pavel Flachs,[1] Simon Hawley,[7] Benoit Viollet,[4,5] and Jan Kopecky[1]

OBJECTIVE—The induction of obesity, dyslipidemia, and insulin resistance by high-fat diet in rodents can be prevented by n-3 long-chain polyunsaturated fatty acids (LC-PUFAs). We tested a hypothesis whether AMP-activated protein kinase (AMPK) has a role in the beneficial effects of n-3 LC-PUFAs.

RESEARCH DESIGN AND METHODS—Mice with a whole-body deletion of the α2 catalytic subunit of AMPK (AMPKα2$^{-/-}$) and their wild-type littermates were fed on either a low-fat chow, or a corn oil-based high-fat diet (cHF), or a cHF diet with 15% lipids replaced by n-3 LC-PUFA concentrate (cHF+F).

RESULTS—Feeding a cHF diet induced obesity, dyslipidemia, hepatic steatosis, and whole-body insulin resistance in mice of both genotypes. Although cHF+F feeding increased hepatic AMPKα2 activity, the body weight gain, dyslipidemia, and the accumulation of hepatic triglycerides were prevented by the cHF+F diet to a similar degree in both AMPKα2$^{-/-}$ and wild-type mice in ad libitum-fed state. However, preservation of hepatic insulin sensitivity by n-3 LC-PUFAs required functional AMPKα2 and correlated with the induction of adiponectin and reduction in liver diacylglycerol content. Under hyperinsulinemic-euglycemic conditions, AMPKα2 was essential for preserving low levels of both hepatic and plasma triglycerides, as well as plasma free fatty acids, in response to the n-3 LC-PUFA treatment.

CONCLUSIONS—Our results show that n-3 LC-PUFAs prevent hepatic insulin resistance in an AMPKα2-dependent manner and support the role of adiponectin and hepatic diacylglycerols in the regulation of insulin sensitivity. AMPKα2 is also essential for hypolipidemic and antisteatotic effects of n-3 LC-PUFA under insulin-stimulated conditions. ***Diabetes*** **59:2737–2746, 2010**

From the [1]Department of Adipose Tissue Biology and the [2]Department of Analysis of Biologically Important Compounds, Institute of Physiology of the Academy of Sciences of the Czech Republic, v.v.i., Prague, Czech Republic; the [3]Department of Physiology, Medical University of Bialystok, Poland; the [4]Institut Cochin, Université Paris Descartes, CNRS (UMR 8104), Paris, France; [5]INSERM, U1016, Paris, France; the [6]Molecular Physiology Group, Copenhagen Muscle Research Centre, Department of Exercise and Sport Sciences, Section of Human Physiology, University of Copenhagen, Copenhagen, Denmark; and the [7]Division of Molecular Physiology, College of Life Sciences, University of Dundee, Scotland, U.K.

Corresponding author: Jan Kopecky, kopecky@biomed.cas.cz.

Received 20 November 2009 and accepted 26 July 2010. Published ahead of print at http://diabetes.diabetesjournals.org on 6 August 2010. DOI: 10.2337/db09-1716.

T.J. and M.R. contributed equally to this study.

Naturally occurring n-3 long-chain polyunsaturated fatty acids (LC-PUFAs)—namely, eicosapentaenoic acid (20:5n-3) and docosahexaenoic acid (22:6n-3)—which are abundant in sea fish, act as hypolipidemics, reduce cardiac events, and decrease the progression of atherosclerosis [reviewed in refs (1,2).]. Studies of obese humans have also demonstrated a reduction in adiposity after n-3 LC-PUFA supplementation (3,4). In rodents fed a high-fat diet, n-3 LC-PUFAs efficiently prevented the development of obesity, hepatic steatosis, and dyslipidemia (5–8), as well as impaired glucose tolerance (8–10). However, in diabetic patients, n-3 LC-PUFAs appear to have little effect on glycemic control (3,11,12).

The hypolipidemic and antiobesity effects of n-3 LC-PUFAs depend on both the suppression of lipogenesis and the increase in fatty acid oxidation in several tissues, including the liver (13,14), adipose tissue (6), and intestine (15). This metabolic switch may reduce the accumulation of toxic fatty acid derivatives, while protecting insulin signaling in the liver and muscle (9,10,16). Our previous work has documented that the preservation of whole-body insulin sensitivity by n-3 LC-PUFAs in mice fed a high-fat diet mainly reflects improved hepatic insulin sensitivity (8). The effects of n-3 LC-PUFAs and their active metabolites (17,18) are mediated by peroxisome proliferator-activated receptors (PPAR), with PPAR-α and PPAR-δ (-β) being the main targets (14,16), although PPAR-γ, liver X receptor-α, hepatic nuclear factor-4, sterol regulatory element binding protein-1c (SREBP-1c) and carbohydrate-responsive element-binding protein are also involved (16,19–21).

It has been demonstrated that n-3 LC-PUFAs enhanced AMP-activated protein kinase (AMPK) activity in the liver (22), intestine (23), and adipose tissue (18,24). AMPK is a heterotrimeric protein consisting of a catalytic α-subunit and regulatory β- and γ-subunits, with multiple isoforms identified for each subunit [α1, α2, β1, β2, γ1, γ2, and γ3; reviewed in ref (25)]. Experiments using whole-body AMPKα2 null [AMPKα2$^{-/-}$; ref (26)] mice showed the importance of the AMPKα2 subunit for whole-body insulin action, while liver-specific AMPKα2 knockout mice (27) as well as adenovirus-mediated activation of AMPKα2 in the liver (28) implicated the hepatic AMPKα2 isoform in the suppression of hepatic glucose production and maintenance of fasting blood glucose levels. Furthermore, AMPK controls metabolic fluxes in response to changing cellular

energy levels, namely, the partitioning between lipid oxidation and lipogenesis (29,30).

We hypothesized that the effects of n-3 LC-PUFA on insulin sensitivity and lipid metabolism in mice fed an obesogenic high-fat diet require a functional AMPKα2 isoform. To test this hypothesis in vivo, AMPKα2$^{-/-}$ and wild-type mice were fed either a low-fat chow diet (Chow), a corn oil-based high-fat (cHF) diet, or cHF diet in which 15% of the lipids were replaced by n-3 LC-PUFA concentrate (cHF+F). Our results demonstrate an AMPKα2-dependent action of n-3 LC-PUFAs, in *1*) the preservation of hepatic and muscle insulin sensitivity; *2*) the changes in hepatic diacylglycerol content and composition; and *3*) the antisteatotic effect in the liver and hypolipidemic effect under insulin-stimulated conditions, such as during hyperinsulinemic-euglycemic clamp, but not when the organism depends on lipids as substrates.

RESEARCH DESIGN AND METHODS

Four-month-old whole-body AMPKα2$^{-/-}$ mice (29) backcrossed to C57BL/6J mice for nine generations, and wild-type littermate controls were fed on either Chow, cHF, or cHF+F diet for nine weeks. Body weight and food consumption were recorded, and EDTA-plasma and tissues were collected for various analyses as described in the online appendix, available at http://diabetes.diabetesjournals.org/cgi/content/full/db09-1716/DC1. Male mice were used for all the experiments, except for the measurements of hepatic AMPK activity, which were performed on female mice. The experiments were conducted under the guidelines for the use and care of laboratory animals of the Institute of Physiology and followed the "Principles of laboratory animal care" (National Institutes of Health publication no. 85-23, revised 1985).

Blood and plasma parameters. Blood glucose was measured using calibrated glucometers (LifeScan, Milpitas, CA). Nonesterified fatty acids (NEFAs), triglycerides, and total cholesterol were determined in plasma using the following enzymatic photometric tests: NEFA-C (Wako Chemicals, Neuss, Germany), triacylglycerols liquid, and cholesterol liquid (Pliva-Lachema Diagnostika, Brno, Czech Republic), respectively. Plasma insulin was measured using the Sensitive Rat Insulin RIA Kit (LINCO Research, St. Charles, MO). Total adiponectin levels and adiponectin multimeric complexes were determined using Western blotting (31).

Lipid content and gene expression in the liver. The tissue content of triglycerides was estimated in ethanolic KOH tissue lysates as described before (8). The content and fatty acid composition of the phospholipid, diacylglycerol, triglyceride, and ceramide fractions were assessed in tissue lipid extracts; gene expression was evaluated using real-time RT-PCR (see online appendix).

Activity of α1 and α2 AMPK isoforms. Livers were collected by freeze-clamping, AMPK was immunoprecipitated from tissue extracts, and the activity was assayed using a peptide substrate (32); see the online appendix.

Hyperinsulinemic-euglycemic clamp. Five days before the experiment, an indwelling catheter was placed into the left femoral vein under anesthesia (33). Mice were allowed to recover for 5–7 days, followed by a 6-h fast (8:00 A.M.–2:00 P.M.) prior to the experiment. The whole-body glucose turnover was determined under basal (nonstimulated) and insulin-stimulated conditions (hyperinsulinemic-euglycemic clamp), using separate groups of mice. Insulin (Actrapid, Novo Nordisk Pharma, Denmark) was infused at a constant rate of 4.8 mU/kg·min for 3 h, while D-[3-^{3}H]glucose (Perkin Elmer, Boston, MA) was infused at a rate of 15.9 kBq/min. Throughout the infusion, glucose concentration and D-[3-^{3}H]glucose specific activity (during the last hour of infusion) were determined in tail blood. Euglycemia (~5.55 mmol/l) was maintained by periodically adjusting a variable infusion of 33% glucose (33). At the end of a 3-h infusion period, mice were first anesthetized by diethylether, exsanguinated through the cervical incision, and then killed by cervical dislocation, and tissues (liver and quadriceps muscle) and EDTA-plasma were collected for biochemical analyses (see supplementary Table 1 and Research Design and Methods of the online appendix for details on basic clamp parameters and methodology).

Primary cultures of hepatocytes. Hepatocytes were isolated from livers of fed mice by a modification of the collagenase method (34) and seeded at a density of 0.5×10^6 cells per each 35-mm Petri dish. Rates of basal and insulin-stimulated de novo lipogenesis and AICAR-stimulated fatty acid oxidation were measured using [1-^{14}C] acetate and [1-^{14}C] palmitate, respectively (see online appendix).

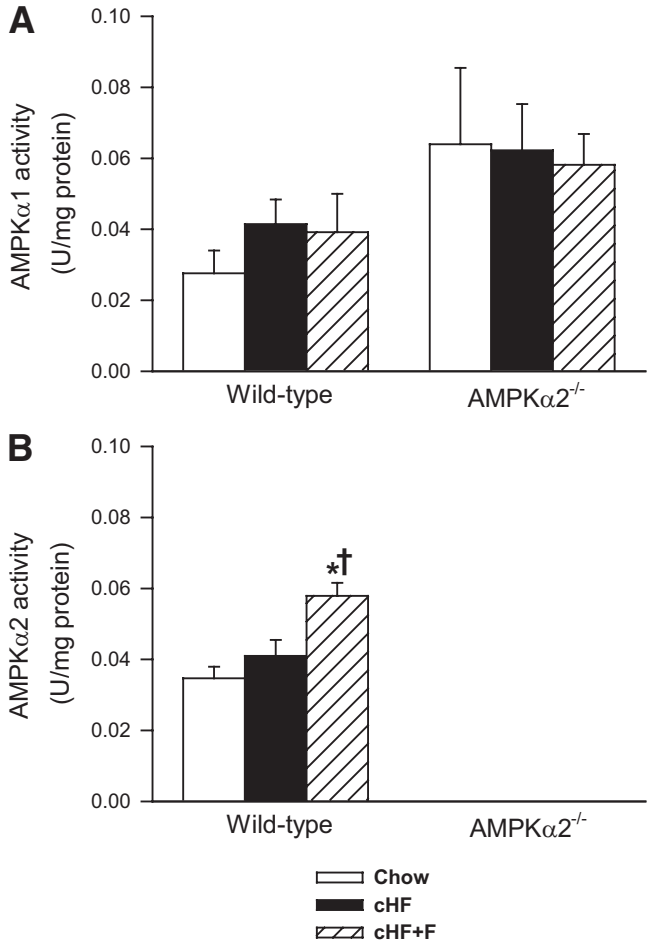

FIG. 1. Liver AMPKα1 (*A*) and AMPKα2 (*B*) activity in wild-type and AMPKα2$^{-/-}$ mice fed either a Chow diet, cHF, or cHF+F for 9 weeks. The data are the means ± SE (n = 5–8). In the AMPKα2$^{-/-}$ mice, AMPKα2 activity was below the detection limit. *P < 0.05 versus genotype Chow; †P < 0.05 versus genotype cHF.

Statistics. All values are presented as means ± SE. Data were analyzed by two-way ANOVA. Comparisons were judged to be significant at $P \leq 0.05$.

RESULTS

Enhancement of hepatic AMPKα2 activity by n-3 LC-PUFAs. Specific activities of AMPKα1 and AMPKα2 were evaluated in the liver of ad libitum-fed mice after nine weeks of the differential dietary treatment (Fig. 1). No significant effect of either diet (Chow, cHF, and cHF+F) or genotype (wild-type versus AMPKα2$^{-/-}$) on AMPKα1-specific activity was observed, although the AMPKα1 activity tended to be higher in the AMPKα2$^{-/-}$ mice (Fig. 1*A*). In contrast, AMPKα2 activity was stimulated by n-3 LC-PUFAs (cHF+F diet; Fig. 1*B*). AMPKα2 activity was not detected in the AMPKα2$^{-/-}$ mice (Fig. 1*B*). No changes were detected in the activity of AMPKα1 and AMPKα2 in the quadriceps muscle in response to n-3 LC-PUFAs (not shown).

AMPKα2 is not required for antiobesity and hypolipidemic effects of n-3 LC-PUFAs in ad libitum-fed mice. At four months of age, at the beginning of dietary treatments, wild-type and AMPKα2$^{-/-}$ mice fed the Chow diet exhibited similar body weights (Table 1). In mice of both genotypes, cHF-feeding for nine weeks resulted in greater body weight gain compared with the Chow-fed mice. However, this effect was less pronounced in AMPKα2$^{-/-}$

TABLE 1
Metabolic and plasma parameters in wild-type and AMPKα2$^{-/-}$ mice

Metabolic parameters	Wild-type			AMPKα2$^{-/-}$		
	Chow	cHF	cHF+F	Chow	cHF	cHF+F
Food consumption (kJ/g · day)	2.0 ± 0.1	1.8 ± 0.1	1.9 ± 0.0	2.0 ± 0.1	1.8 ± 0.1	2.0 ± 0.1
Initial body weight (g)	27.8 ± 0.5	27.9 ± 0.5	27.7 ± 0.5	27.1 ± 0.3	27.7 ± 0.4	27.3 ± 0.4
Body weight gain (g)	1.4 ± 0.2	7.0 ± 1.1*	2.8 ± 0.7†	1.8 ± 0.3	4.6 ± 0.7*‡	1.2 ± 0.4†
Adiposity						
Epididymal AT (g)	0.43 ± 0.02	1.52 ± 0.19*	1.12 ± 0.14*†	0.37 ± 0.03	1.19 ± 0.16*‡	0.64 ± 0.07*†‡
Subcutaneous AT (g)	0.20 ± 0.01	0.54 ± 0.05*	0.42 ± 0.04*†	0.17 ± 0.01	0.34 ± 0.03*‡	0.23 ± 0.01†‡
Epididymal adipocytes size (μm^2)	ND	15,971 ± 1,784	10,232 ± 185†	ND	13,298 ± 1,632	8 593 ± 896†
Subcutaneous adipocytes size (μm^2)	2,916 ± 610	6,775 ± 1,718*	7,311 ± 1,308*	3,395 ± 139	6,625 ± 926*	5,432 ± 648*
Plasma metabolites						
Triglycerides (mmol/l)	1.17 ± 0.08	1.23 ± 0.11	0.62 ± 0.07*†	1.04 ± 0.06	1.22 ± 0.08	0.73 ± 0.06*†
NEFAs (mmol/l)	0.90 ± 0.05	0.94 ± 0.05	0.59 ± 0.04*†	0.88 ± 0.04	0.99 ± 0.06	0.68 ± 0.04*†
Cholesterol (mmol/l)	2.25 ± 0.08	4.12 ± 0.25*	3.10 ± 0.20*†	2.10 ± 0.06	3.94 ± 0.18*	2.75 ± 0.14*†
Glucose (mmol/l)	9.9 ± 0.4	10.7 ± 0.5	10.4 ± 0.3	9.7 ± 0.4	10.0 ± 0.4	9.4 ± 0.4
Plasma hormones						
Insulin fed (ng/ml)	0.66 ± 0.11	1.73 ± 0.29*	1.47 ± 0.28*	0.60 ± 0.07	1.34 ± 0.20*	0.95 ± 0.12*
Insulin fasted (ng/ml)	0.13 ± 0.01	0.39 ± 0.06*	0.19 ± 0.05†	0.16 ± 0.02	0.22 ± 0.03‡	0.15 ± 0.01
Total adiponectin (A.U.)	1.15 ± 0.09	0.97 ± 0.10	1.33 ± 0.09†	0.82 ± 0.09‡	0.80 ± 0.07	0.97 ± 0.08‡
HMW: total adiponectin	0.38 ± 0.02	0.36 ± 0.02	0.44 ± 0.02†	0.35 ± 0.02	0.34 ± 0.02	0.39 ± 0.02

Data are means ± SE of 27–30 mice for metabolic parameters and 13–15 mice for other measures. AMPKα2$^{-/-}$ and wild-type mice were fed either a Chow diet, cHF, or cHF+F for nine weeks. Food consumption was measured weekly for nine weeks. Body weight gain (see supplementary Fig. 1) and plasma parameters were assessed in ad libitum-fed mice after nine weeks. Plasma insulin levels were also assessed in fasted mice after eight weeks. AT, adipose tissue; A.U., arbitary units; HMW, total adiponectin, ratio of high molecular weight to total adiponectin (for levels of all molecular weight forms of adiponectin; ND, no data; see supplementary Fig. 2); *$P < 0.05$ vs. genotype Chow; †$P < 0.05$ vs. genotype cHF; ‡$P < 0.05$ vs. wild-type on respective diet.

mice (Table 1). In both wild-type and AMPKα2$^{-/-}$ mice, the cHF+F diet induced smaller body weight gain than the cHF diet (Table 1 and supplementary Figure 1). None of the differences in body weight gain could be explained by caloric intake, which was similar in all experimental groups (Table 1). The weight of fat depots increased in response to cHF feeding, while the cHF+F diet partially prevented this increase (Table 1). Triglycerides and NEFA levels in plasma of ad libitum-fed mice were similar in the Chow- and cHF-fed mice, while cholesterol levels were markedly and significantly elevated by the cHF diet. n-3 LC-PUFAs lowered plasma lipid levels independently of AMPKα2. Triglycerides and NEFA levels were strongly reduced, even below the levels observed in the Chow-fed mice (Table 1).

AMPKα2 is essential for the preservation of insulin sensitivity in response to n-3 LC-PUFAs. After nine weeks of dietary treatment, no change was observed in blood glucose, but elevations were observed in plasma insulin levels in response to the cHF diet in ad libitum-fed mice of both genotypes. However, the increase in plasma insulin levels was less pronounced in AMPKα2$^{-/-}$ mice, closely reflecting the genotype-dependent differences in body weight gain (Table 1). A similar pattern of changes in insulin levels was also observed in fasted mice, in which n-3 LC-PUFAs significantly reduced insulin levels only in wild-type animals (Table 1). As expected, plasma levels of total as well as high molecular weight form of adiponectin, an adipokine associated with increased insulin sensitivity (35), were increased ~1.4- and ~1.2-fold, respectively, in wild-type mice in response to n-3 LC-PUFA supplementation (Table 1 and supplementary Fig. 2, available in an online appendix); however, no significant increase of plasma adiponectin by n-3 LC-PUFAs was observed in AMPKα2$^{-/-}$ mice.

In further experiments, hyperinsulinemic-euglycemic clamps were performed to evaluate whole-body insulin sensitivity. Under basal conditions, glucose turnover rate (GTO; i.e., glucose uptake in peripheral tissues) was similar in all groups of mice (supplementary Table 1). Under insulin-stimulated conditions (Fig. 2*A–F*), the amount of exogenous glucose required to maintain euglycemia during the clamp, i.e., the glucose infusion rate (GIR), was ~1.3-fold lower in AMPKα2$^{-/-}$ than in wild-type mice fed the Chow diet (Fig. 2*A*). On the other hand, GIR was decreased by the cHF diet to a similar level in mice of both genotypes, manifesting diet-induced insulin resistance. This was attributed to a decreased GTO and, in particular, to an impaired suppression of hepatic glucose production (HGP) by insulin, with HGP being ~8.5-fold higher in the cHF-fed compared with the Chow-fed wild-type mice (Fig. 2*C*). In wild-type mice, cHF+F diet feeding increased GIR and GTO (~1.9- and ~1.2-fold increase, respectively) as compared with cHF-fed mice, while HGP was lowered to a similar level as in the Chow-fed mice. These results document the protective effects of n-3 LC-PUFAs from high-fat diet-induced insulin resistance in wild-type mice, namely, at the level of HGP. In contrast, none of these beneficial effects of n-3 LC-PUFAs was observed in AMPKα2$^{-/-}$ mice, in which neither the GIR (Fig. 2*A*) nor the GTO (Fig. 2*B*) differed between the cHF+F-fed and the cHF-fed mice, whereas the rate of HGP was even higher in the cHF+F-fed than in the cHF-fed AMPKα2$^{-/-}$ mice (Fig. 2*C*). Although whole-body glycolysis was similar in all the groups (Fig. 2*D*), the rate of whole-body glycogen synthesis, which reflects insulin sensitivity of muscle glucose metabolism, was dependent on both diet and genotype (Fig. 2*E*). In the Chow-fed mice, the rate of whole-body glycogen synthesis tended to be higher in wild-type mice than in AMPKα2$^{-/-}$ mice. Only in the former mice was it significantly affected by dietary treatment. Thus, in wild-type mice, glycogen synthesis was

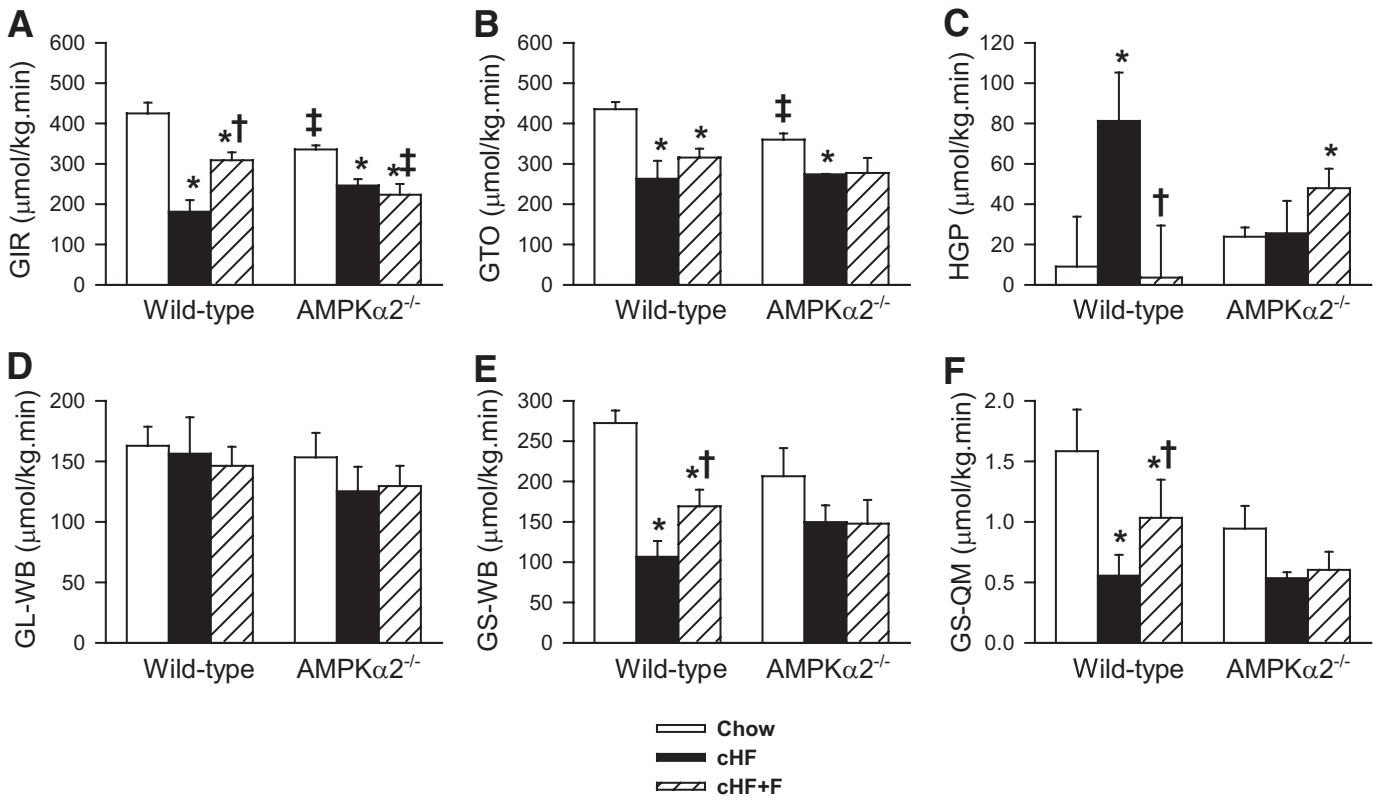

FIG. 2. Insulin sensitivity assessed by hyperinsulinemic-euglycemic clamp. GIR (*A*), GTO (*B*), HGP (*C*), whole-body glycolysis (GL-WB; *D*), whole-body glycogen synthesis (GS-WB; *E*); and glycogen synthesis in quadriceps muscle (GS-QM; *F*) were measured in wild-type and AMPKα2$^{-/-}$ mice fed either a Chow diet, cHF, or cHF+F for 9 weeks. The data are the means ± SE (n = 5–8). *P < 0.05 versus genotype Chow; †P < 0.05 versus genotype cHF; ‡P < 0.05 versus wild-type on respective diet.

decreased ~2.4-fold in response to the cHF diet, while n-3 LC-PUFAs provided a partial protection from this decrease (Fig. 2*E*). A similar pattern of changes in the glycogen synthesis rate in response to n-3 LC-PUFAs was observed when measured directly in the skeletal muscle (Fig. 2*F*). Thus, in accordance with the previous study (26), the results of clamp studies suggested impairment of insulin sensitivity in response to whole-body ablation of AMPKα2 in Chow-fed mice. However, AMPKα2$^{-/-}$ mice seemed to be partially protected against cHF-induced insulin resistance, while AMPKα2 was required for preservation of insulin sensitivity in the skeletal muscle and especially in the liver in response to n-3 LC-PUFA feeding.

Unmasking the role of AMPKα2 in the lipid-lowering effect of n-3 LC-PUFAs under hyperinsulinemic-euglycemic conditions. In addition to the ad libitum-fed mice (Table 1), plasma lipid levels were also measured in fasted mice, as well as in mice subjected to hyperinsulinemic-euglycemic clamp (supplementary Table 2). In contrast to the ad libitum-fed state, cHF+F diet did not affect either triglyceride or NEFA levels under fasting conditions. Under the hyperinsulinemic-euglycemic conditions, both triglyceride and NEFA levels were lower in the cHF+F-fed than in the cHF-fed wild-type mice (~1.6-fold and ~1.4-fold difference, respectively), but no such difference between the diets was observed in AMPKα2$^{-/-}$ mice. Cholesterol levels were consistently decreased by n-3 LC-PUFAs independently of both the metabolic state and genotype (supplementary Table 2).

In ad libitum-fed mice of both genotypes, the hepatic triglyceride content was increased ~twofold by cHF compared with the Chow diet, while triglyceride accumulation was increased only ~1.3-fold by cHF+F diet in both genotypes, documenting a protection against hepatic triglyceride accumulation by n-3 LC-PUFAs (Fig. 3*A*). Under hyperinsulinemic-euglycemic conditions, n-3 LC-PUFAs also protected livers of wild-type mice against the cHF-induced accumulation of triglycerides. However, this effect was absent in AMPKα2$^{-/-}$ mice (Fig. 3*B*). Moreover, a strong correlation was found between plasma NEFA levels and hepatic triglyceride content assessed under the clamp conditions in the cHF+F-fed AMPKα2$^{-/-}$ mice (R^2 = 0.43, P < 0.05) but not in wild-type mice (R^2 = 0.08, P = 0.40).

Dietary n-3 LC-PUFAs increase 5-aminoimidazole-4-carboxamide-1-β-D-ribofuranoside–stimulated fatty acid oxidation and insulin-stimulated lipogenesis in cultured hepatocytes from wild-type but not from AMPKα2$^{-/-}$ mice. We sought to determine whether the differential effect of n-3 LC-PUFAs on accumulation of liver triglycerides in wild-type and AMPKα2$^{-/-}$ mice under the clamp conditions could be explained by hepatic lipid metabolism. In cultured hepatocytes isolated from mice following the different dietary treatments, activities of both fatty acid oxidation and de novo fatty acid synthesis were evaluated. The stimulatory effects of 5-aminoimidazole-4-carboxamide-1-β-D-ribofuranoside (AICAR), an AMPK activator, and insulin on fatty acid oxidation and synthesis are shown in Fig. 4*A* and *B*, respectively (for corresponding basal metabolic activities, see supplementary Table 3, available in an online appendix). In hepatocytes from both Chow and cHF diet-fed mice, the absence of AMPKα2 was associated with a trend for lower AICAR-stimulated fatty acid oxidation. Although hepatocytes

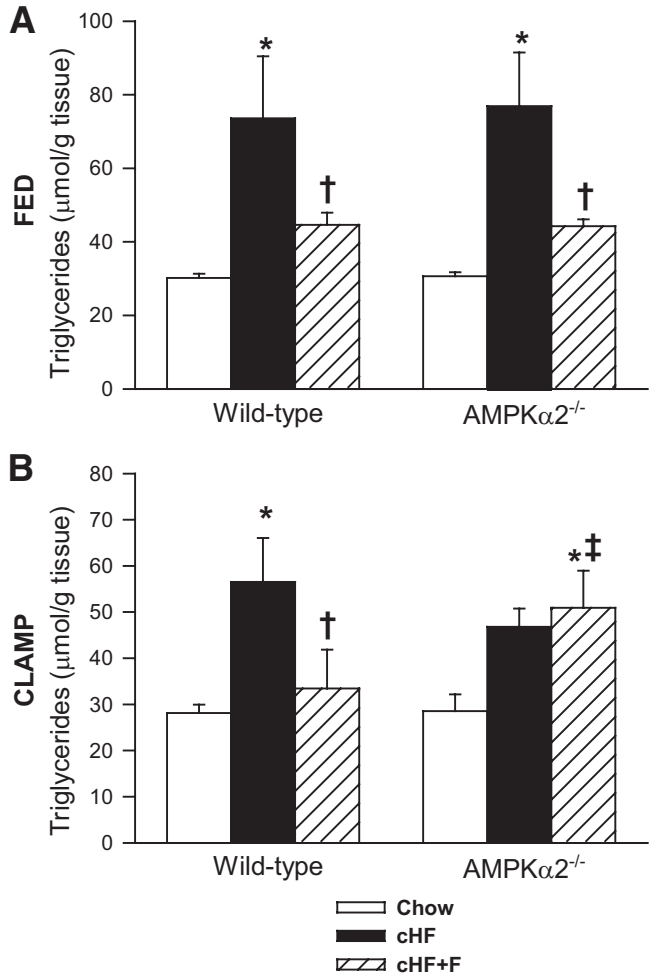

FIG. 3. Triglyceride concentration in the livers of ad libitum-fed mice (*A*) and mice killed at the end of a 3-h infusion period of the hyperinsulinemic-euglycemic clamp (*B*). Wild-type and AMPKα2$^{-/-}$ mice were fed either a Chow diet, cHF, or cHF+F for 9 weeks. The data are the means ± SE (*A*, n = 13–15; *B*, n = 8–14). *P < 0.05 versus genotype Chow; †P < 0.05 versus genotype cHF; ‡P < 0.05 versus wild-type on respective diet. For the detailed fatty acid composition of triglyceride fractions in the livers of ad libitum-fed mice, see supplementary Table 4.

from cHF-fed mice showed reduced stimulatory effect of AICAR irrespective of the genotype, cHF+F feeding normalized this defect in wild-type but not in AMPKα2$^{-/-}$ hepatocytes (Fig. 5*A*), suggesting AMPK-dependent induction of capacity for fatty acid oxidation by n-3 LC-PUFAs in the liver. The stimulatory effect of insulin on de novo fatty acid synthesis was reduced in hepatocytes from cHF-fed wild-type mice, whereas it was retained in the hepatocytes from cHF-fed AMPKα2$^{-/-}$ mice (Fig. 4*B*). cHF+F feeding tended to restore the stimulatory effect of insulin only in wild-type hepatocytes (Fig. 4*B*).

To further characterize hepatic effects of differential dietary treatment, the expression of selected genes was quantified in total RNA isolated from the livers of mice subjected to hyperinsulinemic-euglycemic clamp (Fig. 4*C* and *D*). Feeding cHF diet suppressed expression of lipogenic genes stearoyl-CoA desaturase (SCD-1) and SREBP-1c in all groups (except for SREBP-1c in AMPKα2$^{-/-}$ mice). This suppression was partially counteracted by cHF+F diet in wild-type but not AMPKα2$^{-/-}$ mice (Fig. 4*C* and *D*). Together with the de novo fatty acid synthesis data, these results further support the AMPKα2-dependent improvement of liver insulin sensitivity by n-3 LC-PUFAs.

Changes in hepatic diacylglycerol levels are associated with insulin-sensitizing effects of n-3 LC-PUFAs. To identify factors predisposing animals to insulin resistance in an AMPKα2-dependent manner, a detailed analysis of hepatic lipids in ad libitum-fed mice was performed. No major genotype-dependent differences in the contents of either ceramides or phospholipids were observed (supplementary Table 4). In contrast, hepatic content of diacylglycerols was affected in a genotype- and diet-dependent manner (Fig. 5*A*). Wild-type mice fed the cHF+F diet had lower diacylglycerol content than genotype-matched cHF diet-fed mice, while this effect of the cHF+F diet was not observed in AMPKα2$^{-/-}$ mice. Moreover, the analysis of fatty acid composition of the diacylglycerol fraction in the liver revealed that wild-type as well as AMPKα2$^{-/-}$ mice fed cHF diet were characterized by marked increase in the level of PUFA but not monounsaturated or saturated fatty acids (Fig. 5*B*, *C*, and *D* and supplementary Table 4). The increase in the PUFA content tended to be smaller in the wild-type compared with AMPKα2$^{-/-}$ mice (~1.7-fold and ~2.2-fold, respectively). Administration of n-3 LC-PUFAs completely prevented accumulation of hepatic polyunsaturated diacylglycerols in wild-type mice, whereas their level in the AMPKα2$^{-/-}$ animals, although decreased, was still significantly higher compared with genotype-matched Chow-fed mice (Fig. 5*B*). Regarding polyunsaturated diacylglycerols, α-linolenic acid (18:3n-3) appeared to be by far the most differentially regulated PUFA in the diacylglycerol fraction in the two genotypes (supplementary Table 4). In addition, cHF+F diet markedly reduced hepatic content of monounsaturated diacylglycerols in wild-type but not in knockout animals (Fig. 5*C*). Hepatic diacylglycerol levels and their fatty acid composition were also analyzed in mice subjected to hyperinsulinemic-euglycemic clamp (supplementary Table 5 and supplementary Fig. 3). No significant differences among the groups were observed in total diacylglycerols content or in their saturated or monounsaturated fatty acid fractions (supplementary Fig. 3).

DISCUSSION

Previous animal studies demonstrated that n-3 LC-PUFAs could counteract the development of both hepatic steatosis (8,18,36,37) and hepatic insulin resistance (8,9,16), while suppressing lipogenesis and augmenting lipid catabolism in the liver (8,13,19,21). Using mice with a whole-body deletion of AMPKα2 and high-fat feeding, we show for the first time that AMPKα2 is required for the effect of n-3 LC-PUFAs to preserve whole-body, muscle, and especially hepatic insulin sensitivity, as well as to suppress hepatic and plasma triglycerides as well as NEFA levels under hyperinsulinemic-euglycemic clamp conditions. In contrast, AMPKα2 was not required for protection by n-3 LC-PUFAs from hepatic lipid accumulation and dyslipidemia in ad libitum-fed mice.

In addition to AMPKα2, PPARα was previously identified as an important determinant of n-3 LC-PUFA's effect on lipid metabolism, especially short-term modulation of hepatic gene expression (14) and insulin sensitivity (16). Thus, the reduction in hepatic triglyceride concentrations by fish oil feeding did not rescue insulin action in PPARα-null mice, while hepatic diacylglycerol concentrations were decreased by fish oil in a PPARα-dependent manner

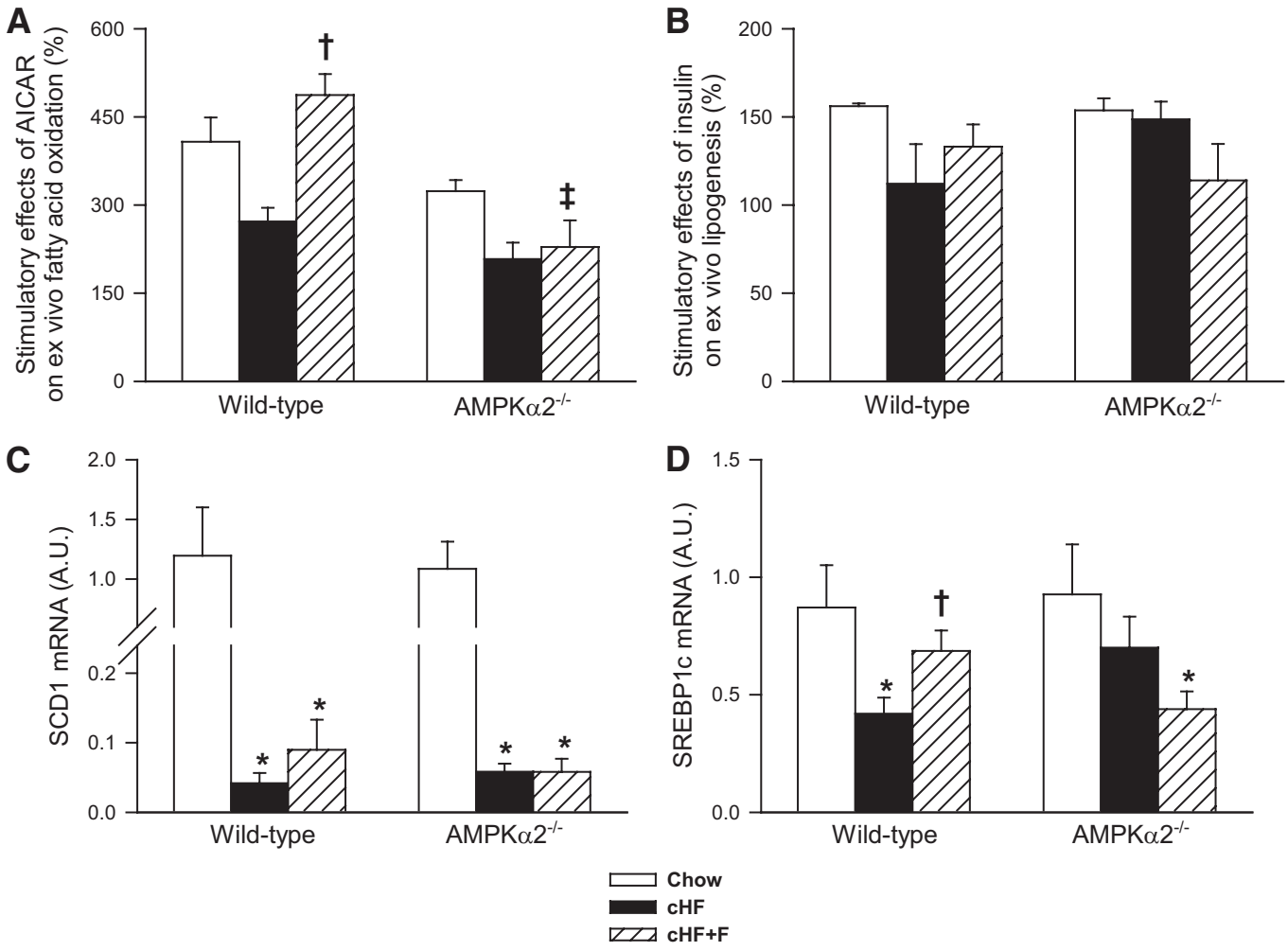

FIG. 4. The effect of differential dietary treatment on the regulation of metabolic fluxes in the liver. AICAR-stimulated fatty acid oxidation (*A*) and insulin-stimulated de novo fatty acid synthesis (*B*) in cultured hepatocytes isolated from wild-type and AMPKα2$^{-/-}$ mice fed for 9 weeks either a Chow diet, cHF, or cHF+F. For basal nonstimulated rates of lipid metabolism, see supplementary Table 3. The expression of SCD-1 (*C*) and SREBP-1c (*D*) genes was quantified in total RNA isolated from the livers of mice subjected to hyperinsulinemic-euglycemic clamp following the differential dietary treatment for 9 weeks. The data are means ± SE (isolated hepatocytes, $n = 3$ in triplets; hepatic gene expression, $n = 5–8$). *$P < 0.05$ versus genotype Chow; †$P < 0.05$ versus genotype cHF; ‡$P < 0.05$ versus wild-type on respective diet. A.U., arbitrary units.

and were associated with a preserved hepatic insulin sensitivity (16). It is generally accepted that *1*) diacylglycerols rather than triglycerides or ceramides mediate hepatic insulin resistance in mice fed a high-fat diet (19,38,39), *2*) diacylglycerol-induced insulin resistance depends on activation of protein kinase C, and *3*) that polyunsaturated diacylglycerols in particular are better protein kinase C activators than saturated diacylglycerol species [reviewed in refs (38,39)]. Also our results showed that cHF diet-induced insulin resistance was associated primarily with the accumulation of PUFA in hepatic diacylglycerols and that n-3 LC-PUFA completely prevented cHF diet-induced increase in PUFA diacylglycerols in wild-type mice, whereas in AMPKα2$^{-/-}$ animals, the content of these lipids was still significantly higher compared with the control. Moreover, it was only in ad libitum-fed mice but not in mice subjected to hyperinsulinemic-euglycemic clamps that the levels of hepatic diacylglycerols and their fatty acid compositions were associated with hepatic insulin sensitivity. It is possible that under clamp conditions AMPKα2-dependent effects of n-3 LC-PUFAs on liver diacylglycerols were masked by metabolic changes occurring during a 3-h infusion of insulin and glucose.

The failure of n-3 LC-PUFAs to decrease hepatic lipids in AMPKα2$^{-/-}$ mice under clamp conditions could be due to primary alterations in metabolic fluxes in the liver, reflecting *1*) increased de novo fatty acid synthesis, *2*) decreased secretion of VLDL triglycerides, or *3*) reduced fatty acid oxidation. De novo fatty acid synthesis was not the responsible factor, because hepatocytes of the n-3 LC-PUFA-fed AMPKα2$^{-/-}$ mice showed decreased insulin-stimulated de novo fatty acid synthesis and reduced expression of SREBP-1c and SCD-1, as compared with hepatocytes isolated from n-3 LC-PUFA-fed wild-type mice, reflecting probably low insulin sensitivity of the liver in AMPKα2$^{-/-}$ mice. Moreover, AICAR-stimulated fatty acid oxidation in hepatocytes from n-3 LC-PUFA-fed AMPKα2$^{-/-}$ mice was markedly reduced as compared with those from wild-type mice, suggesting decreased hepatic capacity for fatty acid oxidation in the absence of AMPKα2, which could contribute to enhanced lipid accumulation. Therefore, these experiments supported a major role of hepatic AMPKα2 in the regulation of both insulin sensitivity and lipid metabolism by n-3 LC-PUFAs. However, the differential modulation of lipid accumulation by n-3 LC-PUFAs in the livers of wild-type and AMPKα2$^{-/-}$

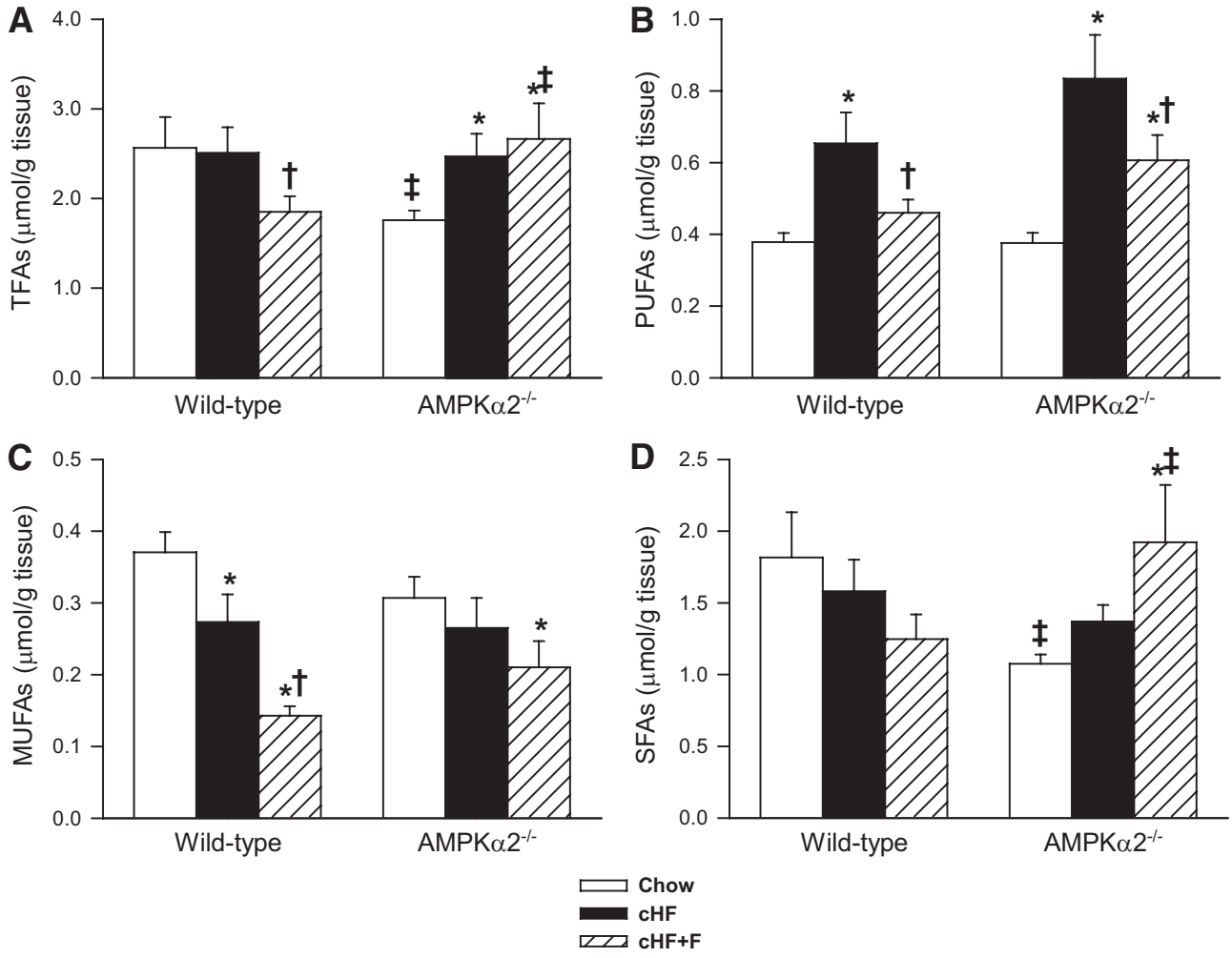

FIG. 5. The composition of fatty acids in hepatic diacylglycerol fraction in ad libitum-fed wild-type and AMPKα2$^{-/-}$ mice: total fatty acids (TFAs; *A*), PUFAs (*B*), monounsaturated fatty acids (MUFAs; *C*), and saturated fatty acids (SFAs; *D*). Animals were fed either a Chow diet, cHF, or cHF+F for 9 weeks. The data are the means ± SE (n = 13–15). *P < 0.05 versus genotype Chow; †P < 0.05 versus genotype cHF; ‡P < 0.05 versus wild-type on respective diet. For the detailed fatty acid composition of diacylglycerol fractions in the livers of ad libitum fed mice, see supplementary Table 4.

mice under clamp conditions could also be secondary to the AMPKα2-dependent effects of n-3 LC-PUFAs in other tissues, resulting in a relatively high hepatic uptake of circulating NEFA in AMPKα2$^{-/-}$ mice. This is supported by persistently elevated plasma levels of NEFA in AMPKα2$^{-/-}$ mice, as well as by a significant correlation between plasma NEFA levels and hepatic triglyceride content observed under clamp conditions in AMPKα2$^{-/-}$ but not wild-type mice fed n-3 LC-PUFA-containing diet. Moreover, it has been shown in humans with nonalcoholic fatty liver disease that most of hepatic triglycerides arise from circulating NEFA (40). That plasma NEFA levels under clamp conditions were reduced only in wild-type but not in AMPKα2$^{-/-}$ mice fed n-3 LC-PUFAs may reflect a role of AMPKα2 in muscle lipid uptake mediated by lipoprotein lipase (41), as well as the antilipolytic effect of AMPK in adipose tissue, documented for AMPKα1 (42). In any case, decreased fatty acid oxidation in situ in the liver and, possibly even more importantly, abundant supply of circulating NEFA could be responsible for the lack of the antisteatotic effect of n-3 LC-PUFAs in AMPKα2$^{-/-}$ mice under clamp conditions (Fig. 6).

Previous studies reported contradictory results, showing either *1*) activation of AMPK in rat liver (22) and murine adipose tissue (24) or *2*) no changes in AMPK activity in the liver, skeletal muscle, and heart of mice (43) in response to dietary n-3 LC-PUFAs. These discrepancies could be related to differences in dietary n-3 LC-PUFA intake, nutritional state of animals, and other parameters. In accordance with the involvement of AMPKα2 in various effects of n-3 LC-PUFAs, our results document activation of AMPKα2 (but not AMPKα1) in the liver of mice by long-term n-3 LC-PUFA treatment, in the absence of significant changes in either the AMP to ATP ratio assessed in whole liver extracts [not shown and ref (44)] or the phosphorylation status of LKB1, an upstream kinase for AMPK [not shown and ref (45)]. In addition, no effect on AMPK activity in either cultured hepatocytes (21) or embryonic kidney cells (not shown) of n-3 LC-PUFAs added to the cell culture medium could be detected. Therefore, the activation of AMPKα2 by n-3 LC-PUFAs probably does not depend on a direct interaction between n-3 LC-PUFAs and AMPK. On the other hand, induction of adiponectin by n-3 LC-PUFAs [results of this study and refs (46,47)] could be involved, because adiponectin activates AMPK in both the liver and skeletal muscle (35). Adiponectin is also required for the activation of AMPK upon administration of PPARγ agonists thiazolidinedio-

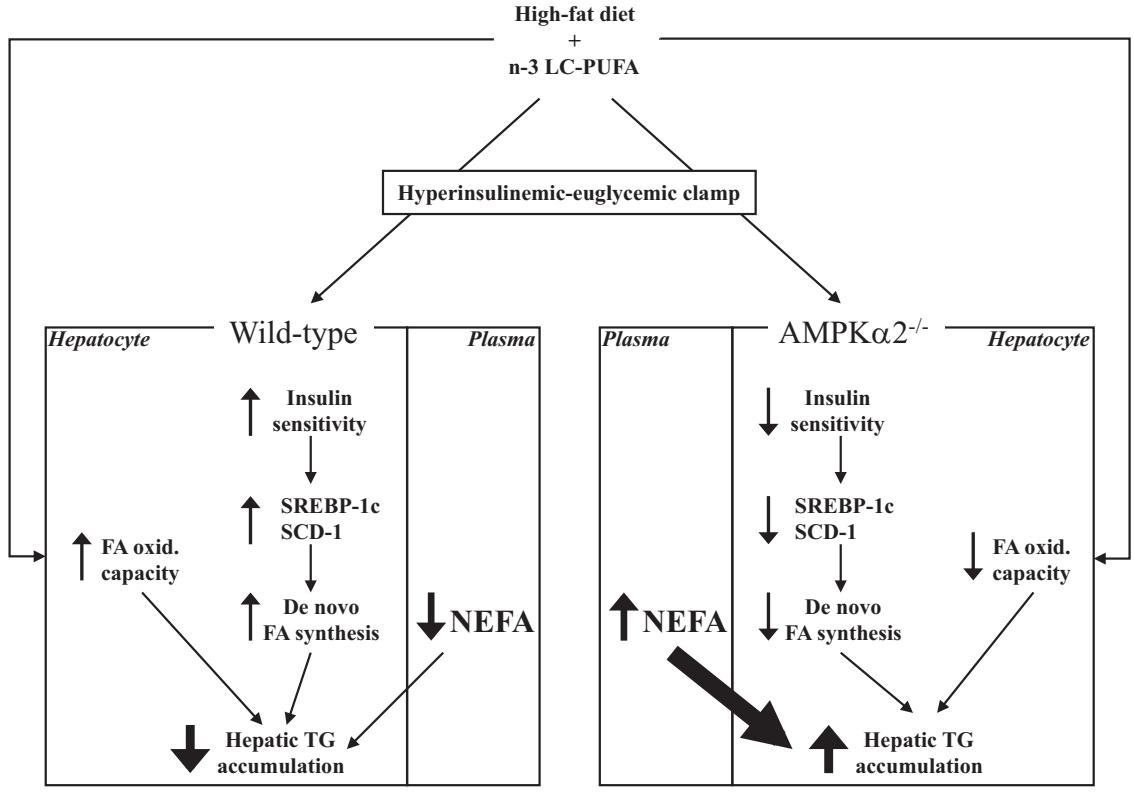

FIG. 6. Putative involvement of AMPKα2 in antisteatotic action of n-3 LC-PUFAs in the liver. Dietary intake of n-3 LC-PUFAs increases the capacity of hepatocytes to oxidize fatty acids in wild-type (left panels) but not in AMPKα2$^{-/-}$ mice (right panels). When insulin and glucose levels are high, such as during hyperinsulinemic-euglycemic clamp, wild-type mice fed n-3 LC-PUFAs exhibit improved hepatic insulin sensitivity and decreased plasma levels of NEFAs as compared with high-fat diet-fed controls. This is associated with increased expression of lipogenic genes such as SREBP-1c and SCD-1 and increased drive for de novo fatty acid synthesis. Despite the elevated lipogenic drive under clamp conditions, the livers of wild-type mice fed n-3 LC-PUFAs show reduced accumulation of triglycerides. However, in AMPKα2$^{-/-}$ mice fed n-3 LC-PUFAs, hepatic triglyceride content is markedly elevated despite reduced rates of de novo fatty acid synthesis. This effect could be secondary to persisting elevated NEFA levels in circulation and thus better substrate availability in AMPKα2$^{-/-}$ mice under clamp conditions. FA, fatty acids; TG, triglycerides.

nes, whereas mice lacking adiponectin show decreased hepatic insulin sensitivity and reduced responsiveness to these compounds (48). Thus, absence of AMPKα2 may blunt adiponectin-mediated effects of n-3 LC-PUFAs. In accordance with the previous study (49), plasma adiponectin levels tended to be reduced in AMPKα2$^{-/-}$ mice. Moreover, the induction of adiponectin by n-3 LC-PUFAs in AMPKα2$^{-/-}$ mice was compromised (Table 1 and supplementary Figure 2).

AMPKα1 and AMPKα2 contribute equally to total AMPK activity in the liver (50). In mice with liver-specific ablation of AMPKα2 (27), hepatic AMPKα2 was essential for suppressing hepatic glucose production and maintaining fasting blood glucose levels; however, the absence of AMPKα2 did not affect inhibitory action of insulin on hepatic glucose production. In our study, although fasting blood glucose levels were unaltered by whole-body ablation of AMPKα2, the beneficial effect of dietary n-3 LC-PUFAs on hepatic insulin sensitivity was clearly AMPKα2-dependent. Differential regulation of glucose homeostasis in the above transgenic models likely reflects the complexity of whole-body (26) versus liver-specific (27) deletion of AMPKα2. In contrast to the previous report, showing induction of adiposity and adipocyte hypertrophy in AMPKα2$^{-/-}$ mice fed a lard-based high-fat diet (49), our study documented a relatively low weight gain, low adiposity, and smaller fat cells in AMPKα2$^{-/-}$ mice fed a corn-oil based high-fat diet. This discrepancy could be related to the differences in the composition of experimental high-fat diets; however, our results are consistent with the elevated sympathetic tonus of AMPKα2$^{-/-}$ mice (26), which may stimulate energy dissipation in these animals. In any case, lower body weight of cHF-fed AMPKα2$^{-/-}$ mice as compared with their wild-type counterparts could be related to better insulin sensitivity of the former mice, as suggested by the differences in insulinemia, results of hyperinsulinemic-euglycemic clamp, stimulatory effect of insulin on lipogenesis, and expression of lipogenic genes in the liver.

In conclusion, the preservation of hepatic insulin sensitivity by n-3 LC-PUFAs in mice fed a high-fat diet depends on AMPKα2. The accumulation of diacylglycerols, which is regulated in an AMPKα2-dependent manner, could contribute to the modulation of hepatic insulin sensitivity in response to dietary n-3 LC-PUFAs. On the other hand, the AMPKα2-dependent acute changes in lipid metabolism and hepatic triglyceride accumulation, which are unmasked under insulin-stimulated conditions such as during hyperinsulinemic-euglycemic clamp, largely reflect the extrahepatic action of n-3 LC-PUFAs. Our results are relevant for the development of novel strategies for prevention and treatment of the metabolic syndrome.

ACKNOWLEDGMENTS

This study was supported by grants from the Czech Science Foundation (301/10/1420) and the Ministry of Education, Youth and Sports (1M6837805002, COST BMB0602-OC08007) of the Czech Republic. Further sup-

port included grants from the European Commission (LSHM-CT-2004-005272, EXGENESIS) and from EPAX AS (Norway), as well as the research project AV0Z50110509. No other potential conflicts of interest relevant to this article were reported.

T.J. and M.R. performed experiments and wrote the manuscript. O.K., Z.M.J., D.M., V.K., M.H., and P.J. performed experiments. I.M. quantified tissue nucleotides. M.B. performed analysis of hepatic lipids and contributed to discussion. J.G. performed analysis of hepatic lipids. S.H. contributed to experiments on hepatocytes. T.E.J. contributed to analysis of muscle metabolism. P.F. introduced AMPK$\alpha 2^{-/-}$ mouse model to the Prague laboratory and contributed to discussion. S.H. performed experiments on kidney cells. B.V. developed AMPK$\alpha 2^{-/-}$ mice and contributed to discussion. J.K. wrote the manuscript.

The authors thank D. Grahame Hardie for the sheep AMPKα1 and AMPKα2 antibodies, Z. Szulc for the gift of *N*-palmitoyl-D-*erythro*-sphingosine (C17 base), and J. Jones (NMR Research Unit, Department of Biochemistry and Center for Neurosciences and Cell Biology, University of Coimbra, Coimbra, Portugal) for critical reading of the manuscript.

REFERENCES

1. Flachs P, Rossmeisl M, Bryhn M, Kopecky J. Cellular and molecular effects of n-3 polyunsaturated fatty acids on adipose tissue biology and metabolism. Clin Sci 2009;116:1–16
2. Nettleton JA, Katz R. n-3 long-chain polyunsaturated fatty acids in type 2 diabetes: a review. J Am Diet Assoc 2005;105:428–440
3. Mori TA, Bao DQ, Burke V, Puddey IB, Watts GF, Beilin LJ. Dietary fish as a major component of a weight-loss diet: effect on serum lipids, glucose, and insulin metabolism in overweight hypertensive subjects. Am J Clin Nutr 1999;70:817–825
4. Couet C, Delarue J, Ritz P, Antoine JM, Lamisse F. Effect of dietary fish oil on body fat mass and basal fat oxidation in healthy adults. Int J Obes 1997;21:637–643
5. Ruzickova J, Rossmeisl M, Prazak T, Flachs P, Sponarova J, Veck M, Tvrzicka E, Bryhn M, Kopecky J. Omega-3 PUFA of marine origin limit diet-induced obesity in mice by reducing cellularity of adipose tissue. Lipids 2004;39:1177–1185
6. Flachs P, Horakova O, Brauner P, Rossmeisl M, Pecina P, Franssen-van Hal N, Ruzickova J, Sponarova J, Drahota Z, Vlcek C, Keijer J, Houstek J, Kopecky J. Polyunsaturated fatty acids of marine origin upregulate mitochondrial biogenesis and induce beta-oxidation in white fat. Diabetologia 2005;48:2365–2375
7. Ikemoto S, Takahashi M, Tsunoda N, Maruyama K, Itakura H, Ezaki O. High-fat diet-induced hyperglycemia and obesity in mice: differential effects of dietary oils. Metabolism 1996;45:1539–1546
8. Kuda O, Jelenik T, Jilkova Z, Flachs P, Rossmeisl M, Hensler M, Kazdova L, Ogston N, Baranowski M, Gorski J, Janovska P, Kus V, Polak J, Mohamed-Ali V, Burcelin R, Cinti S, Bryhn M, Kopecky J. n-3 fatty acids and rosiglitazone improve insulin sensitivity through additive stimulatory effects on muscle glycogen synthesis in mice fed a high-fat diet. Diabetologia 2009;52:941–951
9. Storlien LH, Kraegen EW, Chisholm DJ, Ford GL, Bruce DG, Pascoe WS. Fish oil prevents insulin resistance induced by high-fat feeding in rats. Science 1987;237:885–888
10. Jucker BM, Cline GW, Barucci N, Shulman GI. Differential effects of safflower oil versus fish oil feeding on insulin-stimulated glycogen synthesis, glycolysis, and pyruvate dehydrogenase flux in skeletal muscle: a ^{13}C nuclear magnetic resonance study. Diabetes 1999;48:134–140
11. Fasching P, Ratheiser K, Waldhäusl W, Rohac M, Osterrode W, Nowotny P, Vierhapper H. Metabolic effects of fish-oil supplementation in patients with impaired glucose tolerance. Diabetes 1991;40:583–589
12. Pelikánová T, Kohout M, Válek J, Kazdová L, Base J. Metabolic effects of omega-3 fatty acids in type 2 (non-insulin-dependent) diabetic patients. Ann N Y Acad Sci 1993;683:272–278
13. Teran-Garcia M, Adamson AW, Yu G, Rufo C, Suchankova G, Dreesen TD, Tekle M, Clarke SD, Gettys TW. Polyunsaturated fatty acid suppression of fatty acid synthase (FASN): evidence for dietary modulation of NF-Y binding to the Fasn promoter by SREBP-1c. Biochem J 2007;402:591–600
14. Sanderson LM, de Groot PJ, Hooiveld GJ, Koppen A, Kalkhoven E, Müller M, Kersten S. Effect of synthetic dietary triglycerides: a novel research paradigm for nutrigenomics. PLoS One 2008;3:e1681
15. van Schothorst EM, Flachs P, Franssen-van Hal NL, Kuda O, Bunschoten A, Molthoff J, Vink C, Hooiveld GJ, Kopecky J, Keijer J. Induction of lipid oxidation by polyunsaturated fatty acids of marine origin in small intestine of mice fed a high-fat diet. BMC Genomics 2009;10:110
16. Neschen S, Morino K, Dong J, Wang-Fischer Y, Cline GW, Romanelli AJ, Rossbacher JC, Moore IK, Regittnig W, Munoz DS, Kim JH, Shulman GI. n-3 Fatty acids preserve insulin sensitivity in vivo in a peroxisome proliferator-activated receptor-alpha-dependent manner. Diabetes 2007;56:1034–1041
17. Serhan CN. Novel omega-3-derived local mediators in anti-inflammation and resolution. Pharmacol Ther 2005;105:7–21
18. González-Périz A, Horrillo R, Ferré N, Gronert K, Dong B, Morán-Salvador E, Titos E, Martínez-Clemente M, López-Parra M, Arroyo V, Clària J. Obesity-induced insulin resistance and hepatic steatosis are alleviated by omega-3 fatty acids: a role for resolvins and protectins. FASEB J 2009;23:1946–1957
19. Jump DB. Fatty acid regulation of gene transcription. Crit Rev Clin Lab Sci 2004;41:41–78
20. Neschen S, Morino K, Rossbacher JC, Pongratz RL, Cline GW, Sono S, Gillum M, Shulman GI. Fish oil regulates adiponectin secretion by a peroxisome proliferator-activated receptor-gamma-dependent mechanism in mice. Diabetes 2006;55:924–928
21. Dentin R, Benhamed F, Pégorier JP, Foufelle F, Viollet B, Vaulont S, Girard J, Postic C. Polyunsaturated fatty acids suppress glycolytic and lipogenic genes through the inhibition of ChREBP nuclear protein translocation. J Clin Invest 2005;115:2843–2854
22. Suchankova G, Tekle M, Saha AK, Ruderman NB, Clarke SD, Gettys TW. Dietary polyunsaturated fatty acids enhance hepatic AMP-activated protein kinase activity in rats. Biochem Biophys Res Commun 2005;326:851–858
23. Gabler NK, Radcliffe JS, Spencer JD, Webel DM, Spurlock ME. Feeding long-chain n-3 polyunsaturated fatty acids during gestation increases intestinal glucose absorption potentially via the acute activation of AMPK. J Nutr Biochem 2009;20:17–25
24. Kopecky J, Rossmeisl M, Flachs P, Kuda O, Brauner P, Jilkova Z, Stankova B, Tvrzicka E, Bryhn M. n-3 PUFA: bioavailability and modulation of adipose tissue function. Proc Nutr Soc 2009;68:361–369
25. Carling D. The AMP-activated protein kinase cascade–a unifying system for energy control. Trends Biochem Sci 2004;29:18–24
26. Viollet B, Andreelli F, Jørgensen SB, Perrin C, Geloen A, Flamez D, Mu J, Lenzner C, Baud O, Bennoun M, Gomas E, Nicolas G, Wojtaszewski JF, Kahn A, Carling D, Schuit FC, Birnbaum MJ, Richter EA, Burcelin R, Vaulont S. The AMP-activated protein kinase alpha2 catalytic subunit controls whole-body insulin sensitivity. J Clin Invest 2003;111:91–98
27. Andreelli F, Foretz M, Knauf C, Cani PD, Perrin C, Iglesias MA, Pillot B, Bado A, Tronche F, Mithieux G, Vaulont S, Burcelin R, Viollet B. Liver adenosine monophosphate-activated kinase-alpha2 catalytic subunit is a key target for the control of hepatic glucose production by adiponectin and leptin but not insulin. Endocrinology 2006;147:2432–2441
28. Foretz M, Ancellin N, Andreelli F, Saintillan Y, Grondin P, Kahn A, Thorens B, Vaulont S, Viollet B. Short-term overexpression of a constitutively active form of AMP-activated protein kinase in the liver leads to mild hypoglycemia and fatty liver. Diabetes 2005;54:1331–1339
29. Zhang BB, Zhou G, Li C. AMPK: an emerging drug target for diabetes and the metabolic syndrome. Cell Metab 2009;9:407–416
30. Kahn BB, Alquier T, Carling D, Hardie DG. AMP-activated protein kinase: ancient energy gauge provides clues to modern understanding of metabolism. Cell Metab 2005;1:15–25
31. Polak J, Kovacova Z, Jacek M, Klimcakova E, Kovacikova M, Vitkova M, Kuda O, Sebela M, Samcova E, Stich V. An increase in plasma adiponectin multimeric complexes follows hypocaloric diet-induced weight loss in obese and overweight pre-menopausal women. Clin Sci (Lond) 2007;112:557–565
32. Hardie DG, Salt IP, Davies SP. Analysis of the role of the AMP-activated protein kinase in the response to cellular stress. Methods Mol Biol 2000;99:63–74
33. Burcelin R, Crivelli V, Dacosta A, Roy-Tirelli A, Thorens B. Heterogeneous metabolic adaptation of C57BL/6J mice to high-fat diet. Am J Physiol Endocrinol Metab 2002;282:E834–E842
34. Foretz M, Guichard C, Ferré P, Foufelle F. Sterol regulatory element binding protein-1c is a major mediator of insulin action on the hepatic expression of glucokinase and lipogenesis-related genes. Proc Natl Acad Sci U S A 1999;96:12737–12742
35. Yamauchi T, Kamon J, Minokoshi Y, Ito Y, Waki H, Uchida S, Yamashita S, Noda M, Kita S, Ueki K, Eto K, Akanuma Y, Froguel P, Foufelle F, Ferre P,

Carling D, Kimura S, Nagai R, Kahn BB, Kadowaki T. Adiponectin stimulates glucose utilization and fatty-acid oxidation by activating AMP-activated protein kinase. Nat Med 2002;8:1288–1295
36. Kajikawa S, Harada T, Kawashima A, Imada K, Mizuguchi K. Highly purified eicosapentaenoic acid prevents the progression of hepatic steatosis by repressing monounsaturated fatty acid synthesis in high-fat/high-sucrose diet-fed mice. Prostaglandins Leukot Essent Fatty Acids 2009;80(4):229–238
37. Uyeda K, Repa JJ. Carbohydrate response element binding protein, ChREBP, a transcription factor coupling hepatic glucose utilization and lipid synthesis. Cell Metab 2006;4:107–110
38. Wakelam MJO. Diacylglycerol—when is it an intracellular messenger? BBA-Mol Cell Biol Lipids 1998;1436:117–126
39. Schmitz-Peiffer C, Biden TJ. Protein kinase C function in muscle, liver, and beta-cells and its therapeutic implications for type 2 diabetes. Diabetes 2008;57:1774–1783
40. Donnelly KL, Smith CI, Schwarzenberg SJ, Jessurun J, Boldt MD, Parks EJ. Sources of fatty acids stored in liver and secreted via lipoproteins in patients with nonalcoholic fatty liver disease. J Clin Invest 2005;115:1343–1351
41. Ohira M, Miyashita Y, Murano T, Watanabe F, Shirai K. Metformin promotes induction of lipoprotein lipase in skeletal muscle through activation of adenosine monophosphate-activated protein kinase. Metabolism 2009;58:1408–1414
42. Daval M, Diot-Dupuy F, Bazin R, Hainault I, Viollet B, Vaulont S, Hajduch E, Ferré P, Foufelle F. Anti-lipolytic action of AMP-activated protein kinase in rodent adipocytes. J Biol Chem 2005;280:25250–25257
43. Dobrzyn A, Dobrzyn P, Miyazaki M, Ntambi JM. Polyunsaturated fatty acids do not activate AMP-activated protein kinase in mouse tissues. Biochem Biophys Res Commun 2005;332:892–896
44. Salati LM, Clarke SD. Fatty acid inhibition of hormonal induction of acetyl-coenzyme A carboxylase in hepatocyte monolayers. Arch Biochem Biophys 1986;246:82–89
45. Woods A, Johnstone SR, Dickerson K, Leiper FC, Fryer LG, Neumann D, Schlattner U, Wallimann T, Carlson M, Carling D. LKB1 is the upstream kinase in the AMP-activated protein kinase cascade. Curr Biol 2003;13:2004–2008
46. Flachs P, Mohamed-Ali V, Horakova O, Rossmeisl M, Hosseinzadeh-Attar MJ, Hensler M, Ruzickova J, Kopecky J. Polyunsaturated fatty acids of marine origin induce adiponectin in mice fed a high-fat diet. Diabetologia 2006;49:394–397
47. Itoh M, Suganami T, Satoh N, Tanimoto-Koyama K, Yuan X, Tanaka M, Kawano H, Yano T, Aoe S, Takeya M, Shimatsu A, Kuzuya H, Kamei Y, Ogawa Y. Increased adiponectin secretion by highly purified eicosapentaenoic acid in rodent models of obesity and human obese subjects. Arterioscler Thromb Vasc Biol 2007;27:1918–1925
48. Nawrocki AR, Rajala MW, Tomas E, Pajvani UB, Saha AK, Trumbauer ME, Pang Z, Chen AS, Ruderman NB, Chen H, Rossetti L, Scherer PE. Mice lacking adiponectin show decreased hepatic insulin sensitivity and reduced responsiveness to peroxisome proliferator-activated receptor gamma agonists. J Biol Chem 2006;281:2654–2660
49. Villena JA, Viollet B, Andreelli F, Kahn A, Vaulont S, Sul HS. Induced adiposity and adipocyte hypertrophy in mice lacking the AMP-activated protein kinase-alpha2 subunit. Diabetes 2004;53:2242–2249
50. Cheung PC, Salt IP, Davies SP, Hardie DG, Carling D. Characterization of AMP-activated protein kinase gamma-subunit isoforms and their role in AMP binding. Biochem J 2000;346:659–669

Online-Only Appendix

TABLE 1. Blood glucose and plasma insulin levels during the insulin-stimulated (clamp) conditions and glucose turnover under basal (non-stimulated) conditions in wild-type and AMPKα2$^{-/-}$ mice

	Wild-type			AMPKα2$^{-/-}$		
	Chow	cHF	cHF+F	Chow	cHF	cHF+F
Blood glucose before clamp (mmol/l)	7.0 ± 0.8	8.0 ± 1.0	7.8 ± 0.8	8.5 ± 0.6	5.9 ± 0.1	7.4 ± 0.9
Steady-state blood glucose (mmol/l)	5.7 ± 0.5	5.7 ± 0.2	5.8 ± 0.2	5.8 ± 0.1	5.8 ± 0.7	5.9 ± 0.3
End-point plasma insulin (μU/ml)	30 ± 10	29 ± 7	24 ± 8	21 ± 7	25 ± 7	28 ± 9
Basal glucose turnover (μmol kg^{-1} min^{-1})	108 ± 11	86 ± 15	90 ± 15	118 ± 7	83 ± 23	104 ± 17

The data are presented as means ± SE (n = 5-8). Wild-type and AMPKα2$^{-/-}$ mice were fed either a Chow diet or corn oil-based high-fat diets without (cHF) or with 15% of the lipids in the form of n-3 LC-PUFA concentrate (cHF+F) for 9 weeks.

TABLE 2. Triglycerides, NEFA and cholesterol levels in plasma of wild-type and AMPKα2$^{-/-}$ mice under different metabolic conditions

	Wild-type			AMPKα2$^{-/-}$		
	Chow	cHF	cHF+F	Chow	cHF	cHF+F
Triglycerides (mmol/l)						
Fasted	0.46 ± 0.03	0.49 ± 0.03	0.46 ± 0.04	0.57 ± 0.05	0.44 ± 0.02	0.46 ± 0.02
Fed	1.17 ± 0.08	1.24 ± 0.11	0.62 ± 0.07*†	1.04 ± 0.06	1.22 ± 0.08	0.73 ± 0.07*†
Clamp	0.44 ± 0.05	0.64 ± 0.09	0.41 ± 0.04†	0.38 ± 0.06	0.55 ± 0.05	0.53 ± 0.08
NEFA (mmol/l)						
Fasted	1.16 ± 0.07	0.84 ± 0.08*	0.78 ± 0.05*	1.34 ± 0.05‡	0.89 ± 0.06*	0.87 ± 0.05*
Fed	0.90 ± 0.05	0.94 ± 0.05	0.59 ± 0.05*†	0.88 ± 0.04	0.99 ± 0.06	0.68 ± 0.04*†
Clamp	0.25 ± 0.02	0.39 ± 0.05	0.27 ± 0.03†	0.21 ± 0.03	0.41 ± 0.11	0.37 ± 0.07
Cholesterol (mmol/l)						
Fasted	1.77 ± 0.07	2.81 ± 0.22	2.00 ± 0.15†	1.78 ± 0.04	2.67 ± 0.12	2.02 ± 0.08†
Fed	2.25 ± 0.08	4.12 ± 0.25*	3.10 ± 0.20*†	2.10 ± 0.06	3.94 ± 0.18*	2.75 ± 0.14*†
Clamp	2.26 ± 0.13	2.98 ± 0.22	2.51 ± 0.15	1.83 ± 0.09	2.99 ± 0.24	2.63 ± 0.22

The data are presented as means ± SE (for fasted and fed mice, n = 13-15; for clamp, n = 8-14). Wild-type and AMPKα2$^{-/-}$ mice were fed either a Chow diet or corn oil-based high-fat diets without (cHF) or with 15% of the lipids in the form of n-3 LC-PUFA concentrate (cHF+F) for 9 weeks. Plasma parameters were assessed at 8 weeks (fasted values) or 9 weeks (fed and clamp values), respectively. *$P < 0.05$ vs. genotype Chow; †$P < 0.05$ vs. genotype cHF; ‡$P < 0.05$ vs. wild-type on respective diet.

TABLE 3. The basal rates of lipid metabolism in isolated hepatocytes of wild-type and AMPKα2$^{-/-}$ mice

	Wild-type			AMPKα2$^{-/-}$		
	Chow	cHF	cHF+F	Chow	cHF	cHF+F
Fatty acid oxidation (pmol/h/mg protein)	13 ± 2	8 ± 1*	9 ± 1*	15 ± 2	12 ± 1‡	6 ± 1*†
Lipogenesis (pmol/h/mg protein)	108 ± 9	74 ± 24	43 ± 10*†	79 ± 10	51 ± 6	34 ± 6*

The data are presented as means ± SE (n = 3 analyzed in triplets). Wild-type and AMPKα2$^{-/-}$ mice were fed either a Chow diet or corn oil-based high-fat diets without (cHF) or with 15% of the lipids in the form of n-3 LC-PUFA concentrate (cHF+F) for 9 weeks. *P < 0.05 vs. genotype Chow; †P < 0.05 vs. genotype cHF; ‡P < 0.05 vs. wild-type on respective diet.

TABLE 4. The content and composition of hepatic lipids in wild-type and AMPKα2$^{-/-}$ mice killed in ad libitum fed state

	Wild-type			AMPKα2$^{-/-}$		
	Chow	cHF	cHF+F	Chow	cHF	cHF+F
Total ceramide (nmol/g)	121.45 ± 9.33	119.71 ± 6.43	125.89 ± 14.66	123.34 ± 4.84	117.91 ± 7.53	123.82 ± 6.42
Triglyceride species						
Total fatty acids (μmol/g)	38.10 ± 3.18	116.55 ± 14.51*	80.35 ± 8.80†	50.31 ± 4.60	128.04 ± 18.59*	76.80 ± 6.63†
Myristic (14:0) (μmol/g)	0.38 ± 0.05	1.25 ± 0.22*	0.63 ± 0.08†	0.44 ± 0.04	1.27 ± 0.25*	0.59 ± 0.06†
Palmitic (16:0) (μmol/g)	11.12 ± 0.94	30.39 ± 4.10*	20.27 ± 2.88†	14.44 ± 1.06	35.25 ± 6.10*	17.17 ± 1.86†
Palmitoleic (16:1n7) (μmol/g)	2.82 ± 0.35	1.54 ± 0.46*	0.54 ± 0.10*	3.01 ± 0.37	1.35 ± 0.41*	0.81 ± 0.41*
Stearic (18:0) (μmol/g)	0.85 ± 0.09	1.90 ± 0.15*	1.60 ± 0.08*	0.98 ± 0.08	2.52 ± 0.31*‡	1.83 ± 0.14*†
Oleic (18:1n9) (μmol/g)	13.23 ± 1.22	27.05 ± 3.33	15.08 ± 1.72*†	16.68 ± 1.18	30.81 ± 5.84	15.52 ± 1.60*†
Linoleic (18:2n6) (μmol/g)	7.68 ± 0.61	47.52 ± 5.98*	25.98 ± 2.67*†	12.16 ± 2.60	49.22 ± 5.78*	25.81 ± 2.43*†
Arachidic (20:0) (μmol/g)	0.08 ± 0.01	0.23 ± 0.04*	0.18 ± 0.01*	0.12 ± 0.02	0.28 ± 0.05*	0.19 ± 0.02†
α-Linolenic (C18:3n3) (μmol/g)	0.43 ± 0.03	1.42 ± 0.24*	0.81 ± 0.09†	0.56 ± 0.06	1.52 ± 0.28*	0.79 ± 0.07†
Behenic (22:0) (nmol/g)	71.89 ± 5.67	89.37 ± 11.63	31.13 ± 2.65*†	81.32 ± 3.67	98.81 ± 15.97	43.53 ± 7.20*†
Arachidonic (20:4n6) (μmol/g)	0.56 ± 0.04	3.15 ± 0.58*	0.41 ± 0.04†	0.84 ± 0.12	3.72 ± 0.79*	0.47 ± 0.06†
Lignoceric (24:0) (nmol/g)	7.30 ± 0.80	10.28 ± 1.07	9.93 ± 1.04	8.14 ± 0.70	14.66 ± 3.10*	11.19 ± 0.89
Eicosapentaenoic (20:5n3) (μmol/g)	0.13 ± 0.01	0.25 ± 0.04	1.91 ± 0.21*†	0.13 ± 0.01	0.23 ± 0.05	1.33 ± 0.13*†‡
Nervonic (24:1n9) (nmol/g)	7.43 ± 1.01	8.23 ± 0.58	10.01 ± 0.89	6.94 ± 0.28	10.04 ± 1.30*	12.30 ± 1.17*
Docosahexaenoic (22:6n3) (μmol/g)	0.73 ± 0.06	1.74 ± 0.29	12.90 ± 1.08*†	0.84 ± 0.05	1.75 ± 0.31	12.21 ± 1.21*†
Diacylglycerol species						
Total fatty acids (μmol/g)	2.57 ± 0.34	2.51 ± 0.29	1.85 ± 0.18†	1.76 ± 0.11‡	2.47 ± 0.25*	2.66 ± 0.40*‡
Myristic (14:0) (μmol/g)	0.08 ± 0.01	0.08 ± 0.01	0.06 ± 0.01	0.06 ± 0.00	0.06 ± 0.01	0.06 ± 0.01

Palmitic (16:0) (μmol/g)	1.02 ± 0.13	0.95 ± 0.13	0.70 ± 0.06	0.69 ± 0.05	0.90 ± 0.09	1.12 ± 0.22‡
Palmitoleic (16:1n7) (μmol/g)	0.09 ± 0.01	0.03 ± 0.00*	0.01 ± 0.00*	0.06 ± 0.01‡	0.02 ± 0.00*	0.02 ± 0.01*
Stearic (18:0) (μmol/g)	0.70 ± 0.18	0.54 ± 0.10	0.48 ± 0.11	0.31 ± 0.02	0.40 ± 0.04	0.65 ± 0.16
Oleic (18:1n9) (μmol/g)	0.28 ± 0.02	0.25 ± 0.03	0.13 ± 0.01*†	0.24 ± 0.02	0.25 ± 0.04	0.19 ± 0.03
Linoleic (18:2n6) (μmol/g)	0.23 ± 0.02	0.49 ± 0.07*	0.27 ± 0.03†	0.24 ± 0.02	0.57 ± 0.07*	0.36 ± 0.05†
Arachidic (20:0) (nmol/g)	15.23 ± 4.54	11.84 ± 1.95	11.87 ± 2.85	7.67 ± 0.56	9.47 ± 0.62	10.94 ± 0.92
α-Linolenic (18:3n3) (nmol/g)	12.61 ± 1.52	12.60 ± 1.88	6.55 ± 0.50*†	7.64 ± 0.64‡	10.73 ± 1.52	13.23 ± 2.62‡
Arachidonic (20:4n6) (nmol/g)	72.11 ± 3.89	83.54 ± 5.32	30.86 ± 4.35*†	65.43 ± 4.89	100.95 ± 16.46*	37.75 ± 4.28*†
Eicosapentaenoic (20:5n3) (nmol/g)	10.43 ± 0.75	8.59 ± 0.89	19.97 ± 1.62*†	8.58 ± 0.58	8.37 ± 8.84	20.29 ± 1.27*†
Nervonic (24:1n9) (nmol/g)	0.80 ± 0.10	1.36 ± 0.32	1.18 ± 0.12	0.83 ± 0.06	1.38 ± 0.37	1.38 ± 0.21
Docosahexaenoic (22:6n3) (μmol/g)	0.05 ± 0.00	0.06 ± 0.01	0.13 ± 0.01*†	0.06 ± 0.01	0.14 ± 0.05*‡	0.17 ± 0.02*
Phospholipid species						
Total fatty acids (μmol/g)	67.96 ± 1.61	65.83 ± 1.09	70.75 ± 1.39†	68.20 ± 0.97	67.62 ± 1.40	74.45 ± 2.44*†
Myristic (14:0) (μmol/g)	0.14 ± 0.01	0.22 ± 0.08	0.16 ± 0.01	0.26 ± 0.08	0.15 ± 0.02	0.15 ± 0.01
Palmitic (16:0) (μmol/g)	18.38 ± 0.46	13.80 ± 0.24*	17.38 ± 0.21†	18.16 ± 0.30	14.18 ± 0.34*	18.20 ± 0.87†
Palmitoleic (16:1n7) (μmol/g)	1.40 ± 0.12	0.17 ± 0.01*	0.25 ± 0.11*	1.36 ± 0.06	0.17 ± 0.01*	0.33 ± 0.19*
Stearic (18:0) (μmol/g)	11.21 ± 0.36	14.39 ± 0.28*	13.53 ± 0.47*	11.56 ± 0.25	14.81 ± 0.33*	14.30 ± 0.36*
Oleic (18:1n9) (μmol/g)	5.23 ± 0.21	3.34 ± 0.14*	3.80 ± 0.21*	5.02 ± 0.14	3.42 ± 0.14*	4.11 ± 0.36*†
Linoleic (18:2n6) (μmol/g)	12.37 ± 0.29	14.27 ± 0.39*	14.89 ± 0.42*	12.00 ± 0.21	14.38 ± 0.45*	15.91 ± 0.41*†
Arachidic (20:0) (μmol/g)	0.10 ± 0.01	0.11 ± 0.01	0.15 ± 0.01*†	0.10 ± 0.00	0.11 ± 0.01	0.15 ± 0.01*†
α-Linolenic (C18:3n3) (μmol/g)	0.07 ± 0.01	0.04 ± 0.00*	0.05 ± 0.00	0.07 ± 0.01	0.05 ± 0.00*	0.06 ± 0.01
Behenic (22:0) (μmol/g)	0.13 ± 0.01	0.03 ± 0.01*	0.04 ± 0.01*	0.13 ± 0.01	0.02 ± 0.00*	0.04 ± 0.02*
Arachidonic (20:4n6) (μmol/g)	11.83 ± 0.66	13.70 ± 0.30*	5.60 ± 0.47*†	12.85 ± 0.18	13.75 ± 0.79*	6.62 ± 0.80†
Lignoceric (24:0) (nmol/g)	9.90 ± 1.00	15.69 ± 6.14	11.32 ± 0.70	13.82 ± 3.82	10.46 ± 0.72	10.29 ± 0.83
Eicosapentaenoic (20:5n3) (μmol/g)	0.44 ± 0.08	0.08 ± 0.01*	2.01 ± 0.17*†	0.27 ± 0.01	0.16 ± 0.10	1.78 ± 0.19*†
Docosahexaenoic (22:6n3) (μmol/g)	6.64 ± 0.39	5.64 ± 0.18	12.88 ± 0.65*†	6.42 ± 0.13	6.40 ± 0.53	12.80 ± 0.75*†

The data are the means ± SE (n = 8-14). Wild-type and AMPKα2$^{-/-}$ mice were fed either a Chow diet or corn oil-based high-fat diets without (cHF) or with 15% of the lipids in the form of n-3 LC-PUFA concentrate (cHF+F) for 9 weeks and killed in ad libitum fed state. *P < 0.05 vs. genotype Chow; †P < 0.05 vs. genotype cHF; ‡P < 0.05 vs. wild-type on respective diet.

The intake of n-3 LC-PUFA resulted in a marked increase in EPA and DHA concentration in all lipid fractions, independently of the genotype and with relatively small changes in the diacylglycerol fraction. Except for EPA and DHA (and a relatively low content of arachidonic acid and high content of nervonic acid), levels of individual fatty acids in the triglyceride fraction reflected the total tissue content of triglycerides. The fatty acid profile of the phospholipid fraction was only marginally affected by either diet or genotype. In diacylglycerol fraction, the content of several fatty acids (i.e., palmitic, palmitoleic, oleic, and α-linolenic acid) was differentially affected by the cHF+F diet, depending on the genotype and explaining the effect of the cHF+F diet on total hepatic content of diacylglycerols (see Fig. 5A of the main text). α-linolenic acid was by far the most differentially affected fatty acid, with a ~1.9-fold decrease in response to cHF+F diet in wild-type mice, and a ~1.2-increase produced by the same diet in AMPKα2$^{-/-}$ mice. This fatty acid also contributed to the lower content of liver diacylglycerols in AMPKα2$^{-/-}$ compared to wild-type mice fed the Chow diet.

TABLE 5. The content and composition of hepatic diacylglycerols in wild-type and AMPKα2$^{-/-}$ mice subjected to hyperinsulinemic-euglycemic clamp

	Wild-type			AMPKα2$^{-/-}$		
	Chow	cHF	cHF+F	Chow	cHF	cHF+F
Diacylglycerol species						
Total fatty acids (μmol/g)	1.90 ± 0.21	2.43 ± 0.32	2.57 ± 0.32	1.99 ± 0.12	2.72 ± 0.35	2.43 ± 0.48
Myristic (14:0) (μmol/g)	0.06 ± 0.01	0.05 ± 0.01	0.07 ± 0.01	0.05 ± 0.00	0.06 ± 0.01	0.06 ± 0.01
Palmitic (16:0) (μmol/g)	0.58 ± 0.07	0.67 ± 0.09	0.85 ± 0.17	0.62 ± 0.03	0.73 ± 0.08	0.75 ± 0.15
Palmitoleic (16:1n7) (μmol/g)	0.03 ± 0.00	0.01 ± 0.00*	0.01 ± 0.00*	0.03 ± 0.00	0.01 ± 0.00*	0.01 ± 0.00*
Stearic (18:0) (μmol/g)	0.53 ± 0.18	0.41 ± 0.05	0.68 ± 0.19	0.42 ± 0.05	0.48 ± 0.10	0.68 ± 0.26
Oleic (18:1n9) (μmol/g)	0.24 ± 0.04	0.29 ± 0.05	0.22 ± 0.04	0.31 ± 0.05	0.33 ± 0.05	0.21 ± 0.04
Linoleic (18:2n6) (μmol/g)	0.29 ± 0.05	0.81 ± 0.15*	0.49 ± 0.09	0.35 ± 0.04	0.91 ± 0.14*	0.47 ± 0.08*†
Arachidic (20:0) (nmol/g)	13.16 ± 4.54	9.63 ± 0.72	14.52 ± 3.47	9.63 ± 1.08	11.94 ± 2.51	16.70 ± 6.43
α-Linolenic (18:3n3) (nmol/g)	17.76 ± 5.65	13.88 ± 3.53	13.70 ± 4.46	11.91 ± 1.68	13.03 ± 2.17	11.09 ± 2.80
Arachidonic (20:4n6) (nmol/g)	83.84 ± 14.03	68.67 ± 2.07	33.82 ± 3.17*†	106.37 ± 11.29	80.26 ± 4.40*	39.60 ± 4.58*†
Lignoceric (24:0) (nmol/g)	1.29 ± 0.21	1.09 ± 0.12	1.56 ± 0.23	1.21 ± 0.08	1.02 ± 0.13	1.08 ± 0.21
Eicosapentaenoic (20:5n3) (nmol/g)	5.73 ± 0.45	5.10 ± 0.75	11.96 ± 0.99*†	6.26 ± 0.82	5.40 ± 0.58	12.48 ± 1.12*†
Nervonic (24:1n9) (nmol/g)	11.63 ± 2.56	9.83 ± 2.32	11.61 ± 2.24	10.87 ± 2.25	12.37 ± 2.85	11.64 ± 1.82
Docosahexaenoic (22:6n3) (μmol/g)	0.05 ± 0.01	0.07 ± 0.01	0.16 ± 0.03*†	0.07 ± 0.01	0.08 ± 0.01	0.16 ± 0.04*

The data are the means ± SE (n = 5-8). Wild-type and AMPKα2$^{-/-}$ mice were fed either a Chow diet or corn oil-based high-fat diets without (cHF) or with 15% of the lipids in the form of n-3 LC-PUFA concentrate (cHF+F) for 9 weeks. Liver tissue was collected immediately after the completion of hyperinsulinemic-euglycemic clamp. *$P < 0.05$ vs. genotype Chow; †$P < 0.05$ vs. genotype cHF; ‡$P < 0.05$ vs. wild-type on respective diet.

RESEARCH DESIGN AND METHODS

Animals and treatments. Whole-body AMPKα2$^{-/-}$ mice and wild-type littermate controls generated on a hybrid C57BL/6 and 129/Sv genetic background (1) and backcrossed to C57BL/6J mice for nine generations were used. At four weeks of age, mice were weaned onto a standard laboratory Chow (lipid content ~3.4% wt/wt; extruded R/M-H diet; Ssniff Spezialdiäten, Soest, Germany) and maintained at 22°C on a 12 h light–dark cycle (light on from 6 a.m.) with free access to food and water.

Two separate experiments were performed, in which four-month-old wild-type and AMPKα2$^{-/-}$ mice (n = 13-15), caged in groups of 3-4 mice, were fed the following diets for nine weeks: (i) Chow; (ii) a corn oil-based high-fat diet (cHF; lipid content ~35.2% wt/wt); or (iii) a cHF diet supplemented with n-3 LC-PUFA concentrate (46% DHA, 14% EPA; product EPAX 1050 TG; EPAX, a.s., Lysaker, Norway) replacing 15% of dietary lipids (cHF+F). The macronutrient and fatty acid composition of all diets has been described before (2). Fresh rations of food were distributed every two days, while food consumption and body weights were recorded once a week. Mice from the first experiment in ad libitum fed state were first anesthetized by diethylether, exsanguinated through the cervical incision, then sacrificed by cervical dislocation (between 8 a.m. and 10 a.m.), and EDTA-plasma, liver, quadriceps muscles, epididymal and subcutaneous (dorsolumbar) adipose tissues were collected for various analyses (see below). When indicated, plasma samples were also collected after eight weeks from mice fasted for 15 hours (between 8 a.m. and 11 p.m.). In order to assess insulin sensitivity, mice from the second experiment were studied under hyperinsulinemic-euglycemic conditions.

Real-time RT-PCR analysis. Total RNA was isolated from liver samples (stored in RNA*later* Solution; Ambion, Austin, TX) homogenized in TRIzol Reagent (Invitrogen, Carlsbad, CA). A single-strand cDNA was synthesized from 0.5 µg of total RNA and gene expression was assessed by real-time PCR, using the LightCycler® 480 Instrument and the kit LightCycler® 480 SYBR Green I (Roche Diagnostics, Mannheim, Germany). Transcript levels were normalized according to the expression levels of eukaryotic elongation factor 1a (ELF-1a). The following oligonucleotide primers, designed by Lasergene software (DNAStar, Madison, WI), were used:
SCD1:
sense, 5'-ACTGGGGCTGCTAATCTCTGGGTGTA,
antisense, 3'- GGCTTTATCTCTGGGGTGGGTTTGTTA;
SREBP-1c:
sense, 5'- TACCCGTCCGTGTCCCCCTTTTC,
antisense, 3'- TGCGCTTCTCACCACGGCTCTG;
ELF-1a:
sense 5'- TGACAGCAAAAACGACCCACCAAT,
antisense, 3'- GGGCCATCTTCCAGCTTCTTACCA.

Activity of α1 and α2 AMPK isoforms. Livers were collected by freeze-clamping. AMPK was immunoprecipitated from tissue extracts and the activity was assayed using a peptide substrate (3). AMPKα1 or AMPKα2 isoforms were immunoprecipitated using specific antibodies (gift of Dr. D. Grahame Hardie), which were bound to Protein G Sepharose (Amersham Pharmacia Biotech, Little Chalfont, UK). Immunoprecipitates were mixed with AMP (1 mmol/l), [γ-

^{32}P]ATP (1 mmol/l) and AMARA peptide (1 mmol/l; Vidia, Prague, Czech Republic) dissolved in HEPES-Brij buffer. Reaction proceeded for 30 min at 30°C and it was stopped by dropping the filter spotted with a reaction mixture into 1% phosphoric acid solution. The activity of 1 U/mg protein corresponds to 1 nmol ^{32}P-AMARA peptide/mg protein per min.

The analysis of blood samples from hyperinsulinemic-euglycemic clamps. To assess D-[3-^{3}H]glucose, $^{3}H_2O$ and total glucose concentrations, blood samples were firstly deproteinized by precipitation with a $ZnSO_4/Ba(OH)_2$, followed by centrifugation (4). The first aliquot of the supernatant was evaporated to dryness to determine the radioactivity corresponding to D-[3-^{3}H]glucose. The second aliquot was used to determine the radioactivity of both D-[3-^{3}H]glucose and $^{3}H_2O$. Plasma $^{3}H_2O$ radioactivity was then calculated as the difference between radioactivity in the second and the first aliquot. In the third aliquot of the supernatant, the total glucose concentration was assessed by the glucose oxidase method (Glukosa God 1500, PLIVA-Lachema, Czech Republic). The D-[3-^{3}H]glucose specific activity was calculated by dividing the D-[3-^{3}H]glucose enrichment of plasma (dpm/ml) by the total plasma glucose concentration (mg/ml). Time points, in which the steady-state D-[3-^{3}H]glucose specific activity varied more than ± 15 %, were not taken into account (4). The rates of insulin-stimulated glucose turnover (GTO) were determined as the ratio of the [3-^{3}H]glucose infusion rate (dpm/min) to the specific activity of plasma glucose (5). The rate of glycogen synthesis in quadriceps muscle was quantified by measuring the incorporation of D-[3-^{3}H]glucose into glycogen and calculated by dividing the radioactivity of D-[3-^{3}H]glucosyl units in glycogen (dpm/kg) by the mean specific activity of D-[3-^{3}H]glucose in plasma during the last hour of the clamp.

The rate of lipogenesis in isolated hepatocytes. De novo lipogenesis was assesed using ^{14}C-Acetate (1uCi/ml) (PerkinElmer, USA). Cells were incubated in 2 ml of a medium (M199, Gibco) containing ^{14}C acetate with or without 25 mM glucose and 100 nM insulin (Actrapid MC, Novoindustri, Denmark). After 2 hr of incubation at 37 °C (5% CO_2 and 95% O_2) cells were washed by PBS and harvested into 600 ul KOH (shaking at 70°C). ^{14}C incorporation into saponifiable FA was estimated (6) and expressed as pmol of acetate converted to fatty acid/mg protein per hour. Identical incubations in parallel wells without radioactivity were performed to determine protein concentrations.

The rate of fatty acid oxidation in isolated hepatocytes. Palmitate oxidation was assesed using [1-^{14}C] palmitate (PerkinElmer, USA). Cells were incubated for 45 min at 37°C in 800 ul of a medium (M199) supplemented with 1% BSA, 50 μM cold palmitate and [1-^{14}C] palmitate (0,38 μCi/reaction) with or without 1 mM AICAR. The reactions were terminated by aspiration of the media, cells were washed by PBS and then incubated in 800 ul of 5 % perchloric acid for 15 min at room temperature. Palmitate oxidation was determined by measuring production of ^{14}C-labeled acid-soluble metabolites (ASM), a measure of tricarboxylic acid cycle intermediates and acetyl esters. The ASM were assessed in supernatants of the acid precipitate. Identical incubations in parallel wells without radioactivity were conducted to determine protein concentrations.

Total content and fatty acid composition of phospholipid, diacylglycerol, triglyceride, and ceramide fractions. Liver samples were pulverized in an aluminum mortar precooled in liquid nitrogen. The powder was transferred to a tube containing ice-cold methanol and 0.01%

butylated hydroxytoluene (Sigma) as an antioxidant. Internal standards (1,2-diheptadecanoin, triheptadecanoin and 1,2-diheptadecanoyl-sn-glycero-3-phosphatidylcholine, Larodan Fine Chemicals, Sweden) were then added to the samples and lipids were extracted by the method of Folch. The fractions of total phospholipids, triglycerides and diacylglycerols were separated by thin-layer chromatography (7). Lipid class standards were spotted on the outside lanes of the chromatography plate to enable localization of the sample lipid classes. The gel bands corresponding to the standards were scraped off the plates, transferred to fresh tubes and then transmethylated in 14% methanolic boron trifluoride (Sigma) at 100°C for either 10 or 30 minutes (phospholipids and triglycerides). The content of resulting fatty acid methyl esters was determined by means of gas-liquid chromatography (8). The content of ceramides was determined as described previously (9) with the exception that N-palmitoyl-D-*erythro*-sphingosine (C17 Base; a gift from Dr. Zdzislaw Szulc, Medical University of South Carolina) was used as an internal standard.

FIGURE LEGENDS

Supplemental Figure. 1. Body weight curves of wild-type (WT) and AMPKα2$^{-/-}$ (KO) mice fed either a Chow diet or corn oil-based high-fat diets without (cHF) or with 15% of the lipids in the form of n-3 LC-PUFA concentrate (cHF+F) for 9 weeks. The data are the means ± SE (n = 27-30).

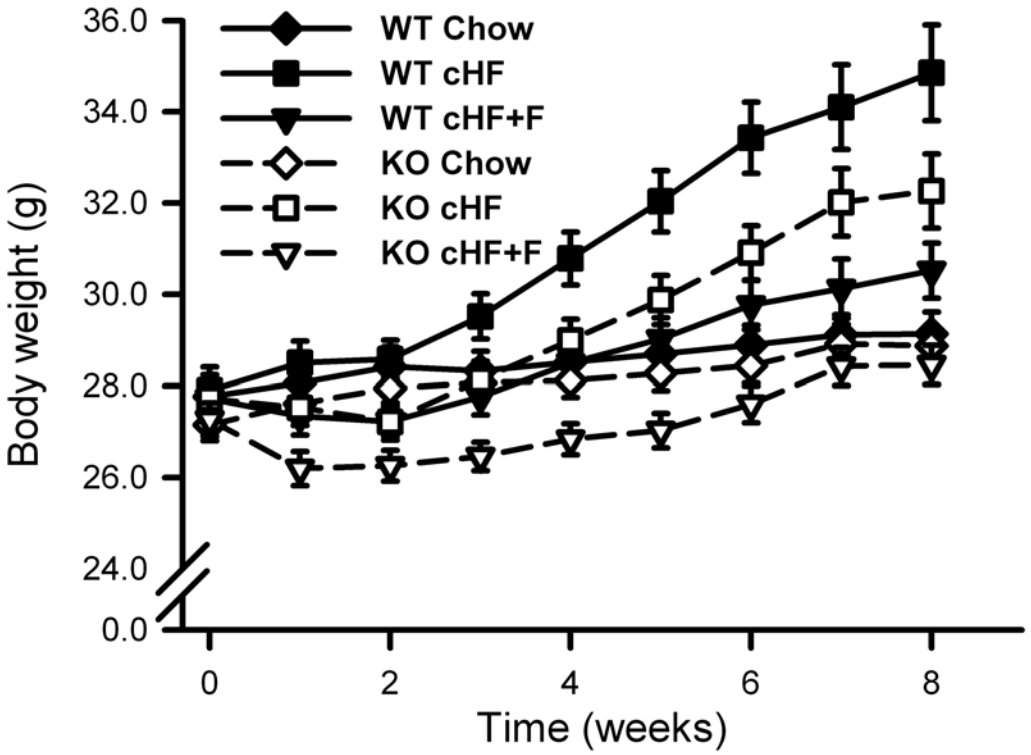

Supplemental Fig. 2. Adiponectin levels in plasma of wild-type and AMPKα2$^{-/-}$ mice fed either a Chow diet or corn oil-based high-fat diets without (cHF) or with 15% of the lipids in the form of n-3 LC-PUFA concentrate (cHF+F) for 9 weeks, and killed in ad libitum fed state. The total adiponectin levels and the distribution of adiponectin multimeric complexes were determined using Western blotting (10). The data are the means ± SE (n = 13-15). **P* < 0.05 vs. genotype Chow; †*P* < 0.05 vs. genotype cHF; ‡*P* < 0.05 vs. wild-type on respective diet. Significance evaluated for the total adiponectin levels. A.U., arbitary units; LMW – low molecular weight; MMW – medium molecular weight; HMW – high molecular weight.

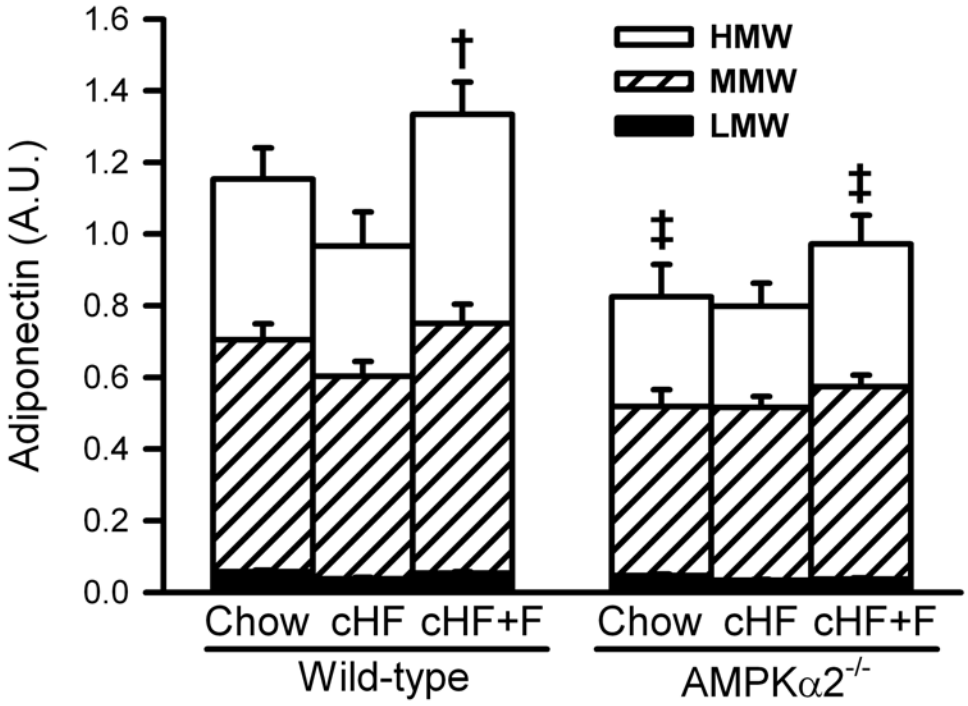

Supplemental Fig. 3. The composition of fatty acids in hepatic diacylglycerol fraction in wild-type and AMPKα2$^{-/-}$ mice subjected to hyperinsulinemic-euglycemic clamp: total fatty acids (TFA; *A*), polyunsaturated fatty acids (PUFA; *B*), monounsaturated fatty acids (MUFA; *C*), saturated fatty acids (SFA; *D*). Animals were fed either a Chow diet or corn oil-based high-fat diets without (cHF) or with 15% of the lipids in the form of n-3 LC-PUFA concentrate (cHF+F) for 9 weeks, and then subjected to hyperinsulinemic-euglycemic clamp. Liver tissue was collected immediately after the completion of the clamp. Data are means ± SE (n = 5-8). **P* < 0.05 vs. genotype Chow; †*P* < 0.05 vs. genotype cHF.

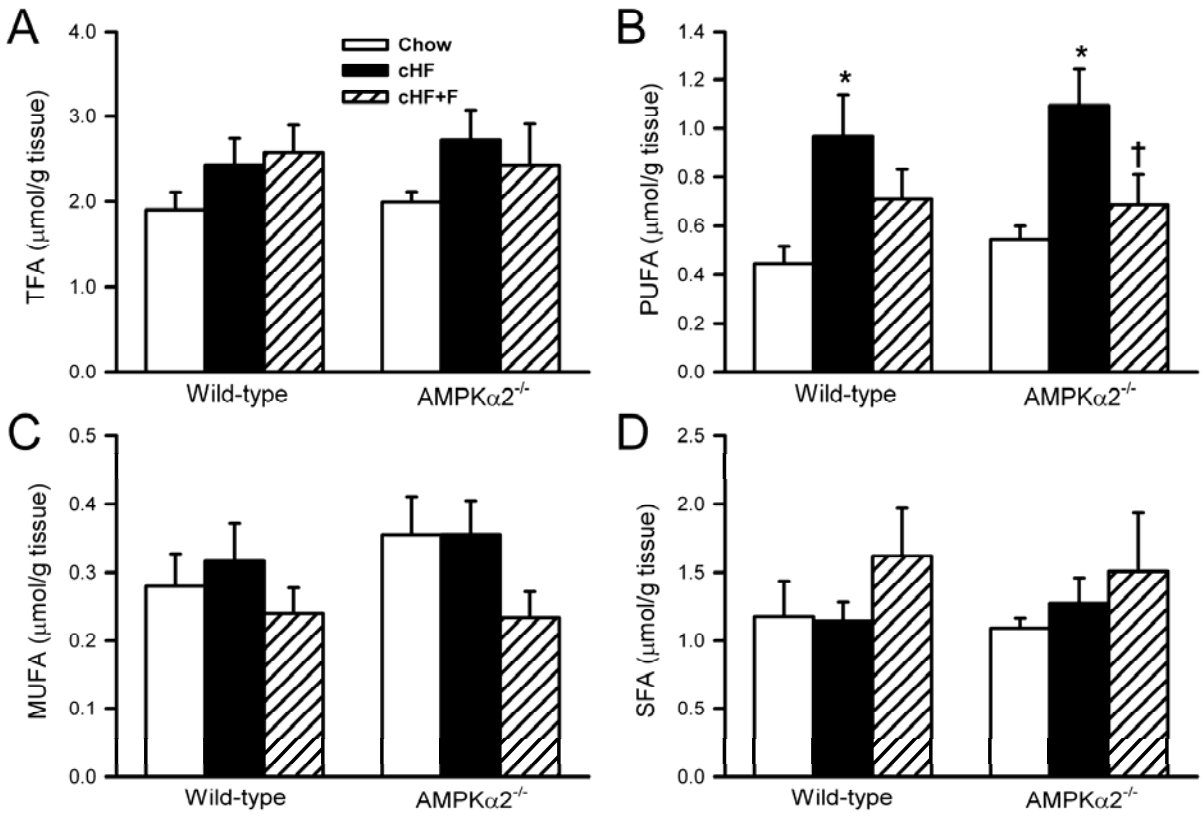

REFERENCE LIST (ONLINE-APPENDIX)

1. Viollet B, Andreelli F, Jorgensen SB, Perrin C, Geloen A, Flamez D, Mu J, Lenzner C, Baud O, Bennoun M, Gomas E, Nicolas G, Wojtaszewski JF, Kahn A, Carling D, Schuit FC, Birnbaum MJ, Richter EA, Burcelin R, Vaulont S: The AMP-activated protein kinase alpha2 catalytic subunit controls whole-body insulin sensitivity. *J Clin Invest* 111:91-98, 2003
2. Kuda O, Jelenik T, Jilkova Z, Flachs P, Rossmeisl M, Hensler M, Kazdova L, Ogston N, Baranowski M, Gorski J, Janovska P, Kus V, Polak J, Mohamed-Ali V, Burcelin R, Cinti S, Bryhn M, Kopecky J: n-3 Fatty acids and rosiglitazone improve insulin sensitivity through additive stimulatory effects on muscle glycogen synthesis in mice fed a high-fat diet. *Diabetologia* 52:941-951, 2009
3. Hardie DG, Salt IP, Davies SP: Analysis of the role of the AMP-activated protein kinase in the response to cellular stress. *Methods Mol Biol* 99:63-74, 2000
4. Burcelin R, Crivelli V, Dacosta A, Roy-Tirelli A, Thorens B: Heterogeneous metabolic adaptation of C57BL/6J mice to high-fat diet. *Am J Physiol Endocrinol Metab* 282:E834-E842, 2002
5. Park SY, Kim HJ, Wang S, Higashimori T, Dong J, Kim YJ, Cline G, Li H, Prentki M, Shulman GI, Mitchell GA, Kim JK: Hormone-sensitive lipase knockout mice have increased hepatic insulin sensitivity and are protected from short-term diet-induced insulin resistance in skeletal muscle and heart. *Am J Physiol Endocrinol Metab* 289:E30-E39, 2005
6. Stansbie D, Brownsey RW, Crettaz M, Denton RM: Acute effect in vivo of anti-insulin serum on rates of fatty acid synthesis and activities of acetyl-coenzyme A carboxylase and pyruvate dehydrogenase in liver and epididymal adipose tissue of fed rats. *Biochem J* 160:413-416, 1976
7. Roemen TH, Van der Vusse GJ: Application of silica gel column chromatography in the assessment of non-esterified fatty acids and phosphoglycerides in myocardial tissue. *J Chromatogr* 344:304-308, 1985
8. Prpic V, Watson PM, Frampton IC, Sabol MA, Jezek GE, Gettys TW: Differential mechanisms and development of leptin resistance in A/J versus C57BL/6J mice during diet-induced obesity. *Endocrinology* 144:1155-1163, 2003
9. Baranowski M, Zabielski P, Blachnio A, Gorski J: Effect of exercise duration on ceramide metabolism in the rat heart. *Acta Physiol (Oxf)* 192:519-529, 2008
10. Polak J, Kovacova Z, Jacek M, Klimcakova E, Kovacikova M, Vitkova M, Kuda O, Sebela M, Samcova E, Stich V: An increase in plasma adiponectin multimeric complexes follows hypocaloric diet-induced weight loss in obese and overweight pre-menopausal women. *Clin Sci (Lond)* 112:557-565, 2007

Publication D

Medrikova D, Macek Jilkova Z, Bardova K, Janovska P, Rossmeisl M, Kopecky J.

Sex differences during the course of diet-induced obesity in mice: adipose tissue expandability and glycaemic control.

Accepted in: *Int J Obes.* (IF = 4.343)

Sex differences during the course of diet-induced obesity in mice: adipose tissue expandability and glycemic control

D Medrikova, Z Macek Jilkova, K Bardova, P Janovska, M Rossmeisl and J Kopecky

Department of Adipose Tissue Biology, Institute of Physiology Academy of Sciences of the Czech Republic v.v.i., Prague, Czech Republic

Running title:

Sex-specific effects of high fat-feeding in mice

Correspondence:

Jan Kopecky, Department of Adipose Tissue Biology, Institute of Physiology Academy of Sciences of the Czech Republic v.v.i.,Videnska 1083, 142 20 Prague, Czech Republic

E-mail: kopecky@biomed.cas.cz.

Abstract

Objective: Adverse effects of obesity on glucose homeostasis are linked to low-grade adipose tissue inflammation and accumulation of lipids in non-adipose tissues. The goal of this study was to evaluate the role of adipose tissue plasticity in a less severe deterioration of glucose homeostasis in females compared to males during the course of high-fat (HF) feeding in mice.

Research Design: Mice of the C57BL/6N strain were fed either a chow or obesogenic HF diet for up to 35 weeks after weaning. Metabolic markers and hormones in plasma, glucose homeostasis, adipocyte size and inflammatory status of gonadal (gWAT) and subcutaneous (scWAT) adipose depots, and liver steatosis were evaluated at 15 and 35 weeks of HF-feeding.

Results: HF-fed males were heavier than females until week ~20, after which the body weight stabilized at a similar level (55-58 g) in both sexes. Greater weight gain and fat accumulation in females were associated with larger adipocytes in gWAT and scWAT at week 35. While adipose tissue macrophage infiltration was in general less frequent in scWAT, it was reduced in both fat depots of female as compared to male mice, however the expression of inflammatory markers in gWAT was similar in both sexes at week 35. In females, later onset of the impairment of glucose homeostasis and better insulin sensitivity were associated with higher plasma levels of adiponectin (week 0, 15 and 35) and reduced hepatosteatosis (week 15 and 35).

Conclusions: Compared to males, female mice demonstrate increased capacity for adipocyte enlargement in response to a long-term HF-feeding, which is associated with reduced adipose tissue macrophage infiltration and lower fat deposition in the liver, and with better insulin sensitivity. Our data suggest that adipose tissue expandability and adiponectin levels might play a role in the sex differences observed in obesity-associated metabolic disorders.

Keywords: sex differences, inflammation, adipose tissue expandability, insulin sensitivity, mice

Introduction

Human [1,2] as well as animal studies [3-7] demonstrate less severe obesity-related metabolic disorders including peripheral tissue insulin resistance and dyslipidaemia (i.e. the components of metabolic syndrome), and/or later onset of these adverse phenotypes in female than in male subjects. However, mechanisms underlying a relatively low susceptibility of females to metabolic syndrome remain largely unknown.

Adverse effects of obesity depend in large on (i) the anatomical site of excessive fat accumulation [8,9], which differ between the sexes [1,10,11], and (ii) on whether growth of adipose tissue is reached by hyperplasia or hypertrophy of adipocytes. Hyperplasia rather than hypertrophy represents a less harmful phenotype associated with a faster turnover of fat cells [12]. Larger adipocytes are less insulin sensitive than smaller ones [7,13,14], and small adipocytes can store more extra fat, while limiting ectopic accumulation of lipids in non-adipose tissues and lipotoxicity [15]. It was suggested that adipose tissue expandability is a more important determinant of obesity-associated metabolic disorders than the absolute amount of adipose tissue an individual possesses [16]. Moreover, larger fat cells are associated with a low-grade adipose tissue inflammation, another key factor linking obesity with insulin resistance [13,14,17-19]. Enhanced secretion of chemoattractants in obese state, like monocyte chemoattractant protein-1 (MCP-1), is believed to promote migration of macrophages [20,21] as well as other immune cells [22] into the tissue accompanied by the phenotypic switch of macrophages to proinflammatory state [23,24]. Higher release of proinflammatory cytokines, like tumor necrosis factor α (TNFα) and interleukin 6 (IL-6), into circulation may disrupt insulin signaling in other tissues [25-27]. Recent studies in mice [19,28] showed that high-fat (HF) diet-induced obesity is associated with increased macrophage infiltration and inflammation in gonadal fat (gWAT) and to a lower extent also in subcutaneous fat (scWAT). Inflammatory state in gWAT correlated with systemic insulin

resistance [28] and with hepatic triglyceride content in rodents [20,21]. It is believed that increased macrophage infiltration of adipose tissue in obesity is triggered by dead adipocytes [29] and that adipocyte size is an important determinant in cell death [30]. At the same time, clearance of dead adipocytes by surrounding macrophages is required for remodeling of adipose tissue [28]. Thus, fat cell size and macrophage infiltration represent interdependent variables affecting adipose tissue expandability.

In contrast to proinflammatory cytokines, the major adipokines released from adipocytes, namely leptin and adiponectin, protect insulin signaling from lipotoxic damage via increasing activity of AMP-activated protein kinase (AMPK; see ref. [31]), reflecting the key role of AMPK in the control of lipid metabolism, as well as by other mechanisms [32]. While secretion of leptin and leptinaemia correlate with adiposity, adiponectin is downregulated in obese and diabetic subjects [33]. This may have a major impact on health due to the antidiabetic, antiinflammatory and antiatherogenic effects of adiponectin [34-37].

Most of the above studies were performed on male subjects. However, studies in humans [38-40] as well as in mice [19] suggest that lower adipose tissue macrophage infiltration [19] and/or smaller fat cell size [19,40] in female subjects could contribute to the sex differences in propensity to the disorders of the metabolic syndrome. In this study performed in mice, we tested a hypothesis that due to a higher stimulation of lipogenesis and stronger antilipolytic effect of insulin in female adipocytes, especially those in gWAT [4,7], (i) prolonged HF-feeding may eventually result in larger fat cells in female than in male animals, and that (ii) glycemic control may be less affected by excessive adiposity in female than in male mice even in the presence of larger adipocytes in the females. During the course of a long-term (35-week) HF-feeding, body weights of male and female mice reached their maxima at a similar level. Adipocytes in both gWAT and scWAT became eventually larger in female than in male mice, while the density of macrophages in adipose tissue remained lower in females. Our results suggest that adiponectin rather than

adipose tissue-derived proinflammatory cytokines is associated with the differential effects of extreme dietary obesity on insulin sensitivity and hepatic steatosis in female and male mice. It is plausible that adipose tissue in female subjects is genetically programmed to store more lipids than in males, thus constituting an important mechanism of a harmless lipid storage.

Materials and methods

Animals and treatments

All experiments were performed using F1 generation of male and female C57BL/6N mice imported from Charles River Laboratories (Sulzfeld, Germany; 20 mice of each sex) maintained (3-4 mice of the same sex per cage) at 22 °C on a 12-hour light-dark cycle (light on from 6:00 am) and allowed free access to food and water. Four weeks after birth (week 0), mice were randomly assigned either to (i) chow (ST; lipid content ~3.4% wt/wt; extruded Ssniff R/M-H diet, SSNIFF Spezialdieten GmbH, Soest, Germany) with protein, fat and carbohydrate forming 33, 9 and 58 energy percent or to (ii) high-fat (HF; lipid content ~35% wt/wt, mainly corn oil) diet with protein, fat and carbohydrate forming 15, 59 and 26 energy percent respectively (see ref. [41] for further details concerning the HF diet composition, including fatty acid composition of dietary lipids). During the treatments, fresh rations were distributed three times a week. Body weight of each mouse was monitored weekly, food intake per cage was monitored weekly between week 4 and week 14 after weaning, and every second week between week 17 and week 30 after weaning, except for the week right after the glucose tolerance tests (see below and Fig. 1). At week 15 or at week 35 after weaning, 10 mice of each sex were sacrificed under diethylether anesthesia by cervical dislocation in a random-fed state. Truncal plasma was collected and stored at -80°C. Liver, gWAT and dorsolumbar scWAT (i.e. fat depot forming a continuum with the inguinal fat [42]) were rapidly dissected. Liver samples were snap-frozen in

liquid nitrogen and stored at -80°C for further histological analysis. Samples of gWAT for mRNA analysis were stored at -80°C in RNA Later (Ambion, Austin, TX). Corresponding contralateral adipose tissue depots were used for light microscopy and immunohistochemical analysis (see below).

All experiments were performed in accordance with the directive of the European Communities Council (68/609/EEC), and the *Principles of Laboratory Animal Care* (NIH publication no. 85-23, revised 1985).

Plasma metabolites, hormones and enzymes

Non-estherified fatty acids (NEFA) and triglycerides (TAG) were determined in EDTA-plasma using respective enzymatic photometric tests: NEFA-C (Wako Chemicals, Neuss, Germany), and Triacylglycerols Liquid (Pliva-Lachema Diagnostika, Brno, Czech Republic). Blood glucose was measured using calibrated glucometers OneTouch Ultra (Life Scan, Milpitas, CA). Multimeric forms of adiponectin were determined similarly as before [43], using Western blotting and primary rabbit anti-mouse polyclonal antibodies (BioVendor, Czech Republic), followed by secondary donkey anti-rabbit IgG infra-red dye conjugated antibodies (IR Dye 800; Rockland, Gilbertsville, PA). Membranes were scanned using Odyssey IR imager (Li-Cor Biosciences, Lincoln, NE). Plasma insulin levels were determined by the Sensitive Rat Insulin RIA Kit , and leptin content was assessed using a Mouse Leptin RIA Kit (both kits from LINCO Research, St. Charles, MO).

Tissue TAG content

Tissue fragments were digested in 0.15 ml of 3 M alcoholic KOH (70°C, 2 hours) and liberated glycerol was assessed by Triacylglycerols Liquid (Pliva-Lachema Diagnostika). TAG content was calculated relative to a Lyonorm Calibrator (Pliva-Lachema Diagnostika).

Adipose tissue DNA content

The DNA content was measured fluorometrically after overnight digestion of the tissue using proteinase K as before [44]. Calf thymus DNA (Sigma-Aldrich, Prague, Czech Republic) was used as a standard.

Light microscopy and immunohistochemical analysis

Adipose tissue samples were fixed in 10% neutral buffered formalin (Sigma-Aldrich) and embedded in paraffin. Sections (5 μm) were stained with hematoxylin-eosin for morphometry, or processed to detect MAC-2/galectin (Cedarlane Laboratories, Burlington, NC) positive macrophages aggregated in crown-like structures (CLS) surrounding dead adipocytes, as described before [29]. Liver lipids were detected in cryosections (8 μm) of the tissue, fixed in 10% neutral buffered formalin and stained with a saturated solution of Oil red O (Sigma-Aldrich) in 70% ethanol; sections were counterstained with hematoxylin. Digital images were captured by Olympus AX70 light microscope and a DP 70 camera (Olympus, Tokyo, Japan). Morphometric analysis was performed using Imaging Software NIS-Elements AR 3.0 (Laboratory Imaging, Prague, Czech Republic). The morphometry data are based on measurements of ~500 cells taken randomly from 3-6 different sections per animal.

Glucose homeostasis

An intraperitoneal glucose tolerance test was performed after overnight fasting (15–16 hours), at week 10, week 25 and week 33. Blood glucose was assessed by tail bleeds at the baseline (fasting blood glucose; just before the glucose injection) and 15, 30, 60, 120 and 180 min after the injection of D-glucose (1 g/kg body weight). Results were expressed as area under the curve (AUC) for glucose [45]. Blood samples collected at the baseline were also used to measure insulinaemia. In addition, to assess changes of glycemia in response to fasted-to-fed transition,

mice scheduled for killing at week 35 were subjected to tail bleeding at week 15. Before the bleeding, one half of mice within each experimental group was either (i) fasted for 14 hours (food was absent in the cage between 8:00 am and 10:00 pm; i.e. fasted state), or (ii) fasted for 10 hours (between 8:00 am and 6:00 pm and allowed free access to food for the following 3 hours; i.e. re-fed state). In each mouse, blood glucose was assessed in both fasted and re-fed state, while altering the above protocols during two subsequent days (adapted procedure, following ref. [46]).

Gene expression analysis

Total RNA was isolated from gWAT using TRIzol Reagent (Invitrogen, Carlsbad, CA). Total RNA (1 µg) was reverse transcribed to cDNA and gene expression was evaluated by quantitative real-time PCR (qRT-PCR), using the LightCycler Instrument 480 (Roche Diagnostics, Mannheim, Germany) and qPCR kit LightCycler 480 SYBR Green I Master (Roche Diagnostics). Oligonucleotide primers were designed using Lasergene software (DNAStar, Madison, WI). The following primer pairs were used: monocyte chemoattractant protein-1 (MCP-1; forward, 5'-GTTAACGCCCCACTCAC-3', reverse, 5'-GGTTCCGATCCAGGTTT-3'); tumor necrosis factor α (Tnfα; forward, 5'- GAAGTTCCCAAATGGCCTCCCTCTC -3', reverse, 5'- GCCACTCCAGCTGCTCCTCCACTTG -3'); macrosialin (Cd68; forward, 5'-CACTTCGGGCCATGTTTCTCTTG-3', reverse, 5'-AGGGGCTGGTAGGTTGATTGTCGT-3'). Levels of transcripts were standardized using the gene encoding eukaryotic translation elongation factor 2 (Eef2; forward, 5'- GAAACGCGCAGATGTCCAAAAGTC-3', reverse, 5'-GCCGGGCTGCAAGTCTAAGG-3').

Statistics

All values are presented as means ± SE. Data were analysed by two-way ANOVA using SigmaStat (SSI, San Jose, CA) statistical software. The Holm-Sidak test for multiple comparisons was used. Changes in glycemia (Fig. 3a) and in plasma insulin levels (Fig. 3d) in individual mice were analysed using repeated measures ANOVA. Threshold of significance was defined at $P \leq 0.05$.

Results

Growth characteristics

At the time of weaning, body weight of male mice was significantly higher than that of females, and males remained heavier during the whole 35-week-period of ST-feeding (Fig. 1 and Table 1). Within a couple of weeks after weaning, mice of both sexes fed HF diet became significantly heavier than their respective ST-fed controls. During ~20 initial weeks, HF-fed male mice showed higher body weight than females, while females gained weight faster than males, and from the week 20 onwards, females showed equal body weight as males, and even tended to be heavier than males eventually (Fig. 1). Thus, females gained more weight during the 35-week feeding period compared to males (Table 1). Food consumption remained stable with age in both sexes and dietary groups. HF-fed males exhibited the same caloric intake as ST-fed males, while caloric intake was higher in HF-fed than ST-fed females. Inter-sex differences in caloric intake were not observed, except for ST-fed female mice during week 4-14 showing lower food intake than ST-fed males (Table 1).

In ST-fed mice, at both week 15 and week 35, no significant differences in weight of either gWAT or scWAT were observed between the sexes, but male mice tended to accumulate more fat. The opposite situation was observed in HF-fed mice, where females displayed the tendency

for a greater accumulation of fat in both depots at week 15. The difference was even more pronounced at week 35, with males exhibiting smaller fat depots, especially in the case of gWAT (~3.8-fold difference) as compared with corresponding female mice (Table 1). Similar trends were observed after normalization of depot weights to total body weight (Table 1).

HF-feeding increased the weight of the liver. However, at both week 15 and week 35 (as well as in ST-fed mice at week 35), the liver was smaller in female than in male mice (Table 1). Female mice were less prone to HF diet-induced liver steatosis, as revealed by the biochemical analysis of the tissue (Table 1) and by its histological staining for lipids (Fig. 2). However, no differences were detected between the sexes with respect to lipid accumulation in skeletal muscle (not shown).

Plasma markers

Levels of lipids and several hormones were measured in plasma of mice killed in *ad libitum* fed state at week 15 and week 35 (Table 2). In ST-fed mice, levels of TAG decreased with age, and especially at week 35, female had lower TAG levels than male mice, while no age- or sex-specific differences in NEFA or cholesterol levels were observed. Except for NEFA, plasma lipid levels were increased in response to HF-feeding; TAG levels were lower in the older mice, and they were also lower in female than in male mice at week 15. No other age- or sex-dependent differences were observed in plasma lipid levels in HF-fed mice (Table 2).

Plasma insulin levels in random-fed state in ST-fed mice were lower in female than in male mice, with the lowest levels observed in females at week 35. Insulin levels increased with HF-feeding and with its duration, suggesting induction of insulin resistance, however, female mice were partially protected, as observed at both week 15 (~2.4-fold difference in plasma insulin) and week 35 (~2-fold difference in plasma insulin) (Table 2).

Plasma leptin levels in ST-fed mice increased with age, and at week 35, the levels were lower in female than in male mice. Leptin levels increased with HF-feeding and with its duration, with female mice at week 35 showing higher levels than the corresponding male mice (Table 2).

Levels of total adiponectin (for a representative Western blot, see Suppl. Fig. 1), especially of its biologically active high molecular weight (HMW) form, which is implicated in enhancement of insulin sensitivity [47], tended to be decreased by HF-feeding, and HMW adiponectin levels were significantly depressed by HF diet at week 15 in male mice and at week 35 in females. Nevertheless, the levels of both total as well as HMW adiponectin were always higher in female than in male mice, with the HMW adiponectin in HF-fed mice showing a bigger difference between the sexes at week 15 than at week 35 (~1.9-fold vs. ~1.6-fold difference, respectively; Table 2). Moreover, in a separate experiment, we have observed higher plasma total adiponectin in female mice already at the time of weaning at 4 weeks of age (0.68 ± 0.04 vs. 1.03 ± 0.06 A.U. in males and females, respectively; n=9, $P \leq 0.01$), with even doubled levels of HMW form (0.24 ± 0.1 vs. 0.49 ± 0.3 A.U. in males and females, respectively; $P \leq 0.01$).

Glucose homeostasis

When evaluated at week 15, mice of both genders fed ST diet, as well as female mice fed HF diet, were able to decrease substantially glycemia during fasting, but HF-fed male mice were not able to do so, indicating metabolic inflexibility to glucose in these mice (Fig. 3a).

To assess the sex differences in the development of HF diet-induced insulin resistance, intraperitoneal glucose tolerance test was performed at week 10, week 25 and week 33 (Fig. 3b,c, and Suppl. Fig. 2). Fasting blood glucose levels at the baseline (Fig. 3b), as well as AUC derived from glycemic curves (Fig. 3c) suggested better glucose tolerance in female than in male mice fed ST diet at all three time points analysed (except for glycemia at week 10), with a mild deterioration of glucose homeostasis with ageing. HF-feeding aggravated glucose intolerance in

both male and female mice. However, in contrast to male mice, which became strongly affected already at week 10, deterioration of glucose tolerance in response to HF-feeding in female mice required longer period to develop, with a significant effect observed at week 25, and even more pronounced effect at week 33, when mice of both sexes showed identical values of both fasting blood glucose and AUC for glycemia during the test.

To further characterize glucose homeostasis at week 33, plasma insulin levels were also determined at the baseline and at 30 min after the glucose injection (Fig. 3d), i.e. at the time of presumed highest insulin response (when plasma glucose levels reach the peak values; see Supp. Fig. 1). In ST-fed mice, insulin levels at the baseline and at 30 min after the glucose injection were similar in the both sexes (Fig. 3d). In the HF-fed mice, already the baseline insulin levels were higher than in the ST-fed mice and the levels increased further in response to glucose reaching significantly higher levels in male than in female mice (Fig. 3d).

Adipose tissue morphology and inflammation

Further analysis was performed to characterise possible links between sex-dependent effects of HF-feeding on glucose homeostasis and changes in adipose tissue morphology and inflammation. Histological analysis combined with morphometry revealed that in ST-fed mice mean area of adipocytes was larger in gWAT as compared to scWAT. However, the mean size of adipocytes was comparable between the sexes and it did not differ between week 15 and week 35 (Fig. 4e,i,g,k). In both sexes and in both fat depots, HF-feeding significantly increased the adipocyte size at week 15 as well as at week 35. As observed before [28], mean adipocyte size in gWAT (Fig. 4e,i), but not in scWAT (Fig. 4g,k) decreased with age. The shift in the mean size of adipocyte in gWAT with the duration of HF-feeding reflected relatively high preponderance of small adipocytes at week 35 (Suppl. Fig. 3). In contrast to gWAT, no major difference in the adipocyte size distribution between week 15 and week 35 was observed in scWAT (Suppl. Fig.

4). At week 15, mean size of adipocytes in both gWAT and scWAT of HF-fed female mice tended to be larger than in male mice fed the same diet (Fig. 4e,g) and at week 35, the mean size of adipocytes in both fat depots was significantly larger in female compared to male mice (Fig. 4i,k).

HF diet-induced hypertrophy of adipose tissue was associated with increased content of macrophages, immunodetected as crown-like structure (CLS) aggregates surrounding individual adipocytes (Fig. 4a-d), and indicating induction of low-grade adipose tissue inflammation [29]. Thus, whereas CLS could be hardly detected in any sample of adipose tissue of ST-fed mice (Fig. 4f,j,h,l), the CLS density was significantly higher in fat depots of HF-fed mice (Fig 4f,j,h,l), and it increased further several fold in gWAT, with a small increase in scWAT, between week 15 and week 35 (Fig 4f,j,h,l). Although the degree of adipose tissue macrophage infiltration is usually correlated with size of adipocytes (see Introduction), adipose tissue of female mice contained much less CLS than their male counterparts. This was most apparent in both fat depots at week 35 (Fig. 4j,l), as well as in gWAT at week 15 (Fig. 4f).

In addition to the histological analysis, cellularity of gWAT was characterized using estimation of tissue DNA. At week 15, lower DNA concentration was found in HF-fed than in ST-fed mice, regardless of the sex (Fig. 5a). At week 35, a different picture was observed. There was no difference between the ST-fed male and female mice, however, HF-feeding increased the DNA concentration only in male mice (Fig. 5b).

Gene expression

To further characterise inflammatory status of adipose tissue in HF-fed mice, expression of several proinflammatory markers was assessed in gWAT, which showed higher induction of macrophage infiltration in response to HF diet than scWAT (see above). In mice of both sexes, HF-feeding markedly increased expression of genes for MCP-1, TNFα and CD68, with a

stronger induction in mice fed HF diet for the longer time (Fig. 6). At week 15, all these genes showed lower expression in female than in male mice (although the difference in TNFα did not reach a statistical significance; Fig. 6a). At week 35, only a trend for lower expression in female mice was observed with TNFα and CD68 (Fig. 6b).

Discussion

In this study, using a murine model of HF diet-induced morbid obesity, we showed that the weight gain, mass of both scWAT and gWAT fat depots, and mean size of adipocytes in these fat depots were all significantly increased in female compared to male mice in response to HF diet administered from weaning for a period of 35 weeks, i.e. HF-feeding of a very long duration until 10 months of age. At this time point, the body weight was stabilized and reached a similar level in both sexes. Although the total content of body lipids was not assessed at the end of HF-feeding, it was also likely increased in females, as supported by their increased plasma leptin levels. Until week 15, males gained more weight and their body mass was higher than in females until week 20. In mice fed a low-fat ST diet, males were heavier, tended to accumulate more fat than females, while no effect on adipocyte size was found during the study. We verified the hypothesis (see Introduction) that the capacity for enlargement is increased in adipocytes of female compared to male mice in response to a long-term HF-feeding, possibly reflecting the higher insulin sensitivity of the female adipocytes. In contrast to similar studies performed previously [6,7,19], the sex-dependent metabolic phenotypes observed in this mouse model of dietary obesity could not be attributed to a lower body weight gain, adiposity, and/or smaller fat cells in females. Most of the results were confirmed by an independent experiment on a separate cohort of animals (not shown).

Study of Grove *et al*., published recently in this journal [19], showed less inflamed gWAT in female than in male C57BL/6 mice fed HF diet for 12 weeks after weaning, with female mice having lower fat mass. Moreover, in female mice, the size of adipocytes tended to be smaller in gWAT, while it was significantly smaller in scWAT [19]. In our experiments, adipose tissue inflammation assessed as the density of CLS was also much lower in gWAT of female compared to male mice at week 15, i.e. the time point when no significant differences in the size of adipocytes were observed between the sexes. However, in contrast to the study by Grove *et al.* [19], we have prolonged the HF-feeding until the week 35, when adipocytes within each fat depot were larger in female compared to male mice. Also at this time point, we observed sex-dependent differences in the CLS accumulation in gWAT and scWAT with females having much lower macrophage accumulation in both fat depots. These results are supported by the data on DNA concentration in gWAT, namely at week 35. At this time, HF-fed mice showed equal (female mice) or higher (male mice) tissue DNA concentration as compared with the ST-fed mice, in spite of larger adipocytes in the HF-fed animals, in agreement with an increased infiltration of adipose tissue with immune cells in response to HF-feeding [22], and with the prominent inflammatory changes occurring in the male mice.

That female mice had lower inflammatory response was a surprising observation, since it is generally believed that macrophage infiltration and inflammation of adipose tissue in obesity is correlated with adipocyte hypertrophy [13,14,19,29,30]. Moreover, in agreement with the published data on extensive remodeling of gWAT in male mice during the course of HF diet-induced obesity [28], our data document smaller adipocytes and lower mass of gWAT depot in males at week 35 than at week 15. In contrast, the mass of gWAT in HF-fed female mice was ~2.8-fold bigger at week 35 than at week 15, indicating very different patterns of gWAT remodeling in the two sexes. Our data also confirmed fat depot-specific differences [19,28] in the induction of adipose tissue macrophage infiltration by HF diet, with a relatively small infiltration in scWAT at either

week 15 or week 35, compared to a much stronger infiltration in gWAT, which increased ~10-fold between week 15 and week 35.

Our observation that hypertrophy of adipocytes can be dissociated from adipose tissue inflammation is not without precedent. Thus, the genetic disruption of MCP-1 receptor gene [48], transport protein lipocalin-2 [49] or disruption of the gene for a component of extracellular matrix, namely collagen VI [17], resulted in larger adipocytes, lower adipose tissue inflammation and attenuated insulin resistance in male mice fed the HF diet. These data suggest a role for extracellular matrix in the mechanisms underlying adipocyte death, due to restriction of adipocytes' enlargement and shear stress [17]. However, we could not find any differences between the sexes concerning the gene expression of the components of extracellular matrix, including collagen VI and lumican (not shown). This suggests that other mechanism(s) than the extracellular matrix-dependent shear stress contributed to reduced inflammation in females' adipose tissue.

Our data confirm the previously observed (see Introduction) sex differences at the level of glycemic control, documenting an earlier onset of glucose intolerance in male as compared to female mice challenged with HF diet. Although blood glucose clearance during the glucose tolerance test was similar in mice of both sexes at the end of the long-term HF-feeding, lower levels of plasma insulin were required in females to maintain the same glucose tolerance as males. We have also examined whether the differences in glycemic control reflected sex-dependent changes in the expression of proinflammatory markers in adipose tissue. Consistent with the previous findings [20,26,50,51] , we observed profound increases in the expression of pro-inflammatory markers such as MCP-1, TNFα, and macrophage marker CD68 in adipose tissue of mice of both sexes during the course of HF diet-induced obesity. In agreement with the sex-dependent differences in macrophage infiltration of gWAT, the expression of MCP-1, TNFα and CD68 was lower in gWAT of females at week 15, however, unexpectedly, no significant

differences in the expression of selected genes (MCP-1, TNFα and CD68) were observed between the sexes at week 35. The lack of correlation between macrophage infiltration and expression of the inflammatory cytokines in gWAT at week 35 remains to be explained. However, it is compatible with other results showing that the absence of MCP-1 does not limit the recruitment of macrophages to gWAT [52], and the lack of a correlation between macrophage content in gWAT and the levels of proinflammatory cytokines in plasma in mice fed HF diet [19,28]. In fact, the previous study [19] in mice fed HF diet for 12 weeks after weaning showed similar plasma levels of TNFα, IL-6, interleukin-1β, MCP-1 and granulocyte-macrophage colony-stimulating factor in male and female mice, in spite of a robust sexual dimorphism in macrophage infiltration and in the expression of genes for inflammatory markers in gWAT. Therefore, the above results suggest that macrophage-released proinflammatory cytokines may not play a major role in the differential induction of systemic insulin resistance by HF diet in male and female mice. On the other hand, macrophages in adipose tissue could contribute to sex-dependent tissue remodeling during the course of HF-feeding [28]. This would be in agreement with the concept (see above) that increased expandability of adipose tissue, reflected by a higher capacity for adipocyte enlargement and lower macrophage infiltration, could counteract ectopic fat deposition and lipotoxicity in females.

Adiponectin or estrogens should be considered among the factors contributing to the sex-dependent differences in insulin sensitivity, since both hormones possess antiinflammatory properties and protect from insulin resistance [34,53,54]. In fact, female mice consistently showed much higher levels of adiponectin in plasma compared to males, including the biologically active HMW form [47], and this feature was independent of the type of diet, expression of inflammatory markers in adipose tissue, and duration of HF-feeding. These results are in accordance with other animal [36,55,56] as well as human [57,58] studies showing higher adiponectin levels in females. Adiponectin may preserve insulin sensitivity in females by various mechanisms, including the

activation of AMPK [31], as well as by promoting the switch between proinflammatory (M1) and antiinflammatory (M2) macrophages in adipose tissue [59]. Thus, relatively low levels of hepatic steatosis in female mice exposed to HF diet could be explained, at least in part, by the AMPK-mediated effect of adiponectin. Indeed, higher phosphorylation of hepatic AMPK was observed in adult female as compared with male mice fed HF diet, suggesting a higher AMPK activity in the females (Jelenik *et al*., unpublished results). However, the involvement of possible sexual dimorphism in macrophage polarization in response to adiponectin and HF diet remains an open question (see Suppl. Tables 2 and 4, ref. [19]).

An important question remains to be answered, whether the increased capacity for adipocyte enlargement in female as compared to male mice is also relevant to human obesity. A carefully conducted study in human subjects has not shown any significant differences between the sexes regarding the curvilinear relationship between body fat mass and fat cell volume in subcutaneous fat, while only a trend for adipocytes in women to grow bigger could be observed (see Fig. 1 a,b of ref. [60]). In this respect, further studies should focus on human subjects with morbid obesity.

In conclusion, in a model of morbid obesity induced in C57BL/6N mice by a long-term (35 weeks) HF-feeding, females eventually accumulated more fat and exhibited larger adipocytes compared to males. In spite of larger adipocytes in gWAT as well as in scWAT, the frequency of dead adipocytes, marked by macrophage infiltration of adipose tissue, was reduced in female compared to male mice. Lower plasma levels of insulin together with a markedly increased adiponectin and less pronounced hepatosteatosis imply better insulin sensitivity in female mice during the course of HF-feeding, independent of the expression of proinflammatory cytokines in adipose tissue. Our results suggest an increased intrinsic capacity for adipocyte enlargement in females in the face of a relatively mild tissue remodeling and macrophage infiltration. Thus,

adipose tissue expandability and adiponectin can substantially contribute to a greater resistance of female mice to deterioration of glycemic control during the development of dietary obesity.

Supplementary information is available at International Journal of Obesity's website.

Conflict of interest

The authors declare no conflict of interest.

Acknowledgements

The research leading to these results has received funding from the European Union's Seventh Framework Programme FP7 2007-2013 under grant agreement nº 244995 (BIOCLAIMS Project), the Czech Science Foundation (303/08/0664), COST Action Mitofood (FA0602), the MSMT of the Czech Republic (OC08008), and EPAX a.s. (Aalesund, Norway). We thank Pavel Flachs for critical reading of the manuscript.

References

1. Krotkiewski M, Bjorntorp P, Sjostrom L, Smith U. Impact of obesity on metabolism in men and women. Importance of regional adipose tissue distribution. *J Clin Invest* 1983;72:1150-1162.

2. Frias JP, Macaraeg GB, Ofrecio J, Yu JG, Olefsky JM, Kruszynska YT. Decreased susceptibility to fatty acid-induced peripheral tissue insulin resistance in women. *Diabetes* 2001;50:1344-1350.

3. Priego T, Sanchez J, Pico C, Palou A. Sex-differential expression of metabolism-related genes in response to a high-fat diet. *Obesity (Silver Spring)* 2008;16:819-826.

4. Guerre-Millo M, Leturque A, Girard J, Lavau M. Increased insulin sensitivity and responsiveness of glucose metabolism in adipocytes from female versus male rats. *J Clin Invest* 1985;76:109-116.

5. Hevener A, Reichart D, Janez A, Olefsky J. Female rats do not exhibit free fatty acid-induced insulin resistance. *Diabetes* 2002;51:1907-1912.

6. Trevaskis JL, Meyer EA, Galgani JE, Butler AA. Counterintuitive effects of double-heterozygous null melanocortin-4 receptor and leptin genes on diet-induced obesity and insulin resistance in C57BL/6J mice. *Endocrinology* 2008;149:174-184.

7. Macotela Y, Boucher J, Tran TT, Kahn CR. Sex and depot differences in adipocyte insulin sensitivity and glucose metabolism. *Diabetes* 2009;58:803-812.

8. Wajchenberg BL. Subcutaneous and visceral adipose tissue: their relation to the metabolic syndrome. *Endocr Rev* 2000;21:697-738.

9. Cnop M, Landchild MJ, Vidal J, Havel PJ, Knowles NG, Carr DR, Wang F, Hull RL, Boyko EJ, Retzlaff BM, Walden CE, Knopp RH, Kahn SE. The concurrent accumulation of intra-abdominal and subcutaneous fat explains the association between insulin resistance and plasma leptin concentrations : distinct metabolic effects of two fat compartments. *Diabetes* 2002;51:1005-1015.

10. Enzi G, Gasparo M, Biondetti PR, Fiore D, Semisa M, Zurlo F. Subcutaneous and visceral fat distribution according to sex, age, and overweight, evaluated by computed tomography. *Am J Clin Nutr* 1986;44:739-746.

11. Clegg DJ, Brown LM, Woods SC, Benoit SC. Gonadal hormones determine sensitivity to central leptin and insulin. *Diabetes* 2006;55:978-987.

12. Arner E, Westermark PO, Spalding KL, Britton T, Ryden M, Frisen J, Bernard S, Arner P. Adipocyte turnover: relevance to human adipose tissue morphology. *Diabetes* 2010;59:105-109.

13. Okuno A, Tamemoto H, Tobe K, Ueki K, Mori Y, Iwamoto K, Umesono K, Akanuma Y, Fujiwara T, Horikoshi H, Yazaki Y, Kadowaki T. Troglitazone increases the number of small adipocytes without the change of white adipose tissue mass in obese zucker rats. *J Clin Invest* 1998;101:1354-1361.

14. Kubota N, Terauchi Y, Miki H, Tamemoto H, Yamauchi T, Komeda K, Satoh S, Nakano R, Ishii C, Sugiyama T, Eto K, Tsubamoto Y, Okuno A, Murakami K, Sekihara H, Hasegawa G, Naito M, Toyoshima Y, Tanaka S, Shiota K, Kitamura T, Fujita T, Ezaki O, Aizawa S, Kadowaki T. PPAR gamma mediates high-fat diet-induced adipocyte hypertrophy and insulin resistance. *Mol Cell* 1999;4:597-609.

15. Danforth E Jr. Failure of adipocyte differentiation causes type II diabetes mellitus? *Nat Genet* 2000;26:13.

16. Virtue S, Vidal-Puig A. It's not how fat you are, it's what you do with it that counts. *PLoS Biol* 2008;6:e237.

17. Khan T, Muise ES, Iyengar P, Wang ZV, Chandalia M, Abate N, Zhang BB, Bonaldo P, Chua S, Scherer PE. Metabolic dysregulation and adipose tissue fibrosis: role of collagen VI. *Mol Cell Biol* 2009;29:1575-1591.

18. Halberg N, Khan T, Trujillo ME, Wernstedt-Asterholm I, Attie AD, Sherwani S, Wang ZV, Landskroner-Eiger S, Dineen S, Magalang UJ, Brekken RA, Scherer PE. Hypoxia-inducible factor 1alpha induces fibrosis and insulin resistance in white adipose tissue. *Mol Cell Biol* 2009;29:4467-4483.

19. Grove KL, Fried SK, Greenberg AS, Xiao XQ, Clegg DJ. A microarray analysis of sexual dimorphism of adipose tissues in high-fat-diet-induced obese mice. *Int J Obes (Lond)* 2010; 34:989-1000.

20. Kanda H, Tateya S, Tamori Y, Kotani K, Hiasa K, Kitazawa R, Kitazawa S, Miyachi H, Maeda S, Egashira K, Kasuga M. MCP-1 contributes to macrophage infiltration into adipose tissue, insulin resistance, and hepatic steatosis in obesity. *J Clin Invest* 2006;116:1494-1505.

21. Kamei N, Tobe K, Suzuki R, Ohsugi M, Watanabe T, Kubota N, Ohtsuka-Kowatari N, Kumagai K, Sakamoto K, Kobayashi M, Yamauchi T, Ueki K, Oishi Y, Nishimura S, Manabe I, Hashimoto H, Ohnishi Y, Ogata H, Tokuyama K, Tsunoda M, Ide T, Murakami K, Nagai R, Kadowaki T. Overexpression of monocyte chemoattractant protein-1 in adipose tissues causes macrophage recruitment and insulin resistance. *J Biol Chem* 2006;281:26602-26614.

22. Anderson EK, Gutierrez DA, Hasty AH. Adipose tissue recruitment of leukocytes. *Curr Opin Lipidol* 2010;21:172-177.

23. Lumeng CN, Bodzin JL, Saltiel AR. Obesity induces a phenotypic switch in adipose tissue macrophage polarization. *J Clin Invest* 2007;117:175-184.

24. Lumeng CN, Delproposto JB, Westcott DJ, Saltiel AR. Phenotypic switching of adipose tissue macrophages with obesity is generated by spatiotemporal differences in macrophage subtypes. *Diabetes* 2008;57:3239-3246.

25. Hotamisligil GS, Murray DL, Choy LN, Spiegelman BM. Tumor necrosis factor alpha inhibits signaling from the insulin receptor. *Proc Natl Acad Sci U S A* 1994;91:4854-4858.

26. Xu H, Barnes GT, Yang Q, Tan G, Yang D, Chou CJ, Sole J, Nichols A, Ross JS, Tartaglia LA, Chen H. Chronic inflammation in fat plays a crucial role in the development of obesity-related insulin resistance. *J Clin Invest* 2003;112:1821-1830.

27. de Luca C, Olefsky JM. Inflammation and insulin resistance. *FEBS Lett* 2008;582:97-105.

28. Strissel KJ, Stancheva Z, Miyoshi H, Perfield JW, DeFuria J, Jick Z, Greenberg AS, Obin MS. Adipocyte death, adipose tissue remodeling, and obesity complications. *Diabetes* 2007;56:2910-2918.

29. Cinti S, Mitchell G, Barbatelli G, Murano I, Ceresi E, Faloia E, Wang S, Fortier M, Greenberg AS, Obin MS. Adipocyte death defines macrophage localization and function in adipose tissue of obese mice and humans. *J Lipid Res* 2005;46:2347-2355.

30. Monteiro R, de Castro PMST, Calhau C, Azevedo I. Adipocyte size and liability to cell death. *Obesity Surgery* 2006;16:804-806.

31. Yamauchi T, Kamon J, Minokoshi Y, Ito Y, Waki H, Uchida S, Yamashita S, Noda M, Kita S, Ueki K, Eto K, Akanuma Y, Froguel P, Foufelle F, Ferre P, Carling D, Kimura S, Nagai R, Kahn BB, Kadowaki T. Adiponectin stimulates glucose utilization and fatty-acid oxidation by activating AMP-activated protein kinase. *Nat Med* 2002;8:1288-1295.

32. Carling D. The AMP-activated protein kinase cascade--a unifying system for energy control. *Trends Biochem Sci* 2004;29:18-24.

33. Hotta K, Funahashi T, Arita Y, Takahashi M, Matsuda M, Okamoto Y, Iwahashi H, Kuriyama H, Ouchi N, Maeda K, Nishida M, Kihara S, Sakai N, Nakajima T, Hasegawa K, Muraguchi M, Ohmoto Y, Nakamura T, Yamashita S, Hanafusa T, Matsuzawa Y. Plasma concentrations of a novel, adipose-specific protein, adiponectin, in type 2 diabetic patients. *Arterioscler Thromb Vasc Biol* 2000;20:1595-1599.

34. Berg AH, Combs TP, Du X, Brownlee M, Scherer PE. The adipocyte-secreted protein Acrp30 enhances hepatic insulin action. *Nat Med* 2001;7:947-953.

35. Yamauchi T, Kamon J, Waki H, Terauchi Y, Kubota N, Hara K, Mori Y, Ide T, Murakami K, Tsuboyama-Kasaoka N, Ezaki O, Akanuma Y, Gavrilova O, Vinson C, Reitman ML, Kagechika H, Shudo K, Yoda M, Nakano Y, Tobe K, Nagai R, Kimura S, Tomita M, Froguel P, Kadowaki T. The fat-derived hormone adiponectin reverses insulin resistance associated with both lipoatrophy and obesity. *Nat Med* 2001;7:941-946.

36. Kim JY, van de WE, Laplante M, Azzara A, Trujillo ME, Hofmann SM, Schraw T, Durand JL, Li H, Li G, Jelicks LA, Mehler MF, Hui DY, Deshaies Y, Shulman GI, Schwartz GJ, Scherer PE. Obesity-associated improvements in metabolic profile through expansion of adipose tissue. *J Clin Invest* 2007;117:2621-2637.

37. Okamoto Y, Kihara S, Ouchi N, Nishida M, Arita Y, Kumada M, Ohashi K, Sakai N, Shimomura I, Kobayashi H, Terasaka N, Inaba T, Funahashi T, Matsuzawa Y. Adiponectin reduces atherosclerosis in apolipoprotein E-deficient mice. *Circulation* 2002;106:2767-2770.

38. Cancello R, Tordjman J, Poitou C, Guilhem G, Bouillot JL, Hugol D, Coussieu C, Basdevant A, Bar HA, Bedossa P, Guerre-Millo M, Clement K. Increased infiltration of macrophages in omental adipose tissue is associated with marked hepatic lesions in morbid human obesity. *Diabetes* 2006;55:1554-1561.

39. Tordjman J, Guerre-Millo M, Clement K. Adipose tissue inflammation and liver pathology in human obesity. *Diabetes Metab* 2008;34:658-663.

40. Hou XG, Moser S, Sarr MG, Thompson GB, Que FG, Jensen MD. Visceral and subcutaneous adipose tissue diacylglycerol acyltransferase activity in humans. *Obesity (Silver Spring)* 2009;17:1129-1134.

41. Kuda O, Jelenik T, Jilkova Z, Flachs P, Rossmeisl M, Hensler M, Kazdova L, Ogston N, Baranowski M, Gorski J, Janovska P, Kus V, Polak J, Mohamed-Ali V, Burcelin R, Cinti S, Bryhn M, Kopecky J. n-3 Fatty acids and rosiglitazone improve insulin sensitivity through additive stimulatory effects on muscle glycogen synthesis in mice fed a high-fat diet. *Diabetologia* 2009;52:941-951.

42. Cinti S. The adipose organ. Milano, Italy: Editrice Kurtis; 1999.

43. Polak J, Kovacova Z, Jacek M, Klimcakova E, Kovacikova M, Vitkova M, Kuda O, Sebela M, Samcova E, Stich V. An increase in plasma adiponectin multimeric complexes follows hypocaloric diet-induced weight loss in obese and overweight pre-menopausal women. *Clin Sci (Lond)* 2007;112:557-565.

44. Ruzickova J, Rossmeisl M, Prazak T, Flachs P, Sponarova J, Vecka M, Tvrzicka E, Bryhn M, Kopecky J. Omega-3 PUFA of marine origin limit diet-induced obesity in mice by reducing cellularity of adipose tissue. *Lipids* 2004;39:1177-1185.

45. Rossmeisl M, Jelenik T, Jilkova Z, Slamova K, Kus V, Hensler M, Medrikova D, Povysil C, Flachs P, Mohamed-Ali V, Bryhn M, Berge K, Holmeide AK, Kopecky J. Prevention and reversal of obesity and glucose intolerance in mice by DHA-derivatives. *Obesity (Silver Spring)* 2009;17:1023-1031.

46. Viollet B, Andreelli F, Jorgensen SB, Perrin C, Geloen A, Flamez D, Mu J, Lenzner C, Baud O, Bennoun M, Gomas E, Nicolas G, Wojtaszewski JF, Kahn A, Carling D, Schuit FC, Birnbaum MJ, Richter EA, Burcelin R, Vaulont S. The AMP-activated protein kinase alpha2 catalytic subunit controls whole-body insulin sensitivity. *J Clin Invest* 2003;111:91-98.

47. Waki H, Yamauchi T, Kamon J, Ito Y, Uchida S, Kita S, Hara K, Hada Y, Vasseur F, Froguel P, Kimura S, Nagai R, Kadowaki T. Impaired multimerization of human adiponectin mutants associated with diabetes - Molecular structure and multimer formation of adiponectin. *J Biol Chem* 2003;278:40352-40363.

48. Weisberg SP, Hunter D, Huber R, Lemieux J, Slaymaker S, Vaddi K, Charo I, Leibel RL, Ferrante AW, Jr. CCR2 modulates inflammatory and metabolic effects of high-fat feeding. *J Clin Invest* 2006;116:115-124.

49. Law IK, Xu A, Lam KS, Berger T, Mak TW, Vanhoutte PM, Liu JT, Sweeney G, Zhou M, Yang B, Wang Y. Lipocalin-2 deficiency attenuates insulin resistance associated with aging and obesity. *Diabetes* 2010;59:872-882.

50. Hotamisligil GS, Shargill NS, Spiegelman BM. Adipose expression of tumor necrosis factor-alpha: direct role in obesity-linked insulin resistance. *Science* 1993;259:87-91.

51. Takahashi K, Mizuarai S, Araki H, Mashiko S, Ishihara A, Kanatani A, Itadani H, Kotani H. Adiposity elevates plasma MCP-1 levels leading to the increased CD11b-positive monocytes in mice. *J Biol Chem* 2003;278:46654-46660.

52. Inouye KE, Shi H, Howard JK, Daly CH, Lord GM, Rollins BJ, Flier JS. Absence of CC chemokine ligand 2 does not limit obesity-associated infiltration of macrophages into adipose tissue. *Diabetes* 2007;56:2242-2250.

53. Ghisletti S, Meda C, Maggi A, Vegeto E. 17beta-estradiol inhibits inflammatory gene expression by controlling NF-kappaB intracellular localization. *Mol Cell Biol* 2005;25:2957-2968.

54. Vegeto E, Belcredito S, Etteri S, Ghisletti S, Brusadelli A, Meda C, Krust A, Dupont S, Ciana P, Chambon P, Maggi A. Estrogen receptor-alpha mediates the brain antiinflammatory activity of estradiol. *Proc Natl Acad Sci U S A* 2003;100:9614-9619.

55. Combs TP, Berg AH, Rajala MW, Klebanov S, Iyengar P, Jimenez-Chillaron JC, Patti ME, Klein SL, Weinstein RS, Scherer PE. Sexual differentiation, pregnancy, calorie restriction, and aging affect the adipocyte-specific secretory protein adiponectin. *Diabetes* 2003;52:268-276.

56. Combs TP, Pajvani UB, Berg AH, Lin Y, Jelicks LA, Laplante M, Nawrocki AR, Rajala MW, Parlow AF, Cheeseboro L, Ding YY, Russell RG, Lindemann D, Hartley A, Baker GR, Obici S, Deshaies Y, Ludgate M, Rossetti L, Scherer PE. A transgenic mouse with a deletion in the collagenous domain of adiponectin displays elevated circulating adiponectin and improved insulin sensitivity. *Endocrinology* 2004;145:367-383.

57. Spranger J, Kroke A, Mohlig M, Bergmann MM, Ristow M, Boeing H, Pfeiffer AF. Adiponectin and protection against type 2 diabetes mellitus. *Lancet* 2003;361:226-228.

58. Snijder MB, Heine RJ, Seidell JC, Bouter LM, Stehouwer CD, Nijpels G, Funahashi T, Matsuzawa Y, Shimomura I, Dekker JM. Associations of adiponectin levels with incident impaired glucose metabolism and type 2 diabetes in older men and women: the hoorn study. *Diabetes Care* 2006;29:2498-2503.

59. Ohashi K, Parker JL, Ouchi N, Higuchi A, Vita JA, Gokce N, Pedersen AA, Kalthoff C, Tullin S, Sams A, Summer R, Walsh K. Adiponectin promotes macrophage polarization toward an anti-inflammatory phenotype. *J Biol Chem* 2010;285:6153-6160.

60. Spalding KL, Arner E, Westermark PO, Bernard S, Buchholz BA, Bergmann O, Blomqvist L, Hoffstedt J, Naslund E, Britton T, Concha H, Hassan M, Ryden M, Frisen J, Arner P. Dynamics of fat cell turnover in humans. *Nature* 2008;453:783-787.

Table 1 Growth characteristics, adiposity, and liver weight and TAG content

	ST		*HF*	
	Male	*Female*	*Male*	*Female*
BW (g)				
Week 0	17.8 ± 0.2	14.3 ± 0.3*	18.2 ± 1.0	14.3 ± 0.3*
Week 15	28.5 ± 0.4	24.1 ± 0.4*	43.6 ± 1.9#	36.4 ± 1.7#*
Week 35	35.3 ± 0.7	27.6 ± 0.8*	55.4 ± 2.2#	57.7 ± 2.6#
BWG (g)				
Week 15	11.6 ± 0.6	10.6 ± 0.5	27.2 ± 1.4#	23.1 ± 2.3#*
Week 35	17.5 ± 0.6	13.2 ± 0.6	37.2 ± 1.8#	43.4 ± 2.4#
FC (kJ/day)				
Week 4-14	66.3 ± 0.7	56.2 ± 1.4*	69.5 ± 2.4	68.5 ± 3.6#
Week 17-30	64.8 ± 1.1	61.1 ± 2.3	66.7 ± 4.1	70.6 ± 2.0#
gWAT (mg)				
Week 15	484 ± 31	364 ± 26	1881 ± 158#	2147 ± 301#
Week 35	1032 ± 107	711 ± 97	1565 ± 95	5989 ± 470#*
gWAT (% of BW)				
Week 15	1.8 ± 0.1	1.62 ± 0.1	4.8 ± 0.4#	5.87 ± 0.5#*
Week 35	2.9 ± 0.3	2.5 ± 0.3	2.8 ± 02	10.2 ± 0.5#*
scWAT (mg)				
Week 15	217 ± 14	195 ± 11	797 ± 95#	873 ± 117#
Week 35	312 ± 35	271 ± 24	1297 ± 113#	1590 ± 133#*
scWAT (% of BW)				
Week 15	0.8 ± 0.0	0.8 ± 0.1	2.0 ± 0.2#	2.4 ±0.2#
Week 35	0.9 ± 01	1.0 ± 0.1	2.3 ± 0.2#	2.7 ± 0.2#*
Liver (mg)				
Week 15	1247 ± 55	1144 ± 29	1606 ± 130#	1236 ± 56*
Week 35	1544 ± 51	1160 ± 56*	2541 ± 231#	1806 ± 111#*
Liver (% of BW)				
Week 15	4.6 ± 0.2	4.9 ± 0.1	4.0 ± 0.1#	3.6 ± 0.1#*
Week 35	4.4 ± 0.1	4.2 ± 0.1	4.5 ± 0.3	3.1 ± 0.1#*
Liver TAG (mg/g of tissue)				
Week 15	28 ± 1	32 ± 3	109 ± 20#	72 ± 6#*
Week 35	34 ± 3	38 ± 3	197 ± 27#	121 ± 8#*

Male and female mice weaned at four weeks of age (week 0) onto ST or HF diet were analysed after 15 weeks or 35 weeks (n=10) of feeding their respective diets. BW, body weight; BWG, body weight gain since week 0; FC, mean food consumption; gWAT, gonadal white adipose tissue; scWAT, subcutaneous white adipose tissue; TAG, triglycerides. Data are means ± SE. *significant differences between sexes within diet, #significant differences between diets within sex (ANOVA).

Table 2 Plasma lipids and hormones

	ST		*HF*	
	Male	*Female*	*Male*	*Female*
TAG (mmol/l)				
Week 15	1.20 ± 0.12	1.01 ± 0.05	1.66 ± 0.21#	1.21 ± 0.14*
Week 35	0.97 ± 0.11	0.61 ± 0.04*	0.96 ± 0.03	0.92 ± 0.06#
NEFA (mmol/l)				
Week 15	0.51 ± 0.04	0.48 ± 0.03	0.59 ± 0.06	0.62 ± 0.06
Week 35	0.40 ± 0.05	0.39 ± 0.03	0.41 ± 0.06	0.46 ± 0.03
Cholesterol (mmol/l)				
Week 15	1.77 ± 0.11	1.54 ± 0.10	4.08 ± 0.30#	3.55 ± 0.20#
Week 35	1.96 ± 0.10	1.47 ± 0.06	4.78 ± 0.38#	4.08 ± 0.25#*
Insulin (ng/ml)				
Week 15	0.88 ± 0.21	0.38 ± 0.04*	2.71 ± 0.54#	1.15 ± 0.23#*
Week 35	0.97 ± 0.16	0.21 ± 0.03*	4.68 ± 0.45#	2.30 ± 0.46#*
Leptin (ng/ml)				
Week 15	6.2 ± 0.7	8.8 ± 0.8	45.5 ± 7.6#	41.7 ± 8.0#
Week 35	17.7 ± 2.0	9.1 ± 1.7*	71.9 ± 4.7#	89.6 ± 2.8#*
Adiponectin (A.U.)				
Week 15				
HMW	0.45 ± 0.03	0.62 ± 0.05*	0.33 ± 0.02#	0.63 ± 0.03*
MMW	0.46 ± 0.02	0.65 ± 0.04*	0.44 ± 0.02	0.60 ± 0.03*
LMW	0.02 ± 0.00	0.02 ± 0.00	0.01 ± 0.00	0.02 ± 0.00*
Total	0.94 ± 0.05	1.29 ± 0.08*	0.78 ± 0.03#	1.25 ± 0.05*
Week 35				
HMW	0.46 ± 0.04	0.86 ± 0.10*	0.40 ± 0.06	0.63 ± 0.07#*
MMW	0.55 ± 0.03	0.80 ± 0.06*	0.50 ± 0.02	0.78 ± 0.07*
LMW	0.04 ± 0.01	0.03 ± 0.00	0.02 ± 0.00#	0.03 ± 0.00
Total	1.06 ± 0.06	1.69 ± 0.15*	0.92 ± 0.07	1.44 ± 0.13*

Male and female mice weaned at four weeks of age onto ST or HF diet were analysed after 15 weeks or 35 weeks (n=10) of feeding their respective diets. A.U., arbitrary units; TAG, triglycerides; NEFA, non-estherified fatty acids; HMW, high molecular weight adiponectin; MMW, medium molecular weight adiponectin; LMW, low molecular weight adiponectin. Data are means ± SE. *significant differences between sexes within diet; #significant differences between diets within sexes (ANOVA).

Legends to figures

Figure 1 Growth curves. Mice of both sexes were weaned to either ST or HF diet at four weeks of age (week 0). Some mice (*n=10* from each sex) were killed at week 15, while the remaining mice were killed at week 35. Data are means ± SE (*n=20* between week 0-15; and *n=10* between week 16-35). Intraperitoneal glucose tolerance test (GTT) was performed at week 10, 25 and 33, respectively.

Figure 2 Liver histology. Oil-red O staining showing triglyceride accumulation (red color) in the liver (sections counterstained with hematoxylin) of male and female mice 35 weeks after weaning to either ST or HF diet. Bar, 0.1 mm.

Figure 3 Glucose homeostasis. **(a)** Plasma glucose levels in fasted and fed mice at week 15 (see text for details). **(b-d)** Intraperitoneal glucose tolerance test was performed at week 10, 25 and 33, respectively, after weaning to either ST or HF diet (see also Supp. Fig. 1). **(b)** Fasting blood glucose at time 0 of the glucose tolerance tests performed at week 10, 25 and 33, respectively. **(c)** Area under the glycemic curve (AUC) of the tests performed at week 10, 25 and 33, respectively. **(d)** Plasma insulin levels at time 0 and 30 min of the test performed at week 33. Data are means ± SE (*n=10*; at week 10, only part of mice was randomly selected for the testing). *significant difference between the sexes within the same diet, $^{\#}$significant difference between the diets within the same sex (ANOVA), ‡significant difference before and after the respective treatment (RM ANOVA).

Figure 4 Adipose tissue histology – morphometry of adipocytes and macrophage infiltration. **(a-d)** Immunodetection of MAC-2 positive macrophages aggregated in crown-like structures

(CLS; brownish color indicated by arrows) in gWAT and scWAT of male (M) and female (F) mice 35 weeks after weaning to either ST or HF diet. Sections were counterstained with hematoxylin-eosin. Bar, 0.1 mm. At week 15 **(e-h)** and week 35 **(i-l)**, size of adipocytes was evaluated by morphometric analysis in hematoxylin-eosin stained sections of gWAT **(e,i)** and scWAT **(g,k)** in both sexes. Frequency of CLS in gWAT **(f,j)** and scWAT **(h,l)** in both sexes. Data are means ± SE (*n=8;* within each group, mouse with the lowest and with the highest body weight, respectively, were not analysed). *significant difference between the sexes within the same diet, #significant difference between the diets within the same sex (ANOVA).

Figure 5 DNA quantification in gWAT of male (M) and female (F) mice fed ST or HF diet at week 15 (**a**) and week 35 (**b**). Data are ± SE *(n=7-10).* *significant difference between the sexes within the same diet, #significant difference between the diets within the same sex (ANOVA).

Figure 6 Quantification of gene expression in gWAT of male and female mice fed ST or HF diet at **(a)** week 15 and **(b)** week 35. Expression of selected genes was evaluated using qRT-PCR and standardized relative to ST diet fed male mice at week 15. Data are means ± SE (*n=7-10*). *significant difference between the sexes within the same diet, #significant difference between the diets within the same sex (ANOVA). MCP-1, monocyte chemoattractant protein-1; TNFα , tumor necrosis factor α; CD68, macrosialin.

Figure 1

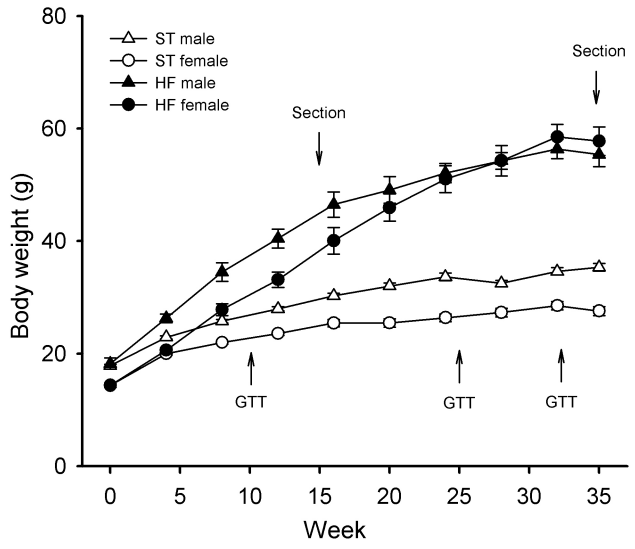

Figure 2

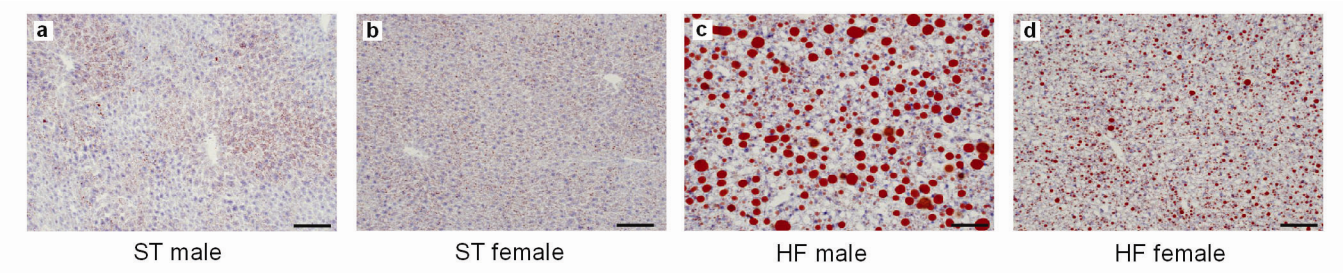

Figure 3

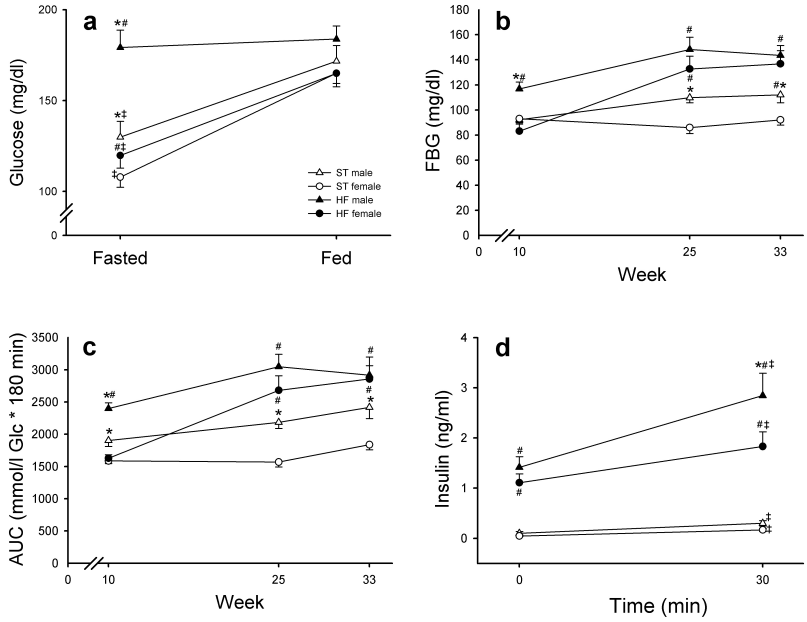

Figure 4

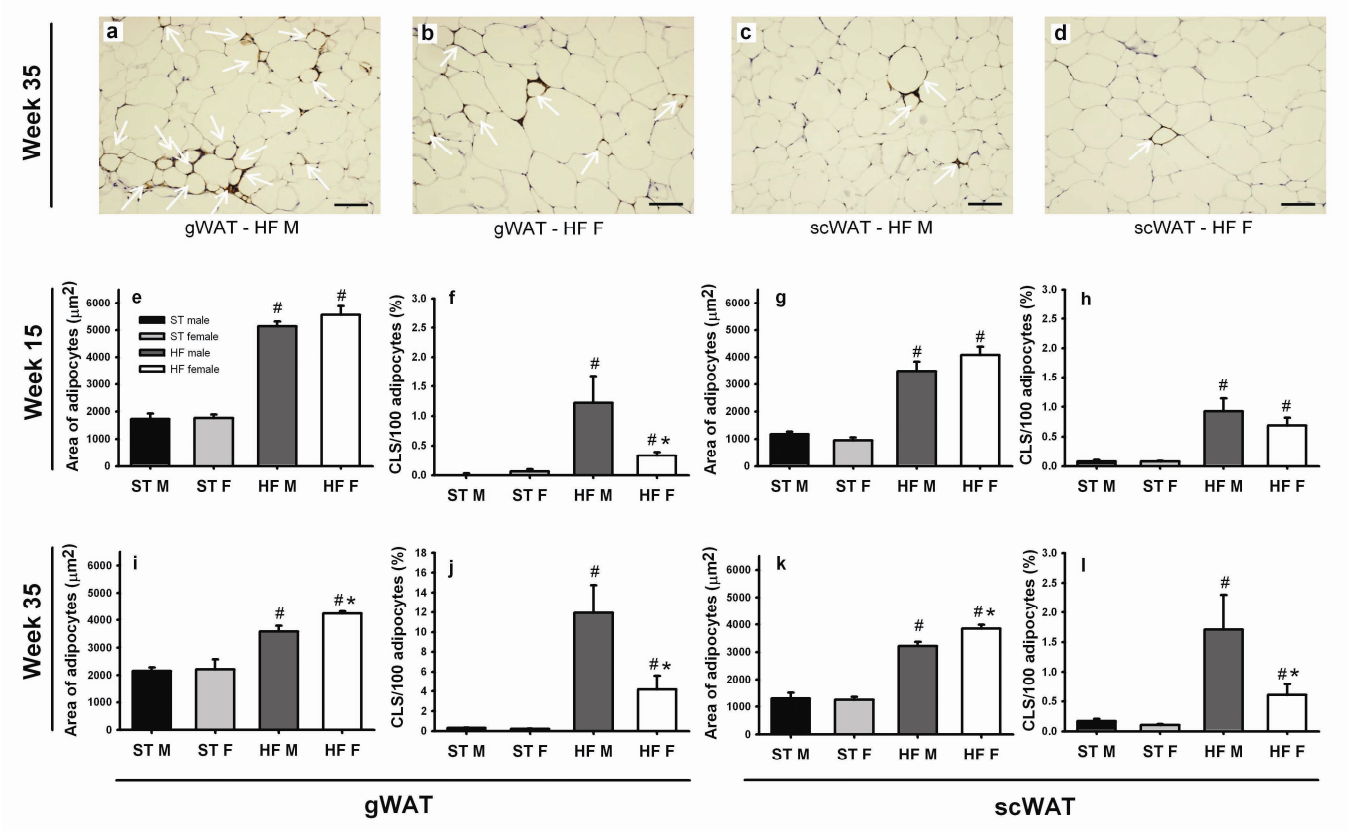

Figure 5

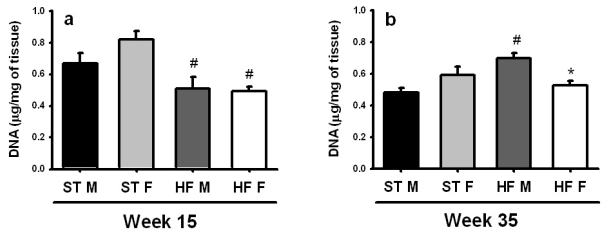

Figure 6